Tribochemistry of Boron-Containing Lubricant Additives on Ferrous Surfaces for Improved Internal Combustion Engine Performance

Lukman Aremu Animashaun

Submitted in accordance with the requirements for the degree of

Doctor of Philosophy

The University of Leeds

School of Mechanical Engineering, Leeds, UK

February, 2017

This candidate confirms that the work submitted is his work. The contribution of the candidate and other contributors has been explicitly indicated below. The candidate confirms that appropriate credit has been given within this thesis where reference has been made to the work and others. X-ray photoelectron spectroscopy undertaken at NEXUS, NanoLAB, in Newcastle. In addition, my sincere thanks to R.T.Vanderbilt Holding Company, Inc. and ARCHOIL Inc. who provided the borate esters additives for the purpose of this research.

This copy has been supplied on the understanding that it is copyright material and that no quotation from this thesis may be published without proper acknowledgement.

Acknowledgments

In memory of my late

mum and grandparents

Abstract

Global concerns for the environmental impact of pollutants from automotive sources require considerable reduction of phosphorus and sulphur-based antiwear additives in lubricating oils. One of such additives used as antiwear/extreme pressure (EP) additives in lubricating oils is Zinc Dialkyl DithioPhosphate (ZDDP). Potential replacements for ZDDP are antiwear/EP boron-based additives. In this study, a comprehensive evaluation of the tribological properties of model oils of different types of borate antiwear additives are considered for comparison to ZDDP on steel surfaces in tribo-contact.

In this thesis, tribological experiments in pure sliding under boundary lubrication conditions were performed using pin-on-reciprocating plate test rig with variations of: additive concentrations in the oil, bulk-oil temperature, sliding process, dissolved, and free water contamination tests. The coefficient of friction response and antiwear performance of tribofilms were evaluated. Bulk oil analysis of the model oils were performed to evaluate their response to different thermal and oxidative conditions in comparison to ZDDP. In addition, chemical characterization of key crystalline boron compounds was done. The physical and chemical aspects of tribofilms generated during tribological tests were evaluated using surface analysis techniques such as: Optical white-light interferometry, Atomic Force Microscopy (AFM), Focused Ion Beam-Scanning Electron Microscopy (FIB-SEM), Raman Spectroscopy, X-ray Photoelectron Spectroscopy (XPS) and Nanoindentation.

One of the key findings of this study is that tribofilms from hydrolytically unstable borates additives gave poor antiwear performance compared to ZDDP and other synthetic borate additives with better resistance to hydrolysis. This study has revealed that boric acid is not directly responsible for the poor antiwear performance as previously understood. Tribochemistry results by this thesis has shown that high atomic concentration of boron and particles such as; boron nitride and carbides acts as third body abrasives, are responsible for the poor antiwear performance. The established antiwear mechanism of borate tribofilms relies on the digestion of abrasive iron oxides by trigonal structural groups in boron oxide. Results at different test conditions from this research have indicated that boric acid, iron oxyhydroxide, and tetragonal structural units in boron oxide plays a major role in this process. The

established friction reducing mechanism of boron-containing tribofilms relies on the weak van der Waal's of boric acid and passivation of its high energy edge-sites by moisture. Another major finding of this PhD thesis is that decomposition and volatility of boric acid at certain temperatures affects the easy shear of the lamellar.

An important finding from this study indicated that the abnormal behaviour of boron oxide effect in borosilicate glass manufacture could also affect the antiwear performance and durability of tribofilms containing nanoparticle alkali borate ester. In addition, the hardness of built-up tribofilms from oils containing hydrated potassium borate was found to be comparable to ZDDP, unlike organic borates which gave significantly higher hardness. Another major finding of this research is that in moisture-rich atmosphere, borate tribofilms formed on ferrous surfaces was more wear-resistant than ZDDP due to their different tribochemistry.

Table of Contents

List of Figures

xiv

xxi

List of Tables

Nomenclature

A_r	Real Contact Area in m^2
k	Dimensional Wear Coefficient (m^3/N-m)
W	Applied Load (N)
L	Sliding Distance (m)
H	Hardness (GPa)
v_i	Wear Volume in m^3
F	Friction Force (N)
μ	Coefficient of Friction (COF)
E	Elastic Modulus (Pa. or N/m^2)
h$_{min}$	Minimum Lubricant Film Thickness
Λ	Lambda Ratio
η_o	Lubricant Viscosity at Ambient Pressure (N.s/m^2)
P	Pressure (N/m^2)
R	Radius of Curvature (m)
k$_i$	Ellipticity Parameter
S	Effective shear stress (N/mm^2)
ABE	Diethanolamine Borate Ester
KBE	Hydrated Potassium Borate Ester
ZDDP	Zinc Dialkyl DithioPhosphate
BTE	Boric Acid Trimethyl Ester
PAO	Polyalpha Olefin
XPS	X-ray Photoelectron Spectroscopy
AFM	Atomic Force Microscopy

Chapter 1
Introduction

1.1 Emission challenges from internal combustion engines

The release of an excess amount of certain heat-trapping gases into the atmosphere is a major global challenge presently facing humanity. This causes a dramatic effect on the climate resulting in the melting of glaciers, rising sea levels, drying forests and extreme weather conditions; more rain followed by longer siccative droughts. In many parts of the world, these factors bring along with it economic instability.

The greenhouse gases emitted to the atmosphere and their relative contributions to greenhouse effects are; methane (CH_4 = 4.4%), Nitrogen (I) Oxide (N_2O = 1.5%), Ozone (O_3 = 8%), Carbon IV Oxide (CO_2 = 26%), water vapour (60%) and others (0.1%) [1]. About 95.7 % of CO_2 in the environment has been estimated to come from natural sources, such as: organic decomposition, ocean release, respiration and volcanoes [2]. The rest are due to anthropogenic sources. However, the second largest emission of CO_2 into the atmosphere through human activity was attributed to combustion of hydrocarbon fuels in internal combustion engines (IC) [3].

The IC engines used in such devices for the transportation of goods and people by land, air and sea have been identified to be responsible for about 22% of the global primary energy consumption. Road transportation accounts for 72% of the 22% total energy use, and 18% of global anthropogenic greenhouse emission as shown in Figure 1-1. Passenger cars have been identified to account for more than 80% of the total CO_2 emissions into the atmosphere [3]; unlike the lower contributions by shipping cargo with about 2.2-2.7 % [4]. This is due to the fact that having personal cars is powerful and pervasive, as it provides freedom, convenience and comfort to their owners. Hence, vehicle demands was estimated to rise from 850 million in 2011 [3] to over 1 billion by 2020 [5].

In view of the consequential outlook of a higher level of CO_2 above the natural balance in the environment, substantial reduction from automotive sources have links to

technological improvement of fuel economy in internal combustion engines. Future engine designs are expected to have lower weight, advanced valve train and combustion systems, with ash-less boundary lubrication target of low friction and wear lubricant additives for the engine oil.
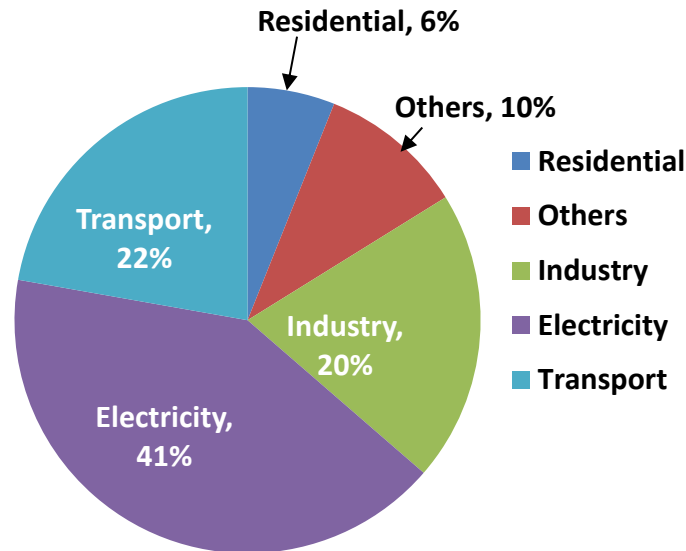
Figure 1-1 Global CO2 emissions contribution into the atmosphere [6]

1.2 Future lubrication schemes for internal combustion engines

Emissions from exhaust fumes could contain carbon monoxide (CO), oxides of nitrogen (NO_x) and unburnt hydrocarbon that could either be oxidized or reduced by emission control system as shown in Equation 1- 1, Equation 1- 2 and Equation 1- 3. Environmental regulatory agencies of many countries in the world have legislative mandate that these catalysts must remain highly effective for up to about 193,000 km of service [7]. Hence, the challenges in pollution control from automotive exhaust system requires expensive catalytic converter system.

However, evidence on how these catalyst degrade points to the volatility of phosphorus in ZDDP. Combustion products of these additives also contain oxides and phosphates that have irreversible and deleterious effects on particulate filters in modern vehicles [8-10]. Hence, ZDDP oil additive is classified as sulphated ash, phosphate and sulphur (SAP) based additives.

$$2CO \quad + \quad O_2 \quad \rightarrow \quad 2CO_2 \qquad\qquad \text{Equation 1- 1}$$

$$C_xH_{2x+2} \quad + \quad \frac{(3x+1)}{2}O_2 \quad \rightarrow \quad xCO_2 \quad + \quad (x+1)H_2O \qquad \text{Equation 1- 2}$$

$$2NO_x \quad \rightarrow \quad xO_2 \quad + \quad N_2 \qquad\qquad \text{Equation 1- 3}$$
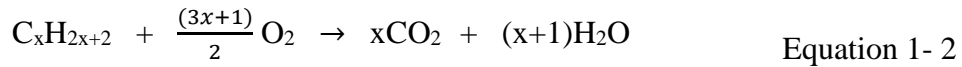
A way of limiting the amount of phosphorus in engine oils is to reduce the concentration of ZDDP in oils. The regulatory framework for achieving these are provided by American Petroleum Institute (API) and International Lubricant Standards and Approval Committee (ILSAC). In 1995, API SI and ILSAC GF-2 limited the phosphorus level to a maximum of 0.1 (mass) %, that was further reduced to 0.08 (mass) % in ILSAC GF-4 [7]. Any further reduction in ZDDP concentration in the oil could adversely affect its antiwear performance and durability of tribofilms formed on the component parts of the IC engines, as shown in Figure 1-2. Hence there is need for a study on how the amount of phosphorus in engine oils can be reduced if not eliminated without sacrificing the antiwear performance and durability of tribo-component parts of IC engines.

In view of environmental restrictions limiting the use of ZDDP additive that boron-containing antiwear/EP lubricant additives are considered as a possible alternative to ZDDP [11-13]. This is based on literature study which showed that vehicles lubricated with oils containing boron antiwear additives produce lower CO emissions than those containing ZDDP [14]. In addition, the same study revealed little differences in terms of wear reduction and cleanliness performance compared to ZDDP. Thus, if boron-containing lubricant additives can lower CO emission and produce comparable antiwear performance to ZDDP in IC engines, then the level of phosphorus in engine oils can be considerably minimized if not eliminated.

Boron is a relatively rare-element in the Earth's crust, but is always found concentrated in water due to its high solubility in form of borate minerals and boric acid. The global proven reserves of boron minerals has been shown to exceed 1.2 billion metric tonnes against a yearly production of about 4 million tonnes per/annum [15]. The countries with the largest deposits of boron compounds are

Turkey and United State of America (USA). They both have a combined share of 90% [16]. Presently, the major global demand for borates are in fiberglass and borosilicate glassware production [15, 17].

The most common contacting surfaces in IC engines that are prone to frictional losses and engine wear are: piston, bearings and valve train assembly. Piston assembly in IC engines accounts for the largest share of mechanical losses. At the piston dead-centres, boundary lubrication dominates and hydrodynamic lubrication at the mid-stroke [18]. For the valve train assembly, boundary and mixed lubrication conditions dominates, unlike the bearing assembly where hydrodynamic regime prevails. The part of valve train that is noted for high wear rates due to asperity contacts is the cam/follower contact configuration. In the cam/follower tribocontact, the operating regime is mainly by boundary lubrication regime [19]. In this lubrication regime, the chemistry of reacted layers plays a more important role than lubricant viscosity. Hence, experiments for this research were carried out under boundary lubrication conditions, based on the highest wear rates occurring at this lubrication regime.
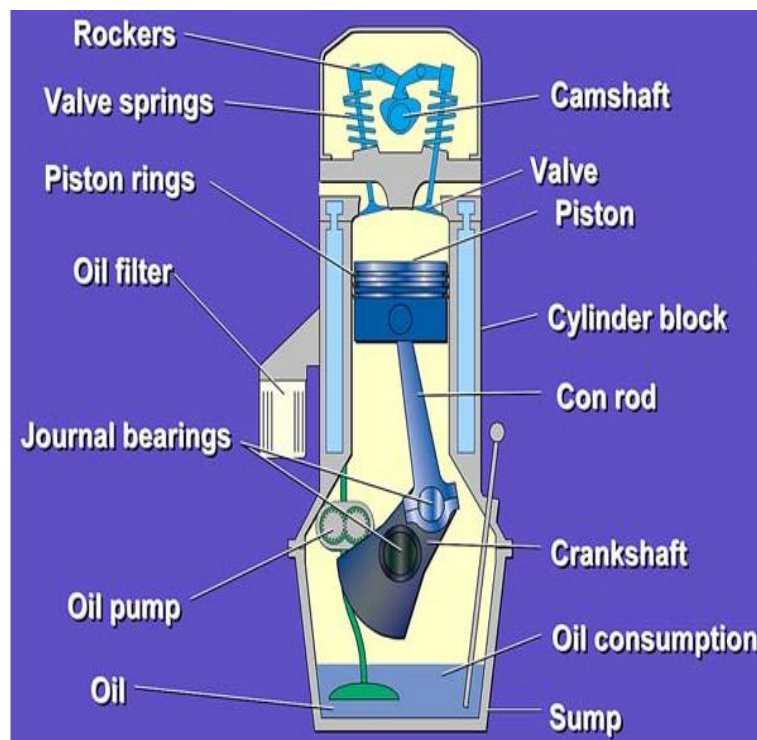
Figure 1-2 A schematic diagram of an internal combustion engine **[20]**

4

The formation of polyphosphate species on ZDDP tribofilms has been shown to depend not only on the wear process, but also on temperature [21]. Hence, a potential substitute for ZDDP should be studied under different test conditions in other to fully understand their antiwear performance and durability behaviour.

The antiwear mechanism established for borate lubricant additives on Fe-based materials have been based on Pearson's Hard Soft Acid Base (HSAB) principle [22]. However, this assumed negligible effect of: hydrolysis by-products, no transformation in borate anions due to changes in physical properties, and effects of boric acid in aqueous solution on oxides of iron. In addition, the friction reducing mechanism of borate tribofilms has been hinged on boric acid; based on its weak van der Waal's [23], and passivation of high energy edge-site of lamellar boric acid [24]. However, these mechanism assumed that boric acid is stable at all temperatures, and more amount of boric acid formed on surfaces would give better friction coefficient reduction. Hence, the study of tribofilms formed by boron-containing oils is necessary under different test conditions in order to elucidate the suitability of borate additives as zero-SAP substitute for ZDDP antiwear/EP additive in engine oils for IC engines.

1.3   Aims and Objectives

The aim of this PhD work was to assess the relative susceptibility to hydrolysis of non-synthetic borate additives to synthetic additives. This study will further investigate the physical nature of reacted layer formed on ferrous surfaces under boundary lubrication regime and different extrinsic conditions by oils containing boron additives using ZDDP as reference.   In addition, the study of lubrication chemistry of borate tribofilms formed at different tribological test conditions under boundary lubrication regime could elucidate on the influence of these conditions on established friction reducing and antiwear mechanisms.

To achieve these aims, a number of objectives were set out, namely to:

- Assess the hydrolytic stability and thermo-oxidative stability of lubricating oils containing synthetic and non-synthetic borate additives in comparison to ZDDP. Following this results, moisture absorption characteristics of oils containing synthetic additives and key crystalline boron compounds are

undertaken. This is to provide an understanding of the differences between synthetic and non-synthetic borate additives, and also between synthetic borate additives and ZDDP in terms of affinity for moisture absorption.

- To assess the tribochemical behaviour of borate additives at different additive concentrations against the ZDDP additive through physical and chemical surface characterization. This is to provide a better understanding of how hydrolytic stability not only affects the tribochemistry of borate tribofilms, but also the borate friction reducing and antiwear mechanisms.

- To explore the effect of temperature on antiwear performance and durability of borate tribofilms. Surface characterization of borate tribofilms formed at different bulk oil temperatures are expected to explain how the established antiwear mechanism could be affected by boric acid decomposition and transformation of B_2O_3 structural units.

- To investigate how borate antiwear mechanism is affected by humidity increase in the surrounding environment through chemical and physical surface analysis of the formed tribofilms. This is to elucidate on the limit of borate tribofilms synergy with moisture for effective antiwear performance.

- To evaluate the friction and antiwear performance of borate additives in comparison to ZDDP with increasing water content in the oil. Post-test surface analysis of boundary films formed under thermal and tribo-oxidation conditions could elucidate the limitation of their tribochemistry with regards to their antiwear mechanism.

1.4   Thesis outline

- Chapter One: This consists of introduction and justification for the study. In addition, the aims and objectives of this thesis and some theories of tribology, lubrication and boron chemistry are discussed

- Chapter Two: Literature review of conventional ZDDP, organic borates and metal borate dispersions antiwear lubricant additives on ferrous surfaces in tribo-contact under various extrinsic conditions

- Chapter Three: Overview of experimental methodology, and details of sample properties, sample preparation procedure, lubricants, test rigs, bulk oil and surface analysis techniques

- Chapter Four: Hydrolytic and thermo-oxidative stability results from bulk oil analysis, moisture absorption of oils and moisture adsorption by major crystalline boron compounds experiments are provided in this chapter

- Chapter Five: Friction and wear experiments and results from variable concentration, temperature, and water-based contaminants are contained in this chapter

- Chapter Six: Physical characterization of tribofilms using Atomic Force Microscope (AFM) images, Nanoindentation and Focussed ion beam-Secondary Electron Microscope (FIB-SEM)

- Chapter Seven: Chemical characterization of tribofilms results using X-ray Photoelectron Spectroscopy (XPS) and Raman Spectroscopy

- Chapter Eight: A comprehensive discussion of the results obtained from various bulk oil analysis tests, tribological experiments and surface analysis in relation to published literatures are presented in this chapter

- Chapter Nine: This chapter contains the main conclusions from this PhD. research and future works.

1.5 Background and Theories

1.5.1 Introduction to tribology

The term 'Tribology' has its prefix rooted from the Greek word 'tribos' implying 'rubbing' or 'to rub', while the suffix, 'ology' means 'the study of', that literary translates to be ' the study of things that rub'. The word was officially used for the first time in 'The Jost Report' to the British Parliament in 1966, while the scientific basis for modern understanding of tribology was established by scientist like; Hertz, Reynolds, Hamrock, Dowson, Bowden and Tabor [3]. Tribology is the science and technology of interacting surfaces in relative motion and of related subject and practices. The transmission of normal or tangential forces between two bodies in relative motion may take place.

In certain engineering systems and mechanics related to our everyday lives, tangential forces are required to be minimized in order to control motion or improve system efficiency by optimizing factors related to tribological interface, as shown in Figure 1-3.
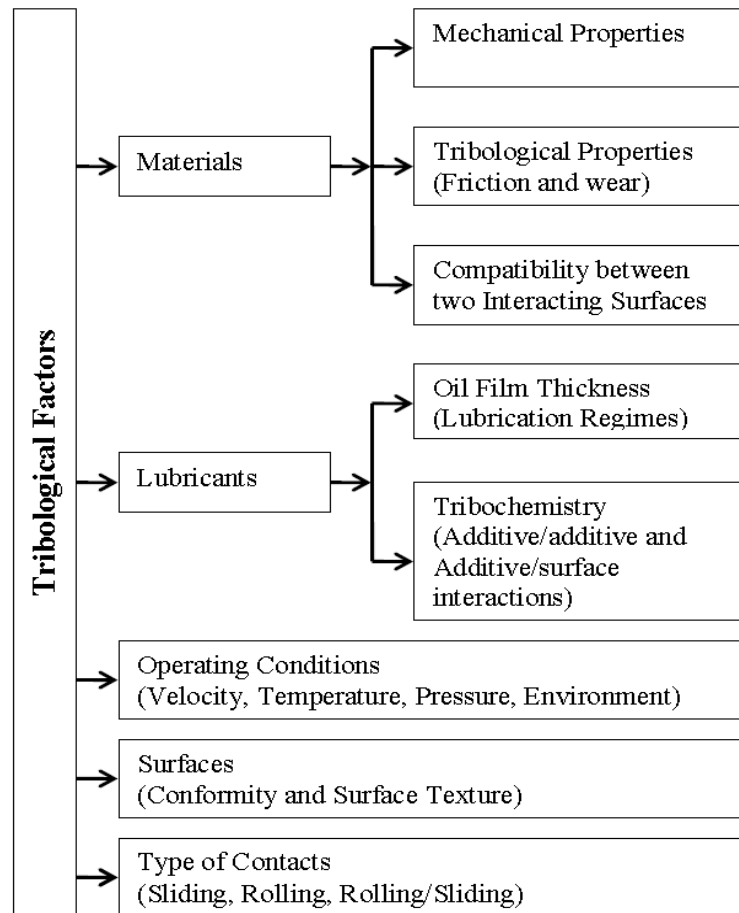
Figure 1-3 Fundamental factors affecting tribology of IC tribo-components **[25]**

1.5.2 Friction

Friction is the force opposing the relative motion of one body in contact with another. The classes of frictional forces are sliding and rolling friction. Sliding friction requires conformal surfaces; contacting surfaces that fits snugly into each other, so that load distribution spreads over a relatively large area. On the other hand, rolling friction involves non-conformal surfaces; here, the full burden of load distribution is concentrated on a small lubrication area [26].

8

The first two laws governing friction for bodies in dry sliding contact conditions as postulated by Leonardo da Vinci (1452-1519) and was re-established by Guilanme Amontons in 1699. The third law of friction was formulated in 1781. The three laws are stated as;

- The first law of friction describes the tangential force opposing motion (friction force, F) as proportional to the normal applied load (W)

- The second law of friction describes frictional force is independent of the size or apparent area of the contacting solids, but rather on the real area of contact. This assumed that apparent area is equal to the real area of contact by assuming that normal load is pressure multiplied by apparent; instead of real area as mostly recognized in most tribological analysis.

- The third law of friction describes kinetic friction (force required to maintain motion) as lower than static friction (force required to start sliding) and is independent of the sliding speed. Initially, there is asperity interlocks between the two contacting surfaces which makes it harder to overcome, but once the interlock is broken it will be easier to sustain the sliding process with less energy.

These laws are generally obeyed by metals, but are found to be different when polymers and rubbers are unlubricated contacting solids [26], which was expressed in Appendix A: Equation A.1.- 1, Equation A.1.- 2 and Equation A.1.- 3. Another expression for coefficient of friction in terms of mechanical properties of the sliding material is shown in Equation A.1.- 4. If the Hertzian contact model is considered, low friction can result by using sliding materials of low shear strength and high contact pressure [27]. This is possible by the formation of a relatively thin low-shear strength layers with increasing contact pressure by using additives in lubricants. The shear strength of MoS_2 has been estimated to be about 24.8 MPa [28] to give low friction coefficient on surfaces and that of boric acid as 22.9 MPa [27]. Hence, the lubricious nature of boric acid based on its friction reducing properties could be an added advantage of the ZDDP additive.

1.5.3 Wear

This is an undesirable consequence of friction, with the progressive physical scathe, because of material loss from the operating surface of a body due to its relative motion. Wear is a system property like friction, and not a material property. There are three broad wear types, which can further be broken down into six interrelated modes, as described in Table A.2.- 1. The general laws of wear are very similar to the laws of friction in dry sliding condition. Wear in tribological systems is often described according to Archard's wear law as the proportionality of wear volume to the product of real area of contact and sliding distance, as shown in Equation A.2.- 1, based on the assumptions that:

- Local contact occurs when asperities interact,
- Each individual asperity contact is circular,
- For metals, asperity deformation is plastic,
- The real contact area is proportional to normal load,
- The region of contact under consideration is isothermal

Adhesive wear is known to be common with metal/metal contact interactions. It is described as the displacement and attachment of wear debris or material from one surface to another. This is unlike abrasive wear that occurs when hard particles are forces against and at the same time moves along the solid surfaces in relative motion. The hard particle sources could be: dirt in the housing, sand or scale from castings, metal wear particles, and particles introduced into housing when filling with lubricating oil. The relationship between Archard's law, adhesive wear and abrasive wear shown in Equation A.2.- 2 and Equation A.2.- 3 are used to assess the relative wear rates of lubricated worn surfaces. In order to minimize the negative effect of friction and wear, most engineering approaches to overcoming the consequences of wear involves:

- Use of special low-friction materials,
- Use of lubrication processes involving the interposition of solid, liquid, or gas medium between the contacting surfaces,
- Conversion of sliding friction into rolling friction with clever designs; since rolling friction is much smaller than sliding friction.

The combination of these approaches could greatly reduce friction and wear, but also the influence of physical properties of interacting surfaces, interposing lubricant and physicochemical interactions of reacted layers with the surroundings. Hence, a careful study of the physical and chemical nature of reacted layers formed by additives used as additives in lubricating oils of internal combustion engines is necessary during tribological process. These chemical agents are expected to act as an alternative to the conventional S- and P-containing IC engine oils in order to meet environmental and legislative challenges.

1.5.4 Lubrication

Lubrication is used in mechanical systems in order to minimize the negative effect of friction and wear of machine components. This is achieved by providing interposing layers between contacting solids in relative motion. The functions of lubricant in an I.C engine are to;

- Form an easily sheared viscous lubricant films with the potential to carry a relatively large applied load,

- Prevent corrosion,

- Transport contaminants from the system,

- Assist in sealing spaces,

- Reduce friction coefficients between interacting surfaces,

- Act as coolant

The variation of coefficient of friction (COF) had been shown to be a function of lubricant film parameter (Λ), or the ratio of the product of the lubricant viscosity and speed to the normal load applied which can be describe by the basic Stribeck curve shown in Figure 1-4. If the lubricant film thickness is large enough to separate the interacting surfaces, hydrodynamic lubrication (HL) lubrication condition or regime is at play. In this type of lubrication regime, the bulk properties of the lubricant (i.e. viscosity) governs the lubrication of the solid surfaces rather than the elastic deformation of the lubricated surfaces. However, if there is considerable elastic deformation of the lubricated surfaces in addition to complete separation by lubricating film, the type of hydrodynamic lubrication that arises is known as elasto-

hydrodynamic lubrication (EHL). In this lubrication regime, the lubricant and material properties are important in controlling friction.
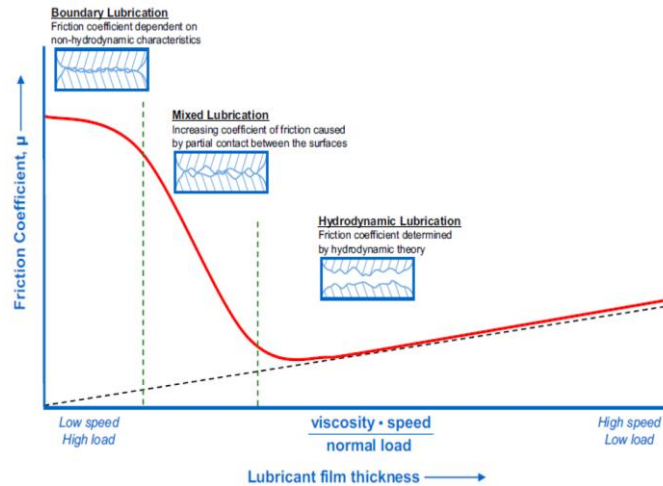
Figure 1-4 Stribeck curve to depict friction coefficient as a function of viscosity, load and speed for a lubricated system **[29]**

The other lubrication regimes are; Boundary lubrication (BL) and Mixed lubrication (ML). In Boundary lubrication (BL) regime there is negligible fluid film effect in separating the contacting surfaces with considerable asperity-to-asperity contact. Here, the friction characteristics of interacting surfaces is governed by the properties of the solids and the lubricant films formed at the common interface. In mixed lubrication (ML) regime, penetration of lubricant film occur due to excessively high pressures or too low running speed in the EHL tribocontact, with a behaviour governed by fluid films and boundary lubrication effects. The different lubrication regimes can be distinguished from one another by determining the film parameter (Λ), defined mathematically in Equation A.3.- 1 to Equation A.3.- 8 as shown in Appendix A.3. The characterisation of the film parameter (Λ) into the various lubrication regimes is possible if Λ is within the range stated below [30];

- Hydrodynamic lubrication; $\mathbf{5} \leq \Lambda < \mathbf{100}$

- Elasto-hydrodynamic lubrication; $\mathbf{3} \leq \Lambda < \mathbf{10}$

- Mixed lubrication; $\mathbf{1} \leq \Lambda < \mathbf{5}$

- Boundary lubrication; $\Lambda < \mathbf{1}$

1.5.5 Introduction to the boron chemistry

Boron is a non-metallic chemical element with symbol **B** belonging to group 13 and period 2 of p-block on the periodic table of chemical elements with a shell structure shown in Figure 1-5 which indicates electron deficiency in its outermost shell. It is the only non-metallic element with vacant valence shell. This makes it have unusual binding conditions and structural complexity. Boron has electronic configuration, atomic number and atomic weight of $1s^2\,2s^2\,2p^1$, 5 and 10.81 respectively.
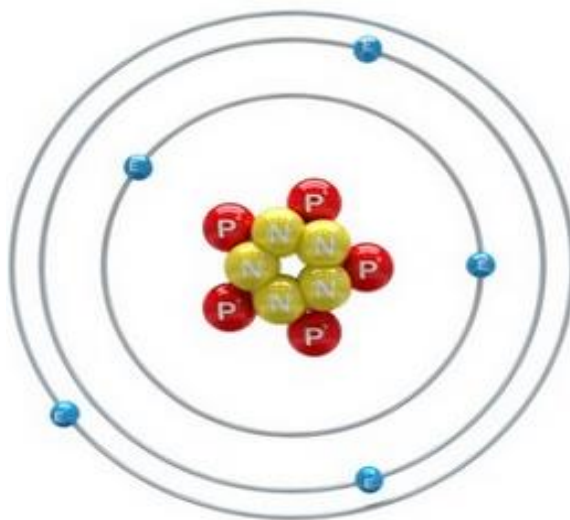
Figure 1-5 Shell structure of boron **[31]**

The first attempt to isolate boron as an element was by reduction of boric acid (H_3BO_3) or $B(OH)_3$ with Sodium (Na) or Magnesium (Mg) to yield about 50 % purity was undertaken by three eminent scientists namely; Humphrey Davy, Joseph Louis Gay-Lussac and Louis Jacques Thenard [32]. However, boron was recognized to be isolated at 99% purity by Ezekiel Weintraub in 1909 [33] who reduced volatile boron halides in hydrogen at very high temperature. Higher purity boron can be produced by decomposition of diborane at high temperature followed by purification. Pure boron does not occur in nature, but rather as ores.

The ores of boron are found in most part of the world with larger deposits concentrated in Turkey and the United State of America in form boron-containing minerals. The majority of these ores are usually in hydrated form of boron oxide or diboron trioxide (B_2O_3) fused with metal oxides such as; Potassium, Sodium, Calcium, Magnesium,

etc. There are about 150 known boron-based ores [34] with tincal, ulexite, colemanite, kernite, probertite and szaibelyite that are of major commercial relevance [35].

In addition, boron atoms have only two stable abundant naturally occurring isotopes. These are ^{10}B and ^{11}B with natural boron containing about 20% of ^{10}B and 80% of ^{11}B. The known allotropes of boron exists in three crystalline forms and two amorphous states. The crystalline polymorphs are; α-rhombohedral, β-rhombohedral and β-tetragonal. The two amorphous forms are glassy solid and finely grounded powder. Since boron atom is electron deficient due to three electrons in its valence shell (oxidation state of +3), it can neither donate electrons nor accept electrons easily. This makes it form a stable covalently bonded molecular network in most of its compounds such as oxides, halides, borides, nitrides and sulphides.

In addition, the empty p-orbitals is easily attacked by nucleophiles such as water to result in either bond cleavage of three-coordinated neutral borate species or the formation of four-coordinated borate species [32]. This behaviour suggests that chemical reactions between boron compounds and a wide variety of other compounds on interacting surfaces to give reacted layers with considerable tribological properties.

1.5.6   Boron interactions with other elements

Since boron has only three electrons in its outermost shell, the ion is un-polarizable and does not hydrate, hence it is not eager to donate electrons in an electrovalent bond, and can also not accept them easily. A small quantity of hyperactive boron reacts with silicon molecules in silicon dioxide (or silica) to form amorphous glass molecules.

This acts like a fluid rather than lined up in a crystalline pattern as used in the manufacture of borosilicate glass with a common trade name called 'PYREX'. However boron is more reactive with carbon than silicon to form boron carbide (B_4C).

When boron and nitrogen react as pure substances a synthetic binary compound known as boron nitride (BN) is formed. The most common boron nitride polymorphs are; hexagonal-BN and cubic-BN. The structure of hexagonal-BN is similar to plate-like microstructure of graphite shown in Figure 1-6 is known to give good lubricating properties.

Boron interactions with the halogens produce volatile, highly reactive, covalently bonded molecular compounds, which can readily accept a pair of electrons into their

vacant un-hybridized p-orbitals to form boron halides; all boron halides are Lewis acid. Boron hydrogen compounds are formed due to trivalent nature of boron. Boron hydrides or boranes are formed when boron combines with di-hydrogen such as; B_2H_6, B_4H_{10}, B_5H_9, B_5H_{11} etc.
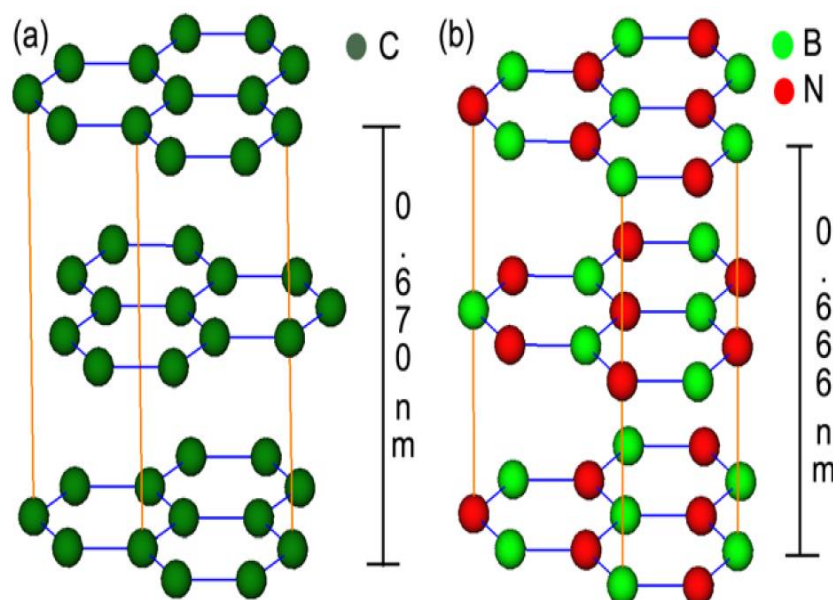
Figure 1-6 Crystal structures of (a) graphite; (b) hexagonal boron nitride **[36]**

The boranes are used; for welding torches, reducing agent in reactors, catalysts in polymerization process and preparing hydrocarbons. Boron reacts with oxygen in the air to form thin films of boron trioxide (B_2O_3) on surfaces to prevent further reaction with oxygen. Due to the high chemical attraction of boron for oxygen, boron compounds form strong covalent boron-oxygen bonds in compounds known as borates; boron atoms in borates can either bond with three or four oxygen atoms to form planar-trigonal BO_3 units or negatively charged tetrahedral BO_4 units.

When boron-rich compounds reacts thermo-chemically with iron-rich surfaces, compounds known as iron borides with formula Fe_xB_y are formed that could either be FeB and Fe_2B. Boron reacts with alkalis to form alkali meta-borates with the evolution of hydrogen. Bonds between boron, oxygen and hydrogen occur in form of water or moisture in air to form a very weak acid known as boric acid (H_3BO_3); H_3BO_3 is weaker than carbonic acid.

1.5.7 Effects and applications of boron

Boron is a vital constituent of the natural world and also finds good use in domestic and industrial applications. The effects of boron which makes it useful for industrial applications are summarized below;

- Boron is a light element which bonds covalently with other elements to form super hard materials that are extremely resistant to external shear stress such as, boron carbide (Vickers hardness = 38 GPa), cubic-boron nitride (Vickers hardness = 76 GPa) [32] and borides (i.e. iron borides with Vickers hardness = 21 GPa, Rhenium borides = 40 GPa) [37-39]. These light-weight compounds of boron are useful in tank armour, antiballistic vest etc.

- Some covalent-bonded boron compounds can also form soft materials that find good use domestically and industrially. Such boron compounds are; boric acid (Brinell Hardness=1.5 GPa) [40], hexagonal-BN (5 GPa) [41] and glassy-boron trioxide (HV=1.5 GPa) [42]. This compounds are used as thin films of solid lubricants on metallic surfaces to provide friction reducing and corrosion resistance characteristics

- Borates are used to modify the structure of glasses due to their excellent resistance to heat and chemical attack. The vitrifying effect of Boron is used in 'Borosilicate glass' or 'Pyrex' glass manufacture, ceramic tiles of space shuttle to provide resistance to extreme stress and heat during the re-entry of space shuttles from outer space back to Earth, and as soldering flux used in Silversmith and Goldsmith works

- Film processing, detergents and fireworks solutions rely on borates due to their chemical properties that serves to provide stable pH or to balance acidity and alkalinity

- Boron is used in nuclear reactor shielding and boron neutron capture therapy in cancer tumour treatment due to boron B^{10} isotope ability to absorb thermal or low energy neutrons

- Boron is an essential component of neodymium-iron-boron ($Nd_2Fe_{14}B$) magnets used in many modern computer and electronic devices such as CD and DVD players, small motors, loudspeakers, communications, power generators, mobile telephone sets and HDD's. The intrinsic characteristics of

these magnets enables a 1 MHz, 41 cm diameter size hard disk drive to be reduced to about 5 cm diameter size

- In the semi-conductor industries, boron is used as a dopant in some elements used as semiconductors such as silicon, germanium and silicon carbide. This is as a result of boron having one valence electron less than the host atom. By donating an electron hole, boron permits the semiconductor to have a conductivity that has a larger positive charged hole concentration than electron concentration. Hence a p-type (or positive charged hole) semiconductor

- Some detergent, laundry detergents, cleaning products and bleaching agents contains sodium perborate ($NaBO_3$) that provides oxygen-containing radicals due to the bleaching effects of boron

- The control of viscosity of paints, adhesives and cosmetics utilize the dispersing effects of borates to bond with other particles in order to ensure that different ingredients are evenly dispersed

- Boric acid is used as an insecticide due to its inhibiting effects on metabolic processes of certain organisms such as control of ants and fungi, water clarifier in swimming pool water treatment and eye antiseptics

- Boron compounds are used as lubricant additives in motor, gear and hydraulic fluids due to their friction-reducing, corrosion inhibition and antiwear properties [13]. In addition, they are known to prevent sludge build-up and CO_2 emission reduction in crankcase engines [43].

Chapter 2
Literature Review

2.1 Introduction

In this chapter, a review of key chemical agents (additives) used to impact antiwear function in IC engines are provided. In order to understand the challenges that new antiwear additives must overcome, a literature review of traditional (ZDDP) and boron-containing chemical agents in lubricants are discussed. A comprehensive review of the literature on how borate and ZDDP antiwear additives behave in oil solutions and as tribofilms in various tribo-oxidative environment are presented. In addition, literature studies on physical and chemical nature of boundary films formed by oils containing ZDDP and borates are expected to elucidate the current understanding of borate friction reducing and antiwear mechanisms. This is to enable results from experiments in this study to be comprehensively discussed and conclusions deduced.

2.2 Zinc Dialkyl DithioPhosphate (ZDDP or ZDTP) additives

2.2.1 Introduction

The use of ZDDP additive in lubricating oils for IC engines is basically due to its antiwear, antioxidant and extreme pressure (EP) properties. The antioxidant potential of ZDDP as an additive was realised in 1941 and was introduced as an additive package. Hence, it has since become the main antiwear additive due to its ability to form quick reaction films that are observed to reduce wear in IC tribo-components [10, 44]. The antiwear chemical agent, ZDDP as an additive consists of elemental species such as: sulphur, zinc, phosphorus, oxygen, carbon and hydrogen that are chemically bonded together. This is possible by reacting alcohols or alkyl phenols with phosphorus penta-sulphide and zinc salts. A simplified molecular structures of various types of ZDDP are shown in Figure 2-1. The three types of ZDDP additives used in lubricating oils for IC engines are; primary ($R=CH_3CH_2CH_2CH_2O$-), secondary ($R=CH_3CH_2CH$ (CH_3) O-) and aryl ZDDP. The differences are due to the type of alcohol used in their manufacturing processes.

ZDDP Types	Molecular structure
primary alkyl ZDDP	
secondary alkyl ZDDP	
aryl ZDDP	
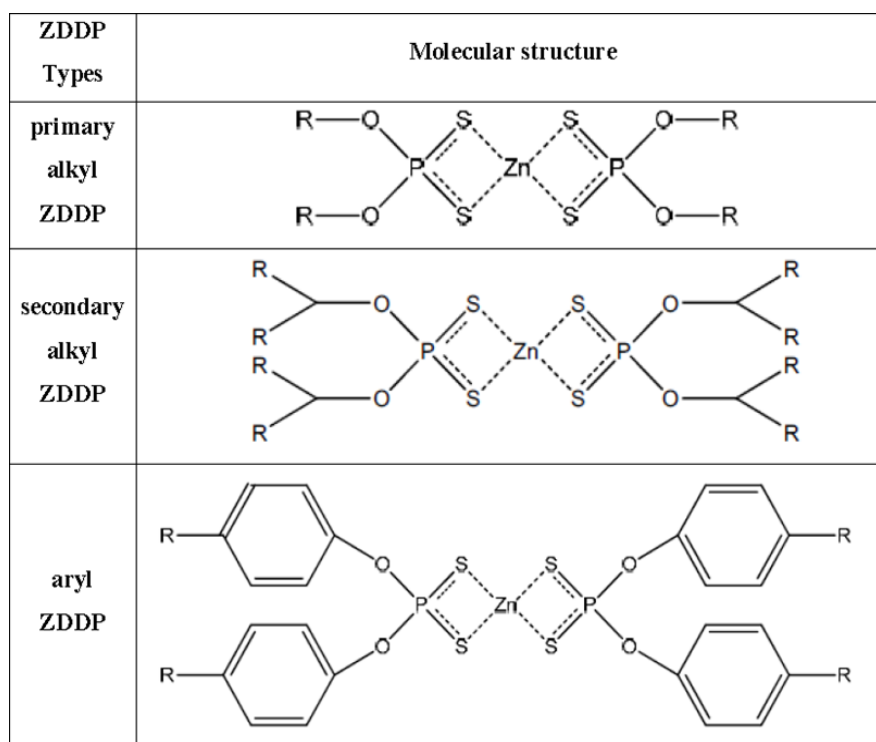
Figure 2-1 Molecular structures of different types of ZDDP **[45]**

Table 2-1 describes different types of ZDDP types in terms of the alcohol used for their manufacture, and rankings in terms of thermal and antiwear behaviour.

Table 2-1 Types of ZDDP and rankings based on thermal and antiwear reactivity

ZDDP TYPE	Alcohol Type Used for Manufacture	Rankings	
		Thermal Stability	Antiwear Reactivity
Aryl	Alkyl phenols	1st	3rd
Primary	Primary Alcohol	2nd	2nd
Secondary	Secondary Alcohol	3rd	1st

These rankings are based on wear rates and different decomposition temperatures of ZDDP types during its tribofilm formation on contacting ferrous surfaces as shown by the discussion of Asseff, P.A. in the literature study of Paul Bennett works [46].

19

The effect of sliding process on the wear rates of ZDDP tribofilms was later confirmed by Yin, Z. et al. [47] and Martin, et al. [48]. In addition, temperature was also shown by Morina et al. [21] to affect ZDDP tribofilm formation. The various types of ZDDP have been customized to function optimally in lubricating oils of one type of IC than other types i.e. ZDDP used in oils for gasoline engines are different to that used in diesel engines. These are based on their different thermal and antiwear reactivity.

2.2.2 Thermal degradation of ZDDP films in solution and on steel

Figure 2-2 shows the main stages of ZDDP reactions in solution and on surfaces in tribological contact. In oil solution, the behaviour of ZDDP is different to how it forms thin films on surfaces.
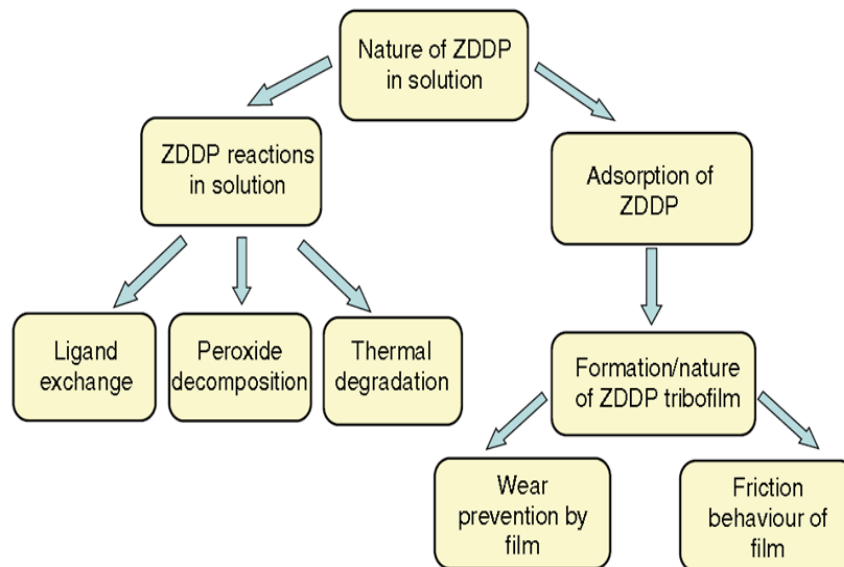
Figure 2-2 Major stages of ZDDP behaviour in solution and on surfaces **[49]**

A feature of ZDDP in solution was identified to dithiophosphate ligands. This was described as a transient chemical species that could easily exchange zinc cation with other metal ions (M) such as iron or copper ions to give a less thermally stable metal dithiophosphate [49, 50] as shown in Equation 2- 1.

$$((RO)_2PSS)_2Zn \ + \ M^{2+} \ \rightarrow \ ((RO)_2PSS)_2M \ + \ Zn^{2+} \qquad \text{Equation 2- 1}$$
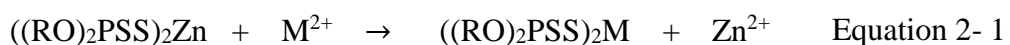
In addition, this behaviour could also take place on surfaces with metal oxides [49].

Metal dithiophosphates (MDDP) are known as metal extraction agents with the potential for exchanging different metal cations with one another [49, 51]. This process was shown to depend on the relative order as described in Equation 2- 2; where cations to the left displace cations to the right of MDDP.

$$Pd^{2+} > Au^{3+} > Ag^+ > Cu^{2+} > Fe^{3+} > Ni^{2+} > Zn^{2+}$$ Equation 2- 2

Another study on how ZDDP in solution behaves indicated that it decomposes both hydro-peroxides and peroxy-radicals in order to stall the peroxide oxidation cycle [52-54] to form reaction products which enhances oxidation inhibition [49, 55]. However, literature studies had shown that when ZDDP behave as peroxide decomposer, the resulting species do not possess enough potential to provide effective zinc phosphate antiwear films [56-58].

In addition, decomposition of ZDDP in solution was attributed to hydrolytic mechanism to form zinc polyphosphate and alkyl sulphide [59, 60]. The study suggested that phosphate species are physically adsorbed on surface oxide layer, and iron sulphide formation when elemental sulphur reacts with alkyl sulphides and Fe_2O_3.

Thermo-oxidative degradation behaviour of ZDDP in solution was shown to yield solid deposits, alkyl sulphides, mercaptans, hydrogen sulphide, olefins and zinc phosphate in the absence of significant levels of peroxy-radicals and hydroperoxides [49, 50]. However, ZDDP degradation temperature could fall between 130°C and 230°C which depends on the type of alkyl groups and metal cation present in ZDDP and contacting surface [49]. Thermo-gravimetric analysis (TGA) of ZDDP-containing oils had been shown to vary between 170°C and 200°C [61, 62].

The product of hydrolysis of ZDDP in solution was suggested to be composed of alkyl sulphides and zinc polyphosphates [59, 60]. In addition, polyphosphates with long chain from ZDDP in solution was shown to hydrolyse/depolymerize to form short chain polyphosphates and phosphoric acid [63, 64]. Thermo-oxidative stability test results of ZDDP in PAO had chemical attack on copper by the reactive sulphur to form deposits on copper coupons as proposed in the works of Jayne et al. [65] and Garcia-Anton et al. [66]. The product of hydrolysis of ZDDP in solution along with zinc polyphosphates, was suggested to be composed of alkyl sulphides [59, 60].

21

The mechanism for thermal degradation was attributed to either Oxygen/Sulphur isomer exchange in ZDDP molecules as shown in Figure 2-3 or polyphosphates formation. This occurs when phosphoryl group from a neighbouring molecule displace the RS groups [49, 63, 67, 68]. Studies on the behaviour of ZDDP molecules on ferrous surfaces showed that adsorption took place through sulphur atoms of P=S bonds [49, 69]. When the temperature of ZDDP in solution was increased to about $60^{o}C$, irreversible adsorption was noted to have occurred due to loss of Zn ions [70]. This was attributed to either cation exchange with iron oxide or hydrolysis by surface water molecules or hydroxides to give iron salts due to free dithiophosphoric acid reaction with Fe_2O_3 [46].
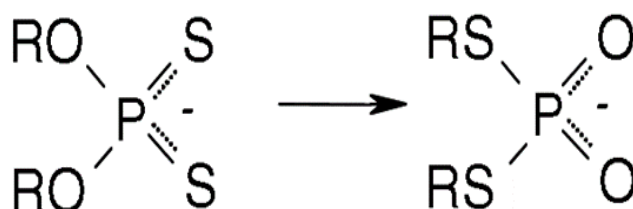
Figure 2-3 Exchange of O/S in ZDDP molecules **[49]**

2.2.3 Tribological behaviour of ZDDP in different conditions

The literature review of tribological behaviour of ZDDP used in lubricating oils of IC engines presented in the following sections refers to secondary alkyl ZDDP with molecular structures shown in Figure 2-1. This review will only cover tribological tests conducted on steel/steel contacts using model oil containing ZDDP in base oil unless otherwise stated. ZDDP in lubricating oils used in internal combustion engines is known to function as an antiwear, antioxidant and extreme pressure additive by forming thick antiwear films on surfaces which do not accumulate oxide debris [71, 72].

In order to provide an effective surface for ZDDP tribofilm growth, Lin and So [73], suggested that contacting surfaces must have identical roughness and hardness numbers [73]. The study suggested that a fully hardened ferrous surface will provide wear reduction to prevent cutting and ploughing action in order to hinder chemical

film growth and longer running-in duration. This was later confirmed by results from Sheasby et al. [71]. On the other hand, increase in load was shown to reduce the sulphur content of tribolayer containing ZDDP which adversely affected its antiwear effectiveness by using the Auger microprobe [74]. This was attributed to reduction in sulphide content of the antiwear films, since sulphides are much harder than phosphates within the tribofilm.

A study of the behaviour of ZDDP antiwear film at different temperatures indicated that physisorption at the surface commenced at about $50^{o}C$ followed by chemisorption around $80^{o}C$. This was attributed to chemical reaction with the surface using energy dispersion spectrometry (EDS) and Auger Electron Spectroscopy (AES) [73].

Physisorption is the physical adsorption process in which the electronic structure of the atom and molecule are barely disturbed upon adsorption unto a surface. It is known to be caused by van der Waals force and can only be observed at relatively low temperature [75, 76]. On the other hand, chemisorption is the alteration of the electronic structure of an atom or molecule to result into new electronic bonds by activation energy; temperature increase [77]. At certain temperature, ZDDP tribofilms had been shown to physisorbed, but will chemisorbed at elevated temperature. However, chemisorption process can be accelerated by rise in temperature between two sliding surfaces [72].

Another tribological study of temperature increase on oils containing ZDDP by Morina et al. [21], attributed enhanced antiwear performance at $30^{o}C$ to $150^{o}C$ bulk oil temperatures to the formation of long chain polyphosphates. By using EDS and XPS to study ZDDP antiwear films from a reciprocating pin-on plate tribocontact, the antiwear performance of ZDDP has been shown to be a function of both temperature [21] and sliding process. This was also confirmed by Gosvami et al. [78] using single asperity sliding nano-contact atomic force microscopy measurements.

However, the stability of polymeric phosphate glass is defined by its glass transformation temperature (T_g) of about $200^{o}C$ [48, 79, 80]. Previous studies on the stability of ZDDP tribofilms at low and high temperature was carried out on both gear oils and lubricating oils containing boron [81, 82]. The study concluded its work without differentiating the role played by ZDDP and boron in the wear-resistant and durability performance.

In addition, the formation and performance of ZDDP antiwear films are greatly affected by many tribological factors such as; sliding mode, temperature, contact pressure, humidity, surface roughness and hardness of the rubbing surfaces. Hence, the study of tribochemistry of tribofilms formed by ZDDP additives on fully-hardened contacting ferrous surfaces at different test conditions will provide a benchmark for any other antiwear chemical agent as a potential substitute.

Humidity of the surrounding environment had been identified to affect tribofilms from oils containing ZDDP [83]. The study observed that as humidity increases, ZDDP tribofilms from a steel ball- on- steel disc unidirectional test rig gave decreased antiwear performance. This was attributed to depolymerisation of longer chain polyphosphates to shorter chain length phosphates and decreasing thickness of the reaction layer using XPS, EDS and scanning electron microscopy (SEM).

However, a detrimental effect on wear was attributed to accelerated oxidation of lubricating oil in the presence of water [84]. In addition, hydrolysis of ZDDP in oils have been identified to lead to formation of alcohols, zinc phosphates, alkyl sulphides and possibly phosphoric acid that could affect ZDDP antiwear mechanism [59, 60, 63].

The other important factors that can affect antiwear functions of ZDDP tribofilm are; concentration [72], thickness of the tribofilm, purity and alkyl group of the ZDDP. The thickness of ZDDP tribofilms on rubbing ferrous surfaces can vary between 50 and 200 nm which consisted of zinc phosphate/polyphosphate materials [10]. In terms of alkyl group, antiwear films from secondary ZDDP gave better antiwear performance than tribofilms from primary ZDDP [72, 85].

At temperatures due to frictional flash heating, ZDDP antiwear films had been shown to give lower friction coefficient than at high temperatures [73, 81, 82]. However, as bulk oil temperature increases, literature studies indicated that boundary films formed by ZDDP gave increased friction coefficient [86, 87]. In addition, similar friction performance was observed on lubricating oils formulated with ZDDP at high temperatures [74, 86, 87].

Increased friction coefficient according to Kubo at al. [88] was attributed to the formation of thicker films using Electron Probe Microanalysis (EPMA) to study tribofilm chemistry. Some other literature studies had confirmed the increasing effect

of rising temperature on friction coefficient between 135 and 150ºC [21, 89]. This was attributed to the formation of higher amount of phosphorus and zinc than at temperatures below 100ºC [21].

However, the effect of humidity on friction coefficient response of ZDDP tribofilm was observed to give a reduction of 30 % [83]. This was attributed to surface film formation [90]. On the other hand, a reduction in antiwear performance of ZDDP-derived boundary films occurred in water-rich environments, which makes it less suitable for use in surroundings that is prone to water contamination.

2.2.4 Antiwear mechanism of ZDDP tribofilm

ZDDP tribofilms are known to form on wear tracks of sliding steel surfaces. The formation could depend on test temperature and type of contact (sliding, rolling or both); where the rate of film formation increases with temperature rise [91, 92]. A comparison of ZDDP tribofilm to its thermal films was identified to be identical in chemical composition, but have different mechanical properties [47, 93].

Chemical analysis of ZDDP tribofilms multi-surface analysis techniques indicated that its outer section consists of zinc phosphate with graded glassy phosphate that could either be pyro- or ortho- phosphate [94-96]. A summary of the results are presented in Figure 2-4

An observation of ZDDP tribofilms by Aktary et al. [97] indicated that long chain polyphosphate island was surrounded by underlying short chain polyphosphate. The raised white pad and dark patches in the works of Morina et al. [98] and Ye et al. [99] were respectively described as long chain polyphosphate and short chain polyphosphate. This was also confirmed by Nicolls et al. [64, 100].
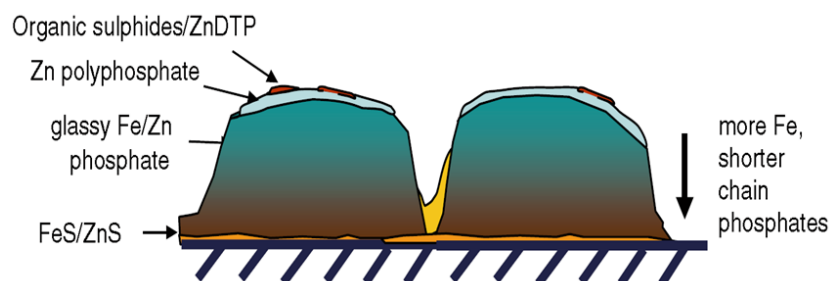
Figure 2-4 Schematic diagram of ZDDP pad-like structure and composition **[49]**

Analysis of elemental species on ZDDP tribofilm suggests the outer section of the pads is mainly composed of Zn cations and inner section closest to the ferrous substrate as rich in iron (Fe). In addition, the presence of sulphur could be in form of zinc or iron sulphide on the metal surface below these pads.

However, Martin et al. [101] disputed these claims by suggesting a two-layer structure of ZDDP tribofilm using AES, XPS and XANES analysis [101] is as shown in Figure 2-5. These layers are thought to consist of long-chain polyphosphate overlaying a mixed transition metal short chain phosphate which was supported by using the Hard Soft Acid Base (HSAB) principle. In view of different intrinsic and extrinsic factors affecting ZDDP formation during boundary lubrication, literature studies considered only three basic model of ZDDP tribofilm antiwear mechanism; formation of a mechanically protective film, removal of corrosive peroxides or peroxy-radicals and digestion of abrasive iron oxide particles using HSAB principle. The third model of ZDDP tribofilms antiwear mechanism involves acid-base reaction between phosphates and iron oxides.
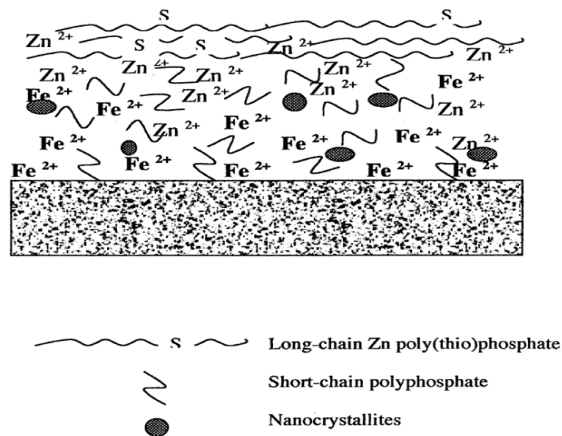
Figure 2-5 Two layer schematic representation of ZDDP tribofilm **[101]**

The mechanically protective model of ZDDP tribofilms suggests the film as acting like a barrier to prevent direct contact and adhesion between metal or metal oxide surfaces [102]. This type of model suggests that once ZDDP tribofilm is formed, all the wear that occurs afterwards is due to ZDDP itself. This is based on the assumptions that ZDDP tribofilm are only slowly worn away, and material loss from the ferrous

substrate is mainly due to iron oxide which reacted with the phosphate films [91, 103]; even when the oil containing ZDDP is replaced with base oil.

The effectiveness of such protective film was dependent on higher film formation rate than film removal rate [104]. Another suggestion on physical attributes of ZDDP antiwear films as acting like a protective barrier between the rubbing surfaces through the formation of softer tribofilm than the substrate [105]. In this way, reduction in the number of contacting asperities is thought to exceed its shakedown limits [105] such that any increment of plastic deformation is due to successive load cycles.

In the acid-base reaction model of ZDDP antiwear mechanism, pad-like ZDDP tribofilm was identified to consist of long chain zinc poly (thio) phosphate at the top. On the other hand, major parts of the pad consists of mixed short chain iron/zinc polyphosphate and metal sulphides as shown in Figure 2-4. In this model, Fe^{3+} was considered as a harder Lewis acid than Zn^{2+} and that cation exchange process between iron oxide (Fe_2O_3) and zinc oxide (ZnO) is energetically more favoured [48]. This was based on Pearson (HSAB) principle [106]. Since most iron oxides and Fe_2O_3 are much harder than zinc oxide, the zinc polyphosphate polymer glass is able to digest the native iron oxide and the abrasive iron oxide particles to reduce wear as shown in Equation 2- 3 [101].

$$5Zn\,(PO_3)_2 \quad + \quad Fe_2O_3 \quad \rightarrow \quad Fe_2Zn_3P_{10}O_{31} \quad + \quad 2ZnO \qquad \text{Equation 2- 3}$$

2.2.5 Physical properties of ZDDP tribofilms

In a study of Warren et al. [107], ZDDP tribofilm was described as anisotropic in topology and later suggested to consists of ridges and trough using AFM and Interfacial Force Microscopy (IFM) [107]. Indentation modulus and shear strength of the ridges was estimated as 81.0 GPa and 2.0 -3.0 GPa respectively. On the other hand, indentation modulus of the trough on ZDDP tribofilms was estimated as 25 GPa [107]. Nanoindentation and IFM techniques was also used by Graham et al. [108], to study ZDDP tribofilms heterogeneity which revealed higher modulus for the central part of large pads as 209 ± 38 GPa to provide significant resistant to plastic flow. This is unlike the edges (87 ± 23 GPa).

In order to understand the mechanical behaviour of tribofilms formed by ZDDP at different sliding distance, Aktary et al. [97] determined the hardness and modulus of

elasticity of ZDDP tribofilm at different test durations using nanoindentation technique. The modulus of elasticity and hardness of ZDDP antiwear films was found to be around 93 GPa and 6 GPa respectively. They described ZDDP tribofilms as soft materials similar to soft sacrificial coatings deposited on hard substrate [97, 109]. However, Bec et al. [110] used nanoindentation, Surface Force Apparatus (SFA) and nanomachining techniques as shown in Figure 2-6 studied the mechanical properties of 'soft mechanically washed' and 'solvent washed' ZDDP tribofilms.
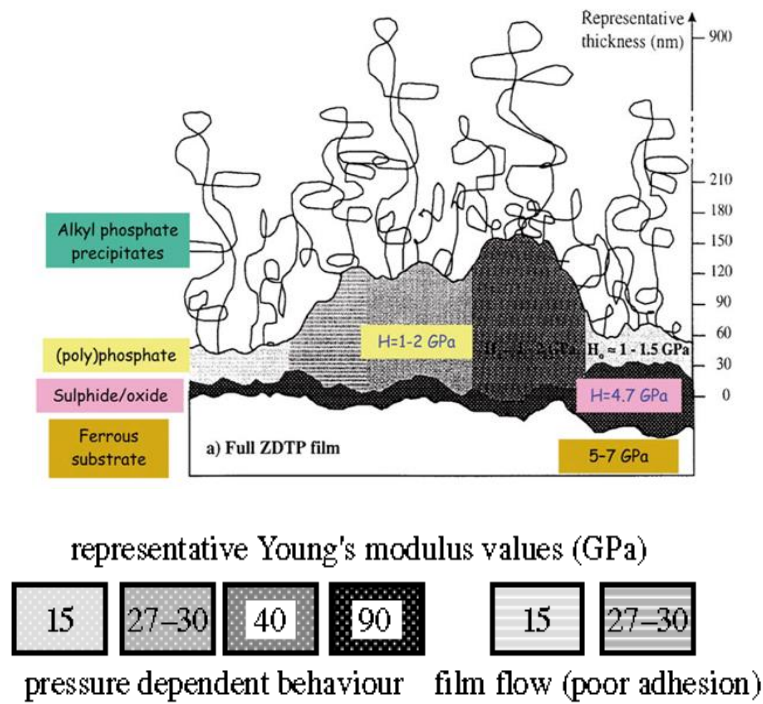
Figure 2-6 Schematic representation of the structure and mechanical properties of different layers of ZDDP tribofilm **[105, 110]**

Results from the study, indicated that ZDDP tribofilm is heterogeneous and composed of two distinct layers. The top layer was noted to consist of soft polymeric film that is characteristic of polyphosphates layer and the inner layer consist of harder sulphide/oxide with estimated thickness of about 150 nm. In addition, exceptional antiwear resistance properties of ZDDP layered film was observed to have unique properties of adaptation to a wide range of imposed conditions. This possibility earned ZDDP antiwear films description as 'SMART' material by providing appropriate level of resistance response imposed by a wide range of conditions on the rubbing

metal surfaces, such as applied load and contact geometry [105]. By using the AFM to investigate ZDDP tribofilm morphology, separate patches of films initially formed on rubbing steel surfaces developed gradually to form continuous pad-like structure that was separated by deep valleys [97, 99, 111]. However, another study described tribofilm formed by ZDDP containing oils as a combination of white patches and dark stripes formed along the sliding directions [98, 99]. Figure 2-7 illustrated the structure and chemical composition of ZDDP pad-like tribofilm in a scale of 1/100th of the vertical height [49].
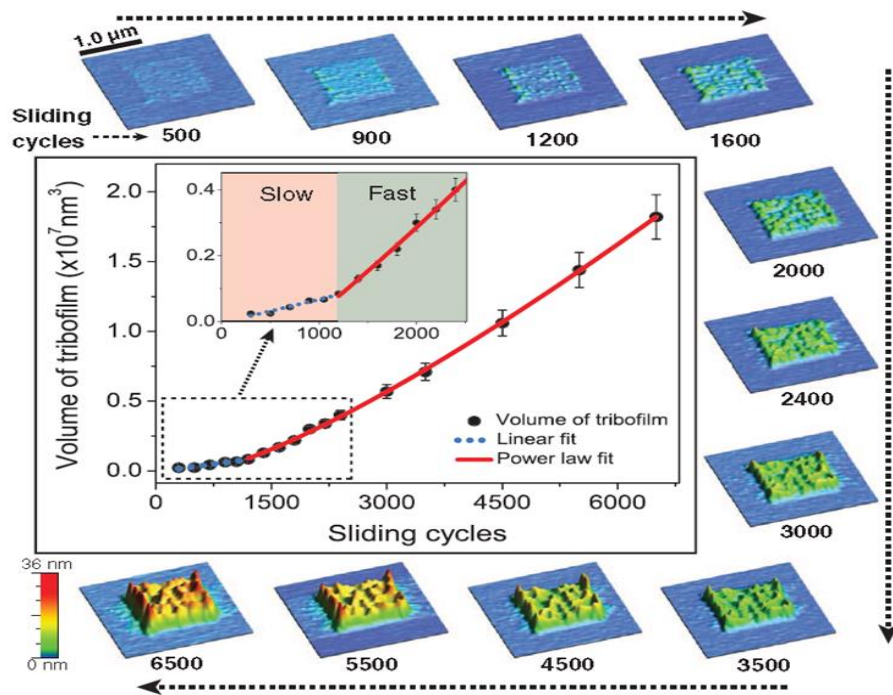
Figure 2-7 Effect of sliding frequency on growth of ZDDP tribofilms **[78]**

The exponential growth rate of ZDDP antiwear films as shown in Figure 2-7 was observed to be due to applied compressive stress and temperature using AFM technique on a single asperity sliding nano-contact [78]. This was attributed to surface-based nucleation growth and thickness saturation of patchy tribofilms as shown in Figure 2-7. However, durability of ZDDP tribofilms in terms of wear-resistance at high temperature under boundary lubrication condition is yet to be investigated. Hence, a study to investigate durability of boundary films containing ZDDP and borate additives is necessary not only in terms of friction coefficient reduction, but also in terms of antiwear performance at different temperature.

29

2.2.6 Additive effect on emission control system of IC engines

Uncontrolled environmental pollution from internal combustion engines arises primarily due to; exhaust emissions, crankcase venting and evaporation of fuel from vehicle storage tank. However, considerable influence of lubricant compositions on exhaust and crankcase emission had been identified, while emissions from fuel evaporation is governed by fuel composition [112].

Exhaust gases from internal combustion engines contain three primary pollutants: unburned or partially burned hydrocarbons (UHCs), Carbon monoxide (CO), and Nitrogen oxides (NO_x), in addition to other compounds such as water, oxygen and oxides of sulphur, among other substances released into the atmosphere [113].

Many countries of the world are enacting various legislations to limit emissions from automotive sources. One of such legislation is the use of low sulphur and unleaded fuel to limit emission. The limitations imposed on phosphorus and sulphur usage in lubricant composition was due to their poisoning and deactivating effect on exhaust catalytic converter of IC engines.

This was attributed to oxides of sulphur and phosphorus [10, 92]. In order to minimize these emissions, catalytic converters have been developed to simultaneously oxidize and reduce pollutants [14, 114]. A study by Rokosz et al. [115] had attributed oil-derived contamination on light-off catalyst from high mileage taxis to two forms of phosphorus contamination. These are; (i) an over layer of Zn, Ca and Mg phosphates, and (ii) aluminium phosphate within the wash coat [115]. A study of the effect of boron-containing additive on three way catalytic (TWC) exhaust catalytic converter in comparison to ZDDP by Twigg et al. [14] revealed that boron additives in lubricating oils gave;

- Lower CO emission compared to oils containing ZDDP

- Comparable hydrocarbon and NO_x reduction to ZDDP containing oils

- Minimal boron losses from the oils in the crankcase compared to constant losses of phosphorus from oils containing ZDDP

- Little difference in engine performance in terms of wear and build of solid carbon deposits on piston grooves (piston cleanliness)

30

In view of the advantage of boron-containing lubricating oil over ZDDP in terms of its effect on catalytic converter and particulate filter of IC engines, that a study of a potential replacement is necessary. Hence, the tribochemistry of boron-containing lubricant additives as an alternative antiwear additive to ZDDP is necessary in other to elucidate its limitations as a potential substitute.

2.3 Boron compounds as lubricant additives

A promising material for development as antiwear lubricant additives in automotive and industrial lubrication system is a wide range of boron compounds that present beneficial tribological properties. These properties are; self-lubrication, antiwear efficiency, good film strength and high temperature resistance. The study of borate esters as an effective antiwear lubricant additives was thought to have started in early 1960s [116]. Boron-containing engine oils had been noted to form boron compounds like; boron oxides, boric acid, and boron nitride on its tribofilms. These are known to enhance the tribological properties of contacting surfaces [11]. Most boron-containing engine oils are known to have features like; antioxidant characteristics, low toxicity, pleasant odour and non-volatility. In nature, boron occurs as borates due to its great affinity for oxygen. Further studies by Kreuz et al. [117], characterized tribofilms from tribenzyl borate in solvent neutral on ferrous tribological system as a physical mixture of iron oxide-boric oxide and an organic phase. A drawback for borates as additives in lubricant oil formulation is its susceptibility to hydrolysis due to the electron deficient boron (B) [118, 119].

2.3.1 Effect of hydrolysis on borate ester as lubricant additives

In view of the electron-deficient boron atoms, various schemes have been adopted in overcoming the negative effect of hydrolysis on borates as additives in lubricating oils over the years. The hydrolysis reaction of borate esters is shown in Figure 2-8.
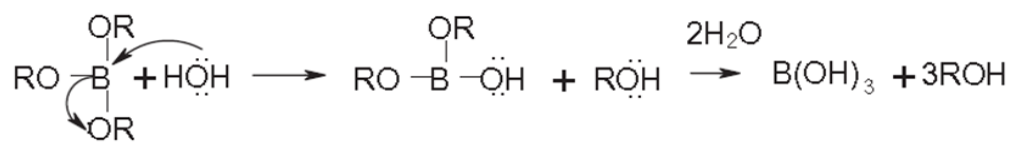
Figure 2-8 Hydrolysis equation for borate ester **[10]**

The improvement of hydrolytic stability of borates as lubricant additives is possible by using various methods. Some of these methods are as listed below;

- Use of hindered phenol to inhibit attack on boron-oxygen bonds [120]

- Inter molecular-coordination bonding of nitrogen to boron by reacting boric acid with amine groups to form a stable five-member ring structure [121, 122]

- Intra molecular-coordination of nitrogen to boron by reacting boric acid and Schiff base in order to introduce an imido group to form a stable six-member ring structure [119]

- Nano-particle dispersion of inorganic metal borate salts [123-129].

Among the several means of assessing hydrolytic stability of synthetic borates as additives in lubricating oils, the most common method is high onset decomposition temperatures in air and nitrogen atmospheres using Thermo-gravimetric analyser (TGA). Some borate additives with onset decomposition temperature around 300°C and 176°C are considered to have good and poor thermo-oxidative stability respectively [130-132]. Other means of assessing resistance to hydrolysis of lubricating oils used in internal combustion engines are copper corrosion resistance in terms of changes in copper colour appearance and physicochemical properties of aged oil [133-137]. Some other means of avoiding hydrolytic effect of water on boron is the use of hard boron-permeated layer. These could be; boron carbide [138], vanadium boride [139], titanium boride [140], iron boride [141-144], boride ceramic [145].The other forms of boron-permeated layers are; zirconium boride/boron carbide composites [145, 146], hexagonal boron nitride (h-BN) as additives [147] and BN composites [148-150], boron-doped diamond-like carbon (DLC) [151].

2.3.2 Tribological tests with boron-containing additives

Literature review in the following sections will refer to tests with organoboron and metal borates as lubricant additives for use in IC engines. The focus of this review will be on tribological tests using steel-steel point contacts and lubricants which contains organoboron or nanoparticle metal borates in base oil; unless otherwise stated. Examples of tribological behaviour of some tribofilms formed by oils

containing borate additives in terms of additive concentration are respectively shown in Figure 2-9 (a) and (b) and Figure 2-10 (a) and (b)
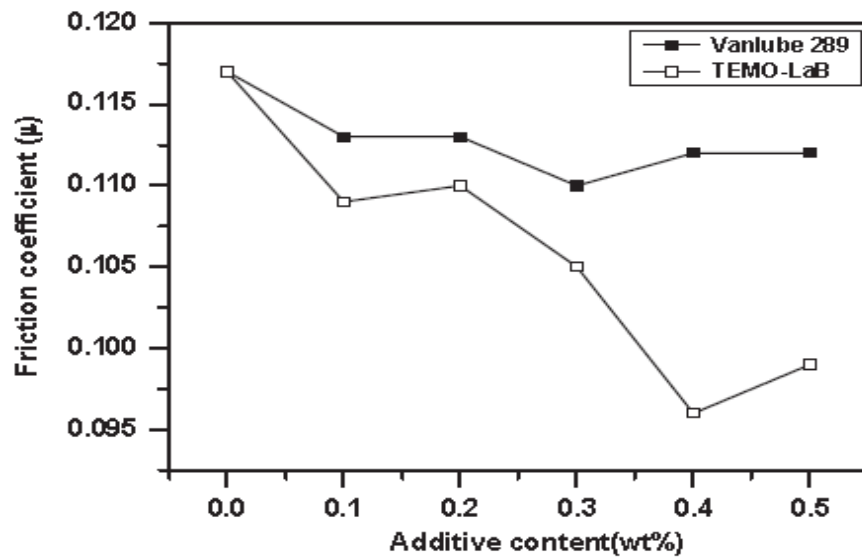
(a)
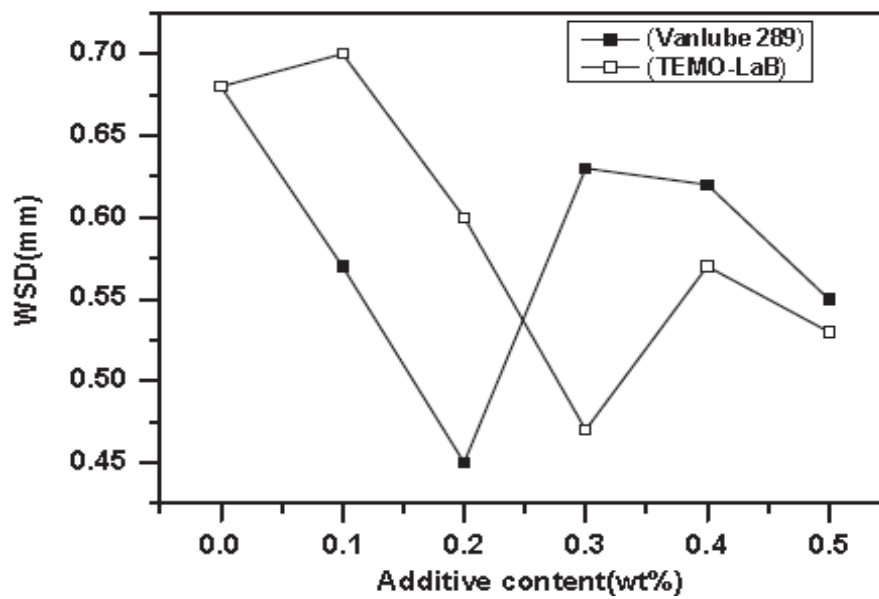
(b)

Figure 2-9 Typical tribological behaviour of oils containing organoboron additives [152]; (a) friction coefficient performance, (b) antiwear performance
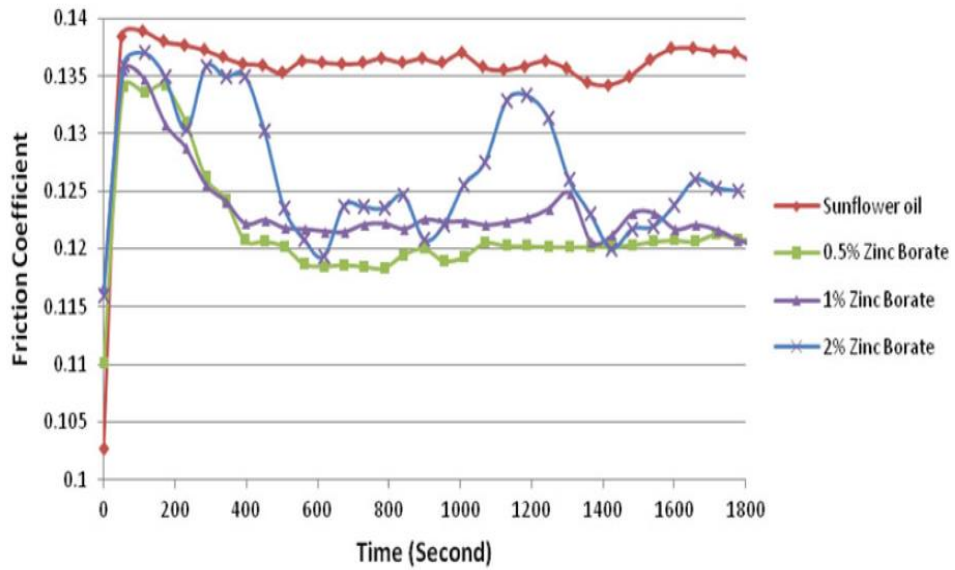
(a)
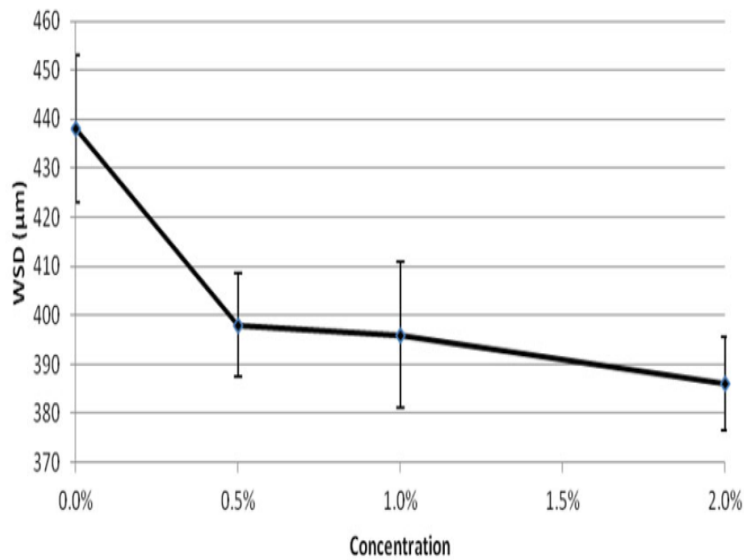
(b)

Figure 2-10 Typical tribological behaviour of oils containing zinc borate ultrafine powder; (a) friction coefficient, and (b) antiwear performance **[153]**

The friction coefficient behaviour of borate additives was attributed to boric acid (H_3BO_3) at the tribocontact which was formed when boron oxide in oils containing boron additives reacts spontaneously with moisture in open air. This is possible due to the negative standard Gibbs free energy of reaction of boric oxide (B_2O_3) [154] with the reaction shown in Equation 2- 4.

$$1/2 \; B_2O_{3(s)} + 3/2 \; H_2O_{(g)} \rightarrow H_3BO_{3(s)}, \Delta_r G_{298} = \text{-28.84 kJmol}^{-1} \qquad \text{Equation 2- 4}$$
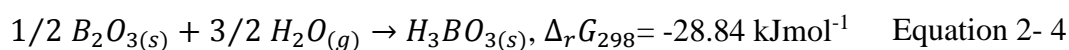
On the other hand, antiwear performance of borate tribofilms was attributed to boron oxide, described as glass network-former such as; As_2O_3, P_2O_5 and GeO_2 [155]. These glass network-former are noted to fuse with metal cations to form inorganic crosslinked polymers glasses. Glass network formers are known to melt without decomposition [80, 155]. However, observations from the literature have shown that friction and wear performance of boron-based lubricants is influenced by intrinsic and extrinsic test conditions. Hence, the effects of various test conditions on tribological performance of boundary films containing boron are reviewed in the following sub-sections.

2.3.3 Effect of concentration on borate tribofilms

The effect of increased additive concentration under frictional flash temperature on tribofilms from organoborate-based oils indicates a reducing friction coefficient response by Hao et al. [152], as shown in Figure 2-9 (a). Another study involving organoborate additives by Jincan et al. [156] has friction coefficient reduction from 0.1 to 0.075 at increased additive concentration up to 3 wt. %.

However, increased concentration of potassium borate nanoparticle at about 3.5 wt. % in the oil formed tribofilms that gave friction coefficient of about 0.037 [157]. Another study on tribofilms formed by zinc borate dispersions in sunflower base oil at low concentration gave better control of friction coefficient compared to low additive concentrations, as shown in Figure 2-10 (b).

The boric acid responsible for friction reduction on borate tribofilms are usually detected by XPS at 192.7 eV or as B-O at 192.6 eV [158]. The other method used to identify boric acid is Raman shifts at 498 and 879 cm^{-1} [159, 160]. It has also been observed that increased concentration of some borate additives as shown in Figure 2-9 and Figure 2-10 can provide increased antiwear performance. Enhanced antiwear performance by tribofilms from organoborate additives were attributed to the formation of wear-resistant boron oxide-iron oxide glass based on surface analysis by XPS technique [80, 158]. On the other hand, tribofilms from metal borate nanoparticle dispersion are known to provide wear-resistant due to shear effect and tribochemical reaction between boron oxide and metallic iron to form iron borides [125].

However, literature studies have suggested that some borate additives that are susceptible to hydrolysis could give poor antiwear performance due to oil insoluble abrasive boric acid [119, 158], and boron partially replaced by metallic iron in the iron oxide films [161]. In addition, boric acid is known to begin decomposition around 70-80°C [162, 163], but also can be volatile with steam [35, 162, 164]. Hence a study of the effect of concentration and hydrolysis at temperature range where boric acid is unstably is necessary in order to elucidate its effect on borate tribochemistry.

2.3.4 Influence of temperature on borate tribofilms

The antiwear performance of borate tribofilms is dependent on boron oxide; an oxide glass former [155]. Under the influence of frictional flash temperature, borate esters are known to mechanically degrade through C-O bond breaking [158]. However, thermal degradation at high temperature had been reported to occur in the alkyl group leading to CH_3 and BO_3 groups in B_2O_3 formation [165, 166].

The effect of temperature on friction behaviour of tribofilms formed by borate containing additives has mostly been studied when blended with ZDDP for use in gear oils and engine oils. In the study of metal borate dispersions in oils containing ZDDP, Kim et al. [81] showed that oil blends with high boron content have tribofilms with superior tribological performance at 100°C than at 32°C higher temperature.

This was attributed to reduction in metal-to-metal adhesion, material transfer and surface ploughing by wear debris using SEM, optical microscopy and surface profilometry. A similar study on gear oils containing boron and ZDDP at high temperature by Komvopoulos et al. [82] have tribofilms with slightly lower friction coefficient and higher wear resistance at elevated temperatures.

These were attributed to faster tribofilm formation. However, these two studies concluded without knowing the actual role played independently by ZDDP and boron. Another study by Varlot et al. [167] at 100°C using X-ray absorption near-edge spectroscopy (XANES) on borate micelles and primary-ZDDP in neutral base oil suggests antagonistic effect of borates on ZDDP antiwear functions. This behaviour was not only attributed to increase in proportion of trigonal boron anions (BO_3) and higher concentration of unreacted calcium borates at the core of the micelles.

On the other hand, a similar study on ZDDP interaction with borated dispersant at 100°C by Zhang et al. [168] indicated good synergy in terms of antiwear effectiveness. The study observed that borated dispersant facilitated decomposition of ZDDP and formation of phosphates on both tribofilms and thermal films. In addition, structural coordination of boron with three oxygen atoms (trigonal units) in the untreated oil changed partially to boron coordination with four oxygen atom (tetrahedral) on the tribofilms formed.

The effect of temperature on wear rate of different types of boron-containing antiwear agent (BSL) in various combinations of synthetic base fluid (PAO 10) and diester (A51) by Weimin et al. [131] between 20 and 110°C is shown in . The study indicated that tribofilms formed by borate additives in lubricating oils could provide effective antiwear performance at high temperature. The antiwear mechanism was attributed to complex chemisorption and tribofilms composition [131].
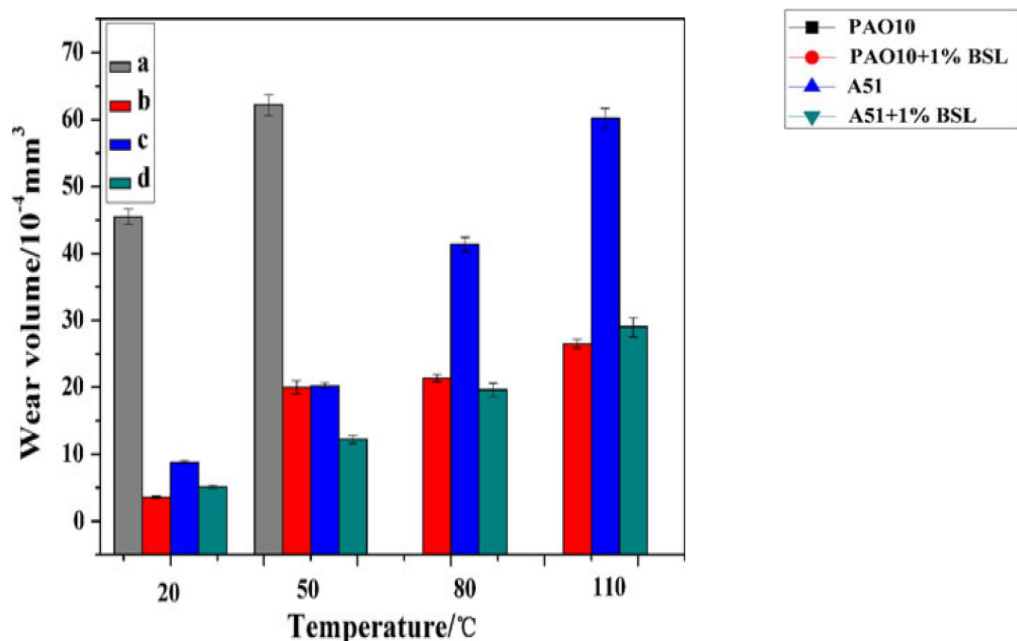
Figure 2-11 Effect of temperature on antiwear functions of borate tribofilms **[131]**

A study of the tribological performance of boron-containing tribofilms at 150°C compared to ZDDP at 100°C revealed that stable, but relatively thin antiwear film was formed that gave better control of friction than ZDDP [169]. Another study

37

investigated the effect of temperature on boric acid based additives in PAO by Elin Johnsson [170]. The study revealed that friction and wear produced by borate tribofilms formed are affected by temperature. Surface analysis of tribofilms formed using EDS and Secondary Ion Mass Spectroscopy (SIMS), revealed that oils containing boron additives hinders the formation of zinc-rich tribofilms.

Boron oxide glass is assumed to consist of a random three-dimensional network of planar BO_3 units with 120° between bond angle and a comparatively high fraction of six-membered boroxol rings [171-173] as shown in Figure 2-12 (a) and (b). The interaction of these structural units in boron oxide with metallic cation could lead to transformation of BO_3 units to BO_4 tetrahedral to form inorganic crosslinked polymer glasses [172, 174, 175]. However, the composition of these metal oxides within the glass structure has been shown to affect many of its physical properties [35, 176, 177] such as; viscosity, density, thermal expansion, hardness and heat content.

Boroxide groups (BO_3^{-3}) | BO_4 linked to BO_3 units

(a)   (b)
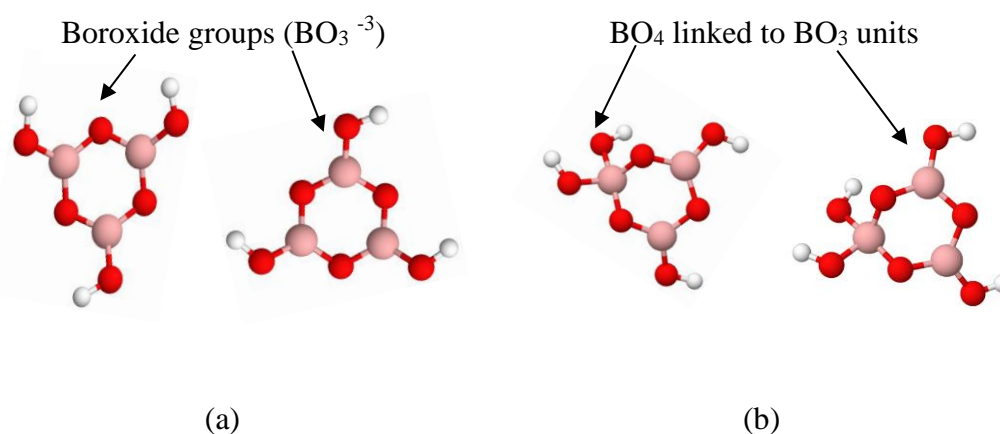
Figure 2-12 Structural units of B_2O_3; (a) Boroxide groups, (b) BO_3 linked to BO_4

A description of the interaction of structural units of B_2O_3 with metal cations are; (a) $B\emptyset_3$, (b) $M^+B\emptyset_2O$ (c) $M^+B\emptyset_4$ (where $\emptyset$ stands for bridging oxygen and O stands for non-bridging oxygen and M^+ is the added modifier cation) [174, 178]. In addition, the rigidity of borate structural units is known to increase with increasing $M^+B\emptyset_4$ and decreases with its lower amount as shown in Figure 2-13.
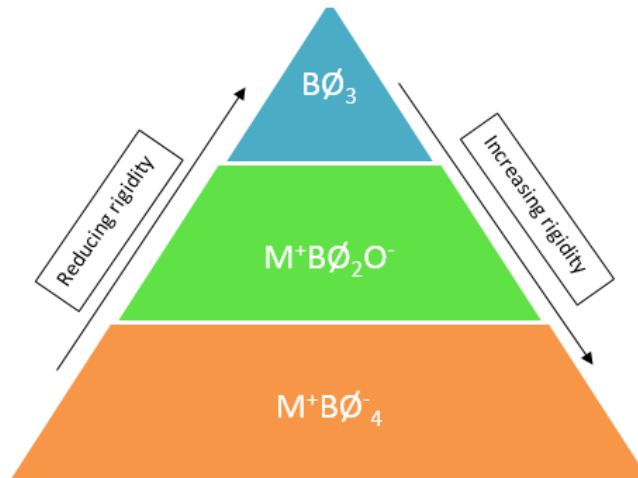
Figure 2-13 Rigidity of borate glass and boron anions **[174, 175, 179]**

The changes in BO_3/BO_4 speciation (N_4) in B_2O_3 was investigated using Raman spectroscopy [180, 181] and XANES [181, 182] spectroscopy methods. On the other hand, phosphate glass formed on ZDDP tribofilms at high temperatures have been shown to provide good wear-resistant. These are known to have glass transition temperature of about 200°C [48, 80]. On the other hand, borate glasses are known to have glass transition temperature around 260°C [79, 80, 183]. Hence, increased temperature could cause changes in the amount of metallic oxide on the glass network former (B_2O_3) and structural units of boron oxide to affect antiwear performance and durability of borate tribofilms.

2.3.5 Influence of water on borate tribofilms

The tribological behaviour of borate tribofilms in terms of friction and wear reduction had been related to moisture from the surrounding air. Boron oxide is known to react spontaneously with moisture in air to form boric acid. On the other hand, boric acid will also decompose to form water and boron oxide at certain temperature and contact pressure as shown in Equation 2- 4.

Most experiment on the effect of water on borate tribofilms have been made on boron permeated system. These are boric acid coated surfaces [24], boron carbide [184, 185]

and boride ceramic [145]. Tribological experiment on the influence of humidity on boron carbide gave reduced friction coefficient with increased dissolved water contamination [145, 184, 185]. The low frictional behaviour with humidity increase was attributed to boric acid formation using Auger Electron Spectroscopy (AES) and XPS [185]. The mechanism of humidity effect on friction coefficient reduction was investigated by Barthel et al. [186] using stainless steel ball against a reciprocating copper substrate coated with boric acid. Surface analysis of the borate tribofilms formed using; AES, Polarisation Modulation-Reflection Absorption Infra-red Spectroscopy (PM-RAIRS), and sum frequency generation (SFG) spectroscopy. The study found that boric acid itself experiences high friction coefficient and catastrophic wear in dry oxygen and nitrogen environment, but gives very low friction coefficient (0.06) in humid and acetone vapour surroundings as shown in Figure 2-14.
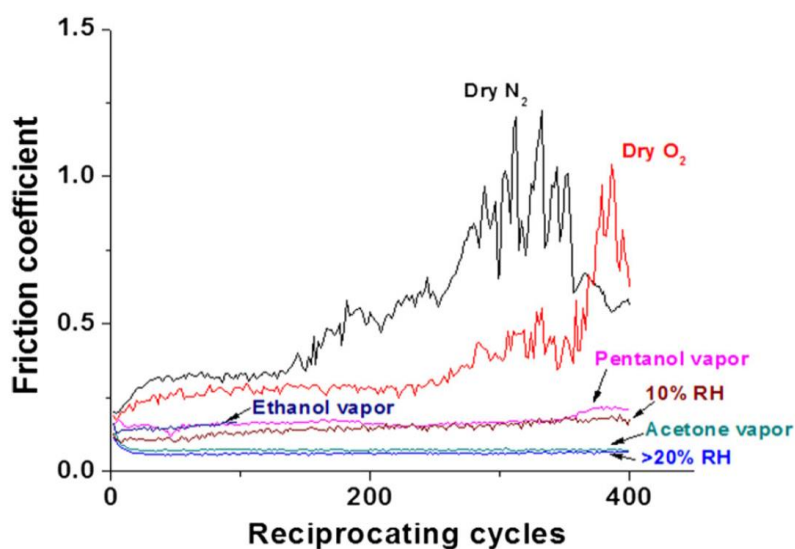
Figure 2-14 Effect of different vapour on friction coefficient of H_3BO_3 **[186]**

This behaviour was attributed to unlocked edge-site of boric acid by water vapour to promote easy shear of the lamellar along the basal plane direction [24, 186, 187]. The behaviour of boric acid in dry and humid environment on boron-rich coated systems similarly gave reduced friction coefficient with increased humidity. However, this behaviour could be affected on ferrous surfaces where some metallic oxides can be hard and less protective. Hence, the need to investigate how humidity affects friction coefficient performance of borate tribofilms formed by oils containing boron additives

on ferrous surfaces. The effect of humidity on wear-resistance borate tribofilms formed on boron carbide by Coung et al. [185] showed that wear rates decreased with rise in moisture content of the surroundings environment, irrespective of sliding distance as shown in Figure 2-15 (a).
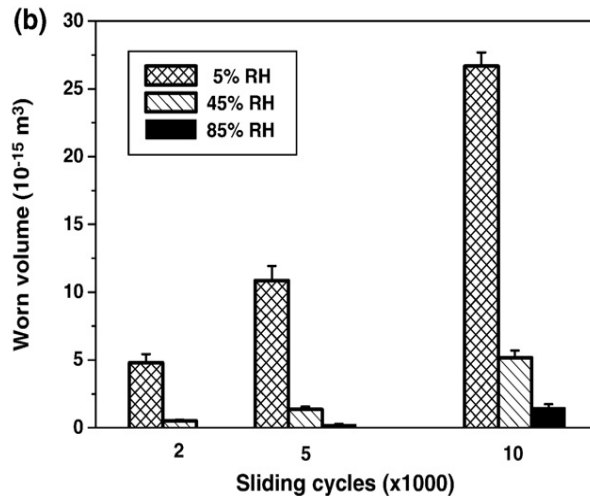
(a)
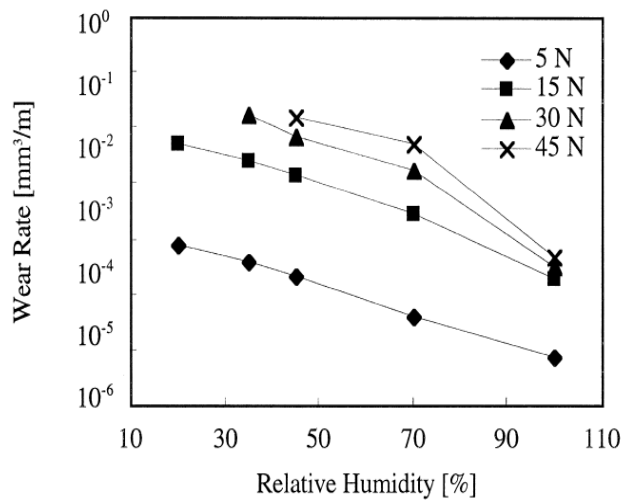
(b)

Figure 2-15 Humidity effect on wear rates reduction of tribofilms formed on borided surfaces due to; (a) sliding cycles **[185]** and (b) load **[184]**

This was attributed to mechanical abrasion at low humidity, but a combination of both mechanical abrasion and complicated chemical wear process at high humidity

41

conditions using XPS and AES. Another study on the influence of humidity on tribofilms formed on boron carbide indicated that wear rate decreases with increasing humidity; irrespective of the applied load [184]. SEM and X-ray diffraction analysis of the tribofilms formed, indicated that humidity effect caused tribochemical surface polishing containing boron oxide and boric acid [184]. The effect of humidity on tribological behaviour of borate tribofilms formed on boron-coated systems suggests a positive synergy with water. Hence the need to study the effect of humidity on wear-resistant potentials of tribofilms formed on ferrous surfaces by oils containing borates.

2.4 Properties of borate tribofilms

In this section, a literature review of the physical and chemical nature of tribofilms from boron containing oils on ferrous surfaces will be undertaken. This is to provide a better understanding of thickness, morphology and mechanical properties of both thermal and tribofilms and associated chemistry of the reacted layers.

2.4.1 Physical properties of borate tribofilms

In the tribological study of tribenzyl borate on steel surface by Kreuz et al. [117], the physical appearance of borate tribofilms was described as dull silvery grey, and dark-colour by another study on zinc borate ultra-fine powder [153]. AFM morphologies and microhardness properties of the dark coloured tribofilms as shown in Figure 2-16 was estimated to have film thickness between 230-360 nm [153].

However, tribofilms containing boron formed at $100^{\circ}C$ have thickness estimated within 100 and 200 nm range using mini traction machine with spacer layer image mapping (MTM-SLIM) technique [10, 80]. This was shown to be in good agreement with earlier estimate by Kreuz et al. [117]. However, the thickness of ZDDP tribofilms has been evaluated using Focused Ion Beam/ SEM technique [188, 189], but has not been used for borate tribofilm thickness investigation. This could offer a better understanding of the heterogeneous nature of borate tribofilms as observed by Kreuz et al. [117]. An early investigation into the mechanical properties of worn surfaces formed by tribenzyl borate on steel substrate using Knoop hardness test [117], suggests higher hardness than new specimens.
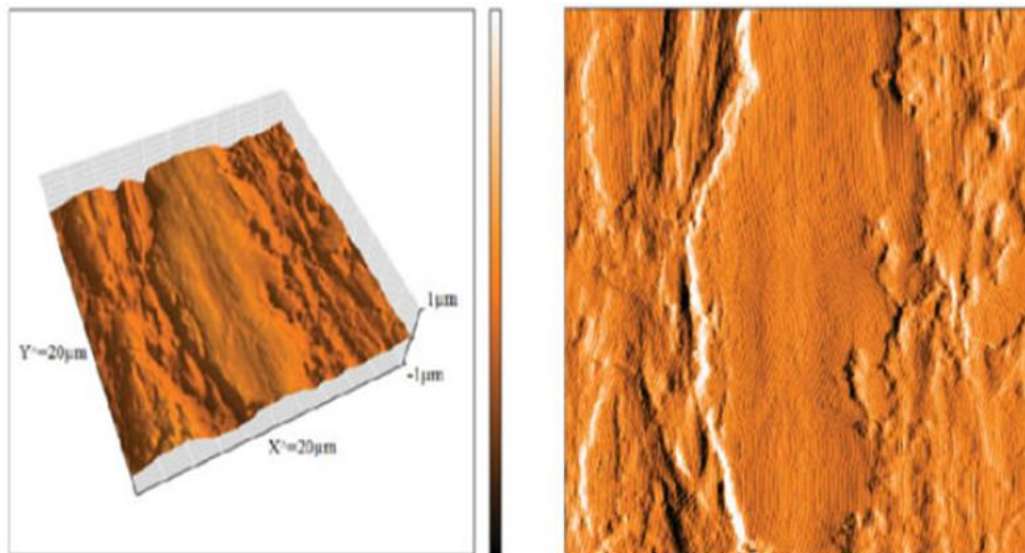
Figure 2-16 AFM images of zinc borate tribofilms formed at 2 wt. % **[153]**

This position was contradicted by lower tribofilm hardness than the ferrous substrate formed by zinc borate ultrafine powder using micro-indentation in the study of Zhao et al. [153]. The study indicated that worn sample surfaces gave hardness between 5.7 and 9.3 GPa compared to 11.5 GPa for the steel substrate. Hence, a study to undertake nanoindentation of worn surfaces lubricated by boron-containing oils; organic and inorganic borates. This is to provide a better understanding of their morphology and mechanical properties.

2.4.2 Chemical composition of borate tribofilms

Chemical characterization of tribofilms from oils containing organic-borates with XPS revealed different types and composition of boron compound and bonds as shown in Figure 2-17 (a) and (b). XPS surface analytical technique was used to identify boron oxide on tribofilms formed by oils containing boron on ferrous surfaces [152, 158]. In addition, the fusion of boron oxide with iron oxide was also identified by XPS analysis [156, 190]. However, most XPS position peaks of B 1s at 192.6 eV, attributed this to either boron oxide and boric acid [158]. The XPS position peaks indicating the interactions of boron-oxygen bond with carbon (C-O-B) and iron (Fe-O-B) are respectively around 532.7 eV [158, 191] and 531.6 eV corresponding to B 1s peaks of 189.7 eV [192, 193].

	Bonding	Binding energy (eV), ± 0.2 eV		Compound	Binding energy (eV)
C1s	Carbide	283.3		B_2O_3	193.1
	C–C/C–H	284.8		$B(OH)_3$	193.0
	C–O	285.9		$B(OH)_3$	192.7
	ads. TMB	287.2		$B(OCH_2CH_2SH)_3$	192.4
	Carbonate	289.5		$B(OCH_2CH_2SC_6H_{13})_3$	191.2
O1s	Oxide	530.0		$B(OC_{12}H_{25})_3$	191.2
	Fe–O–B	531.6		BN	189.7
	C–O–B (TMB)	532.6		Fe_2B	188.4
Fe2P$_{3/2}$	Fe (0)	706.9		FeB	187.9
	Fe oxides	709.1/710.7		$B_{10}H_{14}$	187.6
B1s	B–O (TMB)	192.0		B (powder)	186.7
	B–O (boron oxide/boric acid)	192.6			

(a) (b)

Figure 2-17 XPS characterization of borate tribofilms; (a) peak position of trimethyl borate **[158]** and (b) binding energy of boron compounds **[194, 195]**

The XPS position peaks of iron oxides and iron oxyhydroxide are respectively identified by [196, 197] and [198]. In addition, the stable oxide of potassium identified was potassium dioxide (KO_2) [199, 200].

Hence, the possibility of boron oxide fusing with metallic oxides could be used to describe the wear-resistant behaviour at different tribological test conditions. In order to understand detailed structure of boron compounds within the boundary films, XPS depth profile analysis can also provide information on the intensity of the peak of B 1s as sputtering time increases. Previous studies on XPS depth profile analysis of borate tribofilms had estimated boron permeation of the tribofilms to be between 7.5 nm to 200 nm [80, 169, 193, 201].

This could be due to the small atomic radius of boron [202, 203] and the type of borate oil (organoborate or metal borate). XPS analysis of borate tribofilms clearly provides information on boron oxide, but could not distinguish boron oxide from boric acid at 192.6 eV. However, XPS signal of B 1s peaks are sometimes noisy when there is low atomic concentration of boron compared to Fe 2p peaks [125, 190]. This could make quantitative assessment of boron compounds responsible for friction and wear

reduction difficult using only XPS technique. Raman spectroscopy has been used to study some boron compounds with few of such results shown in Figure 2-18.
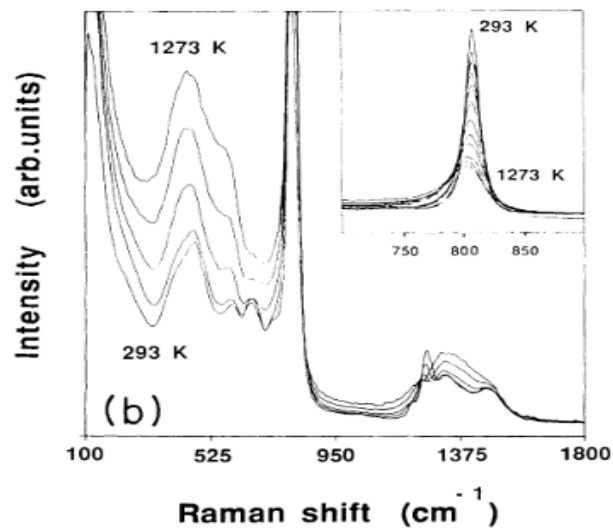
(a)
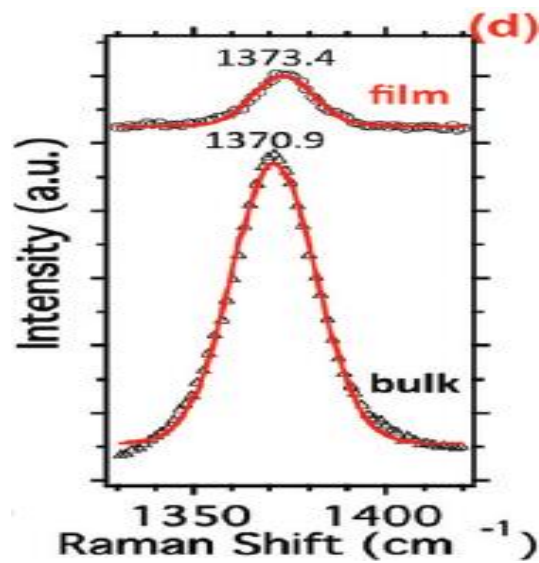
(b)

Figure 2-18 Raman of boron compounds; (a) boron oxide **[204]** and (b) h-BN **[205]**

The boron compounds that are Raman sensitive are; boron nitride (BN) [205, 206], boric acid [139, 160, 207] and B_2O_3 [171, 208-210]. In addition, Raman spectroscopy was used to study the effect of borates on the physical properties of glasses when it interacts with metallic oxides in many literatures as shown in Figure 2-19.
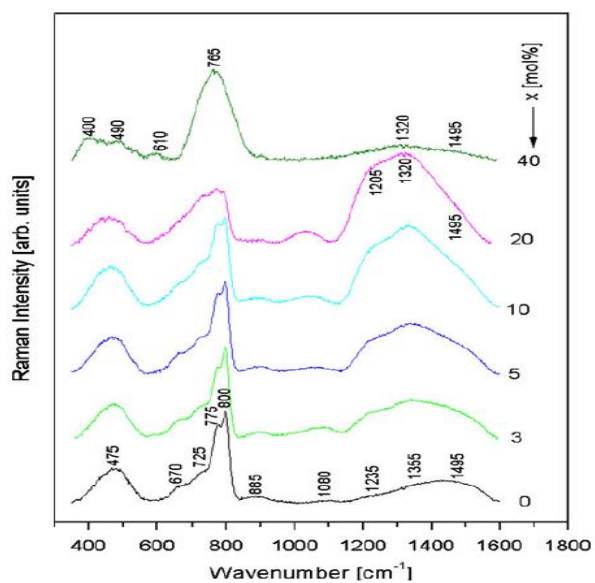
(a)
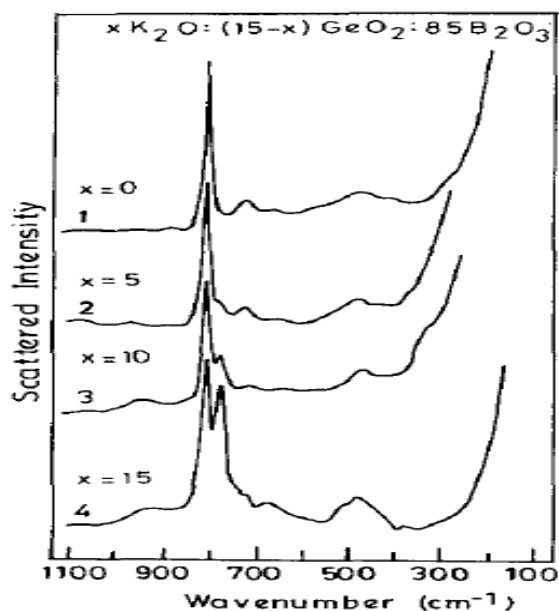
(b)

Figure 2-19 Raman spectra of; (a) iron borate **[211]** and (b) potassium borate **[208]**

Another important use of Raman techniques on borate tribofilms is in identifying changes in structural units of boron oxide [181, 208, 211-213], unlike XPS which cannot distinguish changes in structural units of boron oxide.

Raman spectroscopy technique is widely used in the borosilicate glass industries for bulk alkali-borate glass manufacture [178, 214]. In addition, changes in iron oxides and oxyhydroxide on steel surfaces [215-217] and thin film characterization [218] can also be studied using Raman spectroscopy. On borate tribofilms, Raman spectroscopy had been used to identify many boron compounds on boron permeated layer. These are; boron carbide [159, 219] and vanadium boride surfaces [139]. Hence, this study will investigate changes in the structural units of boron oxide at different temperature, changes on borate tribofilms formed at different additive concentrations and water contamination using Raman spectroscopy. This is to elucidate on how: changes in additives concentrations, high bulk oil temperature effects on structural units of boron oxide, and water contamination effects. These are to elucidate on how changes in extrinsic factors influence the antiwear performance and durability of borate tribofilms formed by oils containing borate additives.

2.5 Tribological mechanisms of borate tribofilms

2.5.1 Mechanisms of low friction of borate tribofilms

The boron containing additives are known as borate esters. These are defined as any compound that contains or supplies boron oxide, or a compound that contains the radical B_2O_3 [16]. The boron oxide in borate ester additives in oils could easily react with moisture in the surrounding air to form boric acid. This is attributed to the negative standard Gibbs free energy of reaction ($\Delta_r G_{298}$ = - 28.84 kJ mol^{-1} [154].

The friction reducing mechanism of borate tribofilms have been attributed to weak van der Waals forces between lamellar sheets of boric acid (H_3BO_3) [220-223]. This was shown to have a low shear strength that is similar to MoS_2 [27, 159, 222]. A description of this processes are summarized by this study in Figure 2-20. Another experiment by Barthel et al. [24] using; Auger Electron Spectroscopy (AES), Polarisation Modulation-Reflection Absorption Infra-red Spectroscopy (PM-RAIRS), and Sum Frequency Generation (SFG) Spectroscopy proposed a new understanding of the friction reducing mechanism of boric acid. This was based on edge-passivation or edge-unlocking mechanism [24] as shown in Figure 2-21, unlike the weak van der Waal mechanism that was earlier proposed [220-223] as shown in Figure 2-21.
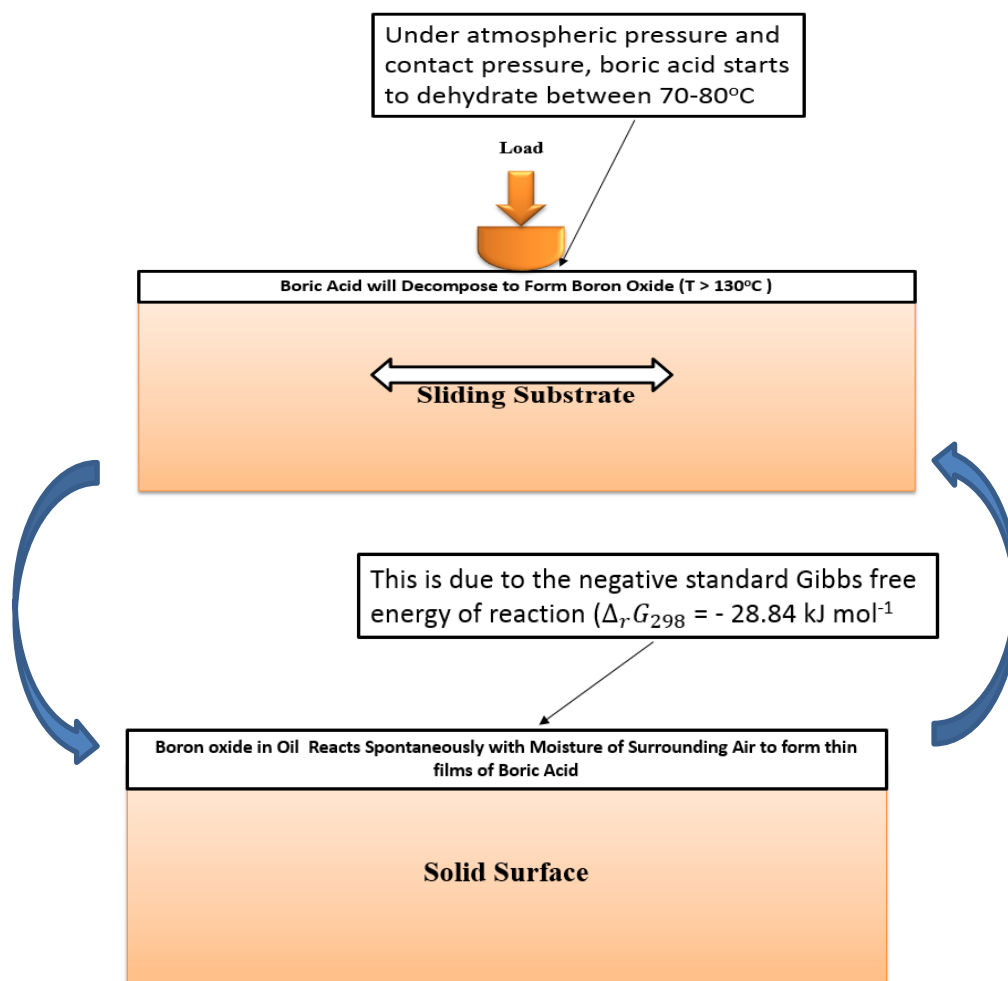
Figure 2-20 An illustration of boric acid weak van der Waal's friction reducing mechanism and formation from boric acid by this study

In the edge-passivation mechanism, vibrational spectroscopy indicates that vapours adsorbs onto the edge site of lamellar rather than on the basal plane of boric acid crystals [24]. The experiment of Barthel et al. [24] resulted into two major observations. Firstly, obtaining ultra-low friction by adsorption of water vapour was shown to be an equilibrium process rather than a kinetic process. Secondly, disturbance of the high energy edge site by physisorbed water molecules is needed for lamellar to shear along the basal plane direction. The study suggested that in dry air, hydrogen bonding interactions between adjacent lamellar exists due hydroxyl groups terminating the edge sites of boric acid. Water vapour presence due to adsorption at the edge sites weakens the hydrogen-bond interactions with water molecules in the basal planes [24], as shown in Figure 2-21.
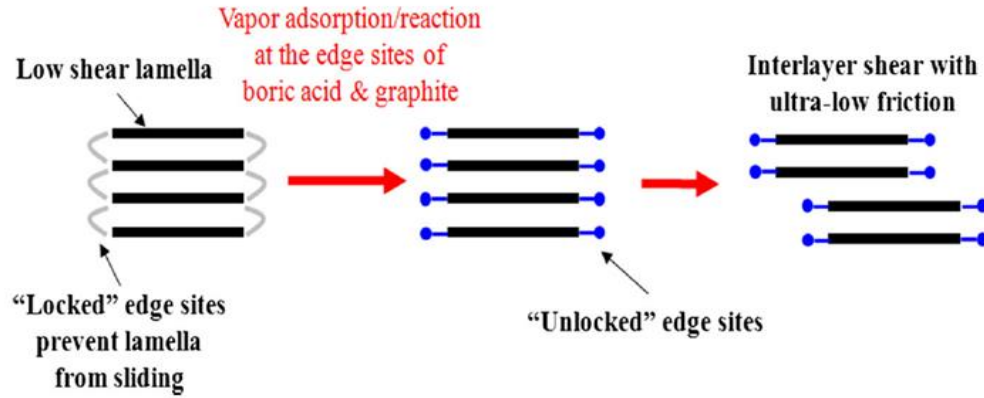
Figure 2-21 Edge-unlocking mechanism for ultra-low friction in lamellar solid lubricants [24]

However, these two mechanisms assumed that sheet-like crystals of boric acid is stable at all temperatures and will decompose to form boron oxide directly. In addition, the two mechanisms suggests that if more boric acid is formed during the friction process could better friction coefficient reduction is possible. These assumed that no intermediate boron compounds could be formed that could significantly affect tribological performance. The thermal decomposition of boric acid has been shown to occur between 70-80°C [163, 224]. In addition, boric acid is known to be volatile with steam [35]. Hence, it is necessary to study the effects of temperature on the friction reducing and antiwear mechanisms of borate additives. This is to elucidate on how the instability of boric acid due to thermal and tribo-oxidative process could affect tribological performance of borate tribofilms.

2.5.2 Antiwear mechanisms of borate tribofilms on steel

In the literature, there are about four different types of antiwear mechanisms for borate tribofilms. These are due to various types of borate additives used in lubricant formulations; some are organoboron compositions and others are metal borate dispersions. The earliest known study of borate tribofilms was by Kreuz et al. [117], which described tribofilms formed by boron additives as consisting of iron oxide-boron oxide and that boron is incapable of oxidative attack on metallic iron. However, the tribological action mechanism of potassium triborate dispersion on a steel substrate was described in the works of Morizur and Teysset [201] as adhesive

film formation on a mechanically-abraded surface. The study described boundary film formed by potassium borate dispersions as consisting of some elements in the organic phase, and others in oxidized state during film formation.

On the other hand, lubricating effectiveness of organoborate ester composition was attributed to the ability of boron to act as electron carrier due to its vacant p-orbital in the study of Guangbin et al. [198]. The study suggests that during the friction process, boron atoms can capture electrons of d- or f- orbital and free electrons on metallic sliding surfaces. These forms a negatively charged B species and positively charged metallic species. The strong attraction between borate ester and metallic sliding surface facilitates the formation of dense adsorbed films [198, 225] to prevent direct contact of the rubbing surfaces to greatly reduce wear.

Another study of nanoparticle dispersions of lanthanum, zinc and titanium borate by Hu et al. [124, 125, 226] used a four-ball tribometer to generate borate tribofilms. Surface characterization using Transmission Electron Microscopy, XPS and XRD noted that reactions took place as shown in Figure 2-22.
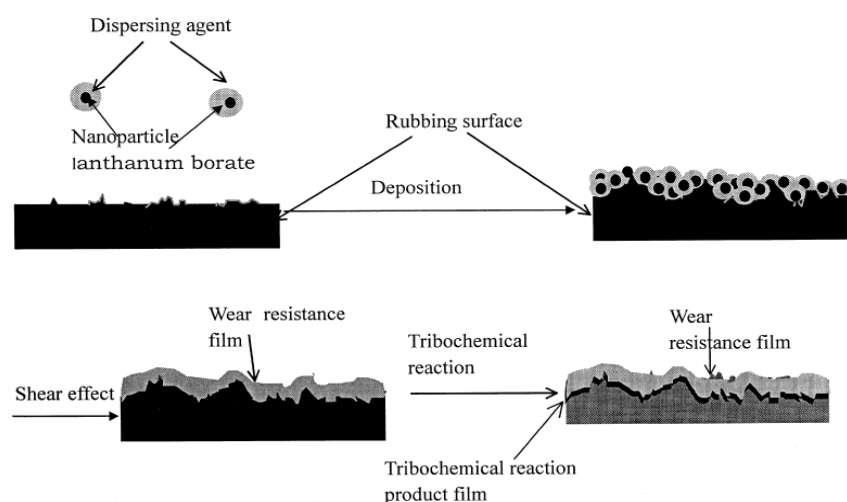
Figure 2-22 Antiwear mechanism of dispersed nanoparticle lanthanum borate [125]

The antiwear mechanism firstly requires a deposition of nanoparticle borate and dispersing agent deposited on the friction zone, after which boron oxide is formed due to shear- and extreme-pressure effects. Tribochemical reaction between boron oxide and substrate produced a wear resistant film consisting of iron boride (FeB). This mechanism was also suggested to apply to other inorganic nanoparticle borate

dispersions involving metals like; magnesium, aluminium, potassium and titanium. Another antiwear mechanism was suggested for tribofilms from organoboron additives based on Hard Soft Acid Base principle (or chemical hardness concept) [106]. The principle states that hard acids (electron acceptor) prefer to coordinate with hard bases (electron donor) to produce ionic compounds, and symmetrically soft acids prefer to coordinate with soft bases to give more covalent species as shown in [48, 106] as shown in Figure 2-23 (a) and (b).

	Acid	Base
Hard	H^+, Fe^{3+}, $B(OR)_3$, R_3C^+	H_2O, OH^-, O^{2-}, $PO_4{}^{3-}$
Borderline	Fe^{2+}, Cu^{2+}	BO_3^{3-}, N_2
Soft	Fe^0, Cu^+, metal atoms	I^-, CO, R_2S

(a)

	Acid	Base
Hard	H^+, Fe^{3+}, Mo^{6+}, Na^+, RPO_2^+, RSO_2^+, CO_2	H_2O, OH^-, CO_3^{2-}, O^{2-}, PO_4^{3-}, ROH, RO^-, SO_4^{2-}
Borderline	Fe^{2+}, NO^+, SO_2, Zn^{2+}	BO_3^{3-}, N_3^-, N_2, SO_3^{2-}
Soft	Cu^+, Fe^0, RH_3, RO^+, metal atoms, bulk metals	R_2S, S^{2-}, RNC, C_2H_4, $S_2O_3^{2-}$

(b)

Figure 2-23 Classification of different species by HSAB principle; (a) borates and iron oxide **[158]** and (b) B, Zn, Mo, P, S and Fe **[48]**

In the proposed antiwear mechanism using XPS and AES, mechanical and/or thermal degradation of borate ester resulted into the formation of methyl groups (CH_3) and boroxide groups BO_3 [158, 165]. However, Figure 2-23 (a) indicated that boroxide groups as a borderline base will react preferentially with borderline acid (Fe^{2+}). This mechanism suggested that hard and less protective iron oxides responsible for

abrasive wear are trapped in the borate tribofilm during the friction process to limit wear effect as shown in Figure 2-24.
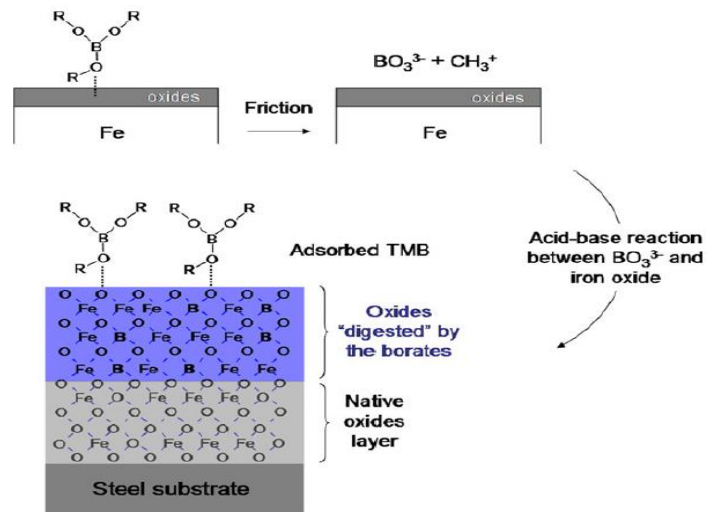
Figure 2-24 Schematic of borate antiwear mechanism **[158]**

This mechanism assumed that no hydrolysis of the borate ester occurred [158]. In addition, assumption was made that boron do not bind directly with metallic iron, which did not support the proposition of Hu et al. [124, 125, 226] on tribofilms formed by nanoparticle borate dispersions. However, in real tribo-oxidative systems involving borate ester, a certain degree of hydrolysis could occur as shown in Figure 2-8 to yield alcohol (ROH) and boric acid. By applying the HSAB principle of Figure 2-23 (b), products of borate ester hydrolysis (ROH and H_2O) are both hard base that will react preferentially with hard acid such as; Fe^{3+} (Fe_2O_3) [48] and K^+ (KO_2 and K_2O). In establishing the antiwear mechanisms of organoboron additives based on hardness concept as shown in Figure 2-24, further assumption made involves protection of tribofilm from oxidation by the oil. In this study, borate tribofilms will be subjected to thermal and tribo-oxidative conditions in order to elucidate more on borate antiwear mechanism on ferrous surfaces.

2.6 Summary

A large amount of research has already been conducted on borate tribochemistry as explored in the thesis chapter. These studies have been able to establish key

mechanisms associated with friction and antiwear behaviour of borate tribofilm on metallic surfaces. The tribological performance of borate tribofilms as shown in the literature review could be greatly influenced by concentration, temperature and water content of the surrounding. In addition, borate tribochemistry is also dependent on the type of borate additives; organoboron or inorganic borate dispersions. The proposed friction reduction and antiwear mechanisms for tribofilms from borate ester on metallic surfaces respectively have boric acid and boron oxide. Subjecting the borate tribofilms to varying extrinsic test conditions could provide a better understanding of these mechanisms.

2.6.1   Knowledge gaps

In the current understanding of borate tribochemistry, there are some knowledge gaps that exists which requires investigating. These are discussed below and form the basis of this Ph.D. research. It is known that borate ester can hydrolyse to form boric acid and ROH (alcohol) as shown in Figure 2-8. However, boric acid is also known to be responsible for friction coefficient reduction. This suggests that boric acid formation from high concentration of borate ester that is susceptible to hydrolysis could produce lower friction coefficient with better resistance to hydrolytic attack.

The current understanding of boric acid could not explain how volatility with steam and thermal decomposition at high temperatures could affect its friction reducing mechanisms. In addition, poor antiwear performance from borate ester as lubricant additives had been attributed to boric acid; described as abrasive despite its low shear strength that is comparable to MoS_2. There has been no study on the effects of hydrolysis by-products induced by tribo-oxidative conditions to show that boric acid was directly responsible for the catastrophic wear provided by tribofilms formed on ferrous surfaces.

Hence, physical and chemical analysis of tribofilms formed by model oils containing different concentrations of synthetic and non-synthetic borates could elucidate; (i) the relative hardness of borate tribofilms with respect to the substrate, (ii) morphology and tribofilm thickness, and (iii) if boric acid is directly responsible for poor antiwear performance of tribofilms from borate ester additives which are prone hydrolysis as previously understood in the literature.

The influence of temperature on the antiwear behaviour and durability of borate tribofilms have mainly been studied with oils containing boron and ZDDP. These studies are able to identify changes in structural units of boron oxide using XANES. Hence, the effect of changes in temperature on antiwear performance and durability of tribofilms from organoborate and alkali borate-containing oils in comparison to ZDDP will elucidate their independent effects on tribofilms containing both additives. However, changes in structural units of boron oxide due to changes in physical properties in alkali borate glass systems is yet to be investigated on borate tribofilms. Hence, the effect of temperature-induced changes in structural units of boron oxide will elucidate its influence on their antiwear performance and durability. In addition mechanical property characterization of borate tribofilms from different tribotests temperatures is yet be investigated. This is expected to elucidate on how changes in temperature affects the hardness of borate tribofilms in comparison to ZDDP, and its relative effect on antiwear performance and durability.

The current understanding on humidity effects on borate tribofilms has been primarily on those formed on boron coated systems. These results suggests a positive synergy between borate tribofilms and humidity. However, there had been no study yet on the effect of humidity on the tribochemistry of borate boundary films due to changes in humidity of the surrounding environment and added water to oils containing boron on ferrous surfaces. In addition, water adsorption rates of oils containing boron additives is yet to be assessed and compared to ZDDP. The tribological behaviour of ZDDP and boron-containing oils in dry and water-rich environments could be affected due to the presence of hard and less protective iron oxides and hydroxides. In order to further understand the limit of this synergy between water-rich environment and borate tribofilms, tribological test under free water contamination conditions could accelerate tribo-oxidative conditions where the antiwear functions of borate tribofilms is noticed to fail.

Chapter 3

Research Methodology, Materials and Surface Analysis Techniques

3.1 Introduction

This chapter outlines information on research methodology, materials and surface analysis techniques used in achieving results. These are an integral part of this PhD research.

3.2 Methodology

This PhD research will adopt two broad experimental methodology as shown in Figure 3-1.
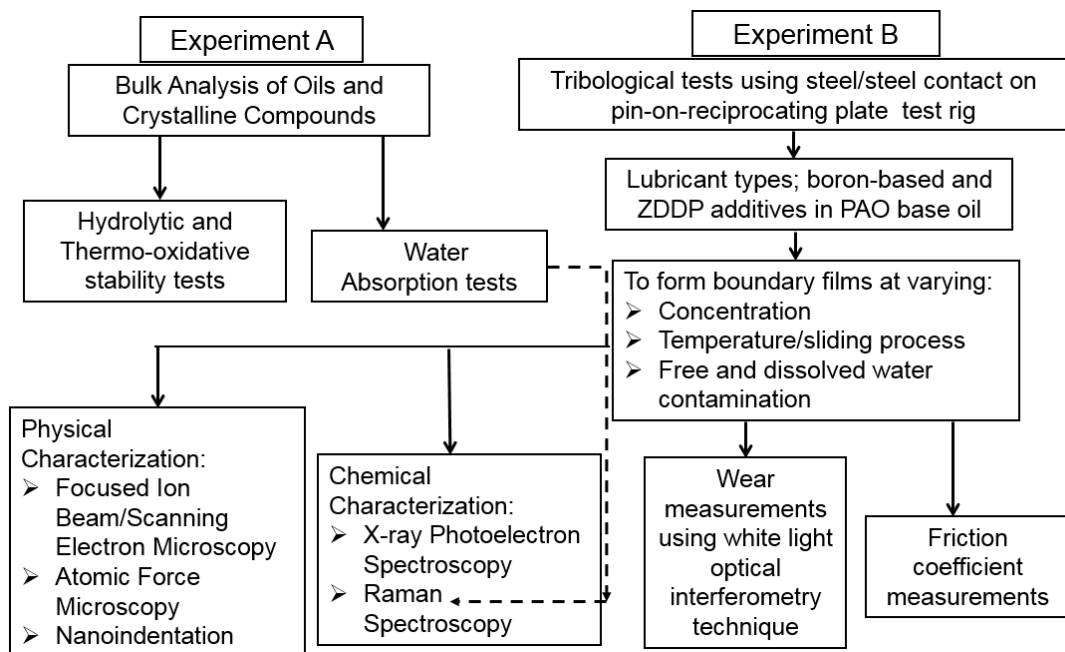
Figure 3-1 Experimental methodology overview

In Figure 3-1, experiment A involves bulk analysis of oils and some key crystalline boron compounds. The first part of this experiment will provide information on the physicochemical behaviour of additives in the base oil in terms of resistance to

hydrolysis under thermal and thermo-oxidative test conditions. This is based on literature studies earlier carried out in chapter 2, that borate esters could be susceptible to hydrolysis due to the vacant valence shell of boron atom which could easily be attacked by nucleophiles, such as water.

Hence the study of susceptibility of borate additives to hydrolysis under thermal and thermo-oxidative conditions is necessary in order to understand the differences between synthetic borate additives and non-synthetic borate additives using ZDDP as reference. In addition, this is to provide a better understanding of the behaviour of synthetic and non-synthetic boron compounds in corrosive and tribo-oxidative conditions

The second part of experiment A as shown in Figure 3-1 involves carrying out water absorption test of oils that are hydrolytically stable under thermal and thermo-oxidative stability. This is to provide information on the relative moisture absorption of additives in oils. In the literature review, some boron-based additives were described to perform their tribological functions by the reaction of boron oxide with moisture of the surrounding environment. The oils that are not hydrolytically stable in the first part of experiment A are not considered for moisture absorption test due to the unsuitability as lubricant additives in engine oils [119].

The third part of this test will undertake water adsorption potentials of key crystalline boron compounds in the absence of tribological process. This is to understand how certain crystalline boron compounds responsible for friction coefficient reduction and antiwear performance interacts with the surrounding air in ambient conditions.

In generating tribofilms from additive-containing oils, experiment B will involve tribological tests at different test conditions. During these tribological tests, friction coefficients are obtained. At the end of these tribological tests, various surface analytical techniques are carried out to assess wear rates of worn samples, physical and chemical characterization of tribofilms. These results are used to provide information on how the chemistry and physical properties of borate tribofilms affects their friction reduction, antiwear performance and durability. In addition, these results will provide a better understanding of the friction reducing and antiwear mechanism of borate additives.

3.3 Information on lubricants

In this research programme, model oils containing four different types of antiwear/EP lubricant additives have been evaluated in base oil. Three of these additives are boron based and ZDDP is the fourth. One out of the three boron-based additives is non-synthetic; boric acid trimethyl ester (BTE). The remaining two borate additives are synthetic borate additives; diethanolamine borate ester (ABE) or Vanlube 289 and hydrated potassium borate dispersed in N-substituted long chain alkenyl succinimides (KBE). The term 'synthetic' in this study implies that appropriate measures had been taken by the manufactures of these additives to prevent hydrolysis. This is unlike non-synthetic borate additives that is not protected against hydrolysis.

Hence, this study will not consider the non-synthetic borate ester as an additive to be used in the lubricating oils of internal combustion engines. However, its use in this study will be limited as a reference to other additives and also a major source of boric acid supply. In addition, tribofilms and thermal films from non-synthetic borate could elucidate the effect of hydrolysis on tribofilms that could be rich in boric acid from varying concentration tests. This is to elucidate on whether boric acid is directly responsible for poor antiwear performance of borate additives that are susceptible to hydrolysis and its effect on friction reducing and antiwear mechanisms of borate tribofilms.

Each of these additives are based in a high performance synthetic basestock that allows high quality lubricants to be formulated. In this research, polyalphaolephene (PAO) from ExxonMobil, SpectraSyn 6 will be used. This is a Group IV base stock with molecular structure as shown in Figure 3-2. This is considered based on its higher viscosity index, better oxidative stability, lower pour point and volatility than the corresponding mineral oils. The physical properties of the PAO used in this study was obtained from its chemical data sheet [227] are highlighted in Table 3-1.

The molecular structure of the borate additives are shown in Figure 3-3 (a) to (d). One of the two synthetic boron-containing lubricant additives is a commercial organic borate ester with 1 % boron content and no metal in the molecular structure with a trade called Vanlube 289 [228] from R.T.Vanderbilt Holding Company, Inc.
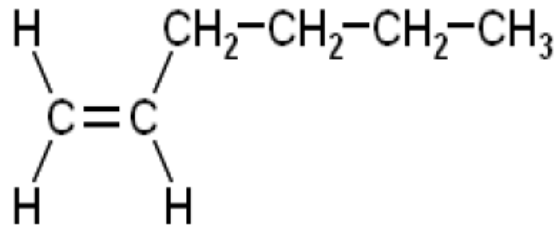
Figure 3-2 Molecular structure of PAO [229]

The molecular structure as shown in Figure 3-3 (c) and physical properties of as shown in Table 3-1 as obtained from the chemical technical data sheet [230].
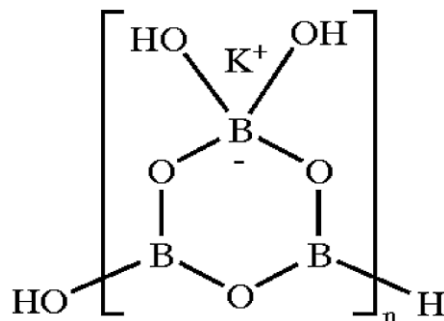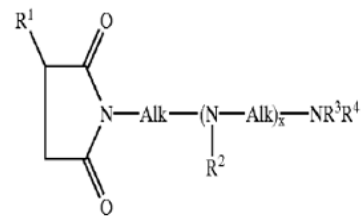
R^1 = alkynyl radical (30 < C atoms < 100)
R^2 to R^4 = alkyl or alkoxy
Alk = alkylene radical with 2 to 6 Carbon

(a)   (b)
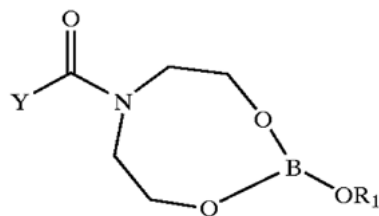
R_1 = alkyl hydrocarbon (C_nH_{2n+1})
Y = glycerol esters of fatty acid
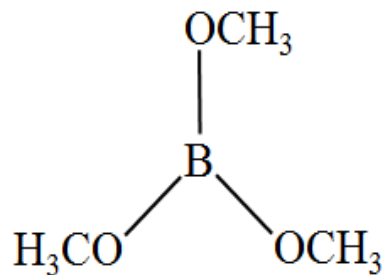
(c)   (d)

Figure 3-3 Molecular structure of; (a) synthetic hydrated potassium borate nanoparticle (KBE) [128, 231], (b) dispersant for KBE nanoparticle [128, 231], (c) synthetic organoborate composition (ABE) [122, 228], (d) non-synthetic boric acid trimethyl ester (BTE)

58

The second synthetic boron-based additive is hydrated potassium borate dispersed in N-substituted long chain alkenyl succinimides with the product name AR9100 oil additive supplied by ARCHOIL Inc. The general formula for potassium borate dispersion (KBE) in terms of ratio of number of moles of hydroxyl groups attached to each mole of boron in KBE is $K_2OxB_2O_3.yH_2O$ [128, 231]. Where the ratio of y to x is from 1.3:1to 2.1: 1); with specific ratio of potassium to boron limited to between 1: 2.75 and 1 : 3.25 [128]. In addition, KBE composition has 1-10 wt. % of potassium tetra borate with nanoparticle size of about 50-100 µm in an organic matrix [129, 157]. The molecular structure of potassium borate dispersion and dispersant are shown in Figure 3-3 (a) and (b) respectively. The physical properties of KBE are shown in Table 3-1 based on the information obtained from chemical data sheets [232].

It should be noted that the temperature at which kinematic viscosity of KBE additive presented by the manufacturer is different to ABE, ZDDP and PAO. This is as a result of the older methods of kinematic viscosity measurement in Saybolt Universal Seconds (SUS) used in USA that requires the measurement at 100^oF and/or 210^oF. In Europe, the older unit of KV measurement is the Redwood second at 100^oF and/or 210^oF. Presently, most countries have switched over to the metric system that uses Centistokes (cSt.) or mm^2/s which measures KV at 40^oC and/or 100^oC.

The third boron additives is trimethyl borate or boric acid trimethyl ester (BTE) with chemical formula $C_3H_9BO_3$ and molecular structure as shown in Figure 3-3 (d). This compound is used as an additive in some polymers [233] and precursor reagent for the organic synthesis of boronic acids used in Suzuki couplings [234]. In addition, gaseous BTE is known to exhibit antioxidant properties in brazing and solder flux metal joining process [235]. The physical properties of BTE are shown in Table 3-1 based on information obtained from the material safety data sheet (MSDS) [236]. The viscosity of BTE was not available as it was not provided on the MSDS.

However, the molecular formula for secondary alkyl ZDDP used for this research has been shown in Chapter 2. Information on the physical properties of the ZDDP used for this research are shown in Table 3-1 based on the works of Jun, Q., et al. [237]. The use of ZDDP in this research is to enable a comparison of the hydrolytic stability and water absorption to borate additives in engine oils. It should be noted that PAO,

KBE and ZDDP are commercially available, but ABE is a proprietary additive that was provided by R.T. Vanlube for the purpose of this research. In addition, tribological properties and physical characterization comparison to ZDDP of the borate tribofilms will elucidate how these extrinsic test conditions could affect their antiwear performance and durability.

Table 3-1 Physical properties of base oil and additives used in this study as obtained from their chemical data sheets/material safety data sheets or the literature; (i) ABE- [230], (ii) KBE- [238], (iii) ZDDP- [237] and (iv) PAO- [227]

Oil Type/ Property Description	ABE (Only)	KBE (Only)	ZDDP (Only)	BTE (Only)	PAO (Only)
KV at 40 ºC in (mm^2/s)	458.0	N.A.	407.6	N.A	31.0
KV at 38 ºC in (mm^2/s)	-	32.0	-	N.A.	-
KV at 100 ºC in (mm^2/s)	22.3	N.A.	13.5	N.A.	5.9
Density (g/cm^3)	0.990 at 15.6ºC	1.0 at 25ºC	1.2 at 15.6ºC	0.932 at 20ºC	0.83 at 15.6ºC

It is assumed that, the inclusion of these additives in PAO at different concentrations did not result in significant changes to the viscosity of PAO. This is based on the assumptions made by similar tribological studies [239]. For the hydrated potassium borate nanoparticles dispersed in N-substituted long chain alkenyl succinimides dispersant additives, and this dispersion was blended in PAO. The assumption is that nanoparticles are stable in the dispersant solution and by changing the concentration of dispersed KBE in base oil, a base oil with variable nanoparticle concentration is

obtained. Hence, every concentration of KBE will therefore represent dispersed hydrated potassium borate nanoparticles.

3.4 Tribological test

3.4.1 Introduction

The objective of this study is to provide further understanding of the behaviour and mechanisms of borate tribofilms formed from synthetic and non-synthetic borate additives in comparison to ZDDP on a ferrous surface. In order for this to be possible, borate and ZDDP containing oils are to be used on a ferrous surface in a tribometer to form tribofilms under boundary lubrication conditions similar to that found in the cam/follower of valve train assembly in IC engines.

3.4.2 Materials

In order for tribofilms to be produced, a Biceri pin-on-reciprocating plate tribometer is utilized. The pin and plate materials chosen for this study are both made of hardened steel AISI 52100 (HRC 58-62) as shown in Figure 3-4. Cylindrical pins of 20 mm lengths and 6 mm diameters are machined on the sliding surface to hemisphere of 40 mm radius of curvature with a surfaces roughness (R_a) of about 0.03-0.05 µm.

(a)   (b)
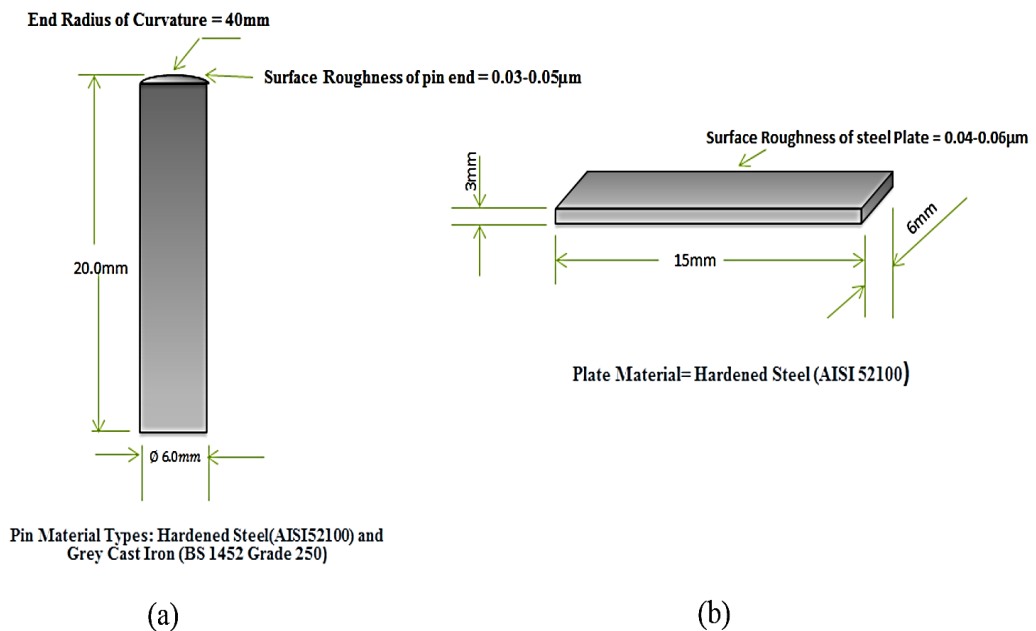
Figure 3-4 Schematics and dimensions of hardened; (a) steel pins and (b) steel plates

On the other hand, plates are of rectangular shape machined to specific dimensions of 15 x 3 x 6 mm^3 and polished to R_a of 0.03-0.06 µm. Nanoindentation hardness measurements of the hardened steel pins and plate samples gave elastic modulus and hardness of 224.7 $\pm$ 13 GPa and 10.8 $\pm$ 0.6 GPa respectively. The tribofilms are formed in pure sliding point contacts under boundary lubrication condition. Tribological tests samples (pins and plates) are cleaned in acetone for 15 minutes and thoroughly dried before use in a tribometer where the hemispheric end is held rigidly over reciprocating plate that is covered with model oil containing the additives.

3.4.3 Tribometer

The test rig consists of a multipurpose adjustable pin-holder with the pin rigidly held against a reciprocating rectangular flat plate that is also rigidly held down on a plate holding base upon which the lubricant is collected in the small bath as shown in Figure 3-5.

A force-post assembly on the test rig is equipped with bi-directional load cell in the range 58.8 N and combined error of -0.0037 N. The combined error being a combination of temperature effect, non-linearity, hysteresis and load cell sensitivity [21]. Frictional force is measured by the load cell, where a data acquisition card (DAQ) converts analogue signal to digital. The acquired digital data is processed and stored in a LABVIEW Window-based software program in a computer.

By using a stroke length of 10 mm and frequency of 1 Hz, frictional force readings are taken every 10 min. for 2 s (120 points); which corresponds to two stroke cycles. The average of 120 data points indicates average frictional force that was used by the software program to calculate friction coefficient.

Steady state friction coefficient is obtained as the average of the last one hour for each experiment. This is plotted as a function of time for the test duration. On the tribometer, sliding motion is made by reciprocating plate against a loaded stationary pins surrounded by lubricating oil. In order to provide heating for the oil and to maintain set temperatures, a thermo-couple heater is installed on the aluminium base plate of reciprocating plate holder. The first stage of tribological test involves investigating the effect of increase in additive concentration in PAO on friction

coefficient and antiwear performance at a fixed temperature of 100°C. At this temperature, boric acid dehydration as shown in the literature [12] could affect the friction reducing and antiwear characteristics of borate tribofilms from the boron additives. The relative tribological performances of these tribofilms are compared to results obtained when the samples are lubricated with only PAO.

The effect of temperature on tribofilms is investigated on additive-containing oils. These are ABE, KBE and ZDDP additives blended in PAO with molecular structure as described in Figure 3-2 and Figure 3-3. The oils containing BTE was not considered for these tests due to its boiling point that was estimated as 68-69°C from the material safety data sheet provided by the chemical supplier [236]. This is due to safety concerns at the test temperature of 135°C, which is far above the boiling point of BTE. Hence, BTE additive was considered unsuitable for this test due to safety reasons.
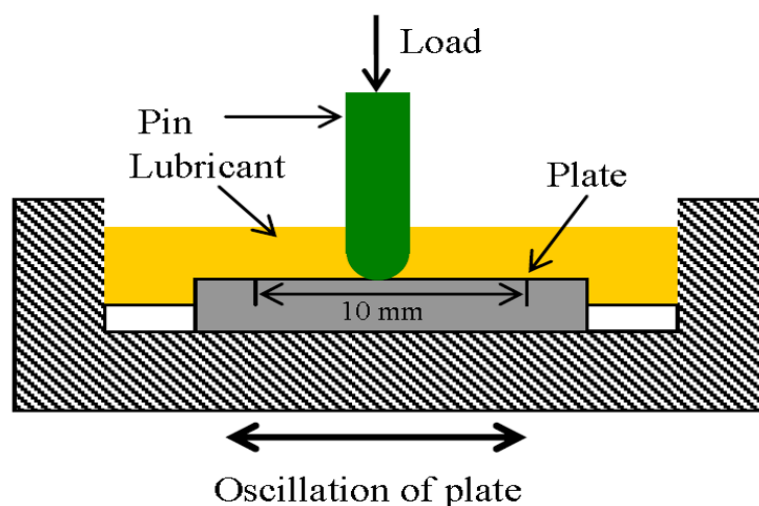
Figure 3-5 Schematic diagram of pin-on-reciprocating plate test rig for; (a) variable concentration and temperature test **[109]**

Previous studies on durability of tribofilms had used the changing oil lubricant approach with only the friction coefficient results used for durability assessment [89, 111]. A literature study of this procedure for evaluating tribofilm stability had indicated that no significant discontinuity in the friction trace could possibly occur due to changing lubricant process in order to ensure non-disturbance of the tribofilms during the friction process [21, 111].

Similarly, this study will use the same approach, but will also consider wear rates of worn samples alongside friction coefficient behaviour in tribofilm durability assessment.

The approach to be adopted in this study in investigating tribofilm durability involves an initial friction test on the tribometer at 1.0 wt. % additive concentration in PAO for 3 hrs (designated as 3 h) and 6 hrs (designated as 6 h) after which wear measurement was carried out using optical interferometry technique. Another friction test is carried out on fresh pair of samples (pin and plate), with additive-containing oils for 3 hrs. This is briefly stopped without replacing the samples, and allowed to cool down. By using a pipette, the oil-containing additives is siphoned out and wiped clean using tissue paper without touching the wear scar before adding fresh base oil (PAO 6).

The discontinued test is re-initiated to run for another three hours with only the base oil under variable temperature conditions; designated as 3r3 tests. At the end of this test, friction coefficient and wear measurement were carried out with the results compared to those obtained from the initial three and six hours tests.

In order to understand the effects of water contamination on tribofilms, two sets of experiments involving free (or added) water in the oil and the other involves humidity effect on tribofilms behaviour. The first part of this test will require the additives in the base oil maintained at 1.0 wt. %. Subsequently, distilled water of known concentrations (0, 0.5, 1.0, 1.5 and 2.0 wt. %) were added to the oil containing additives and properly blended on a magnetic stirrer at about $50^{\circ}C$ for about one hour. Tribological tests are carried out at $80^{\circ}C$ bulk oil temperature for 6 hours. This is to ensure that water in the oil fully dissolves and that thermal and tribo-oxidative condition for 6 hr test duration have a full impact on the tribofilms [83].

In the second part of water contamination tests, moisture effects on the tribological performance of tribofilms are studied by having the tribometer enclosed in a chamber produced from perspex material (68 x 20 x 26 mm^3). On the sides of the humidity chamber, there are inlet holes for ultrasonic humidifier and dehumidifier. These are to allow for the chamber environment to be varied from fully-dry to fully-wet conditions as shown in Figure 3-6.

The humidity chamber has a variable speed fan (400-1500 rpm) which ensures that humid or dry air are not only circulated evenly throughout the chamber, but also provides a means of humidity control. In addition, factory calibrated temperature and humidity probe (0-97 % RH) with a standard deviation of $\pm$ 2 % along with the fan are connected to a LabVIEW programme on a computer for continuous monitoring and control.

Hence, the humidity control chamber over the tribometer provides a good level of humidity monitoring and control for this study. This is to enable the tribological effect of moisture conditions of the surrounding air on tribofilms formation to be investigated appropriately. The relative tribological performances of tribofilms from ABE, KBE and ZDDP additives in PAO can be assessed. This was carried out at fixed additive concentration of 1.0 wt. % and different relative humidity conditions of; 5, 35, 65 and 95 % relative humidity for 3 hrs test durations under boundary lubrication regime.
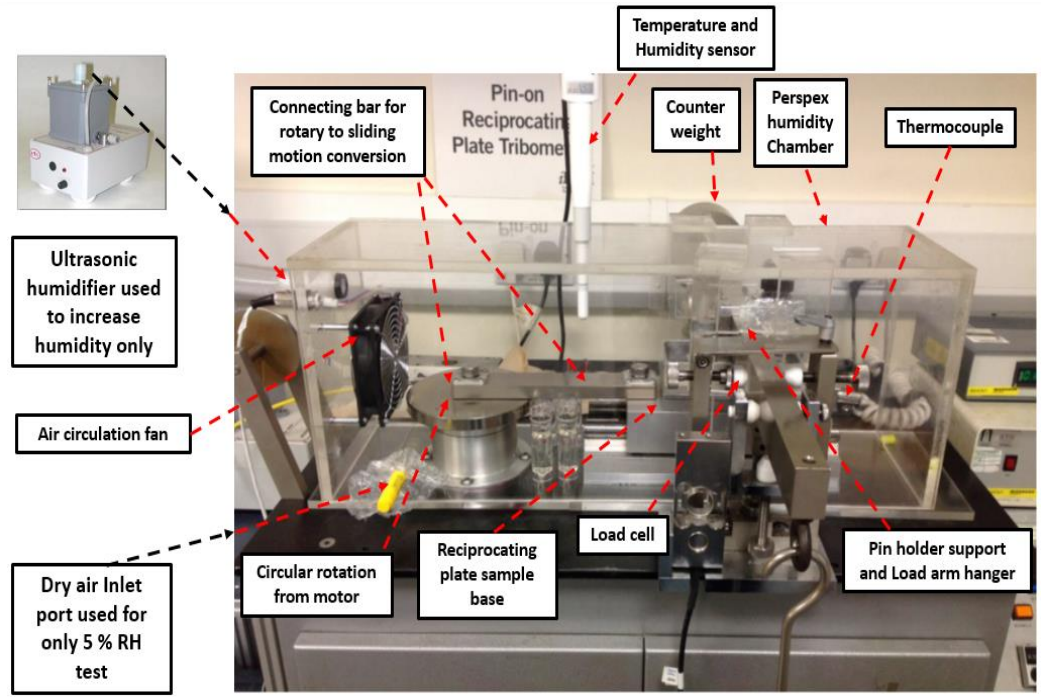
Figure 3-6 Tribometer enclosed in humidity controlled chamber

Similar tests on the effects of humidity on boron coated systems was carried out at room temperature [145, 184, 185]. Hence, experiments on the effect of humidity on tribological performance of borate tribofilms at room temperature of about 19°C. This will elucidate on how dry air and moisture-rich environment affect the tribological performance of borate tribofilms from oils containing borate additives.

In addition to tribological tests at varying humidity conditions, water absorption potentials of oils containing each additives will be assessed. This was carried out by filling a 20 ml open bottles with additive-containing oils. These are exposed to varying humidity environments in the humidity chamber enclosing the tribometer as shown in Figure 3-6. In this experiment 3 bottles for each additives are exposed in the humidity chamber to make a total of nine bottles. This is to ensure that measured water content level in the oils are reproducible.

At the end of each tribological tests under varying humidity conditions, the water content of oils are measured and compared to that existing prior to the time of placing them in the humidity chamber during tribological tests. Hence, this result will not only investigate the effect of humidity on the tribochemistry of some additive containing oils, but also on their water absorption potentials.

3.4.4 Test conditions for pin-on-reciprocating plate tribotests

Following the description of lubricants, tribometer and materials in sections 3.3.2 and 3.3.3, tribotests are carried out at test conditions in Table 3-2. In addition, Table 3-3 shows the chart for experiments carried out in the course of this study. In order to simulate the contact configuration of valve train system under boundary lubrication condition, this study will consider a contact pressure that is similar to cam/follower which was estimated as 0.6 MPa [240]. For this to be possible on the tribometer, a normal load of 172 N, with effective modulus E^* of steel samples as 247 GPa, Poisson's ratio of 0.3 and 40 mm pin radius of curvature for the pins to give a contact pressure of 0.68 GPa.

This was possible using the online software for initial point contact Hertzian contact pressure calculator [241]. In determining the boundary lubrication regime under which each test was performed, the Hamrock and Dowson [242] equation for elasto-hydrodynamic point contact as shown in Equation A.3.- 1 to Equation A.3.- 8

with the entrainment speed taken as 0.02 m/s are used. Hence, a contact pressure of 0.68 GPa will be used throughout the tribological tests for this study. For each tests, about 3 ml of lubricating oil will be used to cover the reciprocating plate and pin contacts. Each test was replicated three times with average friction coefficient and standard deviation of about ± 0.003 in the last hour of the six hours tests was recorded. It is assumed that changes in test conditions did not significantly affect the viscosity of oils as to prevent lubrication regime from leaving the boundary region.

Table 3-2 Test conditions during pin-on-reciprocating plate tribological tests

Parameters	Type of Tribological Tests			
	Variable additive concentration	Influence of temperature	Humidity tests	Water in oil tests
Temperature of Bulk oil (ºC)	100	19, 80, 100 and 135	19	80
Contact Pressure (GPa)	0.68	0.68	0.68	0.68
Sliding durations	6 hr	3 hr/6 hr/3r3	3 hr	6 hr
Lambda ratio, (Λ)	0.04	0.245-0.039	0.241–0.306	0.037-0.04
Additive conc. (wt. %)	0, 0.5, 1.0 and 2.0	1.0 wt. %	1.0 wt. %	1.0 wt. %
Humidity (% RH)	45-52	43-58	5, 35, 65, 95	-
Added water (wt. %)	-	-	-	0, 0.5, 1.0, 1.5 and 2.0

Tribological tests at low, medium and very high additive concentration are chosen to enable tribofilms formed to be assessed under boundary lubrication at a fixed bulk oil temperature of 100°C for a sliding duration of 6 hr under the prevailing humidity condition of the environment. The test temperature of 100°Cwas chosen in order to also investigate how the volatility of boric acid with steam [35] will affect the tribological performance of borate tribofilms.

In addition, this temperature falls within the region where boric acid is unstable [163, 224]. Hence, a study of reacted layers formed by synthetic and non-synthetic borate additives at different concentration and 100°C is necessary. This is to elucidate through the use of different surface characterization techniques whether boric acid is directly responsible for poor antiwear performance of tribofilms from non-synthetic borate additives or not. Two of the synthetic additives contain borates (ABE and KBE) and the third is the commercial ZDDP. The non-synthetic borate additive (BTE) contains a high concentration of boron and boric acid compared to the synthetic borate additives (ABE and KBE). This is to enable the tribological behaviour of different borate additives to be assessed in order to understand how the presence of rich and lean blend of these additives affects borate tribochemistry. Another set of test was carried out with fixed concentration of the synthetic additives in the oil (1.0 wt. %), but at different bulk oil temperature of 19, 80, 100 and 135°C under boundary lubrication condition.

There are few literatures on the effect of temperature on the antiwear and durability of borate tribofilms. Some of these tribological tests at variable temperature were carried out when ZDDP and borate additives are used together in the additive package.

The concluding results of these tests could not distinguish the role played by borates in the chemistry of the tribofilms formed [81, 82]. Another literature study on borate tribofilms without ZDDP stopped the temperature variation at 110°C [131]. However, at this highest test temperature, boric acid is yet to fully decompose to boron oxide due to its step-wise decomposition behaviour in forming boron oxide [163, 224]. Hence, this research will investigate the influence of temperature on tribofilms up to 135°C bulk oil temperature on the antiwear performance and durability of tribofilms from synthetic borate additives (ABE and KBE) in comparison to ZDDP.

Table 3-3 Chart for tribological experiments

Experimental Details			
S/N	Tribological tests	Test Duration	Surface Analysis
(1)	Friction coefficient measurements of ABE, BTE, KBE and ZDDP in PAO at different concentrations and fixed temperature compared to only PAO	6 hr.	Wear measurement, FIB-SEM, AFM, Nanoindentation, XPS and Raman Spectroscopy
(2)	Tribological tests involving tribofilms formed by the borate additives at fixed concentration and variable temperature	3 hr, 6 hr and 3r3	Wear measurements, AFM, Nanoindentation, XPS and/ or Raman Spectroscopy
	Tribological tests involving tribofilms formed by ZDDP additive at fixed concentration and variable temperature	3 hr, 6 hr and 3r3	Wear measurements, AFM, Nanoindentation
(3)	Tribological tests on the effects of water contamination on tribofilms (a) Humidity tests (b) Expose oil samples to humid atmosphere (c) Free water in oil test		
		3 hr	Wear measurements, AFM, XPS and Raman Spectroscopy
		6 hr	Wear measurements, AFM, and Raman Spectroscopy

However, oils containing BTE was not considered for this test. The highest test temperature of 135°C is far above the boiling point of BTE that was estimated as 68-69°C in the material safety data sheet provided by the chemical supplier [236]. Hence, BTE was considered unsuitable for this test due to safety reasons. This test will enable the tribofilms formed at different temperature and sliding process to be

studied in order to provide a better insight to their chemical and physical behaviour under these conditions.

In order to understand how tribofilms formed by borate in oils are influenced by dissolved water contamination, the experimental methodology was designed to compare tribological performance in water-rich environment to moisture-free atmosphere for 3 hr test duration. In moisture-free atmosphere, dry air supply line from a dehumidifier was connected to the air inlet of the humidity chamber to provide dry air, after which tribological test is carried out for 3 hr and relative humidity measured and recorded. At the end of dry air tests, the dry air hose is disconnected and the valve connecting this line closed, before commencing experiments in moisture-rich atmosphere. The tribological test in moisture-rich environments requires another hose to link the moist air from the outlet of ultrasonic humidifier to the moist air inlet of the humidity chamber at 35, 65 and 95% RH. This test is carried out at room temperature without heating the oil. The oil samples exposed to water-rich environments provides a means of measuring the increase of water content of the oil with respect to the initial water content.

In the free-water contamination in oil, specific amount of distilled water was blended with the oil to form either an emulsion or free-water in oil. The additives used for this test are both synthetic and non-synthetic borates. In order to investigate the tribological effects of free-water tribofilms formed by oils containing borate additives, this study will utilize the technique used by Cen et al. [83] to study the effect of dissolved- and free-water on ZDDP tribofilms. In these tests, tribological experiments was carried out with oils containing free-water was carried out for 6 hrs at $80^{\circ}C$ where most of the free-water was observed to have dissolved. Tribological tests are carried out at $80^{\circ}C$ and a sliding time of 6 hr. This is to ensure that water in the oil fully dissolves and that thermal and tribo-oxidative conditions have a full impact on the tribofilms. This was based on increase in saturation level with temperature [243].

There is yet to be a study on the effects of free-water on the formation of borate tribofilms. Hence, tribological experiments on the effects of free-water on tribofilms from oils containing some borate additives using ZDDP as reference. This is to enable surface analysis of the formed tribofilms provide a better understanding on the tribochemistry of borate tribofilms synergy with water (free or dissolved).

70

3.5 Bulk oil analysis

3.5.1 Tendency for hydrolysis

The tendency for borate esters or esters in general to breakdown into alcohol and acid is a measure of their resistance to hydrolysis. As a potential substitute for ZDDP additive in oils, they are required to be hydrolytically stable when exposed to humid air or when in contact with appreciable quantities of moisture. The experimental detail of physicochemical assessment of oils and some boron compounds are shown in Table 3-4.

Table 3-4 Physicochemical analysis of oils and some boron compounds

S/N	Tendency for hydrolysis tests	Physicochemical analysis of the bulk oil
(1)	Hydrolytic stability of additives in oils using sealed-tube tests	➢ Changes in Kinematic Viscosity ➢ Changes in Total Acid Number ➢ Changes in Copper Weight Loss ➢ Copper appearance after the tests
(2)	Thermo-oxidative stability tests	Thermo-Gravimetric Analysis of Additives in Oils Under Different Gas Test Conditions: (a) Air (b) Nitrogen
(3)	(a) Moisture absorption potentials of additive-containing oils (b) Moisture adsorption of boron oxide and boric acid	Changes in water content of the oils Weight gain using the micro analyser and Raman Spectroscopy

The test method employed is a more rigorous version of ASTM D2619-09 test standard for petroleum or synthetic based hydraulic fluids in terms of test temperature and duration as proposed by [136]. This test method differentiates the relative stability of petroleum or synthetic–based hydraulic fluids in the presence of water under the conditions of likely usage. The test method requires a certain quantity of water to be added in a sealed bottle containing copper coupons. This is heated to a particular temperature in an oven for a specific amount of time, such as 48 hours or more. At the end of this test, changes in viscosity, total acid number, copper weight loss or gain and copper colour appearance are used to assess the degree of hydrolytic stability of the oil.

In this study, hydrolysis was accelerated by adopting the wet heating treatment method which requires adjusting 100 ml of lubricant to have a water content of 2000 ppm in a borosilicate glass bottle. Mixing is possible by using a magnetic stirrer at a temperature of 50℃ for about 40 minutes to form water in oil mixture. Each of the copper coupons (Cu C106) is dropped into the sealed borosilicate glass bottles which are placed in the closed oven. The consideration of steel coupons for this test could have provided a better information on the rust inhibition potential of the oils on the steel samples for tribological tests, in terms of weight loss or gain. However, copper coupons will not only provide weight loss or gain, but also colour changes due to oxidation effect of the additive-based oil on copper. Heating of the oils was carried out at 135°C set temperature for 10 days. The degree of hydrolysis was determined by changes in viscosity, total acid number, weight loss and coupons (copper) appearance before and after the heating process.

Pre-and–post heating values of the total acid number (TAN) that conforms to ASTM D664 or Institute of Petroleum (IP)/Energy Institute (EI) 177 test procedure are noted. In determining TAN changes that took place for the mixture during the test, the on-site fuel and lube oil analysis test kit is utilized [244]. This has an accuracy of $\pm$ 0.2 TAN as shown in Figure 3-8. The results are compared to hydraulic fluids and oils (HF-O) test limits. Changes in kinematic viscosity of additives-containing oils are obtained from measured values of dynamic viscosity divided by the corresponding measured values of density before and after the heating processes. Dynamic viscosity measurement was possible by making use of a rotational rheometer with cone and

plate gap loading geometry using a Newtonian model fit, under controlled shear stress mode based on ASTM D2983 test standard. This test method uses rotational viscometers within a torque range and specific spindle speed for the determination of the low shear rate viscosity of some lubricants, automatic transmission fluids and hydraulic fluids. The protocols used for this tests are; (i) minimum shear stress of 0.06 Pa., (ii) maximum shear stress of 50 Pa., total time of 750 sec (delay time of 5 sec. and maximum time out of 5 sec.), gap setting of 150 µm between plates of 4°/40mm diameter geometry.

In order to obtain kinematic viscosity of oils containing each of the additives, the densities of oils are determined at 40°C using instrumented pycnometric method from Micromeritics (Accupyc 1330). This has a measurement error of about 0.001 g/cm^3. The kinematic viscosity of each test oils are determined at 40°C by dividing the measured viscosity with the corresponding density before and after heating these oils in the oven. Results from these tests were compared with ISO Viscosity Grade standard 220 (ISO VG 220). In addition, the weights of copper coupons was determined using a micro analyser that can measure weight changes up to five decimal places before and after heating in the oven, while their colour changes was also obtained before and after heating in the oven at 20 x magnification.

3.5.2 Thermo-oxidative stability tests

The thermo-oxidative stability of known weights of test oils was evaluated using a SHIMADZU TGA-50 thermo-gravimetric analyser as shown in Figure 3-7.

Figure 3-7 Thermo-gravimetric analyser (TGA) used for thermal and oxidative decomposition of oils

73

By using PAO alone and each of the antiwear additive blends in the base oil at 2.5 wt. %. TGA tests were carried out separately in static atmospheres of nitrogen (thermal) and air (oxidative) at 50 cm³/min flow rate. Each sample was heated under a linearly increased temperature programme of 10°C/min to 600°C for one hour. Under these conditions, weight changes with time measurements was possible on the TGA analyser at the beginning (onset temperature) and end (endset temperature) of the experiment to provide an insight on their dynamic decomposition behaviour in thermal and oxidative atmospheres.

3.5.3 Moisture effects on oils and some crystalline boron compounds

In order to understand how borate additives in the base oil interact with humid air to influence friction and wear performance, a quantitative assessment of increase in water content of synthetic borate-based oils is necessary in comparison to ZDDP oil. This can either be a physical or chemical process in which moisture enters the bulk phase of the absorbent. In this experiment, the absorbent is the additive containing oils, as it distributes the absorbed moisture throughout the bulk phase of the additive containing oils. This is possible by determining the increase in concentration of dissolved water in sample oils containing each additives (ABE, KBE and ZDDP) when exposed to different humidity conditions for 3 hr compared to unexposed oils. The various methods of determining the water content of oils are; Crackle test, Calcium hydride test, Karl Fischer and Fourier Transform Infra-Red. In this experiment, lube oil analysis was carried out using test kit from KITTIWAKE Parker [244] to determine water in oil. This method employs the calcium hydride test technique as shown in Figure 3-8.

The calcium hydride test water in oil test works on the principle that oils reacting with calcium hydride reagent in a pressurised oil-containing cell forms hydrogen gas. This reaction is accelerated by shaking the test cell vigorously. A change in pressure due to hydrogen build-up is detected by a pressure sensor which converts the pressure build-up to water content in % or ppm of water in 9 oil samples. Three of these samples are for each additive in order to ensure experimental reproducibility. This test conforms with IP386/ASTME D4928 standard with an error limits of ± 0.1 % [244]. The differences between water concentration in oil samples exposed to moisture

contamination is compared to corresponding water content in oils unexposed to moisture contamination, gives an indication of water adsorption potentials of the additives in the base oil.

In order to determine the moisture adsorption potentials of crystalline boron oxide and boric acid, commercially-available laboratory grades boric acid having an Assay greater than 99.5% and boron oxide with 99% are obtained. The adsorption of moisture on the surface of crystalline boron oxide or boric acid is assessed by using the micro-analyser for weight change determinations. The initial weights of eight samples of some quantities of these crystalline boron compounds are placed in a petri-dish are determined (4 petri-dish each for boron oxide and boric acid). With open lids to the moisture of the surrounding air, the weights of these petri-dish containing boron oxide and boric acid are subsequently determined every one hour up to 9 hrs exposure time. Another sets of eight samples of crystalline boron compounds are exposed to the surrounding environment for 24 hrs. These sets of experiment are repeated four times, with the three sets of samples weighed, and the fourth set of samples taken for Raman spectroscopy analysis.
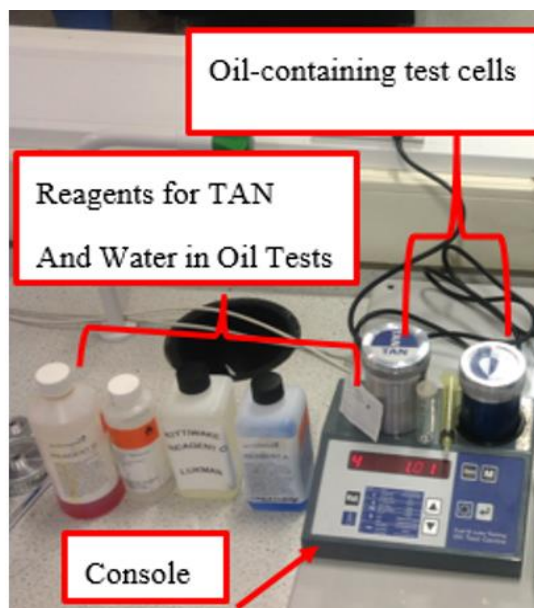
Figure 3-8 Lubricating oil analysis test kit **[245]**

3.6 Post-test surface analytical techniques

3.6.1 Wear measurements; Non-contact profilometry

In order to fully characterize the material loss due to tribological processes, post-test wear analysis are carried out using scanning white light interferometry on a Brucker NP FLEX^{TM} interferometry. For data analysis, 'Vision64' software suite is used to determine volume losses and other surface parameters of worn samples after removing surface bias such as; curvature and tilt. All measurements are made using vertical scanning interferometry mode (VSI), scan speed of x 3 magnification of x 2.5. The profilometry data are converted to dimensional wear coefficients using Archard's wear equation as shown in Equation 3- 1; wear volume obtained from white light interferometry divided by sliding distance (m) and multiplied by the unit load (N)

$$V_{PL} = \ k_{pl} \ \times \ F_N \ \times L \ ; \ V_{pi} = \ k_{pi} \ \times \ F_N \ \times L \qquad \text{Equation 3- 1}$$

Where: $V_{Pi} \ and \ V_{PL}$ in m^3 are measured wear volumes for both the plates and pins; k_{pl} and k_{pi} in m^3/N-m are dimensionless wear coefficients for plates and pins; F_N in Newton is normal load and L in metres is sliding distance.

3.6.2 Focused Ion Beam (FIB)

In order to estimate tribofilms thickness of worn samples from tribological test, a focused ion beam for milling a trench is coupled with scanning electron microscopy will be employed. This enables a cross-section of worn area to be milled and imaged with appropriate optical techniques to not only give an estimate of the tribofilm thickness, but also an indication of its heterogeneity.

In order for this to be possible, a high resolution FEI Nova200, NanoLAB field electron gun scanning microscope (FEGSEM) with precise focused ion beam (FIB) was utilized to image and etch into the wear scar of samples. Prior to milling, the area of interest on the tribofilms is protected from destructive ion beam with an initial protective layer of platinum ($\cong 0.2 \ \mu$m) using an electron beam. Another bulk layer of platinum ($\cong 1.5 \ \mu$m) is laid over the first layer.

Nano-machining was used to sputter a rectangular trench of about 8 x 10 µm^2 using Gallium ion beam at 30 kV on worn samples from the 1.0 wt. % additive-containing

oils. The tribofilm thickness was estimated from a secondary electron image of the trench at an angle relative to the surface that was similar to that used in the literature (54°) [246], and 40-50° [247].

3.6.3 Atomic Force Microscopy (AFM)

In order to obtain high resolution topography images of the tribolayer of worn plate samples, the Atomic Force Microscopy (AFM) is utilized as shown in Figure 3-9 (a). The basic principle of AFM operation involves bringing a sharp probe closely to a sample surface which is subsequently moved relative to each other in a raster scanning pattern of a pre-defined area.
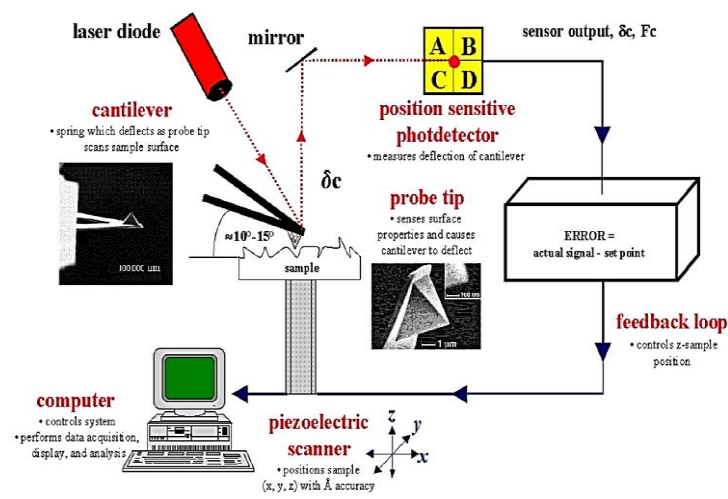
(a)
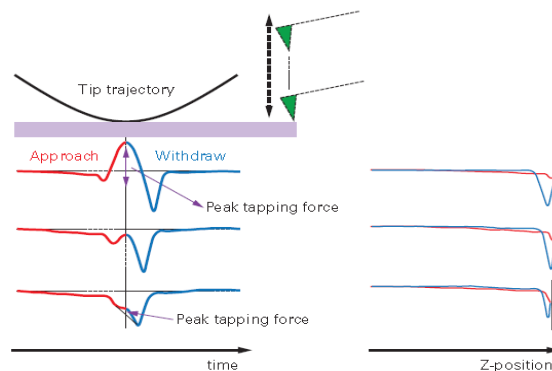
(b)

Figure 3-9 AFM techniques for morphology imaging; (a) schematic diagram and (b) cantilever force curves operated in Peak-Force tapping **[248]**

Height profiling is possible based on the deflection of the tip due to repulsive van der Waals forces experienced from the sample surface. High resolution AFM images were obtained using Bruker Inc. (Dimension icon) under the peak force-quantitative nanomechanical tapping mode with silicon nitride cantilever.

The cantilever resonance frequency is 0.977 Hz with spring constant of 40 N/m. This method avoids lateral forces due to intermittent contacts with the sample as it operates in a non-resonance mode at the turn-around points; z-position is modulated by a sine wave as shown in Figure 3-9 (b) and not a triangular type. On the other hand, this method is also more advantageous than the contact mode which is relatively easy to operate, but with the inherent drawback of high lateral force exerted on the sample.

This can result into sample damage or the movement of relatively loose objects attached to the tip. Tribofilms and/ or thermal films formed by each antiwear additive on plate samples were imaged over scan area of 5.0 x 5.0 μm^2 and 50 x 50 μm^2 at six positions on the wear scars for a representative image to be selected. This is to ensure that morphology image are captured on small and larger scales in order to obtain a good representation of the tribolayer.

In characterising the images obtained from the AFM, surface roughness and height sensor scale bar attached to the images are used to give an indication of deviations of the wear scar regions from the original unworn surfaces. The height sensor is the step height differences between the brightest and darkest regions of the images over scanned area as a signal from z-piezo position sensor.

3.6.4 Nano-mechanical properties measurements

A mechanical property characterization of the tribofilms formed from tribological tests was carried out using instrumented nanoindentation technique. This is used to obtain accurate hardness (H), reduced modulus (E_r), stiffness and fracture toughness of thin films formed on the wear scar of surfaces from tribological tests as shown in Figure 3-10.

The test instrument used for this purpose is Nanotest^{TM} NTX platform system with NanoTest NTX series controller, as shown in Figure 3-10 (a) is manufactured by

Micromaterials Ltd. UK. This equipment is a multi-tasked, flexible nano-mechanical property measurement system that has three independent modules (indentation, scanning and dynamic impact). In addition, the test equipment have two loading regimes; low load heads (0.1-500mN) and high load ''Micro Test'' (0.1-20N) with high resolution microscope (4x, 10x, 20x and 40x).

(a)   (b)
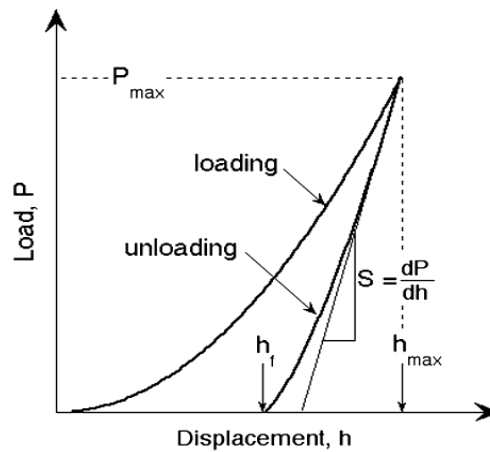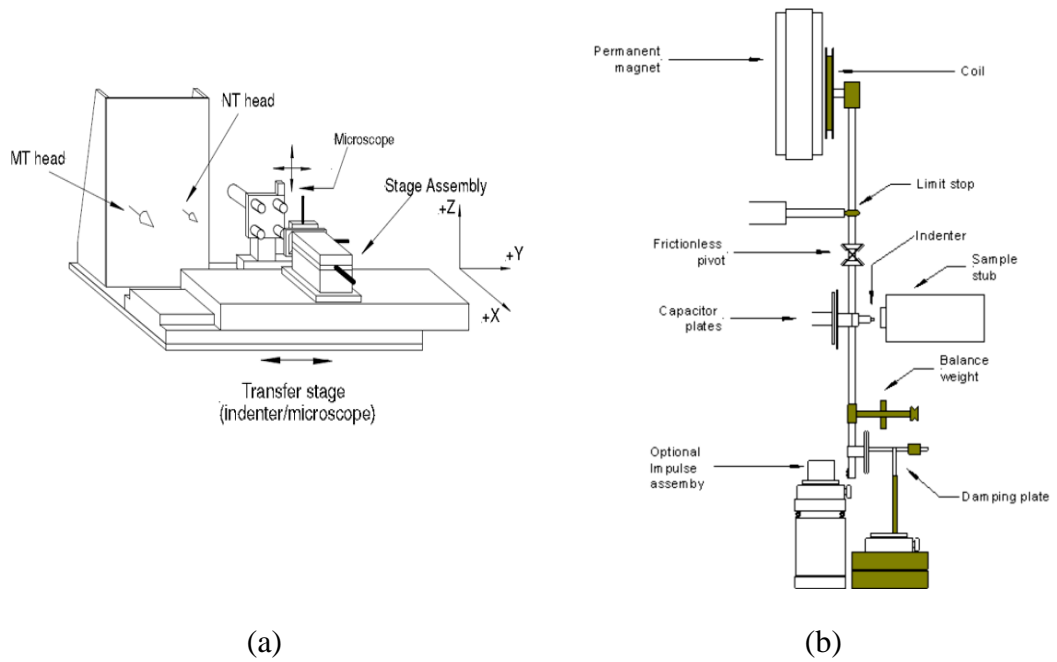
(c)

Figure 3-10 Nanoindentation schemes; (a) Nano Test platform system **[249]**,

(b) Nanotest pendulum **[250]** and (c) Indentation load-displacement curve **[251]**

It is enclosed in a temperature regulated box to prevent the influence of external thermal fluctuations from the surrounding. The dynamic displacement response of thin films to various loadings can be measured through capacitor plates positioned directly behind the indenter tip during indentation events on NanoTest pendulum is shown in Figure 3-10 (b).

This consists of a stiff, ceramic pendulum which is balanced on a frictionless leaf spring pivot. A permanent magnet and electromagnetic coil enable variable loads to be applied. In order to obtain, analyse and interpret data, the micro-capture camera and NanoTest platform software suite is used.

The instrument is equipped with optical microscope for sample imaging before test in order to locate a flat indent area on top of the tribofilms. In addition, the indenter used for this instrument was equipped with a Berkovich diamond tip with nominal radius of curvature in the range of 50 nm. By using high strength adhesives, all samples can be mounted to the sample holder.

After mounting the samples, a series of sequential nano indentations around the same location were made at 600 µN indentation loads which are 50 µm apart on various worn samples. This was based on the approximate film thickness measurements from FIB-SEM in order to ensure that penetration depth into the film is within 10 % of film thickness. The hardness measurement methods suggested by Oliver and Pharr [252] and ISO 14577-1 protocol. This involves experimental algorithm of loading and unloading time of 10 s with each at 0.5 µm/s velocity and 0.5 mN/s sequential loading rates. The test control procedure can be either displacement-controlled or force-controlled. In the force-controlled procedure to be adopted for this test, the test load is constant for a designated period while recording measurements of the changes in the indentation depth as a function of time. The load-displacement curves as shown in Figure 3-10 (c) enables the reduced elastic modulus (E_r) to be measured.

In order to avoid the effect of substrate on the mechanical properties of thin films, some literature adopted certain percentage of the estimated film thickness as the rule of thumb for the indenter penetration depths into the films; 5% [253], 10% [254, 255] and 25% [256, 257]. In this study efforts will be made to maintain the indentation within 10% of tribofilm thickness. The elastic modulus of tested specimen is obtained

from Equation 3- 2, if the Poisson's ratios (v_s and v_i) for the specimen and indenter are taken as 0.3 and 0.07 respectively and the elastic modulus of indenter (E_i) is taken as 1140 GPa. The hardness and/ or elastic modulus of worn samples lubricated by additive-containing oils are compared with the base oil

$$\frac{1}{E_r} \quad = \quad \frac{1- v_s^2}{E_s} \quad + \quad \frac{1- v_i^2}{E_i} \qquad\qquad \text{Equation 3- 2}$$

3.6.5 X-ray Photoelectron Spectroscopy (XPS)

The XPS technique also referred to, as electron spectroscopy for chemical analysis (ESCA), is used to investigate the chemistry at the surface of a sample. These could be; element composition, chemical information about the local environment and valence bond electronic structure of sample surface. This technique works by irradiating a specimen with mono-energetic soft X-ray beam such that photons of specific energy are used to excite the electronic states of atoms below the sample surface in a high vacuum environment. Hence, photoelectrons are ejected from the sample surface, which are energy filtered through a hemispheric analyser (HAS) before a detector identifies the intensity for a defined energy. The resulting energy spectra exhibits resonance peaks characteristics of the electronic structure of atoms on the sample surface due to quantization of the core level electrons in solid-state atoms.

The elemental analysis of worn surfaces was quantitatively analysed by using XPS to obtain more information about the tribochemical reaction products due to different tribological processes. XPS was performed at NEXUS facility nanoLAB with a Theta Probe MK (II). This instrument employs a high-power monochromatic Al$K\alpha$ X-ray source at 1486.68 eV which was focused on the wear scars in 400 μm^2 area of worn plate samples surface in a vacuum of about 10^{-9} milli bar. A low resolution scan was obtained to identify the elements present at pass energy of 200 eV, 5 mm slit size and 1.0 eV step interval; after which long scans at 40 eV and pass energy of 0.1 eV of selected peaks were acquired in spatial mode.

XPS depth profiling experiment was performed on worn samples using ion gun monatomic bombardment at 1.03 nm/min sputtering rate; where energy was set at 40 eV and step interval of 0.1 eV from. This was based on results from similar tests used

in the literature for XPS depth profiling of borate tribofilm that used sputtering rates between 1.5 and 3.0 nm/min [193]. In this test, care was made by choosing lower sputtering rate in order to avoid damage to the tribofilms.

Depth profiling was specifically chosen in order to investigate the chemical species formed deep down the tribolayer. Peaks obtained were analysed using CasaXPS software for curve fitting after calibration of C1s peak for contaminated carbon as reference at 284.8 eV [258]. In order to display data, OriginPro 9.4 software was used. The acquired spectra were compared with standard spectra from XPS handbooks and tabulated spectra from various references [119, 158, 198]. The background used for curve fitting is the more commonly used Shirley background. This type of background goes up in proportion to the total number of photoelectrons below its binding energy position [259]. It is unlike linear background which suffers from large peak area changes that depends on the chosen end points. On the other hand, Tougaard background is impracticable for use when there are numerous peak overlaps [260, 261].

3.6.6 Raman Spectroscopy

In order to complement results from XPS spectroscopy, the Raman spectroscopy is considered for further chemical analysis of the tribofilms above other vibrational spectroscopy. One type of vibrations spectroscopy is the infrared spectroscopy that is based on what is termed mid-infrared (4000 cm^{-1} to 400 cm^{-1}), where region covers the fundamental vibrations of most organic compounds [262]. The other type of vibrations spectroscopy is known as near-infrared (NIR) with spectral region around 4000 cm^{-1} which falls between the infrared and the visible spectrum. A description of these vibration transition processes are shown in Figure 3-11 (a). Third type of vibrational spectroscopy is Raman spectroscopy. This type of vibrational spectroscopy provides information about the molecular structure and interactions within the sample. It measures vibrational energy levels which are associated with; chemical energy to identify bonds, structure characterization, and reaction monitoring. This technique involves illuminating a sample with an intense single frequency light source (i.e. laser) and detecting the scattered light as shown in Figure 3-11 (b).
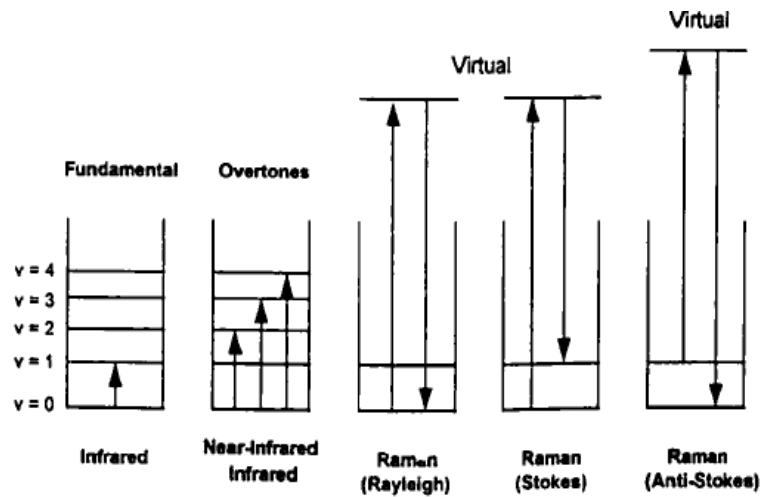
(a)
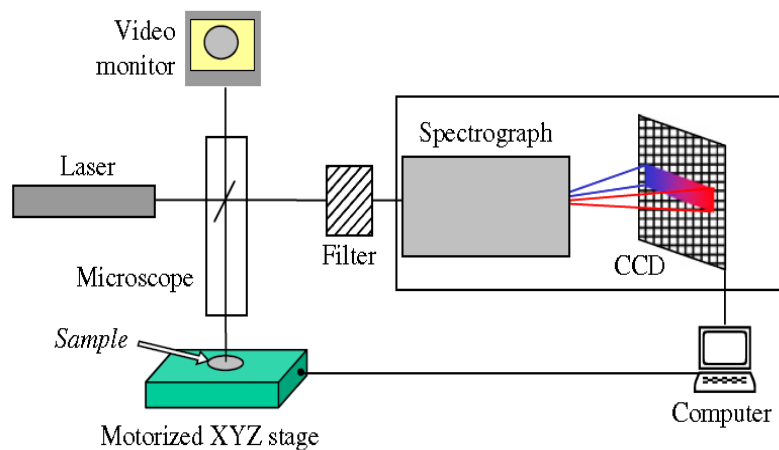
(b)

Figure 3-11 Vibrational spectroscopy; (a) vibration transition processes **[262]**, and (b) schematic representation of Raman spectroscopy [263]

Most of the scattered light could have same frequency as the excitation source, but sometimes are not. This could be related to the force exerted by electromagnetic field on charged particles to form induced dipoles. When the induced dipole oscillates at angular frequency equal to that of incident light, Rayleigh or elastic scattering occurs.

On the other hand, stokes Raman scattering occur when induced dipoles oscillate at lower frequency than incident light, and anti-stokes Raman scattering at oscillating frequency higher than that of incident light. A comparison of different vibration

transition processes are shown in Figure 3-11 (b). A requirement for a vibration to be Raman-active is for such molecules to have change in polarizability (i.e. a change in shape, size or orientation of the electron cloud that surrounds the molecule). This is a molecular vector quantity which describes the ease with which electrons can move by the electromagnetic radiation relative to the nuclear framework. The Raman-active boron compounds that could be found on tribofilms are; boron oxide, boric acid and boron nitride. In order to study structural changes and properties of different borate groups within the tribofilms, we applied room temperature Raman spectroscopy to infer the vibration transitions of the wear-resistant borate glass network. This was based on Krogh-Moe hypothesis that by comparing the Raman spectra of glasses with those of borate compounds whose crystal structure is known, it is possible to obtain information on the presence of certain structural units of glasses [264, 265]. This hypothesis assumed that structural units or groups present in oxide liquids and oxide glasses resemble the units or groups present in the corresponding crystalline compounds [264, 266].

In this study, the Renishaw-inVia Raman spectroscopy was used to analyse worn surfaces of plate samples. In addition, Raman spectroscopy of some crystalline boron compounds could provide a better understanding of borate tribofilms formed during tribo-oxidative interaction with moisture of the surroundings. The key boron compounds are boric acid and boron oxide. All Raman measurements were made using Nd-YAG laser with 488 nm wavelength excitation, and 10 mW laser power on the sample surfaces. The laser beam was focused on worn samples to do spot-to spot mapping of 25 x 25 μm^2 area with intensity integrated in 10 sec. of detector exposure time with one accumulation. Spectral analysis was performed using WiRE 3.4 software (inVia) to collect data.

Band fitting was carried out using a Lorentz-Gauss cross-product function with the minimum number of component bands for the fitting process. Reproducible fitting was carried out until squared correlations of r^2 is greater than 0.995; OriginPro 9.4 software was used to display data. In most of the test results, the spectra will be plotted on the same scale and shifted vertically for clarity. In this way, changes of difference in the Raman spectra can be identified due to different test conditions.

Chapter 4

Tendency for Hydrolysis and Water Absorption of Oils and Key Crystalline Boron Compounds

4.1 Introduction

The first part of this chapter presents results of hydrolytic stability assessment of oils containing borates (ABE, KBE and BTE) and ZDDP additives in PAO. The results focuses on how their breakdown under thermal and/or oxidative conditions using various techniques affects copper coupons. The second part reports results of thermal and oxidative stability of oils containing about 2.5 wt. % additives in PAO using a thermo-gravimetric analyser.

The third part presents results of moisture adsorption by oils containing some additives. Finally, the results of moisture absorption by major crystalline boron compounds such as boron oxide and boric acid are presented. This results are expected to elucidate on the susceptibility of the additives in base oil to corrosion risk under thermo-oxidative conditions. In addition, the results will enable moisture adsorption potentials of these additives in the base oil with the understanding of which boron compounds is responsible for this interactions.

4.2 Results

4.2.1 Hydrolytic stability

A summary of results from hydrolytic stability measurements are shown Figure 4-1. The aged additive-free PAO and BTE were observed to have increased kinematic viscosity (KV) indicated as (+ve), that was higher than the maximum value of 6% recommended by ISO 3104 or ASTM D445. For the aged-tested sample oil containing ABE, KBE and ZDDP additives, a decrease in KV (-ve) were observed which was lower than pre-aged KV values. Above all, aged BTE additive in PAO gave the highest KV change than all other oil-containing additives that is indicative of the adverse effect of ageing on its rheology.

Changes in total acid number (TAN) of test oils were below the recommended 4 mg KOH/g limits for hydraulic fluids and oils (HF-O) standard. However, aged-oils containing BTE additives had TAN values of about four times higher than aged base oil. This is an indication of the adverse effects of the formed acid on copper coupons by certain boron compounds present in BTE aged-oils when compared to aged PAO and oils containing other additives based on results shown in Figure 4-1.
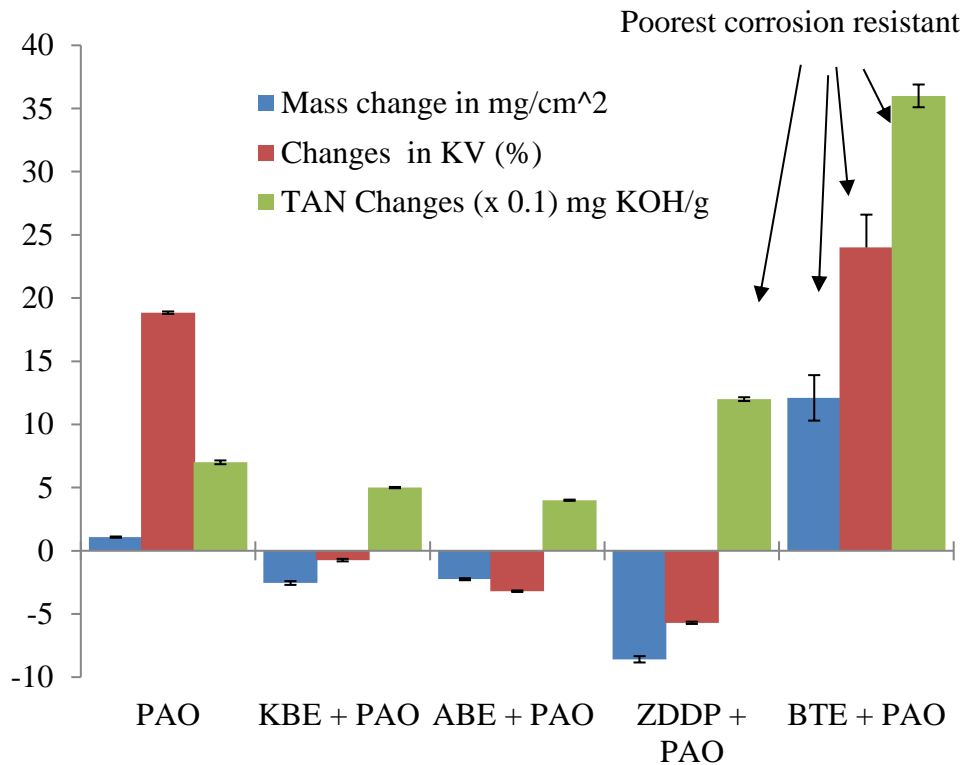
Figure 4-1 Artificial aging of oils test results using seal-bottle containing oils and copper coupons in the oven at 135ºC for 10 days

In addition, copper coupons in aged ABE, KBE and ZDDP-containing oils gave mass gain values that were below the recommended limits 0.3 mg/cm^2 for mass loss [137], but BTE gave mass loss that was higher than the recommended limit. This is an indication that oils containing ABE and KBE additives have better hydrolytic stability than BTE. The oxidation and subsequent corrosion risk to machinery and metallic surfaces with regards to lubricant degradation in service, indicated that BTE possesses

the highest corrosion risk compared to other borate additives (ABE and KBE) and ZDDP.

4.2.2 Corrosion resistant of additive-containing oils

Hydrolytic stability test results based on copper corrosion resistance of other synthetic antiwear additives are shown in Figure 4-2. The colour appearance of copper coupons in aged oils after 3 repeated tests were compared to a new coupon and standard reference chart [267]. Based on ASTM D130, the copper appearances of oils containing ABE additives and only PAO, have grades 1b (dark orange) as shown in Figure 4-2 (b) and (c) respectively. On the other hand, copper coupons in oils containing KBE additives have grade 1a (light orange) as shown in Figure 4-2 (d) that was similar to that of a fresh copper coupon.

Grades	1a	1b	1b	1a	4a	2e
	(a)	(b)	(c)	(d)	(e)	(f)
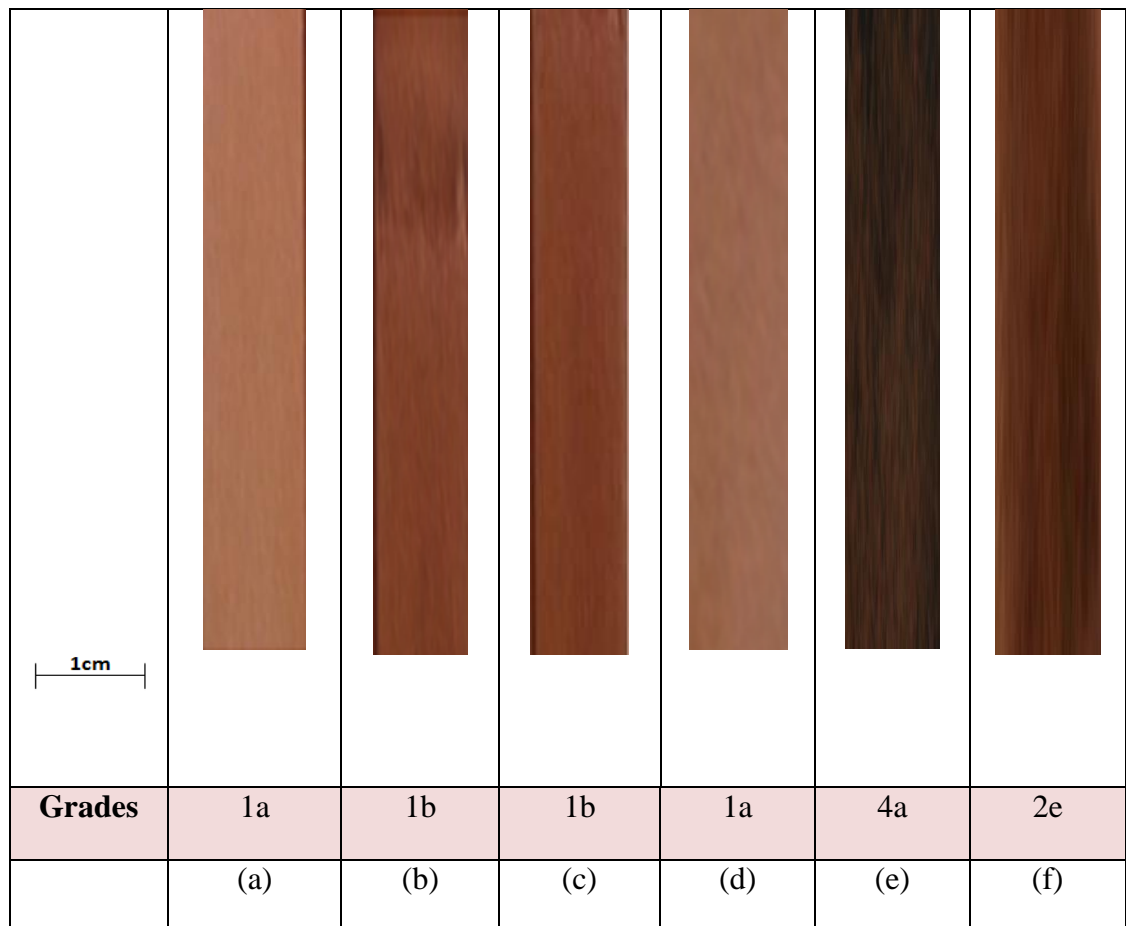
Figure 4-2 Copper coupons colour change from sealed-tube tests in; (a) New coupons with no oil, (b) Aged PAO, (c) Aged ABE, (d) Aged KBE, (e) Aged ZDDP, (f) Aged BTE

Hence, the resistance to corrosion of copper coupons by KBE-containing oils with grade 1a is considered highest, followed by ABE and PAO with grade 1b. Previous studies on hydrolytic stability of boron-containing oils has borate-based oils with grades 1a and 1b represents more stable and stable resistance to hydrolysis [133, 134]. The sealed-tube test results with copper coupons in ZDDP-containing oils gave colour grade 4a as shown in Figure 4-2 (e). This is an indication of poor chemical reaction on copper by water attack on ZDDP due to reactive sulphur in ZDDP-containing oil to form deposits on copper coupons. This was a similar result obtained by Jayne et al. [65] and Garcia-Anton et al. [66]. The copper colour changes in aged BTE-containing oils is 2e as shown in Figure 4-2 (f); moderate tarnish or brassy gold that could be an indication of poor corrosion compared to coupons from oils containing ABE and KBE. Hence, this test was able to show that ABE and KBE additives are not only more hydrolytically stable than BTE, but also have better corrosion resistance.

4.2.3 Thermo-oxidative stability

A representative thermo-gravimetric analysis (TGA) curve obtained for KBE additive in PAO is shown in Figure 4-3.
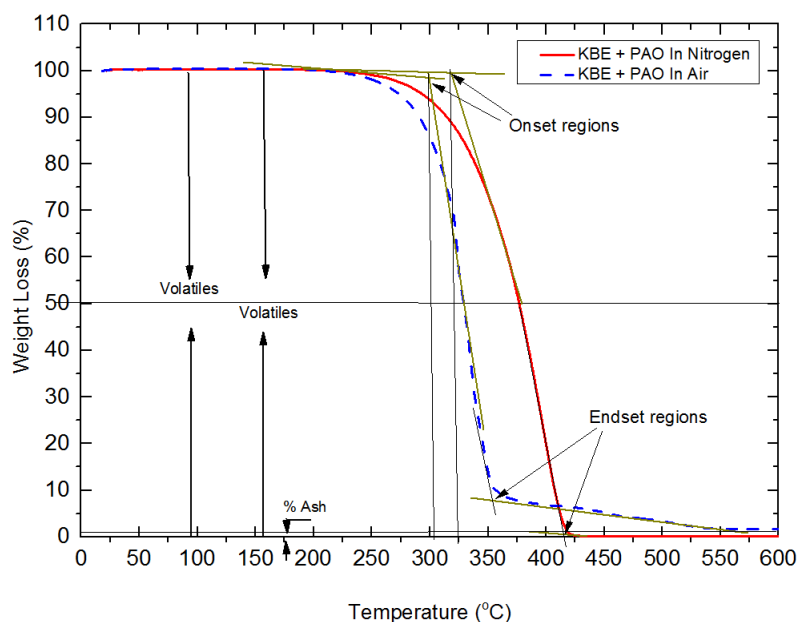
Figure 4-3 A typical TGA plot of KBE additive in oils showing thermal and oxidative degradation in nitrogen and air environments

The TGA curves for all the oils tested indicates that a two-stage thermal decomposition took place when the experiment was performed in air, unlike the single-stage thermal decomposition that was observed for all the oils tested in a nitrogen atmosphere. Table 4-1 summarizes the average onset and endset decomposition temperatures in air and nitrogen atmosphere respectively for all the antiwear additives. The onset and end set decomposition temperatures are the vertical lines through the point of intersection of the tangents to curves at both the onset and end set regions. At the onset regions, both evaporation of hydrocarbon present in the low end of the molecular weight distribution, and degradation of base oil component occurs [268]. The endset region was also attributed to decomposition of long chain hydrocarbons by the same study. Results shown in Table 4-1 indicated that thermal and oxidative decomposition of ABE and KBE are higher than BTE and ZDDP when compared to PAO.

Table 4-1 Thermal and oxidative decomposition temperature of additives

Type of Oil Sample	Onset Temperature (^{o}C)		Endset Temperature (^{o}C)	
	Air	Nitrogen	Air	Nitrogen
PAO	302.7	316.6	550.1	413.3
ABE + PAO	308.8	327.3	505.9	408.0
KBE + PAO	316.0	324.0	506.6	398.2
ZDDP + PAO	249.4	263.5	506.5	361.2
BTE + PAO	223.1	241.5	527.7	358.1

4.2.4 Moisture absorption of oils containing synthetic additives

The effects of dissolved water contamination on exposed additive-containing oils that were placed in humidity controlled chamber were used as samples for this analysis. These are used to investigate water content in the oil samples using the on-site fuel and lube oil analysis test kit as described in Chapter 3.The initial concentration of dissolved water in the oils before placing them in the humidity chamber were used as

reference. This is to obtain the relative increase of water in the oils measured with initial water content in oils measured as; ABE (0.04-0.03 %), KBE (0.06-0.07 %) and (0.04-0.05 %). Oils containing BTE additive was not considered for these test due to its immediate hydrolysis as specified in its MSDS. This is due to continuous moisture adsorption if not properly sealed in its container that will likely affect the accuracy of its results.

The differences between water content in the oils at the end of humidity tests and initial water content are shown in Figure 4-1. This result provides a quantitative analysis of how borate additives in the base oil interacts with humid air. Previous studies in the literature on the effect of humidity effect on the tribochemistry of additives have considered humidity as an extrinsic factor that can influence friction and wear performance surfaces in tribocontact. The results shown in Figure 4-4 indicated the relative increase in water content of additive-containing oils due to changes in relative humidity of the surrounding environment.
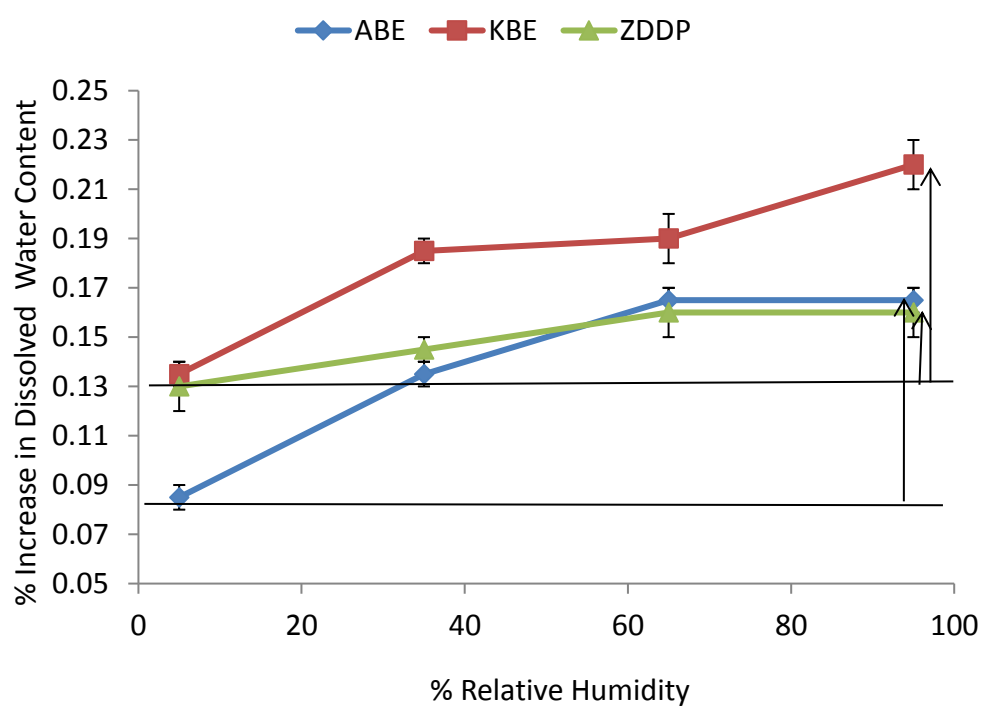
Figure 4-4 Average increase in water content of additive-containing oils due to exposure to different humidity conditions of the surrounding environment. Error is measured as standard deviation of results from three repeated samples

The increase in relative humidity between 5 and 95 %, indicated that boron-containing oils gave water content increase that are higher than ZDDP. Increased water content of the borate-containing oils was about 3 times higher than ZDDP-based oils and could have played a role in their friction response and antiwear performance in comparison to ZDDP. This is an indication that certain boron compounds in the oils could be responsible for water absorption. These could either be boron oxide or boric acid.

4.2.5 Moisture adsorption analysis of crystalline boron compounds

Figure 4-5 and Figure 4-6 shows the results of weight gain per cm^2 of crystalline boron oxide and boric acid exposed to high humidity environment at 53 ± 1.3 % RH and 20^oC of the surrounding air for a period of 24 hrs. Weight gain measurements were determined using analytical balance with a resolution of 0.01/0.1mg.
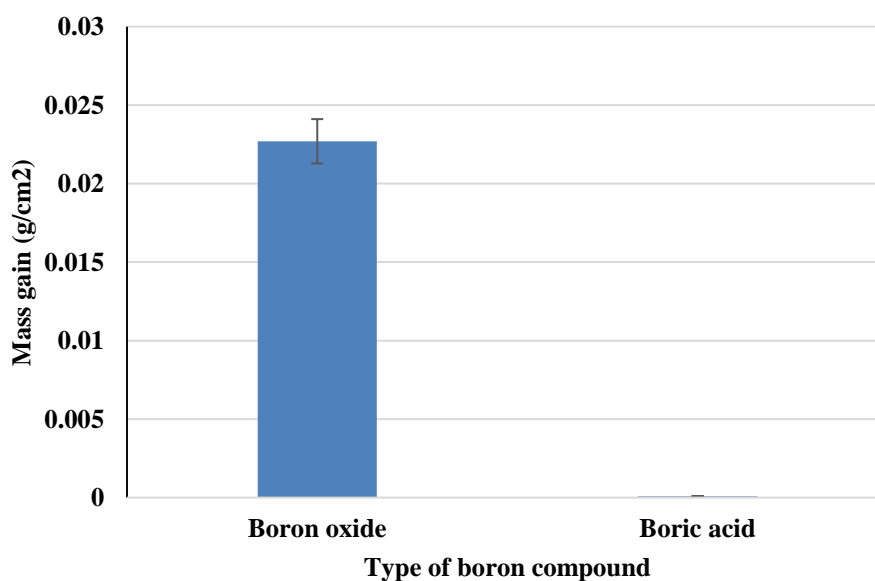
Figure 4-5 Effect of moisture on long duration exposure of boron oxide and boric acid in open air in 24 hrs exposure period. Error in these tests are measured as standard deviations of the averages of 3 test samples at $\pm$ 6.2% for boron oxide and $\pm$ 2% for boric acid

Weight changes were taken every one hour of exposing samples of boron oxide to the surrounding air for a total of 10 hour period. In addition, weight changes of exposed crystalline samples of boron oxide and boric acid to surrounding air for 24 hours were recorded as shown in Figure 4-5. The result indicated that boron oxide gave significantly more weight gain per cm^2 than boric acid within 24 hrs exposure period as shown in Figure 4-5.

However, the result of hourly weight gain per cm^2 of boron oxide as shown in Figure 4-6 is comparable to results from similar studies in the literature [269]. This is an indication that weight gain by exposed boron oxide to atmospheric air is indicative of its moisture adsorption potential, unlike boric acid. In order to further understand the chemical effect of boron oxide exposure to air of the surrounding environment, chemical characterization of crystalline boron oxide and boric acid is necessary.
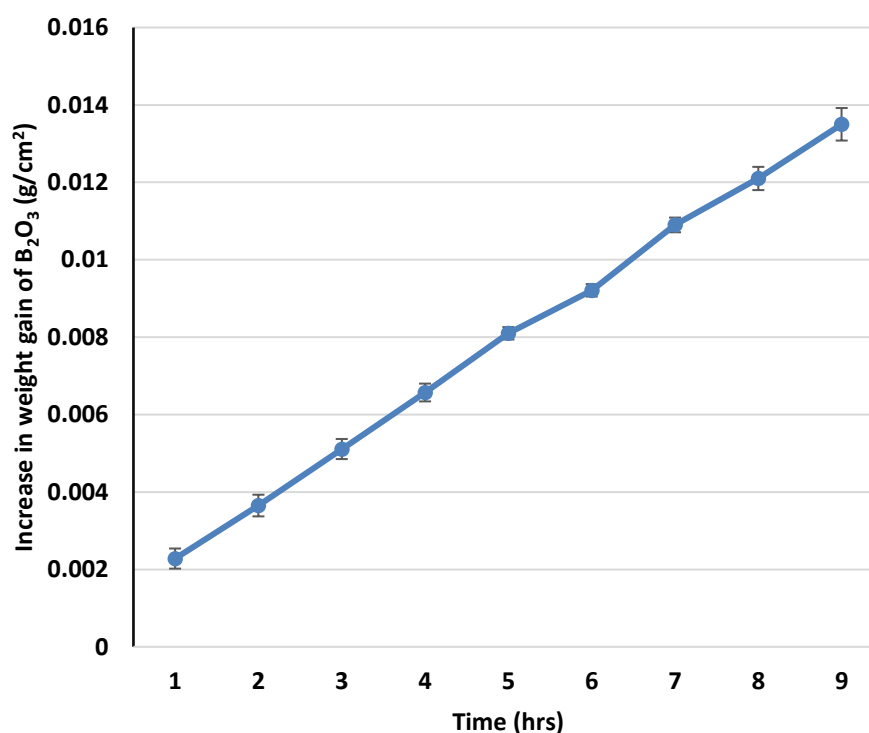
Figure 4-6 Hourly weight gain of exposed boron oxide. Error bars shown are within statistical limits of standard deviation for average of three samples

4.2.6 Raman spectroscopy of crystalline boron compounds

The results of changes in room temperature Raman vibrational spectroscopy of crystalline boric acid and boron oxide exposed to moisture-rich environment at different time intervals are shown in Figure 4-7. The results indicates that within the first one hour of boron oxide exposure to humid air, changes in its crystalline structure commences, but there was little changes in boric acid crystalline structure. After about 24 hrs exposure, most of the boron oxide peaks have changed to boric acid peaks.

The results indicate that when boron oxide with Raman shift of around 806 cm^{-1} is exposed to moisture-rich environment for long duration, boric acid is formed with its characteristic Raman peaks at 499 cm^{-1} and 867 cm^{-1} [138, 207, 221]. This result suggests that when oils containing borates are exposed to atmospheres with some appreciable quantities of moisture, boron oxide in the oil reacts with moisture to form boric acid.
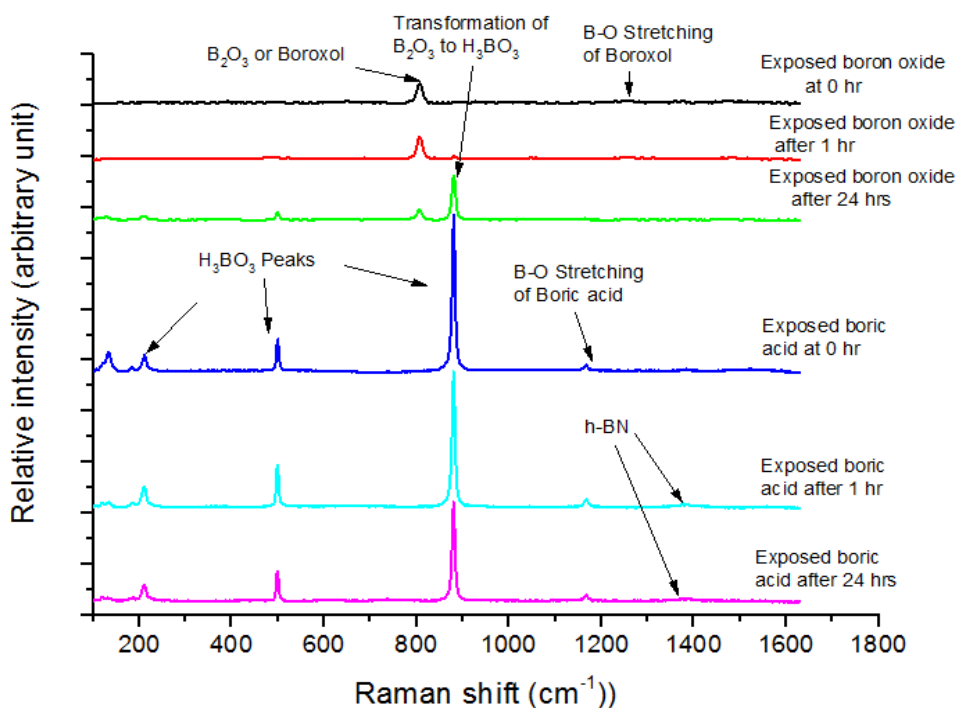
Figure 4-7 Raman of crystalline boron oxide and boric acid at different test duration. Reproducible fittings of analysed area was carried out until squared correlations of r^2 is greater than 0.995. The spectra are plotted on the same scale and have been shifted vertically for clarity

On the other hand, the Raman shift for boric acid remained unchanged throughout the exposure duration both in terms of moisture adsorption and chemical structure except for some little peaks of h-BN after longer duration above 1 hr. This could be as a result of manufacturing process as the purity of boric acid used for this experiment is about 99.5% or due to contamination by some nitrogen-containing compounds in air.

In air, Nitrogen constitutes about 78.084% by volume, 0.5 ppm of nitrous oxide (N_2O) and 0.02 ppm of NO_2 [270]. Any of these sources of nitrogen and its compounds could have been responsible for boron nitride formation. The behaviour of boric acid when exposed to moisture-rich environment to form boron nitride could likely affect its tribological behaviour in terms of wear rate, but not significantly in terms of friction coefficient reduction. This is due to the layered structure of h-BN as show in Figure 1-6.

4.3 Summary

The following key points can be made on the thermal and oxidative effects of boron-containing additives and ZDDP in PAO on their resistance to hydrolysis and thermo-oxidative stabilities. In addition, water absorption of oils and adsorption by certain crystalline boron compounds potentials are presented:

- The synthetic borate additives (ABE and KBE) have been shown to possess better hydrolytic stability than non-synthetic borate additives (BTE)

- The resistance to copper corrosion by synthetic borate additives was shown to be significantly higher than ZDDP and BTE-containing oils

- Higher onset decomposition temperature of synthetic borate additives than ZDDP and BTE is indicative of their higher thermo-oxidative stability

- Lower hydrolytic and thermo-oxidative performance of BTE compared to ABE, KBE and ZDDP raised the possibility of likely adverse effect on its tribological performance

- The result of moisture absorbing potential of oils containing boron indicates that more moisture is absorbed by oils containing boron additives than ZDDP

- Increased water absorption by boron-based oils were observed to be as a result of boron oxide in the oil than boric acid

- The presence of boron nitride on exposed crystalline boric acid is an indication that BN could form on oils or tribolayer containing crystalline boric acid without necessarily having nitrogen in the molecular structure of the borate additive. This is possible if the borate additive have high concentration of boric acid as in the case of BTE used in this study.

Chapter 5

Tribological Results at Variable Extrinsic Test Conditions

5.1 Introduction

Boron compounds as antiwear additives in lubricants used in IC engines have been considered as potential substitutes for conventional ZDDP and other P- and S-containing additives due to their classification as zero-SAP additives. Studies of the existing literature on boron-based additives in Chapter 2, suggest that there are deficiencies in the understanding of friction, wear and durability of borate-based tribofilms.

Hence, a tribochemistry study of borate additives under different extrinsic conditions is essential in understanding the use of borates in lubricant formulation. The conditions to be considered in this study are; concentration of the additives, bulk oil temperature and sliding process, humidity effects and level of water in additive-based oils. In this chapter, tribological results obtained from lubricated sliding steel pin-on- reciprocating steel plate by antiwear additives in PAO6 base oil are presented.

The first part of this experiment will investigate the effect of different borate additives in oils on the friction reduction and antiwear performance of tribofilms at different concentrations. Using the ZDDP as a reference, a comparison of friction and wear results of tribofilms from synthetic and non-synthetic borates can elucidate more on their different tribological behaviour.

A literature survey of the existing work on the effect of hydrolysis on the tribochemistry of tribofilms from borate additives as shown in chapter 2 is limited to friction reduction. In this section of Chapter 5, the effect of hydrolytic stability on the antiwear performance of certain borate additives will be investigated. The second part of this chapter will investigate the effects of temperature and sliding process influence on the antiwear performance and durability of wear-resistant metallic oxide-boric oxide glass from the synthetic borates. The literature survey in Chapter 2, showed that changes in metallic oxide composition and structural transformation in boric oxide anions as practiced in borosilicate glass manufacture, could affect the physical

properties of glasses. There is yet to be a tribological study on how transformation in boron anions and changes in boron oxide and metallic oxide compositions affects the wear-resistant and durability of borate tribofilms.

This test is sub-divided into two stages. The first stage involves carrying out friction and wear tests on additive-containing oils for 3 hr and 6 hr in order to provide an understanding of tribological response of borate tribofilms to temperature changes. The next stage involves carrying out tribofilm durability experiments using the changing oil lubricant procedure experiment at different temperatures as described in chapter 3. The tribofilm is formed with the additive present for 3 hr and stopped. The oil is replaced with additive-free base oil and the test continued for another 3 hr. This is designated as 3r3 tests.

The third part of this chapter investigates the friction and wear performance of borate-based tribofilms with respect to ZDDP additives under different levels of dissolved and free-water in the oil at room and elevated temperature. In the dissolved water experiments, the friction test rig was enclosed in a chamber fabricated from Perspex. An air circulation fan and humidity sensor was connected to the chamber. The combination of ultrasonic humidifier and air drier ensured that moist air at varying levels of dryness enters the chamber. This is to provide controlled chamber environment from fully-dry to fully-wet conditions. The conditions for the friction experiments and humidity conditions are as described in Chapter 3. Friction coefficient and wear measurements of worn plate samples from these experiments are to elucidate the antiwear behaviour of borate additives in dry air and moisture-rich atmospheres.

5.2 Friction and wear results due to changes in concentration

The tribological results of variable additive concentration at 100°C bulk oil temperature as described in section 3.43 and section 3.44 are shown in Figure 5-1 (a). In addition, the influence of base oil on the antiwear performance of oil additives containing oils on both plates and pins are included in Figure 5-1 (b). The friction coefficient results indicated that all the borate additives gave lower friction coefficient than ZDDP at 0.5 wt. % as shown in Figure 5-1 (a).
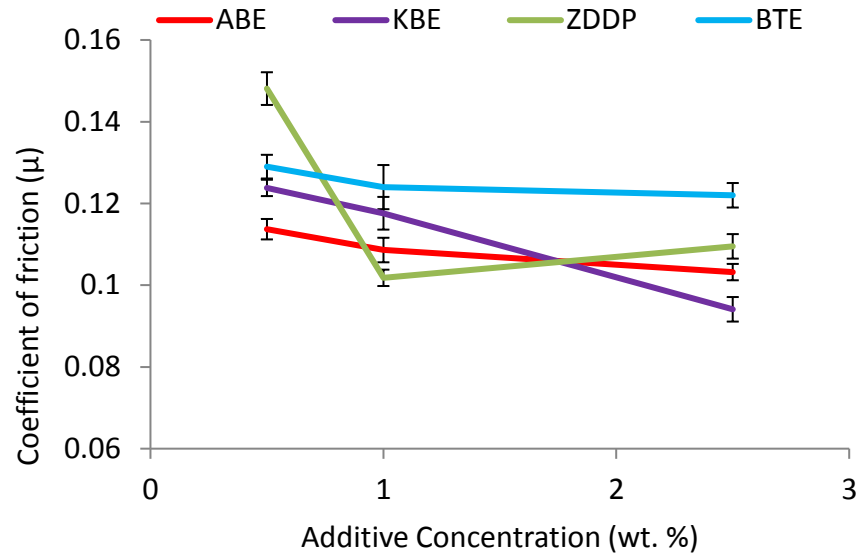
(a)
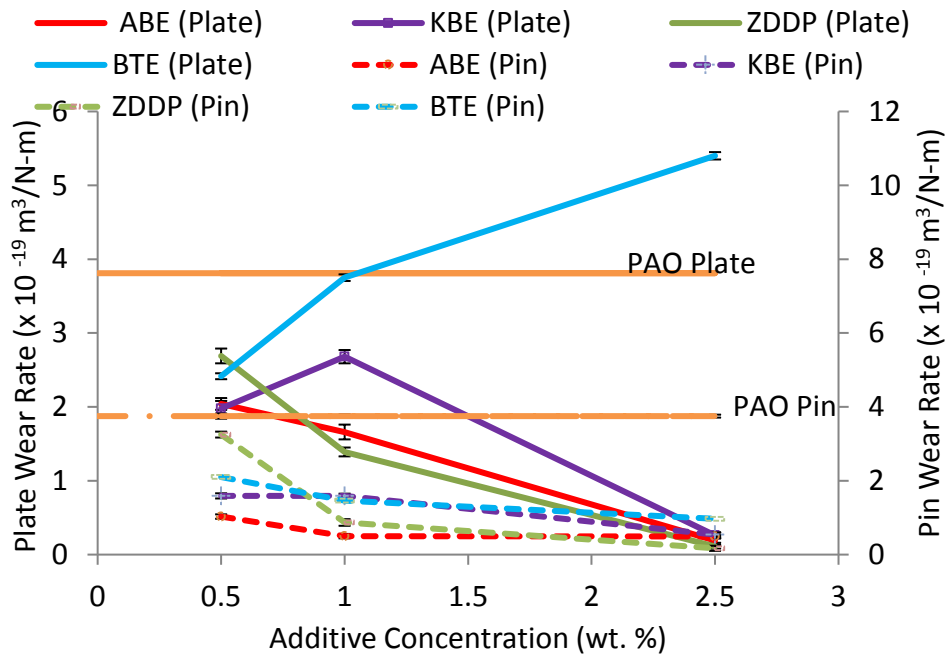
(b)

Figure 5-1 Average tribological results of different additives and concentrations at 100°C and 6 hr test duration for three repeated results with error bars to show the standard deviations; (a) steady state friction coefficient over the last one hour, and (b) pin and plate wear rates

At 1.0 wt. %, this switched completely, and ZDDP gave the lowest friction coefficient values. However, ZDDP is well known to give relatively higher friction coefficient values due to the pad-like structure of its tribofilms. At the highest concentration of 2.5 wt. %, only BTE gave higher friction coefficient values than ZDDP.

An investigation of the friction coefficient performance of tribofilms formed by oils containing KBE additive at 3.5 wt. % concentration in neutral base oil showed friction coefficient values of 0.035 [157]. The lower friction coefficient obtained in the literature could be attributed to the higher concentration of KBE additive used compared to that used in this research. However, increased friction coefficient performance of KBE with increasing additive concentration was attributed to KBE-nanoparticles not being sufficient enough within the friction zone [129, 157].

In addition, friction coefficient performance of ABE was in the range of 0.1 to 0.12. This was observed to be consistent with results from similar studies in the literature [152, 228]. The friction coefficient trace with time at 1.0 and 2.5 wt. % concentrations of the all the additive are shown in Figure 5-2 (a) and (b) respectively. The friction trace results shown in Figure 5-2, indicated that during the first 1 hr, of tribofilm formation, oils containing ABE and KBE gave lower friction coefficient than BTE. A similar friction coefficient behaviour of BTE tribofilms at 2.5 wt. % concentration was obtained as shown in Figure 5-2 (b). This could be related to the quicker formation of certain lubricious boron compound on ABE and KBE tribofilms than BTE.

However, high friction coefficient was not observed on BTE tribofilms within the first one hour of the friction test, but was comparable to that provided by ABE and KBE at 0.5 wt. % concentration as shown in Figure 5-2 (a). The high and unsteady friction coefficient behaviour of BTE during the running-in period could considerably affect its antiwear performance at 1.0 and 2.5 wt. % additive concentration. This is unlike KBE tribofilms where significant friction coefficient reduction occurred. Hence, the friction coefficient performance of the borate additives could be related to the formation and alignment of plate-like crystallites of certain low shear strength boron compounds along the sliding direction on the wear tracks of worn steel samples [27, 222, 271].
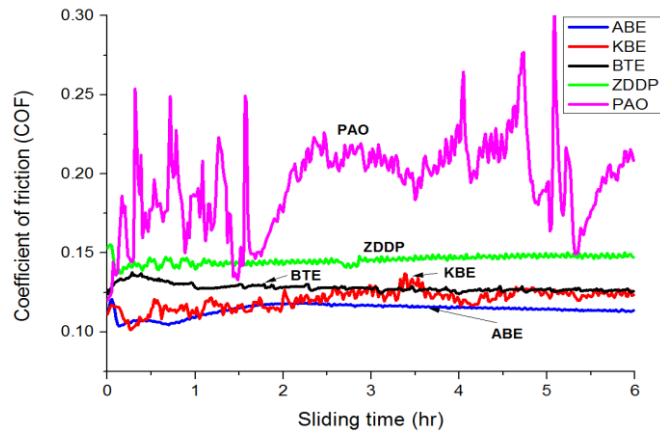
(a)
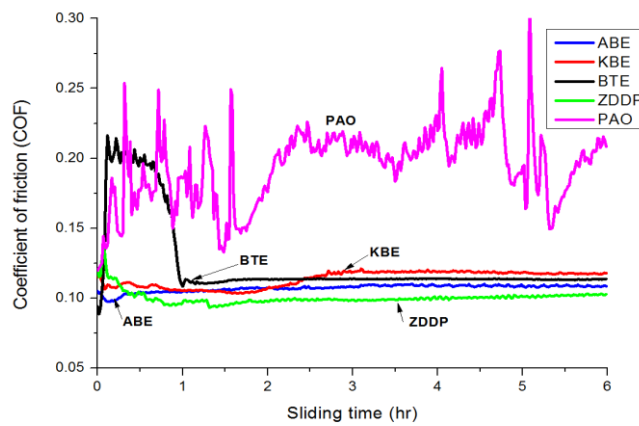
(b)
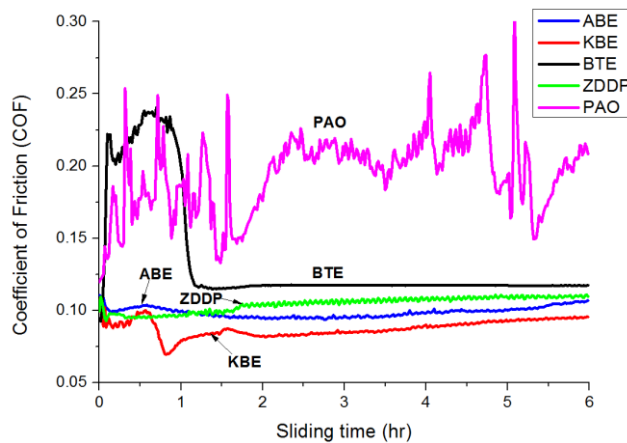
(c)

Figure 5-2 Friction coefficient trace of tribofilms formed by oils containing each additives at 100ºC test temperature and 6 hr test duration respect to PAO at different additive concentrations; (a) 0.5 wt. %, (b) 1.0 wt. % and (c) 2.5 wt. %. The error bars are excluded for clarity

However, results shown in Figure 5-2 (a) and (b) suggests that boric acid formation rate on tribofilms formed by synthetic borate additives (ABE and KBE) are different to that on non-synthetic borates ester (BTE). Results from Figure 5-2 indicated that this occurred on tribofilms formed by BTE when the additive concentration was raised above 0.5 wt. %.

The antiwear performance of non-synthetic borate additives (BTE) on the plates was distinctly different from that of other additives as shown in Figure 5-1 (b). The antiwear performance of BTE tribofilms on the plates was very poor. Higher wear rates with increasing concentration of BTE additive occurred. However, wear rate results of BTE on the pins gave comparable performance to other additives.

The poor antiwear performance by BTE tribofilms on worn steel plates compared to wear rates of the pins could be related to different tribochemistry of the reacted layers on both surfaces. This antiwear performance of ABE tribofilms in comparison to ZDDP on the plates and pins are similar to antiwear performance results from previous studies [119, 169, 272] on hydrolytically stable borate additives.

However, tribofilms on samples lubricated by KBE-containing oil was observed to give comparable plate wear performance to ABE tribofilms at all concentrations; except at 1.0 wt. %. This could be due to temperature under which the test was performed or chemistry of the tribofilms which could not provide the necessary antiwear protection.

5.3 Effect of temperature and wear process

The friction coefficient performance of synthetic borates and ZDDP tribofilms for a range of temperature and wear process as described in section 3.43 and section 3.44 are shown in Figure 5-3 (a) and (b). The results shown in Figure 5-3 (a) indicated that friction coefficient performance by tribofilms from ABE and ZDDP-containing oils are not too different from one another (± 3.3 %) at 19°C when the sliding distance was doubled (from 3 h to 6 h). However, the friction coefficient increased when the sliding time was double on tribofilms formed by oils containing KBE additives at 19°C bulk oil temperature rose to about 13.0 %.
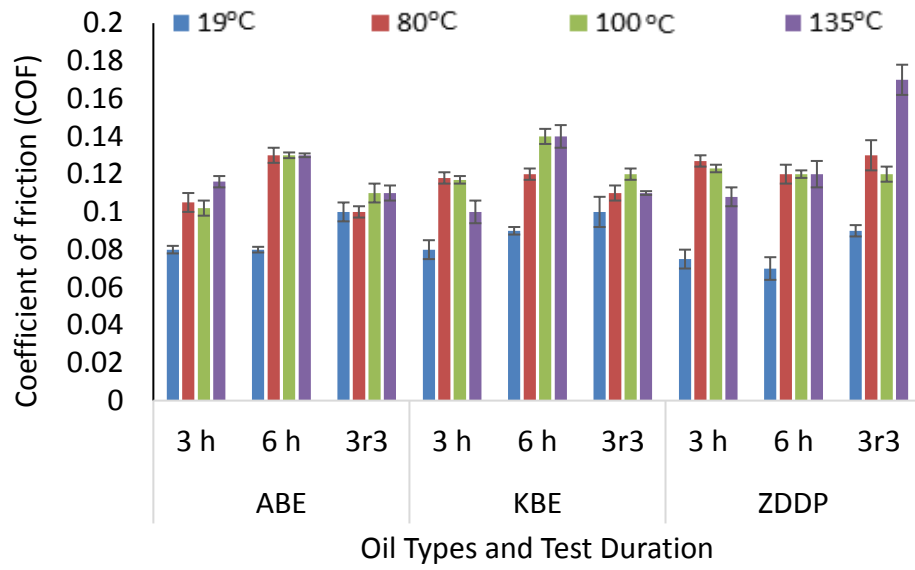
(a)
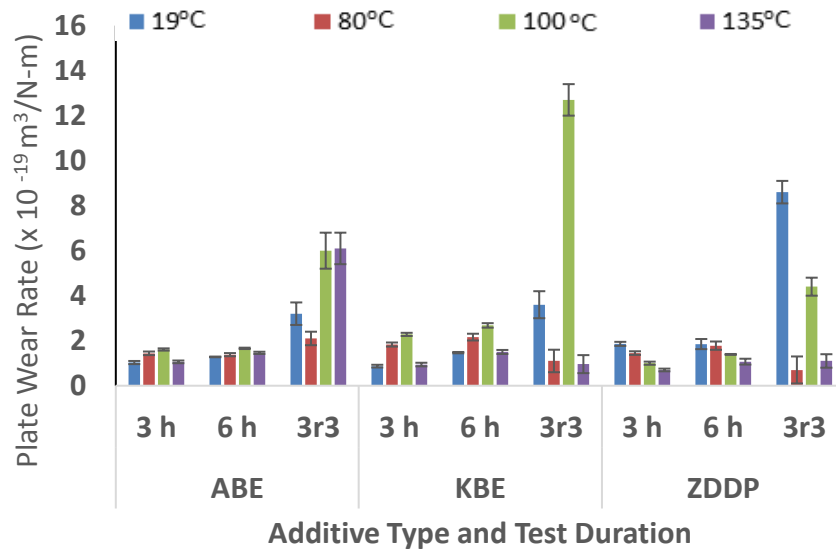
(b)

Figure 5-3 Average tribological test results for a range of temperature and wear process with error bars for three repeated samples to show the variability of the test results; (a) friction coefficient, (b) plate wear rates

In addition, tribofilms formed by each of the additives in base oil gave significantly higher friction coefficient when the sliding process was changed from 3h to 3r3; ABE (20%), KBE (13.0 %) and ZDDP (20%). This behaviour could partly be attributed to the effect of PAO or partly due to the effect of certain abrasive iron oxide that adversely affects friction reduction. At 80°C bulk oil test temperature, the friction coefficient results was higher than at 19°C. In addition, there was no significant changes in friction coefficient when the sliding distance was doubled (from 3 h to 6 h) on tribofilms formed by oils containing KBE (± 2.0 %) and ZDDP (6.0 %); but was considerably higher for ABE (24.0 %). However, when the sliding process was changed from 3 hr to 3r3 at 80°C, there was no significant increase in the friction coefficient performance of tribofilms from oils containing ABE and KBE additives. On the other hand, ZDDP tribofilms gave considerable increase in friction coefficient performance at 80°C when the sliding process was changed to 3r3 compared to 3 h tests. A similar friction coefficient response increase was observed from ZDDP tribofilms at different temperatures [21, 89]. The friction coefficient behaviour of tribofilms formed by ABE and KBE increased at 100°C when the sliding process was doubled (from 3 h to 6 h), unlike that of ZDDP that remained unaffected by this increase. A similar situation occurred when the sliding process was changed to 3r3 at 100°C. This is an indication that friction coefficient of ZDDP tribofilms is not significantly affected by sliding process at the test temperature of 100°C.

At 135°C tribotests temperature, the friction coefficient performance of tribofilms from all the antiwear additives increased when the sliding distance was increased from 3 h to 6 h. However, when the sliding process was changed from 3 hr to 3r3, tribofilms formed by the borates gave reduction in friction coefficient; ABE (11.0 %) and KBE (23%). On the other hand, ZDDP tribofilm gave increased friction coefficient (57.0 %) at 135°C tribotest temperature. This is an indication that durability of borate tribofilms in terms of friction coefficient is better than ZDDP at 135°C tribological test temperature. Hence, the different friction coefficient results from the antiwear films subjected to different temperatures and sliding distance could be related to the chemistry of their formation. These appears to depend on temperature and the sliding process as previously observed in the literature for ZDDP tribofilm [21, 47, 48].

The wear coefficient results shown in Figure 5-3 (b) indicated that all the antiwear additives gave higher wear rates with increasing temperature. However, wear rates of tribofilms from borate tribofilm increased up to 100°C temperature before decreasing

at 135°C to wear rate values that is similar to that one obtained at 19°C. This could be related to the physical and chemical nature of their tribofilms.

This behaviour was quite different to that of ZDDP tribofilm which gave decreasing antiwear performance that was consistent with results from similar study by Morina et al. [21]. At 100°C tribotests temperature, the boron-containing tribofilms both gave higher antiwear performance irrespective of the sliding distance. This behaviour could be related to the chemistry of the reacted layers at this temperature. For the borate-containing tribofilms, there were no significant changes in their antiwear performance when the sliding distance was doubled; unlike the antiwear performance of ZDDP antiwear films that varies with temperature and sliding distance. However, the antiwear behaviour of borate-based tribofilms at 3 hr and 6 hr test durations appeared to be sensitive to temperature rather than sliding process.

Durability performance in terms of wear rates during the 3r3 test conditions as shown in Figure 5-3 (b) indicated that borate-based tribofilms are more durable than ZDDP at 19°C. As temperature increases to 135°C, ZDDP tribofilms gave better durability performance than ABE and KBE-based tribofilms within this test temperatures; except at 135°C, where KBE-based tribofilms gave comparable antiwear performance to ZDDP.

In addition, durability of the borate tribofilms at 100°C was very poor when compared to ZDDP. This could be related to changes in the physical and chemical structure of the borates at this temperature. A tribological study of boron-containing oil at 100°C had observed weaknesses in the wear resistance potential of the borates at this temperature [273]. The result from this study could be used to elucidate the influence of borates and ZDDP in gear and lubricating engine oils as described by Kim et al. [81] and Komvopoulos et al. [82] respectively. Based on the results from this study, ZDDP in fully formulated oils containing borates plays a major role in providing better antiwear protection and durability than the borate additives at 100°C. On the other hand, antiwear performance and durability at ambient temperature and boundary lubrication regime could have been enhanced by borates in lubricating oils of IC engines during cold-starting operations.

5.4   Effect of water-based contaminants on friction and wear

The average friction and wear performance of all the antiwear additives under the influence of dissolved and free water are shown in Figure 5-4 (a) and (b) respectively. In Figure 5-4 (a), friction reduction by ABE and KBE-containing tribofilms when the relative humidity (RH) was varied between 5 and 95% RH indicated that both borate tribofilms gave friction coefficient performance that was lower than tribofilms formed without free- or added-water. However, friction coefficient performance of ZDDP tribofilms was not significantly different to its friction response without added water. This frictional behaviour of ZDDP tribofilms with water contamination was similar to that observed in the works of Cen et al. [83].

The performance of borate tribofilms between 65 % and 95 % RH suggests an interaction with moisture to form certain borate compounds with low shear strength and lubricious tribolayer. The decreasing coefficient of friction trends are similar to that from boron permeated surfaces [145, 184]. The literatures studies in Chapter 2 had shown that friction reduction performance of borate additives is due to the formation of certain low shear strength boron compounds within the friction zone. Friction results shown in Figure 5-4 (b) indicated that changes in free water content in oils containing ABE was lower than KBE and ZDDP up to 1.5 wt. % before drastically increasing by about 28 %.

In addition, ZDDP friction response at different added water concentrations was observed to be comparable to KBE-based tribofilms; except at 2.5 wt. % water content. Literature studies in chapter 2, had attributed friction reduction performance to the presence of low shear strength magnetite film (Fe_3O_4) and the protective oxide film formed by oxygen could reduce metal-to-metal contact under boundary lubrication [274, 275]. The relative antiwear performances of tribofilms from all the additives-containing oils and contaminated with free-water will be assessed and compared to the wear rates of tribofilms when there was no free-water added to the oil as shown in Figure 5-4 (b). The results indicated that tribofilms from all the additives gave increased antiwear performances up to 1.0 wt. % free-water in oil. However, when the free-water in the oil rose to 1.5 wt. %, the antiwear performance of ABE-containing tribofilms reduced, unlike KBE and ZDDP.
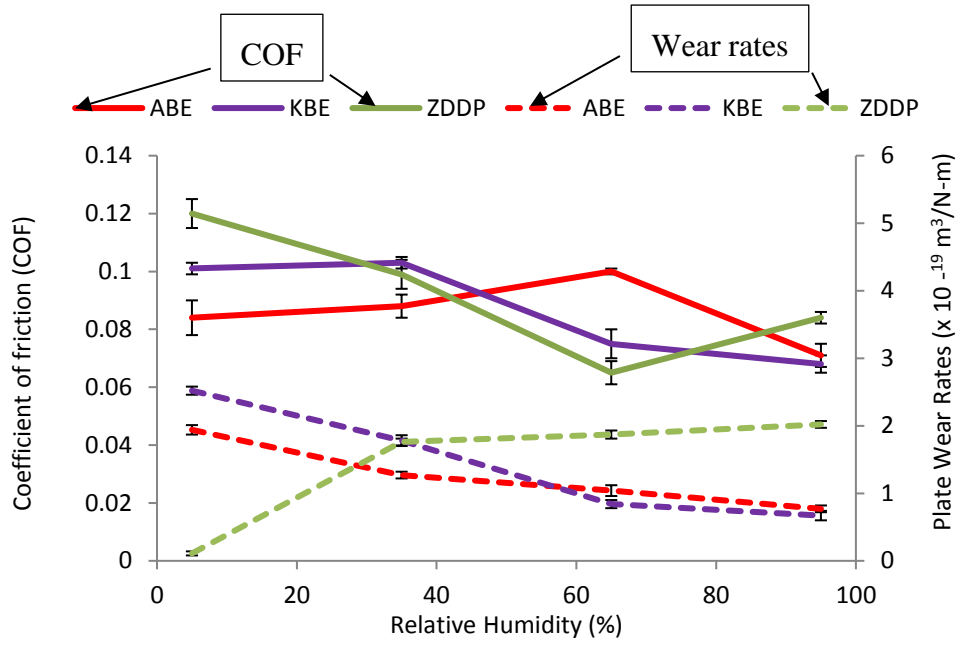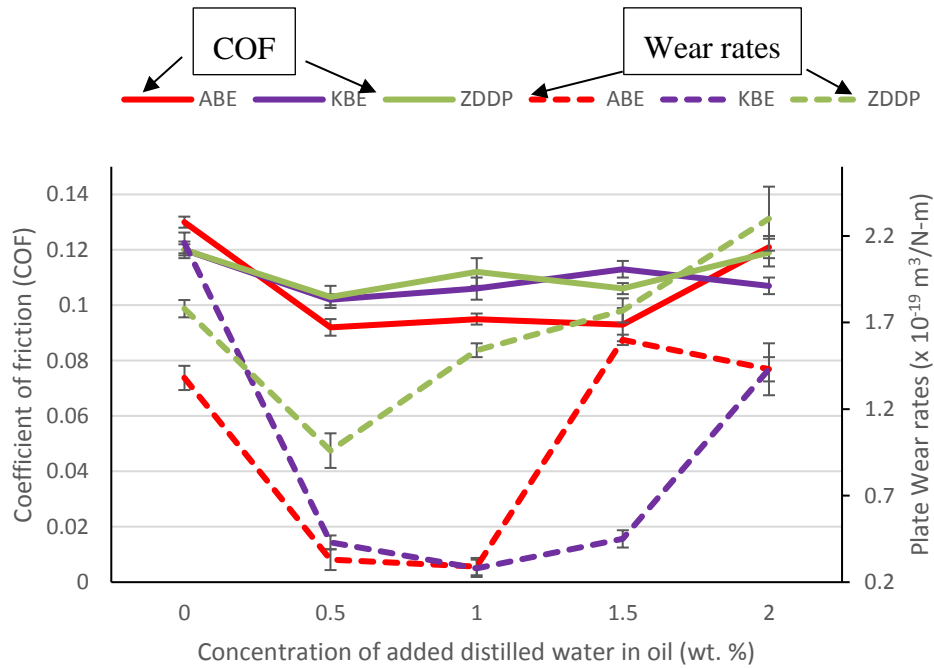
Figure 5-4 Average tribological test results due to; (a) dissolved water for 3 hrs at 19°C, and (b) free water for 6 hrs at 80°C. Error bars indicates standard deviations of three repeated experiments

106

As the level of free-water contamination of oils containing the additives was increased to 2.0 wt. %, the antiwear performance of ZDDP tribofilms was reduced, unlike the enhancement provided by ABE and KBE. These results are consistence with similar work in the literature on the interaction of humidity with tribofilms from boron coated systems [145, 184, 185]. However, wear rates of ZDDP-based tribofilms at 0.5 wt. % was observed to increase with increasing water content that was consistence with increasing wear trends with respect to increasing free-water content of the oil in the work of Cen et al. [83]. This is an indication that tribofilms formed by oils containing KBE additives contaminated by 2.0 wt. % free water formed a more effective antiwear film ABE and ZDDP.

5.5 Summary

Tribological test results are summarized as follows:

- At 0.5 wt. % additive concentration, tribofilms formed by oils containing boron gave better tribological performance than ZDDP

- The tribofilms formed at 2.5 wt. % concentration by synthetic borate additives (ABE and KBE) gave comparable tribological performance to ZDDP, unlike BTE that gave catastrophic wear rates

- The tribofilms formed by ZDDP-containing oils had been shown in the literature to be influenced by bulk oil test temperature and wear process. In this study, borate tribofilms was also shown to be influenced not only by temperature, but also by the sliding process

- The durability of borate tribofilms in terms of friction coefficient performance was found to be comparable to ZDDP at 19, 80 and 100°C tribotest temperature, but were significantly better than ZDDP at 135°C

- The antiwear performance of tribofilms from ZDDP-containing oils was found to increase with increasing temperature. This is unlike tribofilms from oils containing boron additives that gave decreasing antiwear performance at 80 and 100°C. However, at 135°C tribotest temperature, tribofilms from oils containing ABE and ZDDP gave decreased antiwear performance

- The durability of tribofilms from oils containing ABE and KBE in terms of wear rates were observed to be better that ZDDP at 19°C. However, tribofilms

from oils containing ZDDP gave better durability than borate-containing oils at 80 and 100ºC. In addition, enhanced durability in terms of wear rates was provided by tribofilms from oils containing KBE compared to ZDDP at 135ºC

- Tribological tests results indicates that in dry air, tribofilms formed by ZDDP-based oils gave better antiwear performance than oils containing borate additives. However, lubricious boron compound was formed on the borate tribofilms that provided better friction reduction than ZDDP in moisture-rich environment

- As humidity of the surrounding environment increases, antiwear performances of tribofilms formed by the borates increases, but that of ZDDP decreases. This result confirmed the earlier results from the literature that dissolved water contamination did not enhance the antiwear functions of tribofilms formed by ZDDP, unlike those formed by oils containing synthetic borate additives

- Tribological test results on the effects of free water contamination on the antiwear functions of borate tribofilms indicated a positive synergy. This is unlike tribofilms formed by oils containing ZDDP additives that gave adverse antiwear performance when the free-water added into the oil exceeds about 1.5 wt. % concentration.

In order to fully understand the tribochemistry that took place at variable; additive concentration, temperature and sliding time/process, induced tribo-oxidation due to humidity and free-water in the oil, further surface characterization of the tribofilms are necessary. The results of physical and chemical characterization of tribofilms formed under variable test conditions are presented in subsequent chapters. Physical characterization of tribofilms is to provide answers on how changes in morphology, thickness and hardness of the tribofilms affect their tribological behaviour. On the other hand, chemical analysis of the borate tribofilms will elucidate on how the friction reducing and antiwear mechanisms of borate tribofilms are influenced by different extrinsic test conditions.

Chapter 6

Results of Tribofilm Physical Characterization

6.1   Introduction

In this chapter, the physical nature of tribofilms generated from tribological tests results were presented from the preceding chapter are assessed using various surface analytical techniques described in chapter 3. Characterization of tribofilms are necessary in order to understand how changes in the physical nature of the tribofilms affects tribological performance. These physical parameters are; (a) variation in thicknesses of different tribolayer from one additive type to the other, (b) changes in tribofilm morphology with additive concentration, temperature and sliding time/process, and water contamination, (c) changes in the nanomechanical response of tribofilms formed at; (a) different concentrations of additives in oils, and (b) temperature and sliding time/process.

6.2   FIB-SEM experiment results

Figure 6-1 shows the high magnification focused ion beam and secondary electron (FIB-SEM) images of the tribofilm cross-section formed by oils containing BTE additives at 1.0 wt. % concentration in PAO, 100$^{\text{o}}$C test temperature and 6 hr test duration as described in Chapter 3. The cross section of SEM image of the milled tribofilm at x 1000 magnification is shown in Figure 6-1 (a). In order to determine the thickness of the tribofilms, SEM image of the trench at 54$^{\text{o}}$ angle relative to the surface and x 15000 magnification shown in Figure 6-1 (b). The differences between contrasting layers due to electron densities of different materials are taken as tribofilm film thickness at four points on the milled section. This same technique was used in estimating tribofilm thickness from oils containing ABE, KBE and ZDDP. The thicknesses of the antiwear films were averaged along the cut as observed in the literature [188, 276]. The summary of FIB-SEM results for tribofilm thicknesses of all the antiwear additives are shown in Table 6-1. Figure 6-1 (b) indicates that built-up tribofilms are heterogeneous based on different thickness results measured along the milled sections as shown in Figure 6-1(a) to (d). Similar heterogeneity was

observed on tribofilms containing other additives. Results from samples lubricated by ZDDP-containing oils gave tribofilm average thickness of about 78 nm.
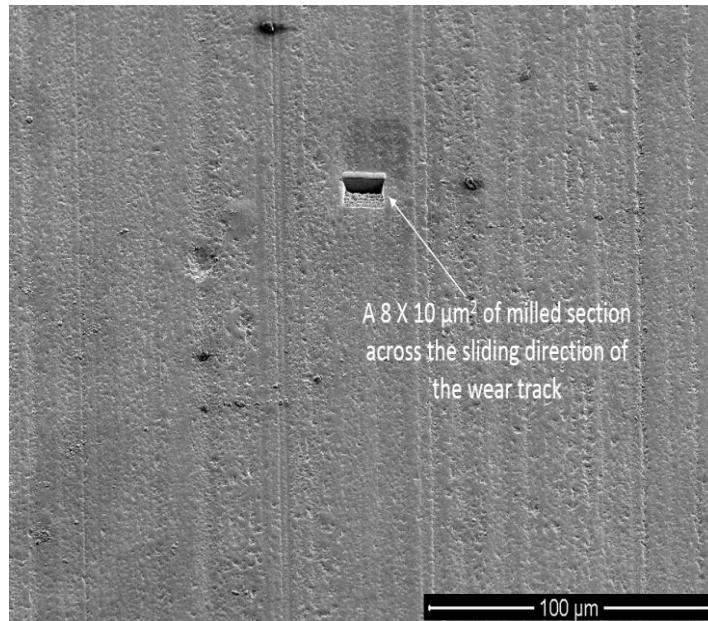
(a)
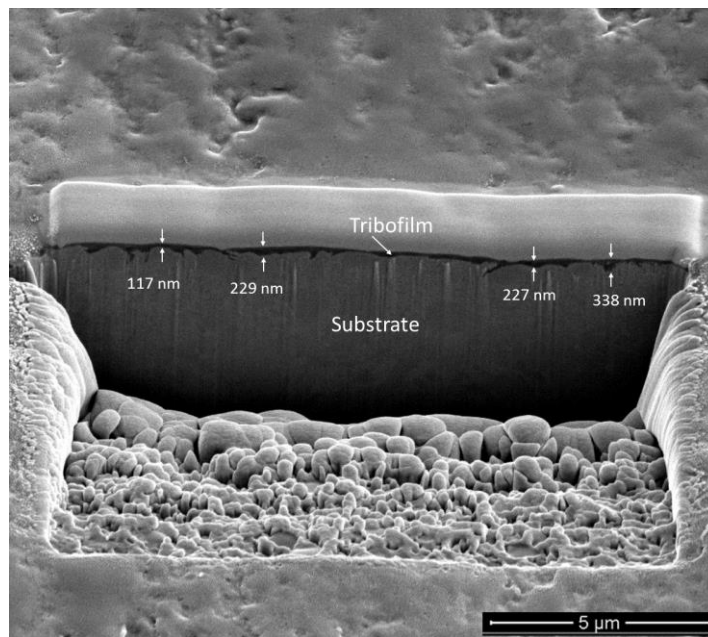
(b)

Figure 6-1 FIB-SEM image of the trench at 54° angle relative to the surface on tribofilm milled on the wear scar of steel plate sample lubricated by oil containing 1 wt.% concentration of BTE additives at 100°C and 6 hrs test duration of (a) milled section at x 1000 magnification, (b) milled section at x 15000 magnification

Results shown in Table 6-1 indicates that the thickness of borate-containing tribofilms vary from about 66 nm to about 230 nm. This is in good agreement with literature studies which estimated borate tribofilms thickness in the range of 100 nm to 200 nm [10, 80, 117]. Tribofilms from BTE gave the highest film thickness, but with poor antiwear performance as shown in section 5.2 of chapter 5. The results of tribofilms thickness of the small section on the wear tracks as shown in Figure 6-1 and Table 6-1 may not represent their thicknesses across the entire surface, but gave an indication of their variability and heterogeneity. This is due to the likely differences between thicknesses of thermal films formed outside the friction zone and tribofilms formed to protect the contacting asperities.

Table 6-1 FIB-SEM tribofilm thickness of worn samples lubricated by 1.0 wt. % additive concentrations at 100ºC tribotest temperature

Additive Type	Tribofilm thickness at different points on milled sections (nm)				Average tribofilm thickness (nm)
	1	2	3	4	
ABE	45	55	55	111	66 ± 26
KBE	57	96	102	128	96± 25
BTE	117	229	227	338	228 ± 78
ZDDP	55	106	66	86	78 ± 19

Unlike thicker BTE-based tribofilm thickness, thinner ABE-containing tribofilms provided adequate wear protection to sliding surfaces despite its low tribofilm thickness, as shown in Figure 5-1 (b). This could be related to the chemical composition of its wear resistant glass or its mechanical properties. However, KBE-based tribofilms gave thicker films than ABE, but with poor antiwear performance compared to ABE at 1.0 wt. % additive concentration as shown in Figure 5-1 (b). Hence, results from this study suggests that thick tribofilms do not

necessarily confer better antiwear performance, but rather the chemical nature of reacted layers also plays a role.

6.3 AFM topography results

An approach for adoption in this investigation is to use the AFM as described in Chapter 3 to obtain morphology image of the tribofilms. AFM measurements were acquired in two sizes. One is to have a qualitative assessment of the tribofilms image over a larger area on worn plate sample surface over a scan area of 50 x 50 µm in order to have a better overview of the surface. The other approach is to have a quantitative evaluation of a smaller scan area of 5 x 5 µm in order to assess tribofilm in terms of surface roughness and distance between dark and bright regions.

By measuring the surface roughness and distance between dark and bright regions (in form of image height sensor) on plate samples for six AFM image scans of the small area, a comparison of tribofilms morphology and thickness will be possible. This is to provide a better insight into the morphology of tribofilms formed by organoborate, metal borate dispersions and ZDDP at different test conditions as comprehensively described in chapter 3. These test conditions are; variable; additive concentration, temperature, sliding time and process, humidity and free-water in oil contamination.

The tribofilms formed by borate-containing oils on ferrous surfaces are known to contain boric acid and boron oxide due to their self-replenishing and self-lubrication properties [221]. On systems containing only these compounds, the morphology of tribolayer formed was described as plate-like crystallites [220]. However, on ferrous surfaces, zinc borate containing oils were shown to form small and patchy pieces of tribofilms with irregular and stretched shaped that was scattered over the worn surface [153]. The description of this morphology in the study could neither be linked to borates in the oil or presence of zinc.

In addition, the morphology of tribofilms formed by organoborate in oils could be significantly different to metal borate dispersions. Hence, it is necessary to investigate how borates in the oil affect tribofilm morphology compared to ZDDP at different concentrations, water contamination, temperatures, sliding distances and sliding process.

6.3.1 AFM results for varying additive concentrations

The AFM morphology at 50 x 50 μm^2 of tribofilms formed on worn plate by different antiwear additives at 1.0 wt. % concentration in the base oil at 100°C tribotest temperature are shown Figure 6-2 (a) to (d). This was particularly considered based on the tribological test results in section 5 which indicates that tribofilms containing KBE and BTE gave poor antiwear performance at 100°C test temperature compared to ABE and ZDDP-containing tribofilms.

Images shown in Figure 6-2 are assumed to represent the entire worn surface. The morphologies of ABE and ZDDP as shown in Figure 6-2 (a) and (d) appears to form smoother surfaces than KBE and BTE as shown in Figure 6-2 (b) and (c).

(a)   (b)

(c)   (d)
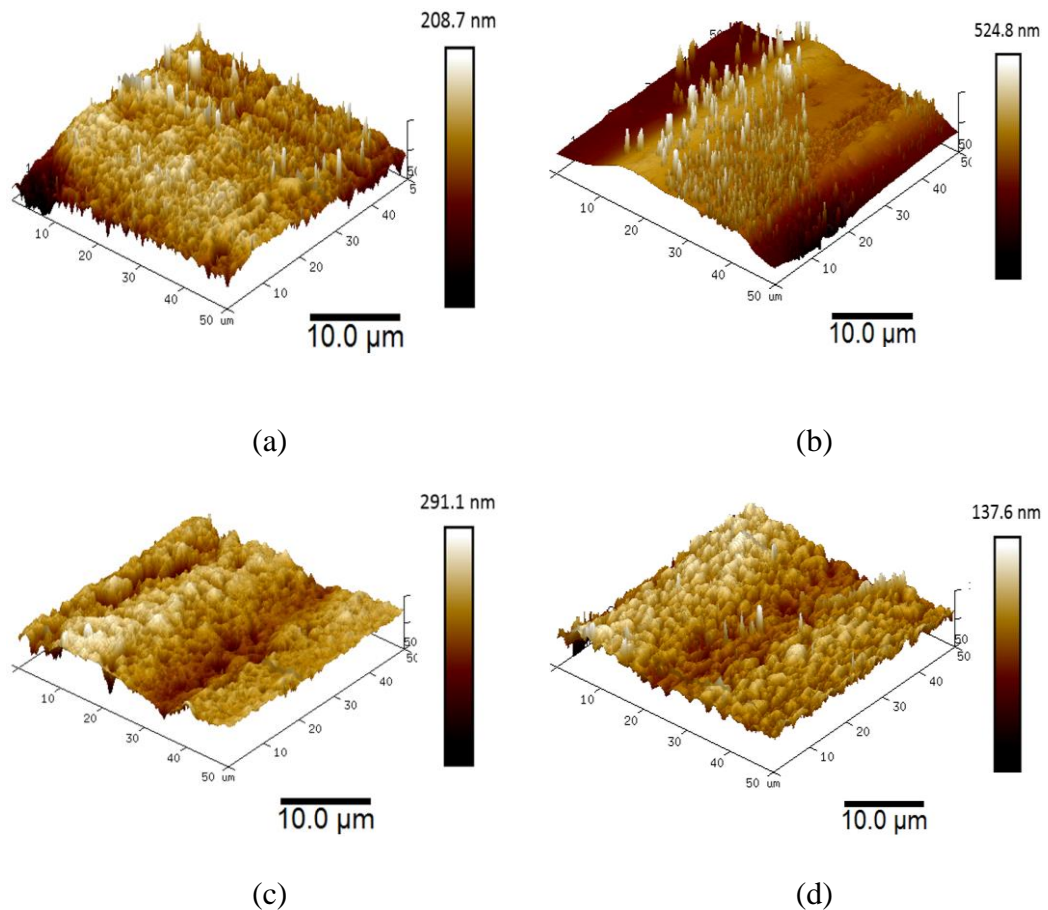
Figure 6-2 Representative AFM images at six points on the tribofilms formed at 100°C tribotest temperature for 6 hr duration and 1.0 wt. % additive concentration over a 50 x 50 µm area; (a) ABE, (b) KBE, (c) BTE and (d) ZDDP

Tribofilms formed by the organoborate (ABE and BTE) are similar to that of ZDDP, but different to metal borate nanoparticle dispersion. The white regions on AFM morphology of ZDDP tribofilms have been described in the literature to represent the top of the tribofilm that consisted of polyphosphates and dark regions represent the unreacted layers of additive [19, 49, 111]. This could also be a physical mixture of boron oxide and iron oxide as described in the literature [117]. The whitish appearance on borate tribofilms was described in the literature [40] as boric acid crystallites formed when boron oxide interacts with moisture of the surroundings.
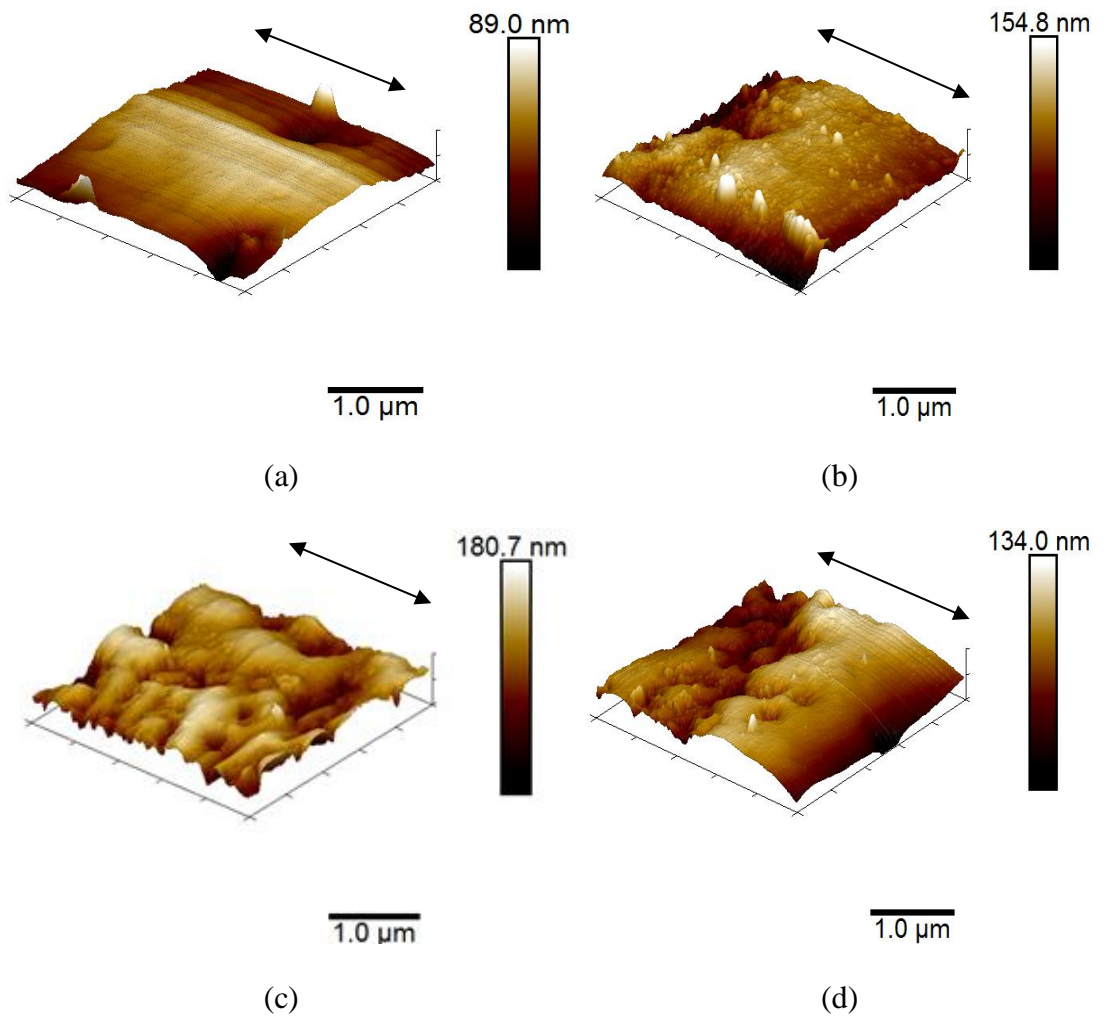
Figure 6-3 Representative AFM images at points on the tribofilms formed at 100°C for 6 hr test duration evolution of antiwear additives at 0.5 wt. % additive concentration and 100°C; (a) ABE, (b) KBE, (c) BTE and (d) ZDDP

Figure 6-3 (a) to (d) shows the topographic image of the tribofilms formed at 0.5 wt. % concentration by all the additives over an area of 5 x 5 μm^2. The morphology of BTE-containing tribofilms images formed by at 0.5 wt. % additive was shown in order to elucidate on its physical characteristics that provided better tribological performance than tribofilms formed at 1.0 and 2.5 wt. %. A quantitative assessment of tribofilms formed at different concentrations in terms of surface roughness and distances between peaks (bright regions) and valley (dark regions) on tribofilms for ABE, KBE and ZDDP are presented in Figure 6-4 (a) and (b). The image height sensor is the vertical distance between the bright and dark regions on the image. These were deduced from the morphology of images formed over 5 x 5 μm^2 scan area on wear tracks of worn samples at different additive concentrations. This distances are larger on BTE-based tribofilms compared to those from other additives at all concentrations. Hence, these results supported the FIB-SEM tribofilm thickness measurements in section 6.2, where tribofilms formed by BTE were shown to have the highest film thickness.

At low concentration; up to 1.0 wt.%, the build-up of KBE-containing tribofilms was observed to contain some nanoparticles that was estimated around 100 nm size [129, 157]. The thicker tribofilms formed by BTE over other additives does not translate to better antiwear performance. In order to further elucidate on how thick tribofilms formed by BTE additives at 1.0 and 2.5 wt. % concentration in the oils are, a combination of image height sensor results and surface roughness characterization of tribofilm morphology are shown in Figure 6-2 (a) and (b). Results of surface roughness with increasing additive concentration indicates that significant variations did not occur on ABE and ZDDP, but did occur on BTE and KBE. Figure 6-2 indicated that tribofilms formed by oils containing BTE at 1.0 wt. % concentration is not only thick, but also rough. The changes on BTE tribofilms at 2.5 wt. % are observed to be higher than those from PAO lubricated steel samples. On the other hand, the thickness of tribofilms formed by KBE at all concentration were comparable, but higher surface roughness at 1.0 wt. % than at 0.5 resulted into higher wear rates as shown in Figure 5-1 (b). In addition, high tribofilm thickness formed at 1.0 and 2.5 wt. % additive concentration of BTE additive, both gave poor antiwear performances. However, the wear rates of BTE at 1.0 and 2.5 wt. % concentration in the oil is very high compared to PAO as shown in Figure 5-1 (b). The image height

sensor appeared to provide results that did not agree with wear and surface roughness trends in this instant Figure 6-4 (a) and (b). Hence, tribofilm thickness measurement using FIB/SEM method appear to be more reliable than AFM technique. However, when the concentration of KBE was increased to 2.5 wt. %, the resulting surface roughness and wear rates was comparable to ABE and ZDDP tribofilms, unlike BTE.
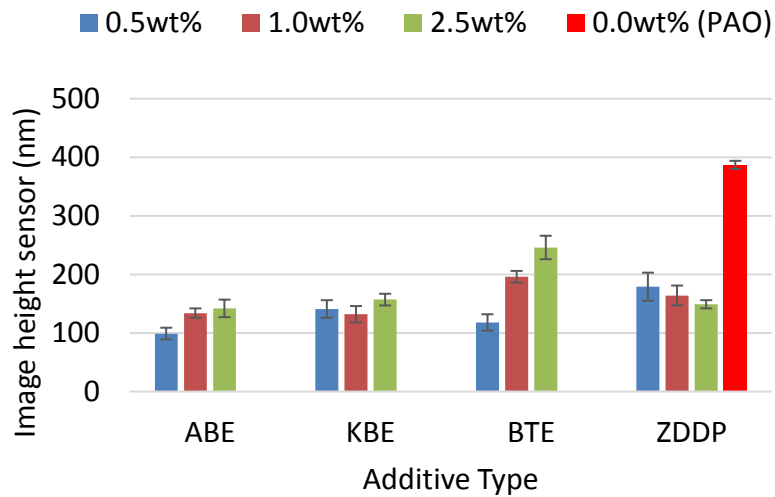
(a)
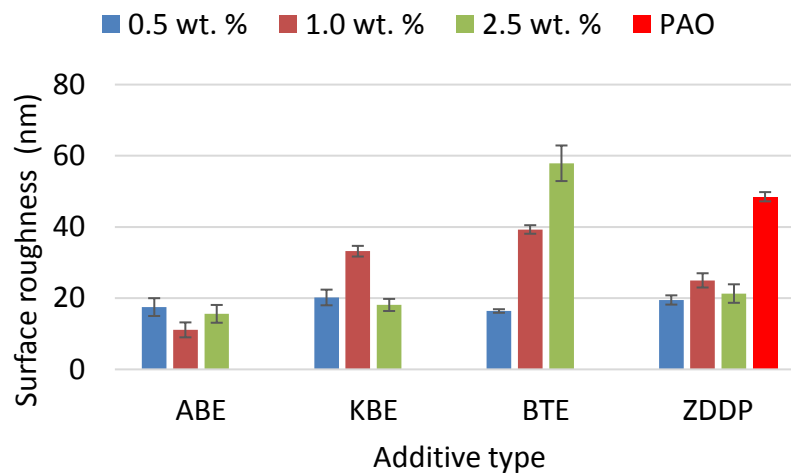
(b)

Figure 6-4 Average AFM morphology characterization of tribofilms formed at 100ºC from variable concentrations tribotests for 6 hr duration at; (a) image height sensor, (b) surface roughness. The error bar indicates the standard deviation of six points on the tribofilm

This suggests that increased concentration of KBE in base oil could affect its tribofilm morphology to give comparable antiwear performance to ABE and ZDDP as shown in Figure 5-1 (b), and as obtained in the literature [129, 157].

6.3.2 AFM images for a range of temperatures and test durations

Figure 6-5 (a) to (c) represent changes in morphology of tribofilms formed by all the additive-containing oils at 19°C and sliding distances except for BTE. This was excluded because of its poor thermo-oxidative stability performance and antiwear performance as shown in Chapter 4 and Chapter 5 respectively.

The choice of images from 19°C tribotest was considered due to most tribological test results at room temperatures indicated that tribofilms formed by borates at this temperature gave enhanced antiwear performance and durability compared to ZDDP [152, 153, 277]. In addition, boron oxide is known to react spontaneously with moisture of the surrounding environment to form boric acid [154, 220], which was also confirmed by this study in section 4.2.5. Hence, it will be interesting to present the morphology of borate films formed under tribo-oxidative condition due to frictional flash temperature. The images of morphologies of tribofilms from all the additives at 19°C are shown in Figure 6-5.

These images indicated that morphology of all the tribofilms formed are different. Tribolayer formed by ZDDP appeared to form thin and rough patches stretched along the sliding directions. However, the tribolayer formed by ABE appeared to not only be thicker, but also was smoother than KBE and ZDDP. The AFM results as shown in Figure 6-5 (a) and (b) suggests differences in morphology of tribofilms between both organoborate additives and metal borate dispersions. A summary of the average peak to valley heights are shown in Figure 6-6 (a). In addition, the average surface roughness of the 5 x 5 µm² at different spots on the tribofilms is shown in Figure 6-6 (b). The reacted layers formed by KBE have patchy and irregularly shaped tribofilms protecting the asperities. AFM morphology results of borate tribofilms suggest that different borates as additives in lubricating oils have different morphology response to concentration changes in oils. In this case, quantitative analysis of these tribofilms will provide a better understanding of these changes. Representative average peak to

valleys heights of antiwear films from all the additives at different temperature and sliding time are shown in Figure 6-6 (a).

Thick protective tribolayer

(a)

Big, patchy and irregular shaped stretched tribofilm
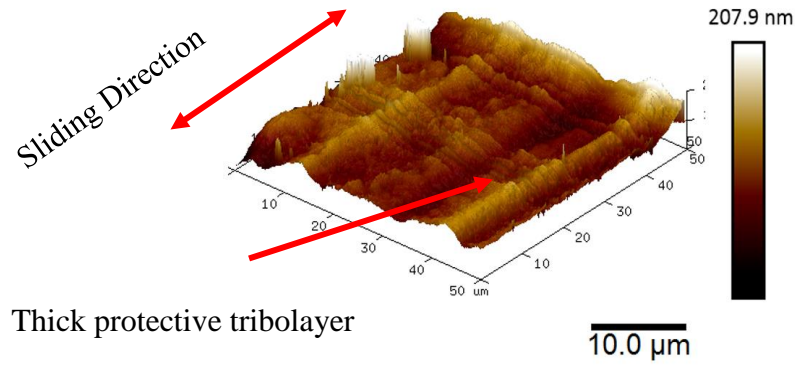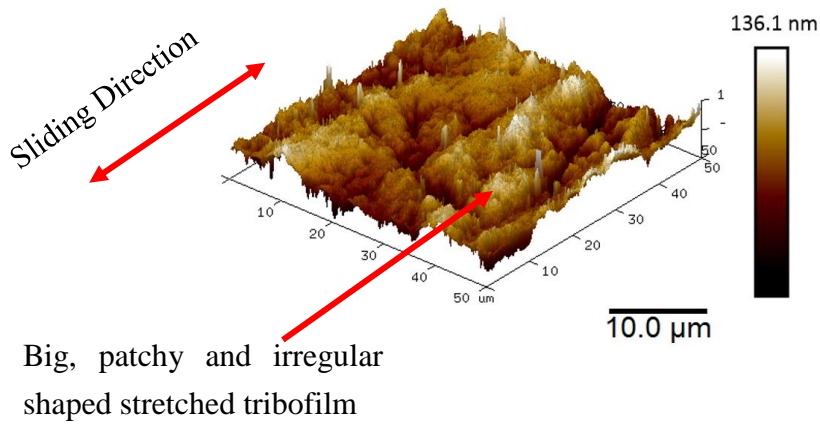
(b)
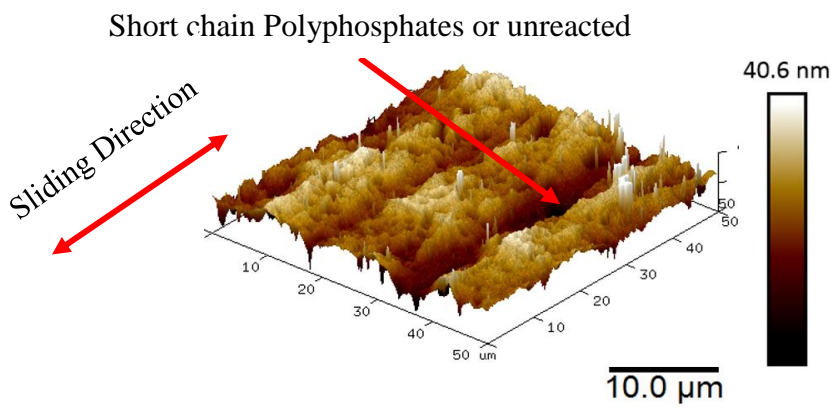
(c)

Figure 6-5 Representative AFM images at six points on the tribofilms formed at 19°C tribotest temperature and 1.0 wt. % additive concentration in the oil for 3 hr test durations over a 50 x 50 µm² area; (a) ABE, (b) KBE and (c) ZDDP

Height differences between the white and dark regions on ZDDP tribofilms between 3 hr and 6 hr are in agreement with the film thickness under similar condition for secondary ZDDP in the literature [91, 92].
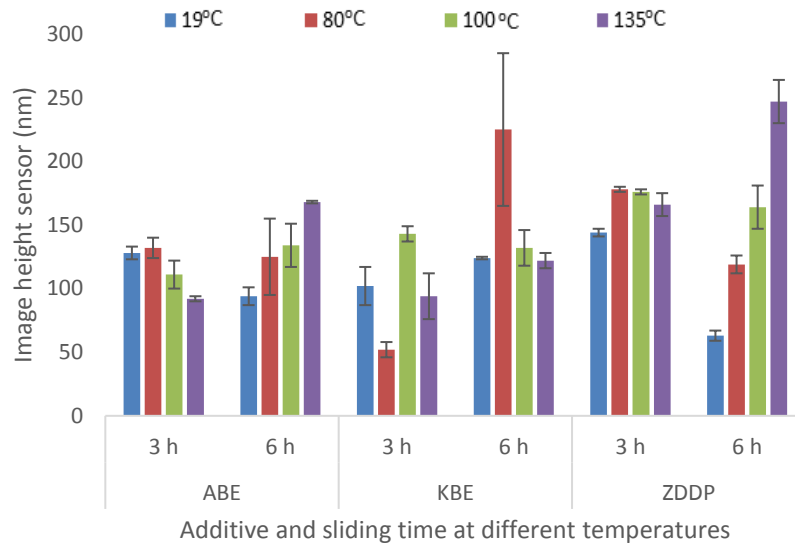
(a)
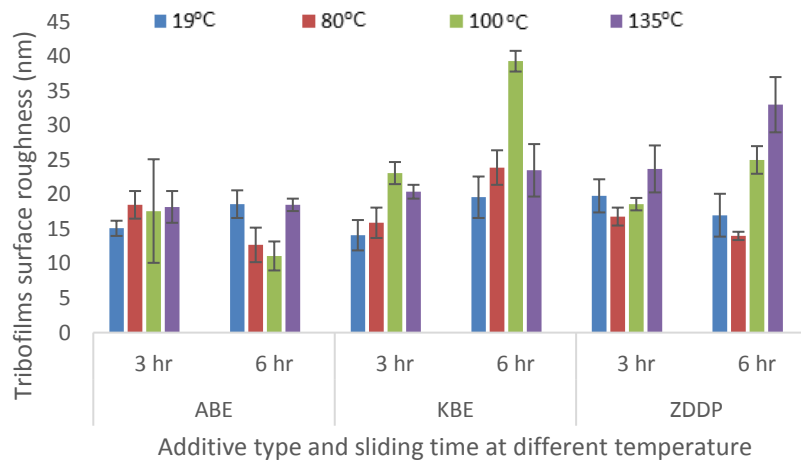
(b)

Figure 6-6 Changes AFM topography characterization at six points on the tribofilms at different temperatures and sliding time and temperature; (a) image height sensor, (b) surface roughness. The variability of the measurements are indicated by the error bars associated with the average of repeated values

The thickness or image height of ZDDP tribofilms is believed to result from rapid formation of a reaction product that promotes film removal [91, 92]. Hence the thickness of the tribofilms formed by oils containing ZDDP were observed to depend on temperature and sliding distance. At lower temperatures (e.g. 19, 80 and 100°C), the height differences between the white and dark regions on ABE-based tribolayer followed similar trend as that from ZDDP; increased temperature and sliding rates resulted into increased tribofilm thickness. On the other hand, significant change in height difference between white and dark regions on KBE tribofilms occurred only at 80°C; when the sliding time was doubled.

Figure 6-6 (b) shows that no significant changes in surface roughness occurred between 3 and 6 hr on ABE tribofilms at all temperatures. However, the significant changes that occurred in surface roughness of KBE tribofilms between 3 and 6 hr was mainly at 100°C. Similar changes in surface roughness was also observed on ZDDP tribofilms at 135°C. Hence, the roughness of borate tribofilms appears to be more stable than ZDDP at 135°C tribotests temperature that could be attributed to different chemistry of their reacted layers.

6.3.3 AFM Image of pre-formed tribofilm after 3r3 tests

In these tests, the morphology of tribofilms formed during the durability experiment at different temperatures were assessed using the AFM. These are tribofilms formed by additive-containing oils for 3 hrs test durations and briefly stopped without disturbing the preformed tribofilm to allow for the replacement of the oil with PAO only for another 3 hr tests. In this way, changes in the morphology of preformed tribofilms can be assessed and linked to tribological performances shown in Figure 5-3. The morphology of pre-formed tribofilms for all tribofilms from the additives after lubrication with PAO at 135°C shown in Figure 6-7 (a-f) revealed how the stabilities of these tribofilms are affected by sliding process. In this instance, there are more white regions on preformed antiwear films of ABE and ZDDP than KBE at the end of 3r3 tests. This is an indication that under these test conditions, more reacted layers are formed on preformed tribofilms of ABE and ZDDP than KBE due to the effect of added base oil.

3hr   **3r3**

(a)   (b)

(c)   (d)

(e)   (f)
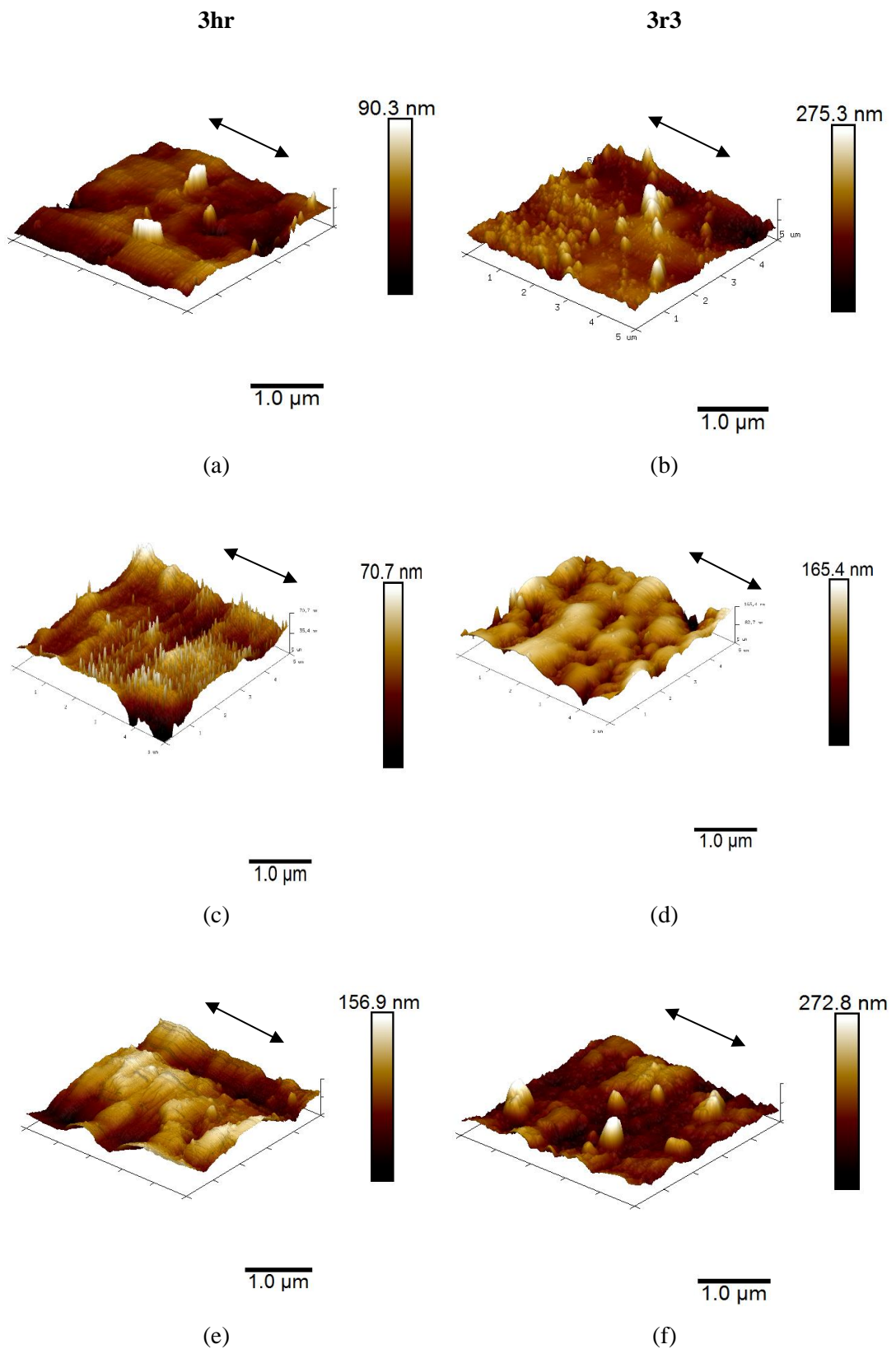
Figure 6-7 Representative six topographic images at 5 x 5 µm size on tribofilms
formed at 135°C and different sliding process; (a) ABE (3hrs), (b) ABE (3r3),
(c) KBE (3hr), (d) KBE (3r3), (e) ZDDP (3hr) and (f) ZDDP (3r3)

121

In addition, adsorption mechanisms of ABE and ZDDP tribofilms compared to the adhesion and electrophoresis mechanisms of nanoparticle metal borates (KBE) [201] could have played a role in this morphology behaviour.
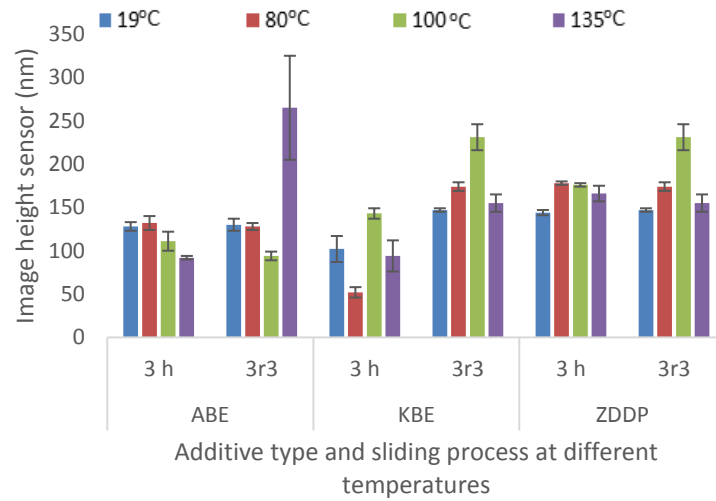
(a)
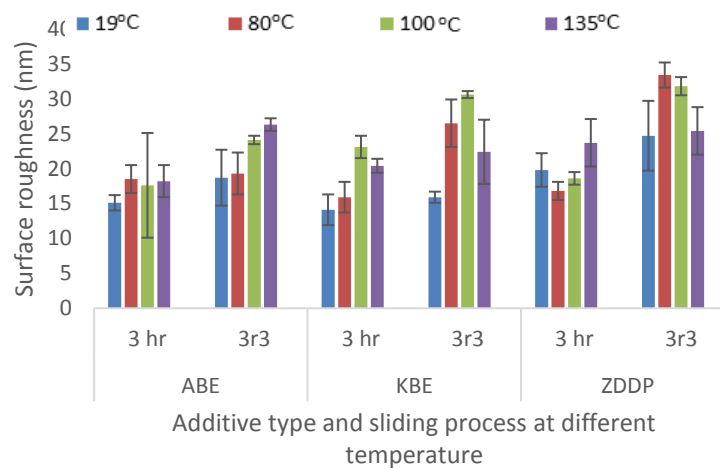
(b)

Figure 6-8 Average effects of temperature and sliding process on AFM morphology parameter on tribofilms formed by the antiwear additives; (a) image height sensor, (b) surface roughness. Error bars represents standard deviation of the average of six experimental points on the tribofilms

The effect of PAO on preformed KBE resulted in tribofilm build-up with less visible nanoparticles potassium borates as shown in Figure 6-7 (c) and (d). At 3 hr sliding process, antiwear films formed by ABE had less dotted spots on the surface than at 3r3 tests. Figure 6-8 shows the effects of PAO on preformed tribofilms at different sliding process based on image height. Results indicated that distances between the white and dark regions on pre-formed ZDDP and ABE tribofilms were not greatly affected by PAO at all temperatures, except at 100°C and 135°C respectively. On the other hand, height difference between the white and dark regions on pre-formed KBE tribofilms was greatly affected at all temperature due to the effect of added PAO. In addition, changes in the surface roughness of preformed tribofilms at different temperatures are shown in Figure 6-8 (b). The surface roughness of pre-formed ZDDP and KBE tribofilms were greatly affected at 80 and 100°C by PAO addition.

On the other hand, the surface roughness of preformed ABE tribofilms was significantly affected at 135°C. This is an indication that surface roughness of different borate tribofilms are considerably affected between 80 and 135 $^{\circ}$C. This is unlike ZDDP at 135 $^{\circ}$C which was not significantly affected. The errors on surface roughness measurements appeared to be higher than image height sensor reading. Hence, combining the two parameters enable morphology assessment of tribofilms to be qualitatively and quantitatively analysed in order to link their effects to tribological performance.

6.3.4 AFM morphology changes due to humidity contamination

Representative AFM topographic images of wear scars of worn samples from dissolved water are shown in Figure 6-9. AFM results in Figure 6-9 (a), (b) and (c) indicate that in dry air, there are more tribofilm patches on ZDDP than ABE and KBE. This is an indication that chemical reactions due to tribological processes involving borate containing oils in dry air was less than ZDDP; as there are many regions of unreacted surface exposed for AFM detection. However, Figure 6-10 (d), (e) and (f) shows that in moisture-rich environments, there are less dark patches on the borate tribofilms than in dry air. This indicates that more chemical reactions took place in moisture-rich environment than in dry air.

The average changes in heights of AFM topographic images of tribofilms from oils lubricated by ABE, KBE and ZDDP during dissolved water contamination for all relative humidity conditions are shown Figure 6-10 (a) and (b).

(a)

(b)

(c)

(d)

(e)

(f)
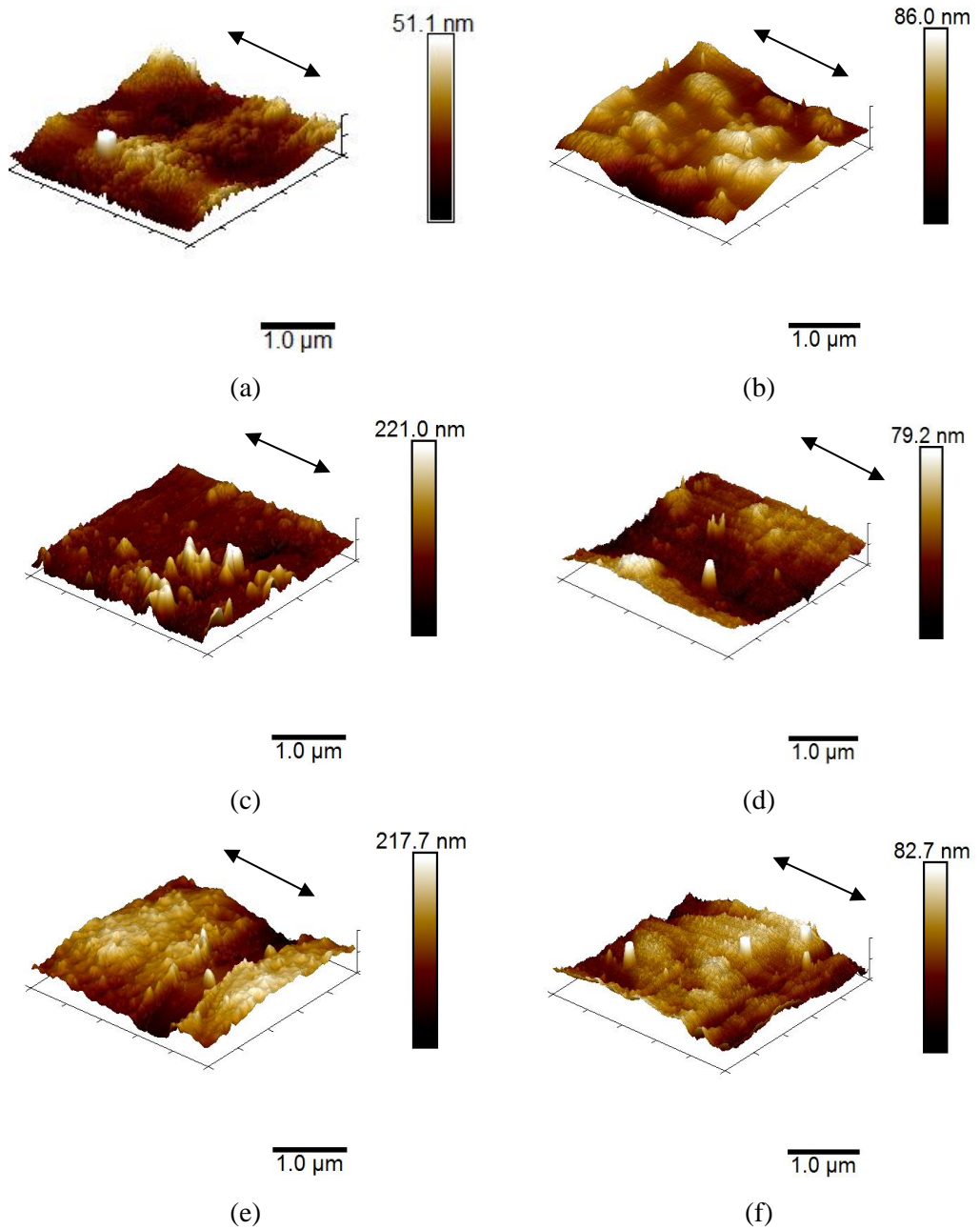
Figure 6-9 Representative AFM morphology of six points on tribofilms formed at extreme relative humidity conditions; (a) ABE-5%, (b) ABE-95%, (c) KBE-5%, (d) KBE-95%, (e) ZDDP-5%, and (f) ZDDP-95%

In this instant, changes in morphology of tribofilms for all the additives took place within the range of humidity test conditions under which the test was carried out as described in chapter 3. In Figure 6-10 (a), there was no significant difference on the image height sensor of ABE tribofilms with increasing humidity, unlike KBE that was significantly affected.
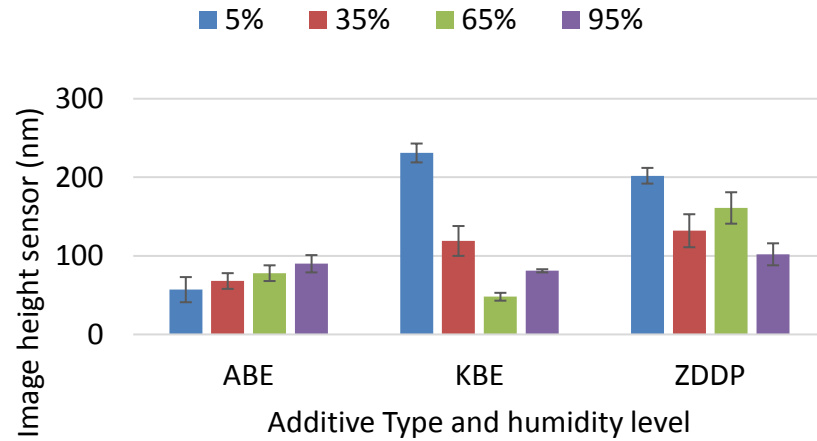
(a)
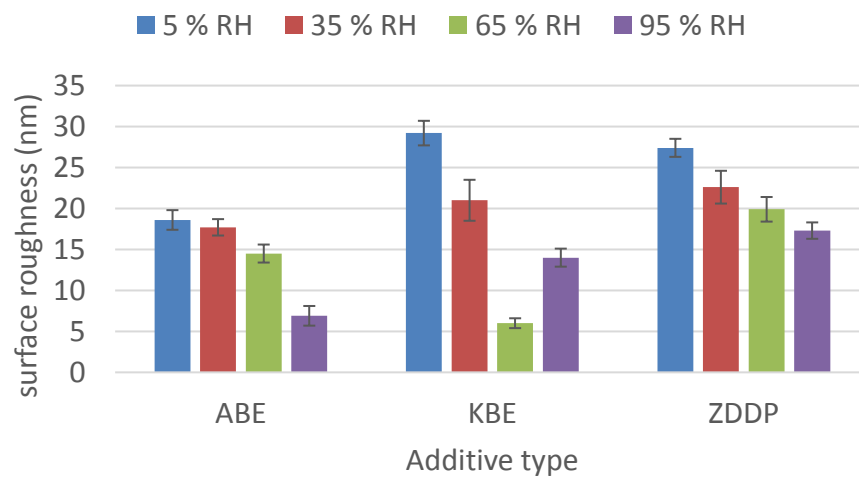
(b)

Figure 6-10 Average AFM parameters of images on tribofilms from six different points formed by additives at different levels of dissolved water contaminations on the wear scars; (a) peak to valley heights and (b) surface roughness. Errors bars represents the standard deviation of the average of six data points on the tribofilms

However, height differences between white and dark regions on tribofilms formed by ZDDP are greatly affected in dry air and moisture-rich environments. AFM surface roughness results shown in Figure 6-10 (b) of the tribofilms formed by all the antiwear additives at different humidity level indicates decreasing roughness with increasing humidity. The lowest height sensor and surface roughness was given by KBE tribofilms at 65 % RH. Results of decreasing surface roughness with increasing humidity from this study are consistent with results from similar studies in the literature which attributed this behaviour to tribochemical surface polishing [184, 185]. Previous studies on the morphology of tribofilms containing borates was shown to consist certain boron compounds with plate-like crystallites of boric acid [27, 138, 278].

The morphology of borate tribofilm formed on ferrous substrate in this study revealed how reacted layers change with dissolved water contamination, but did not identify any plate-like crystallites of boric acid. This is an indication that some other boron compounds that consists of other polyborate could be present on these tribofilms apart from boric acid. Some of the results on roughness could be due to the intrinsic nature of the tribofilm, representing the chemical reactivity. However, it could also be due to worn tip effects during the scan. The tip was changed every two samples due to the time and work load. If the tip was worn, the roughness can be less than what is presented on the graphs.

6.3.5 Nanoindentation results for varying concentration tests

The nanoindentation results of tribofilms lubricated by different additives and concentrations are shown in Figure 6-11. In this test, hardness measurement were carried out to elucidate on the hardness of borate tribofilms in comparison to the ferrous substrate as suggested by Kreuz et al. [117] or not; as investigated by Zhao et al. [153]. In this depth-sensing nanoindentaion test results, KBE tribofilms gave the lowest average hardness results from about 100 indents on a flat section of the central part of the wear scars. The average hardness value for KBE tribofilms was 2.9 ± 0.17 GPa. Micro-indentation test of tribofilms formed by zinc borate ultra-fine powder yielded hardness values of 5.8 - 8.8 GPa that was lower than the ferrous substrate [153]. The average hardness of tribofilms formed by oils with ABE and

ZDDP additives at 1.0 wt. % concentration were 6.74 ± 0.8 GPa and 4.29 ± 0.3 GPa respectively. Previous nanoindentation experiments on ZDDP wear scar had yielded hardness values of 4.7 GPa and 3.6 GPa [97, 279], while hardness results for amine phosphate wear scar that was similar to amine borate gave wear resistance results of 6.0 GPa [280]. The nanohardness response of ABE and KBE tribofilms are not significantly different at different concentrations, unlike BTE that was considerably different at all concentration.
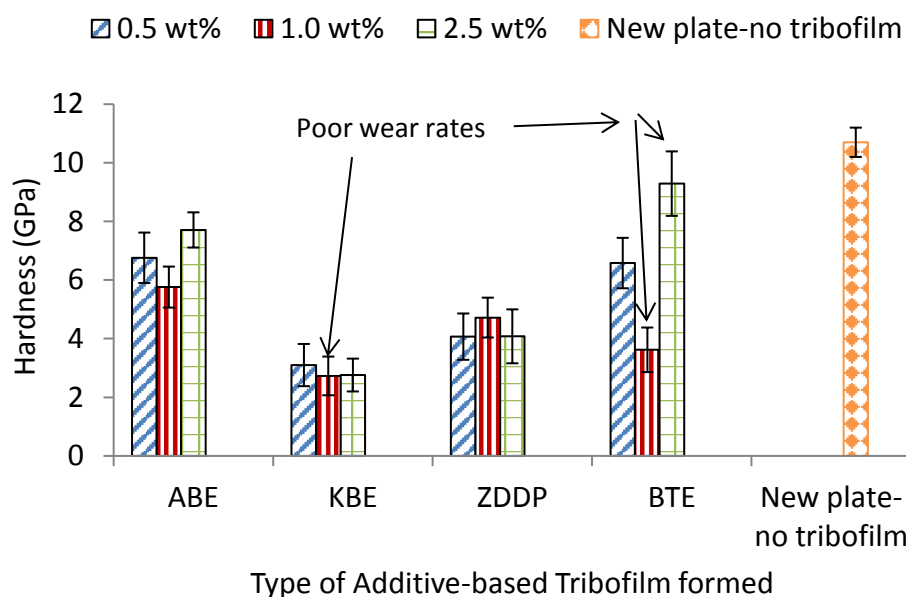
Figure 6-11 Average hardness of tribofilms formed at 1.0 wt. % additive concentration, 6 hr test duration and 100ºC tribotest temperature on worn plate samples lubricated by different additives and plain steel samples before the tribological experiments. Error bars represents the standard deviations of the average of 50-80 data points on the tribofilms

On the other hand, KBE-containing tribofilms gave hardness results that are comparable to ZDDP as shown in Figure 6-11. This could be an indication that KBE tribofilms possess a certain degree of plastic flow which was able to accommodate frictional energy through easily sheared layers formed between the contacting asperities by the nanoparticles as suggested in the literature [281].

6.3.6 Nanoindentation for a range of temperatures and time

The results of hardness and reduced elastic modulus of wear scars of worn samples at varying bulk oil temperatures and sliding distances are shown in Figure 6-12 (a) and (b) respectively.
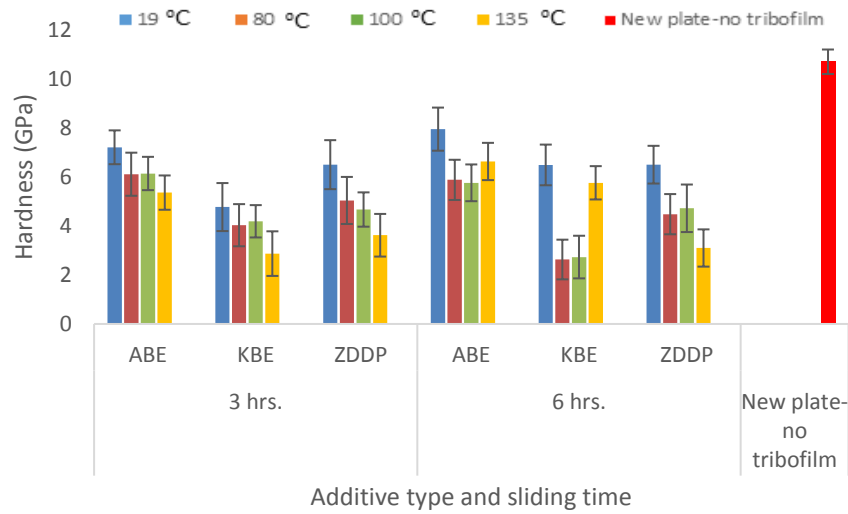
(a)
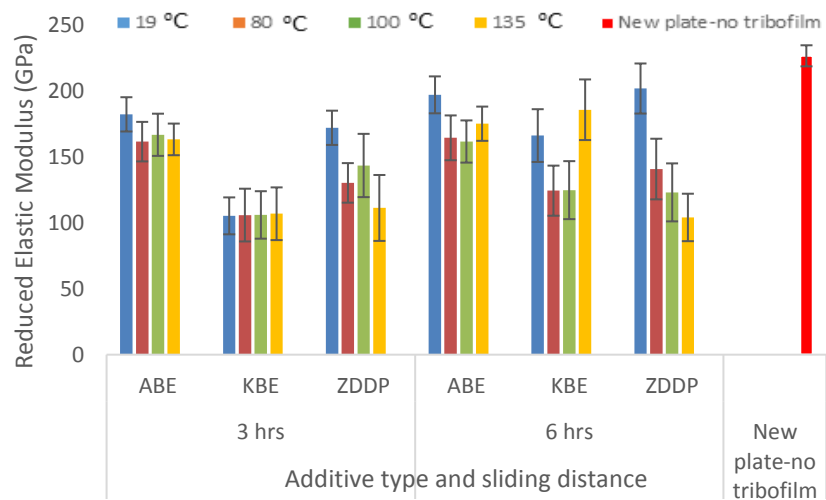
(b)

Figure 6-12 Average nanomechanical properties of tribofilms by different additives at different temperatures and sliding distance; (a) hardness and (b) reduced elastic modulus. Error bars represents the standard deviations of the average of 50-80 data points on the tribofilms

At 3 hr sliding durations, the hardness of tribofilms from all the antiwear additives used in this study decreased with increasing temperature as shown in Figure 6-12 (a). However, there were no significant changes in reduced elastic modulus with temperature, except for ZDDP which occurred between 80°C to 135°C during the 3 hr test duration as shown in Figure 6-12 (b). When the test duration was doubled, changes in hardness with temperature occurred more for KBE and ABE at 135°C than ZDDP tribofilms as indicated in Figure 6-12 (a).

In addition, variation in temperature affected reduced elastic modulus of KBE more than ABE and ZDDP as shown in Figure 6-12 (b). This is an indication that mechanical properties of ABE tribofilms are different to that of KBE irrespective of test temperature. However, the mechanical properties of tribofilms containing KBE are not only affected by temperature, but also the sliding distance.

In addition, the elastic modulus and hardness of ZDDP-containing tribofilms was found to decrease with increasing temperature at the end of 6 hr tests. This is an indication that decreased nanomechanical properties of ZDDP tribofilms occurred due to increased tribotest temperature. This behaviour was attributed to the susceptibility of certain antiwear films to plastic flow or a sacrificial behaviour of the tribolayer in place of harder underlying substrate [281, 282].

The hardness and elastic modulus of ABE-based tribofilms was high compared to KBE and ZDDP based tribofilms irrespective of changes in temperature and sliding duration. This was typical of hardness results of tribofilms from amine phosphate in the works of Komvopoulos et al. [280]. The minor differences in hardness and elastic modulus of ABE and ZDDP tribofilms formed during the 3 hr and 6 hr tests is an indication that its tribofilms are more quickly formed than KBE.

However, when the sliding duration was doubled, the boron-based tribofilms became harder at 135°C than at 80°C and 100°C. At 19°C, the hardness response appeared insignificantly influenced by increased sliding distance. This is an indication that temperature and sliding process could affect not only tribofilm formation as previously observed in the literature [21, 89, 93], but also have considerable effect on nanomechanical properties of tribofilms. The 50 to 80 data points out of 100 indentations made used to obtain the average values and error bars are due to eliminated data that are as a result of pile-up and pop-ins. These can lead to

underestimation of the true area of contact and overestimation of the hardness results if not eliminated.

6.4 Summary

Physical property characterization of tribofilms formed by tribofilms formed by borate antiwear additives indicates that they form tribofilms with average thicknesses around 70-225 nm. The build-up of borate tribofilms based on AFM images are greatly influenced by concentration, temperature, sliding time/process and water contamination. AFM morphologies are all in agreement with small patchy pieces of polyborate antiwear films with irregular and stretched shapes scattered over the worn surfaces [153]. Results from this chapter was able to confirm that changes in temperature and wear processes could affect the antiwear performance and durability of tribofilms formed by oils containing ZDDP and borate additives. In addition, changes in the hardness and elastic modulus of tribofilms formed by oils containing alkali borate nanoparticle dispersions is different to that of organic borates and ZDDP. This could be related to differences in the chemistry of their reacted layers.

Chapter 7
Results of Tribofilms Chemical Characterization

7.1 Introduction

This chapter focuses on the chemical behaviour assessment of boron-based tribofilms formed at different test conditions as described in Chapter 3. This is necessary in order to elucidate how the tribological behaviour of borate additives are affected by extrinsic test conditions. An investigation into the chemistry of tribofilms formed by oils containing alkali metal at different tribotest temperatures could elucidate more on their antiwear and durability behaviour. In addition, chemical analysis of tribofilms from oils containing alkali metal could elucidate on whether 'boric oxide anomaly' [174, 283, 284] have significant effect on its durability. It is well known that metal oxide modifier at low concentration induce transformation of boron coordination with three oxygen atoms structural groups $(BO_3)^{-3}$ in boron oxide to boron coordination with four oxygen atoms $(BO_4)^{-}$ [285, 286]. However, if the metal oxide modifier is an alkali oxide, increased alkali oxide ratio to boron oxide beyond certain limit (16:84) could lead to changes in maximum and minimum values of the glass physical properties [172]. This is termed 'boron anomaly' or 'boron oxide anomaly'.

The physical properties of glass melts that could be affected are; viscosity, density, thermal expansion, heat content and hardness as discussed in Chapter 2 [35]. Hence, chemical analysis in this study could elucidate on how structural changes in borate anions affects antiwear performance, durability and hardness of tribofilms containing ABE and KBE due to temperature effects. In addition, the chemistry of tribofilms formed at different tribo-oxidative conditions by borate additives could elucidate the limits of passivation of ferrous substrate by built-up borate reacted layers. The XPS and Raman spectroscopy as described in Chapter 3 are utilized to analyse tribofilms from borate additives at different test conditions in order to provide a better understanding of tribological results and physical surface analysis from previous sections in this study.

7.2 Chemistry of tribofilms from variable concentrations tests

In this section, the results of tribofilm chemistry as measured by XPS and Raman spectroscopy are presented for tribolayer derived from 6 hr tribotests at 100°C tribotest temperature and different concentration of additives. XPS spectroscopy was used to determine the quantity, state and species of elements and compounds on tribofilms formed on the wear scar of worn plate samples. Raman spectroscopy was utilized to identify the interactions of iron oxides and oxy-hydroxides with some other Raman-sensitive boron compounds such as boric acid and boroxol groups in boron oxide. In addition, the presence of other Raman-sensitive boron compounds such as boron carbide and boron nitride could be identified.

7.2.1 XPS results of tribofilm species at varying concentration

For investigating chemical reactions that took place during the tribological process, a top layer quantification of the XPS spectra of O 1s, B 1s, C 1s, N 1s, Fe 2p and K 2p peaks at three different spots was carried out on tribofilms formed by the boron additives (ABE, KBE and BTE). This was used to determine their elemental compositions, where average values are shown in Figure 7-1 (a). The atomic concentration of C 1s and O 1s spectra are presented separately as shown in Figure 7-1(b) for clarity and scaling constraints when compared to the spectra of B 1s, Fe 2p, K 2p and N 1s.

The amount and species of B 1s peaks on borate tribofilms is of key interest in this study. On tribofilms formed by oils containing BTE additives at increasing additive concentration, B 1s peaks increased significantly compared to tribofilms containing ABE and KBE. However, B 1s atomic concentration increase on tribofilms formed by BTE additive at 1.0 and 2.5 wt. % concentration were respectively about 14 and 19 times higher than at 0.5 wt. % additive concentration. The low B 1s peaks on BTE tribofilms at 0.5 wt. % compared to 1.0 and 2.5 wt. % suggests a reason for its better antiwear performance. This study observed that high atomic concentration B 1s on BTE tribofilm as shown in Figure 7-1(a) resulted into poor antiwear performances at 1.0 and 2.5 wt. % concentrations of BTE in the oil as shown in Figure 5-1 (b). In addition, Figure 7-1 (a) shows that high B 1s atomic concentration on tribofilms formed by KBE at 1.0 wt. % additive concentrations was about 7.8 atm. % that was

132

about twice as much as that formed at 0.5 wt. % additive concentration. In addition, this was also about three times as much as that formed at 2.5 wt. % additive concentration.
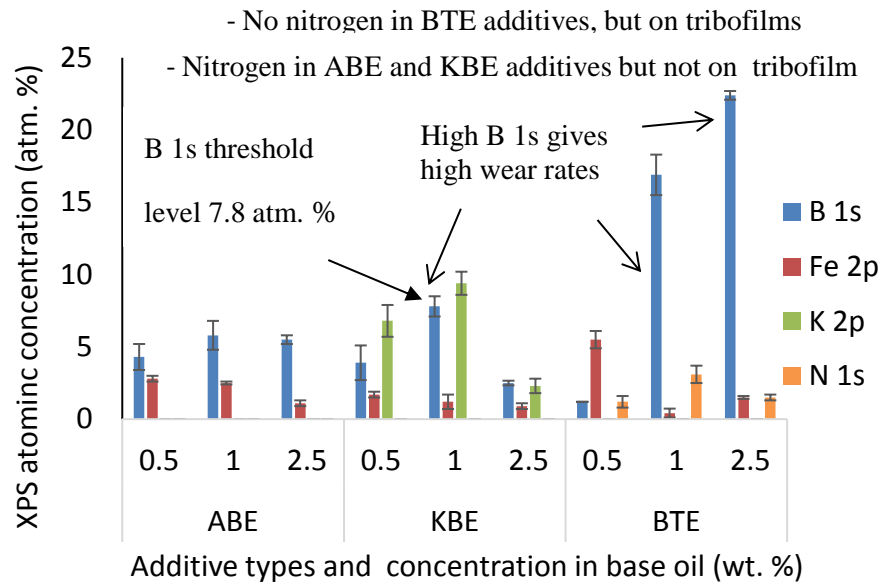
(a)
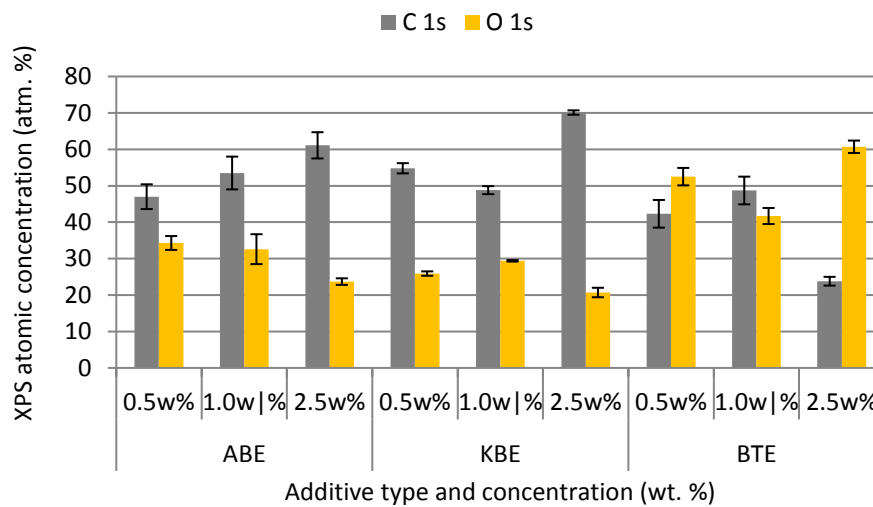
(b)

Figure 7-1 Average XPS atomic concentration of elements at three different spots on the tribofilms formed at different additive concentrations, 6 hr tribotest duration and 100ºC; (a) B 1s, Fe 2p, K 2p and N 1s, (b) O 1s and C 1s. Error bars are the standard deviations of individual average values

However, this did not result into better antiwear performance of tribofilms from oils containing KBE additives at 1.0 wt % than at 0.5 wt. % concentration. Another important observation in Figure 7-1 (a) is KBE tribofilms that gave the lowest atomic concentration of B 1s and K 2p spectra on KBE-containing tribofilms at 2.5 wt. % additive concentration compared to 0.5 wt. % and 1.0 wt. %. These are respectively, 2.5 and 2.3 atm. % which resulted into KBE tribofilms providing better antiwear protection that at 0.5 and 1.0 wt. %. On the other hand, changes in XPS atomic concentration of B 1s on tribofilms formed by ABE with increasing additive concentration was not more than 5.8 atm. %. In addition changes in B 1s atomic concentration with increasing ABE additive concentration in oil as shown in Figure 7-1(a) was not significant compared to tribofilms formed by other borate additives (KBE and BTE).

The XPS peaks of N 1s on ABE and KBE tribofilms at all concentrations gave noisy signals; but were detectable on tribofilms containing BTE, despite the absence of nitrogen on its molecular structure. This is an indication that tribo-oxidative degradation of BTE could have promoted the interaction of either nitrogen-containing compounds or nitrogen in the air with other surface species such as carbon, hydrogen, oxygen and boron. Even though the concentration of nitrogen in the air is about 78 %, there is not enough energy to break the N-N bonds. Hence there is a high probability that nitrogen containing compounds are responsible for these interactions. Higher nitrogen content at the surface of thin films are known to activate phase segregation that could lead to increase in micro-hardness [287].

This appeared to support the high tribofilm thickness of BTE as shown in Chapter 6, but was not the case with ABE-based tribofilms. The highest level of Fe 2p was obtained on tribofilms from oils containing BTE at 0.5 wt. % concentrations when compared to 1.0 and 2.5 wt. %. This could have interacted with certain borate glass former for better antiwear performance at 0.5 wt. % compared to 1.0 and 2.5 wt. % concentrations. The XPS spectra of O 1s on BTE tribofilms shown in Figure 7-1 (b) were observed to be higher than ABE and KBE at all concentration. This is an indication that more oxygen-containing compounds were formed on BTE tribofilms than ABE and KBE. Representative XPS long scan of major elements within wear

scars of samples lubricated by BTE-containing oil at 2.5 wt. % are shown in Figure 7-2 (a) and (b). A summary of the XPS long scan results of B 1s and C 1s peaks for tribofilms formed by ABE, KBE and BTE-containing oils at different additives concentrations are shown in Figure 7-2 (a) and (b). The full width at half maximum (FWHM) used in these analysis for B 1s and C 1s was taken at 1.1-1.3 and 1.4-1.6 respectively.

(a)   (b)
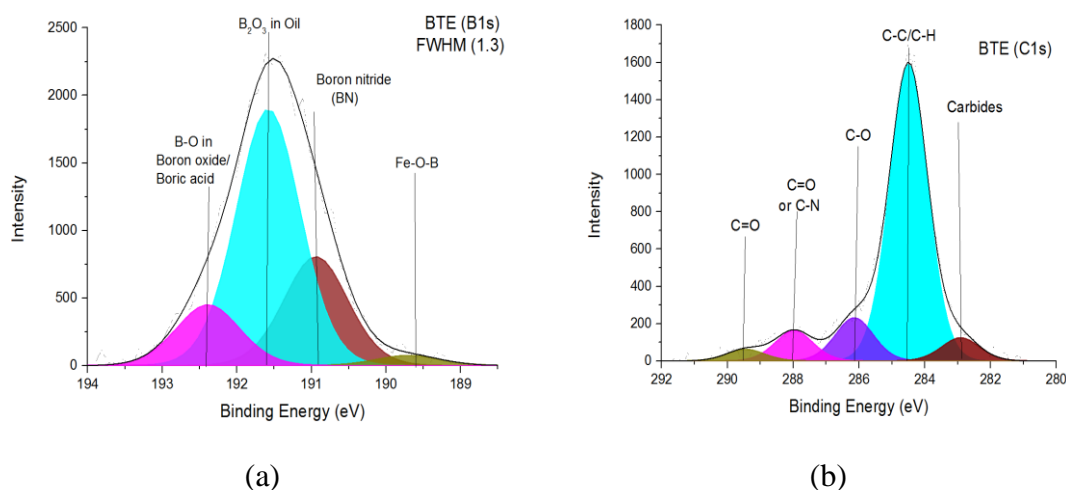
Figure 7-2 Representative XPS peaks at three different spots on BTE tribofilms formed by BTE at 2.5 wt. % additive concentrations at 100°C and 6 hr sliding time;(a) B 1s and (b) C 1s

Table 7-1 (a) shows position peaks for B1s on the wear scars containing ABE at 1.0 wt. % and 2.5 wt.% concentrations, where both tribofilms has boron oxide in oil with binding energy of 191.7 eV [152, 158] and B_2O_3 at about 192 eV [288]. This was found to be different when compared to tribofilms at 0.5 wt. %; which has B_2O_3 or $FeBO_3$ at 192 eV [156, 190]. Hence, an increase in concentration of ABE leads to the formation of boron oxide in oil as shown in the literature studies in Chapter 2 [152, 158]. This could have played a significant role in the antiwear performance of ABE-based tribofilms. However, the B 1s position peaks for KBE-based tribolayer at 0.5 and 1.0 wt. % gave similar boron compounds in form of B-O in boron oxide or boric acid and B_2O_3 [152, 158]. On the other hand, tribofilms from oils containing BTE in the base oil at 0.5 wt. % concentration are mainly composed of orthoboric acid at 193.6 eV [289].

Table 7-1 XPS binding energies, atomic concentration and chemical state at three different spots on the borate tribofilms formed at different concentrations, 100°C tribotest temperature and 6 hr sliding distance; (a) B 1s and (b) C 1s

Additive Type	Binding Energies (eV)/ Molecular wt. %			Compounds or Bond Types		
	0.5 wt. %	1.0wt	2.5 wt. %	0.5 wt. %	1.0 wt. %	2.5 wt. %
ABE	192.0/100.0	191.7/65.5	191.8/63.0	B-O	B_2O_3 in oil	B_2O_3 in oil
	-	192.4/34.5	192.5/37.0	-	B-O	B-O
KBE	192.0/64.3	192.0/59.7	191.5/100	B_2O_3 or $FeBO_3$	B_2O_3 or $FeBO_3$	B_2O_3 in oil
	192.7/35.7	192.7/40.3	-	H_3BO_3 or B_2O_3	H_3BO_3 B_2O_3	-
BTE	193.6/100	191.3/96.3	192.3/13.9	H_3BO_3	$B(OC_{12}H_{25})_3$	B-O
	-	189.3/3.7	191.6/58.8	-	O-Fe-B	B_2O_3 in oil
	-	-	190.9/25.0	-	-	BN
	-	-	189.6/2.3	-	-	O-Fe-B
(a)						
ABE	284.6/77.7	285.3/77.1	285.3/84.6	C-H/C-C	C-C	C-C
	286.0/12.4	286.8/12.4	287.0/9.0	C-O	Ads. ABE	Ads. ABE
	288.4/9.9	289.0/10.5	288.4/6.4	C=O	Carbonates	C=O
KBE	285.4/81.2	285.5/86.5	284.8/89.6	C-C	C-C	C-H/C-C
	286.8/10.0	287.6/8.3	286.4/7.6	Ads. KBE	Ads. KBE	C-O
	288.8/8.7	289.1/5.2	288.2/2.8	C=O	Carbonates	C=O
BTE	284.6/51.0	282.9/3.9	282.7/2.1	C-H/ C-C	Carbides	Carbides
	285.8/24.3	284.6/77.8	284.4/76.6	C-C	C-H/C-C	C-H/C-C
	286.9/10.9	286.1/10.6	286.0/11.1	Ads. BTE	C-O	C-O
	288.2/9.0	287.6/4.8	287.4/5.1	C=O	Ads. BTE	Ads. BTE
	289.4/4.8	288.7/2.9	288.6/5.1	Carbonate	C=O	C=O
(b)						

On the other hand, BTE-based tribofilms at 1.0 and 2.5 wt. % concentration has trialkyl borate at 192.3 eV [158], boron oxide in oil [152, 158], boron nitride (BN) [158, 290, 291] and non-stoichiometric O-Fe-B at about 189.7 eV [192, 193]. XPS results of C1s peaks of borate tribofilms at different concentrations are summarized in Table 7-1(b). The presence of carbides and BN on BTE tribofilms at 1.0 and 2.5 wt. % additive concentrations could have made the antiwear performance poorer than the 0.5 wt. % tribofilms as shown in Chapter 5. The results indicates three major peaks of C 1s on the tribofilms of ABE and KBE; C-C/C-H (chemical state of carbon chain of borate esters or adsorbed carbon) at 284.8 eV, adsorbed ABE at 287.2 eV and C=O bonds at 289.5 eV (carbonates) [31, 57-59]. However, C 1s peaks on BTE-containing tribofilms gave more than three peaks that are indicative of higher interaction of boron with carbon compared to ABE and KBE tribofilms. The C 1s peaks at 282.7-282.9 eV is an indication of the presence of carbides [158]. The presence of carbonyl groups (C=O) at about 288.0-288.9 eV [292, 293] occurred on all the wear scars of the borate additives except at 1.0 wt. % of ABE and KBE tribofilms. Instead of the presence of carbonyl functional group on ABE and KBE tribofilms, carbonates were found at 289.0-289.5 eV [158, 294-296]. The presence of carbonates on ABE and KBE tribofilms could have contributed to its wear-resistant behaviour as suggested in the literature [80].

The antiwear performance of ABE-based tribofilms was not significantly affected, but has considerable effect on KBE. In addition, BTE tribofilms have carbonates on the wear scar at 0.5 wt. % as supported in the literature [158], but was not present at 1.0 and 2.5 wt. % additive concentrations; instead BN and carbides were formed. The presence of carbide on tribofilms formed by BTE is indicative of its poor corrosion potential. This corrosive effect of BTE on ferrous surface could have exposed carbides formed within the microstructure of the ferrous surface during the hardening process of plain carbon steel. This could have been responsible for the poor antiwear performance of BTE at 1.0 and 2.5 wt. % compared to 0.5 wt. %. The summaries of XPS peaks of O 1s, Fe 2p, are shown in Table 7-2 (a) and (b). The FWHM used in the analysis of the peaks are respectively; 1.4, 2.5. The chemical compounds and bonding states of O 1s peaks on tribofilms formed by ABE-containing oils at different concentration as shown in Figure 7-1 are similar.

However, increased molecular concentration of C-O-B at 532.6 eV [158, 191] and B-O at 533.7 eV [190] were observed to rise as additive concentration of ABE in the oil increases. The presence of either C-O-B or B-O appeared to be very important in the antiwear performance of borate-containing tribofilms. In addition, O 1s peaks with binding energy between 531.9 eV and 530.4 eV can be assigned to oxygen atoms in the borate and iron oxides respectively [193]. However, the absence of B-O on tribofilms derived from KBE-containing oil at 1.0 wt. % is an indication that a very low amount of B_2O_3 was formed that affected the formation of adequate wear resistance borate glass. This eventually resulted in increased wear rates as shown in chapter 5. At additive concentrations of 1.0 and 2.5 wt. %, tribofilms from BTE-containing oils also gave low concentration of B_2O_3 at 1.3 and 2.7 atm. % respectively. This could have been responsible for the poor antiwear performance of BTE tribofilms at these concentration, unlike B-O bonds of about 11.2 atm. % from tribofilms formed by BTE at 0.5 wt. % additive concentration.

A summary of Fe 2p peaks for all the borate-based tribofilms formed at 0.5, 1.0 and 2.5 wt. % concentrations are shown in Table 7-2 (b). The result indicated that different phases of iron oxides and iron oxy-hydroxides were present within the borate tribofilms. These could be α-Fe_2O_3 (haematite) at 711 eV [196, 197], FeOOH at 712.9 eV [198]. However, the various phases of FeOOH are present on all the nine borate tribofilms, except for two tribolayer; one on ABE tribolayer at 2.5 wt. % concentration and the other on BTE tribofilms at 1.0 wt. %. The established antiwear mechanism of borate tribofilms [158] did not consider the influence of FeOOH, but took into consideration Fe^{2+} only. XPS peaks of Fe 2p shown in (b) indicated that the presence FeOOH in addition to Fe_2O_3 within borate tribolayer played a role in their antiwear performance. The peaks of K 2p at 293.3 eV on tribofilms from oil containing KBE at 0.5 wt. % and 1.0 wt. % can be attributed to KO_2 (corresponding to O 1s peaks at 530.3 eV) [199, 200]. The presence of potassium oxide and iron oxide indicates the possible fusion of B_2O_3 not only with the abrasive iron oxide, but also with KO_2 to form a two-phased wear resistance borate glass system. However, based on antiwear performance results in Chapter 5, the two-phased glass system formed by KBE-based tribofilms at 1.0 wt. % did not result into better antiwear performance than 0.5 wt. % concentration of KBE.

Table 7-2 XPS binding energies, atomic concentration and chemical state at three different spots on the borate tribofilms formed at different concentrations, 100ºC tribotest temperature and 6 hr sliding distance; (a) O 1s and (b) Fe 2p

Additive Type	Binding Energies (eV)/Molecular wt. %			Bond Types		
	0.5 wt. %	1.0wt	2.5 wt. %	0.5 wt. %	1.0 wt. %	2.5 wt. %
ABE	530.4/43.2	530.6/38.2	530.5/36.5	Fe_2O_3	Fe_2O_3	Fe_2O_3
	531.9/29.9	531.7/33.5	531.6/24.4	Fe-O-B	Fe-O-B	Fe-O-B
	532.7/17.6	532.5/16.9	532.6/21.7	C-O-B	C-O-B	C-O-B
	533.7/9.3	533.5/11.4	533.7/17.4	B-O	B-O	B-O
KBE	530.5/37.3	530.6/32.1	530.0/56.7	Fe_2O_3/KO_2	Fe_2O_3/KO_2	FeO
	531.9/44.9	531.8/46.2	531.2/16.3	Fe-O-B	Fe-O-B	Oxides
	533.0/17.8	532.8/21.6	532.1/22.4	B-O	C-O-B	Fe-OH
	-	-	533.6/4.6	-	-	B-O
BTE	529.6/36.5	527.7/4.5	529.9/21.3	Oxides	Oxides	FeO
	531.1/24.4	529.5/26.5	530.3/25.6	Oxides	α-Fe_2O_3	Fe_2O_3
	532.0/20.9	530.6/43.3	531.0/32.2	Fe-OH	Fe_2O_3	Oxides
	533.0/11.2	531.8/24.4	531.7/18.2	B-O	Fe-O-B	Fe-O-B
	534.2/5.1	533.1/1.3	533.2/2.7	Oxides	B-O	B-O
	535.5/2.1	-	-	Oxides	-	-
(a)						
ABE	711.0/76.0	710.9/71.7	711.0/66.3	α-Fe_2O_3	α-Fe_2O_3	α-Fe_2O_3
	712.9/24	712.9/28.3	713.4/19.4	FeOOH	FeOOH	Non-Stoic Fe oxides
	-	-	708.4/14.3	-	-	Fe_3O_4
KBE	710.6/50.4	711.1/76.7	710.4/74.9	Fe Oxides	α-Fe_2O_3	γ-FeOOH
	711.6/30.5	712.9/23.3	712.5/25.1	α-FeOOH	FeOOH	FeOOH
	713.0/19.1	-	-	FeOOH	-	-
BTE	709.7/54.3	710.6/86.1	708.5/10.7	FeO	Oxides	Fe_3O_4
	711.4/31.9	714.0/13.9	710.3/52.4	α-FeOOH	Sate. Fe	γ-FeOOH
	712.6/13.8	-	711.8/22.0	FeOOH	-	α-FeOOH
	-	-	713.6/11.3	-	-	Fe oxides
	-	-	715.3/3.6	-	-	Sate. Fe
(b)						

On the other hand, the near absence of KO_2 on the tribofilms formed at 2.5 wt. % concentration of KBE-containing oil is an indication that a certain level of KO_2 are required on the KBE-based tribofilms for better antiwear performance. The peak position of N 1s on ABE and KBE tribofilms at all test concentrations gave noisy signals. However, tribofilms containing BTE gave different N 1s peak positions at different test concentrations even though nitrogen was absent in the molecular structure of BTE. The presence of N 1s at 399.9, 399.5 and 390 eV corresponding to additive concentration of 0.5, 1.0 and 2.5 wt. % on the tribofilms containing BTE was attributed to $CONH_2$ or $-NH_2$, nitrogen in organic matrix [297, 298] and ionic bonding of boron atom to nitrogen respectively [119]. The tribofilms of KBE at all concentration had potassium dioxide on its tribofilms with a binding energy of 293.3 eV. XPS results from this study indicates that nitrogen-containing compounds in the air could have interacted with very high concentration of boron to form BN. However, this did not enhance the antiwear performance of tribofilms formed by BTE that could be attributed to lack of nitrogen coordination from the surrounding air with the electron deficient boron [119, 121]. The chemistry of reacted layers formed by different borates in the oils and at different concentration are summarized below;

- Synthetic borate containing tribofilms has very little amount of nitrogen on the tribofilm surface, unlike non-synthetic borates with no nitrogen in their molecular structure that has considerable N 1s peaks

- The composition of tribofilms formed by KBE is different to ABE and BTE due to the presence of oxides of potassium or other potassium compounds

- The amount of B 1s on tribofilms containing ABE does not change significantly with increasing concentration, unlike KBE and BTE. This could have been responsible for their different tribological performance

- Under certain additive concentrations, tribofilms formed by KBE and BTE could have carbonates, carbides and boron nitrides, unlike ABE that is mainly composed of the fusion of boron oxide with metallic oxides and carbonates

- At different additive concentrations, BTE tribofilm had nitrogen mainly as organic matrix, but formed boron nitride at 2.5 wt. % when B 1s concentration rose above 20 atm. %.

- The boron nitride and carbides formed on BTE tribofilms at higher additive concentration acted as third body abrasives.

7.2.2 Raman of tribofilms at varying additive concentration tests

Raman spectroscopy analysis results of mapped area on tribofilms of worn plates and pins samples lubricated by ABE are shown in Figure 7-3 (a) and (b) respectively.
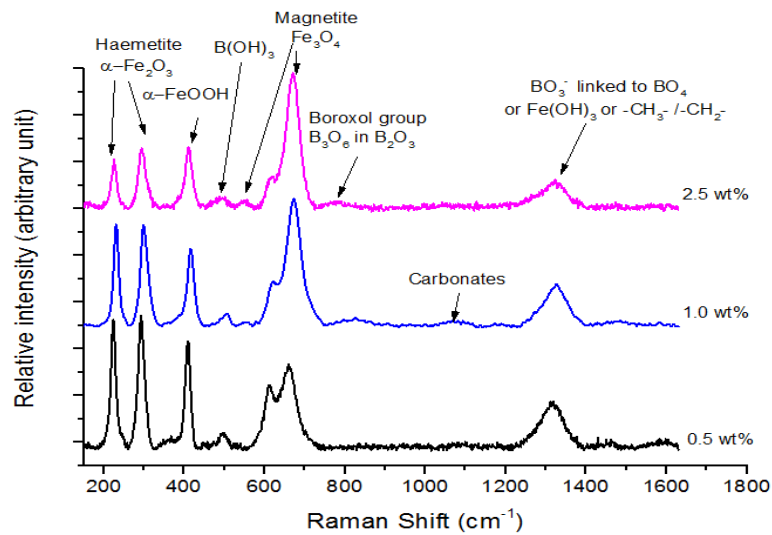
(a)
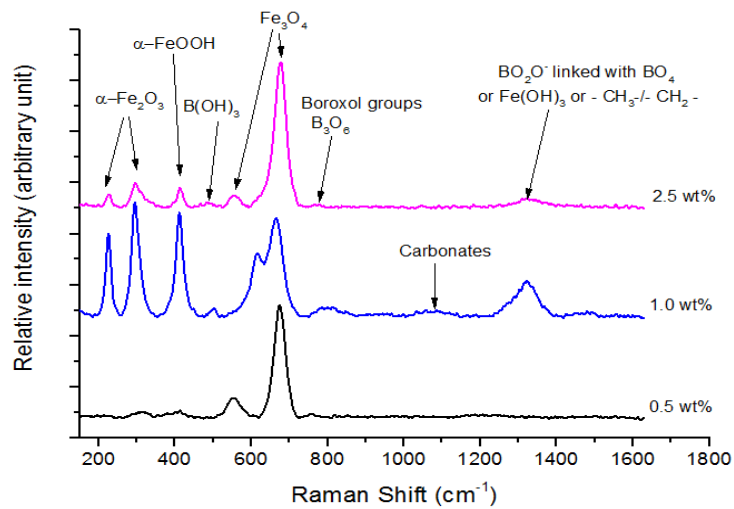
(b)

Figure 7-3 Representative Raman spectra obtained on ABE-based tribofilms from 6 hrs tribotests, 100°C at different additive concentrations; (a) plate and (b) pins

The objectives of analysing the tribofilms formed was to determine the changes that took place on some Raman active boron compounds, iron oxides and oxyhydroxides on worn plates and pins from tribological tests. This is to elucidate on how boric acid, and its ratio to boron oxide affects friction and antiwear performance of the borate tribofilms. In addition, ratios of iron oxides could be used to elucidate how changes in oxides of iron could affect friction and antiwear performance of borate tribofilms. Similar results for tribofilms lubricated by KBE and BTE are shown in Figure 7-4 and Figure 7-5 respectively.
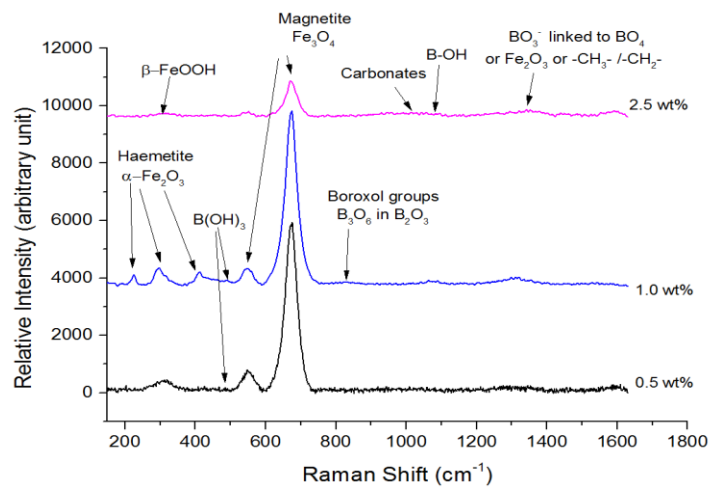
(a)
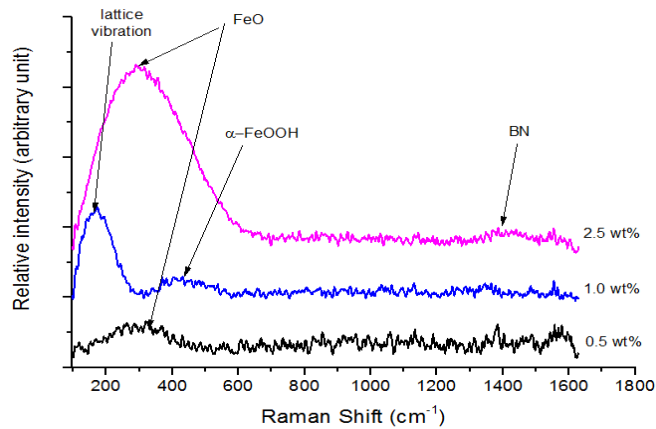
(b)

Figure 7-4 Representative Raman spectra obtained on KBE-based tribofilms from 6 hrs tribotests, 100°C at different additive concentrations; (a) plate and (b) pins

The results were based on Raman spectrometer measurement and analysis as described in Chapter 3 (Depth of analysis compared to XPS). The key features of Raman analysis are: decreasing intensities of haematite bands at 226, 294 and 410 cm^{-1}, and magnetite bands at 309, 534, 614 and 663 cm^{-1} [299] with increasing concentration. Raman sensitive boron compounds are; bands around 495 and 879 cm^{-1} identified as boric acid [138, 160], boroxol groups in B_2O_3 with peaks at 809 cm^{-1} [171, 210, 300, 301] and boroxol linked to at least one BO_4 tetrahedral located around 769-785 cm^{-1} [208, 213, 302].
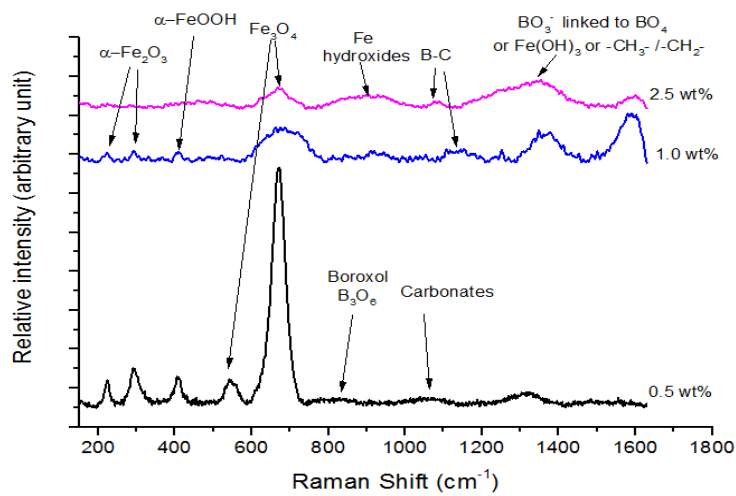
(a)
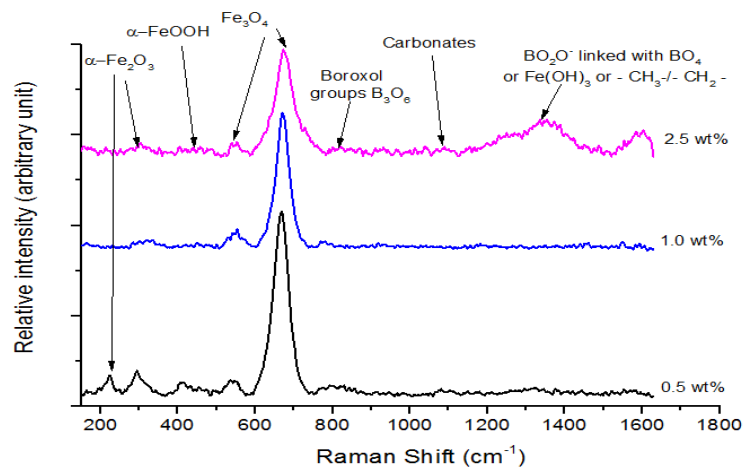
(b)

Figure 7-5 Representative Raman spectra obtained on BTE-based tribofilms from 6 hrs tribotests, 100°C at different additive concentrations; (a) plate and (b) pins

The presence of carbonates was identified at 1060 ± 10 cm^{-1} bands [191, 213]. In addition, Raman peaks near 1300 ± 10 cm^{-1} could either be any one of the followings: in-phase wagging and deformation of - CH$_3$ - and - CH$_3$ - groups [206], BO$_3$ linked to BO$_4$ units [178, 208, 213, 302] or Fe$_2$O$_3$ [303, 304] that were relatively unaffected by changes in additive concentration.

The behaviour of distinct borate groups, iron oxides and iron oxy-hydroxides could have great influence on the tribological performance of tribofilms from the borate additives. In fresh borate ester additives, trigonal boron structural units (BO$_3$) is predominant in the oil [168]. However, transformation from boroxol to tetrahedral species can occur when changes in physical properties such as viscosity, thermal expansion, density, etc. takes place [35, 174, 305]. On tribofilms formed by ABE, changes in additive concentration as shown in Figure 7-3 (a) resulted into various types of borate structural units and boric acid. However, hard and less protective haematite decreased with increasing additive concentration on the plates, but increased on the pins as shown in Figure 7-3 (b).

The tribofilms formed by KBE at 1.0 wt. % concentration had haematite to give poor antiwear performance compared to β-FeOOH [303, 304] other additive concentrations as shown in Figure 7-6 (a) and Chapter 5. In addition, reduced Raman intensity shown in Figure 7-5 (a) of magnetite on BTE tribofilms on the plates can be related to poor antiwear performance at 0.5 and 2.5 wt. % additive concentrations.

The results from this study indicates that changes in concentration of borate additives not only affect boric acid formation and boric oxide structural units, but also oxides of iron to give different antiwear performance. Raman shift of tribofilms from BTE at 0.5 wt. % for the pins and plates as shown in Figure 7-7 (b) had boroxol and boroxol linked to tetrahedral BO$_4$ units to give better antiwear performance than worn plates.

The formation of carbide spectra [306-309] from Raman analysis hereby confirmed the earlier XPS results in Figure 7-3 (a) and (b). However, the situation was different on the pins, where reduction in the intensity of magnetite on tribofilms formed at 1.0 wt. % and 2.5 wt. % was not substantial compared to 0.5 wt. %. In addition, FeO was found on the tribofilms on the pins from 0.5 and 2.5 wt. % of KBE-containing oils, but not on tribofilms formed by KBE at 1.0 wt. % concentration in the base oil. The presence of boron nitride [205, 310] on tribofilms containing KBE on pins could

have been responsible for comparable antiwear performance to ABE and ZDDP as shown in section 5.2.

.
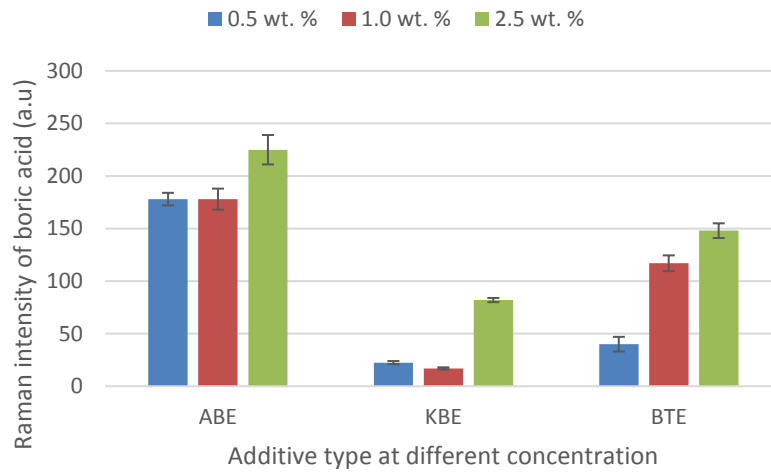
(a)
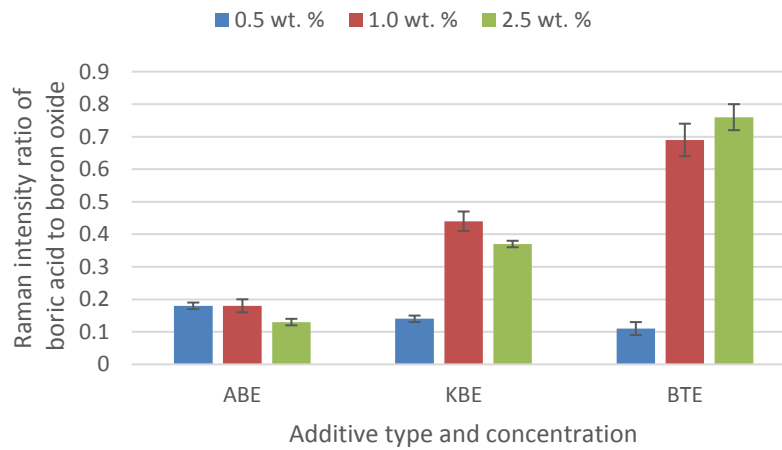
(b)

Figure 7-6 Average Raman intensity on borate tribofilms at different concentration of additives, 100°C and 6 hr sliding durations for; (a) boric acid, and (b) ratio of boric acid to boron oxide. Error is measured over four analysis points

An important feature of the entire Raman spectra of the boron-containing tribofilms in this study are the presence of B_2O_3 as confirmed by the XPS results. On the plates, B_2O_3 exist in form of boroxol groups. However, the pins had boroxol groups and

boroxol linked to tetrahedral BO_4 units. On ABE-containing tribofilms, the presence of either structural units enhanced antiwear performance at different concentrations as shown in Figure 7-3 (a) and (b).

This results confirms similar results on borate tribofilm using XPS for B_2O_3 and Fe_2O_3, FeOOH and carbonates as shown in Table 7-1 and Table 7-2 for the plates. However, XPS analysis was not able to distinguish boric acid from boron oxide on borate tribofilms more compared to results from Raman spectroscopy. The tribofilms containing BTE had boroxol formed on worn plates and pins at 0.5 wt. %, but formed only BO_3 linked to BO_4 structural units at higher concentrations on both plates and pins. On the tribofilms formed by KBE additives, few structural changes in B_2O_3 took place except at 1.0 wt. % on the plates which gave poor antiwear performance. Hence further studies on the effect of structural changes in B_2O_3 are expected to provide better understanding of the established borate antiwear mechanism based on HSAB principle [158].

A summary of the composition of boric acid and boron oxide on the tribofilms of worn plates samples by all the boron additives are shown in Figure 7-6. The result gives an indication of how the major boron compounds responsible for friction coefficient and wear on the tribofilms of worn samples behave at different concentrations.

In Figure 7-6 (a), tribofilms containing ABE gave high boric acid and also sufficient amount of boron oxide to form wear resistant glass as shown in Figure 7-6 (b), irrespective of additive concentration. This was able to provide better antiwear performance at all concentration as shown in Figure 5-1 (b).

In addition, boric acid level on tribofilms containing BTE was not as high as that on ABE-based tribofilms. Hence, the high XPS atomic concentration of B 1s on BTE tribofilms suggest that most of the compounds and bonds formed have considerable amount of other compound present. These were shown to be BN and carbides in Table 7-1 that adversely effected the antiwear performance of tribofilms from BTE additives in the oil at 1.0 and 2.5 wt. % concentrations.

However, tribofilms containing BTE and KBE appeared to have higher boric acid to boron oxide ratio at 1.0 and 2.5 wt. % additive concentrations. This enhanced antiwear performance on KBE tribofilm at 2.5 wt. % additive concentration, but did not on tribofilms formed at 1.0 and 2.5 wt. % concentration of BTE additive in the oil.

In addition, this did not also provide better friction coefficient reduction on BTE tribofilms compared to ABE and KBE as shown in Figure 5-1 (a) and Figure 5-2. Hence, a distinct balance of boric acid and boron oxide appeared to be necessary for borate tribofilms to provide better friction coefficient reduction and antiwear performance.

7.3 Chemistry of tribofilms for a range of temperatures and times

This section is divided into two sub-sections. One section involved XPS analysis of concentration of elements and their chemical states at the top layer of the tribofilms. Another section involved chemical analysis of tribofilms formed at varying temperature at different sliding time and process; from 3 hrs to 6 hrs tests and from 3 hr to 3r3 tests. In addition, depth profile analysis was carried out to investigate tribofilms on samples from the 100°C test temperature for 3 hr test duration. This is due to the fact that depth profiling XPS analysis of sputtered tribofilms can provide a more accurate information of compounds and bond species within the boundary films as a function of depth [21, 193].

7.3.1 XPS analysis of tribofilms species (3hr)

XPS data acquired were used to analyse the tribochemical reaction product involved during the friction process at different tribotests temperatures. The XPS atomic concentration of major elements on ABE and KBE-containing tribofilms are shown in Figure 7-7. The atomic concentration of C 1s and O 1s spectra are presented separately as shown in Figure 7-7 (b) for clarity and scaling constraints when compared to the spectra of B 1s, Fe 2p, K 2p and N 1s. By considering the tribotests at different temperature up to 135°C, BTE-containing tribofilms was not formed due to safety reasons (low boiling temperature range of the additives). The key point of XPS elemental composition analysis of ABE-containing tribofilms from the 3 hr test at different tribotests temperature are; lower atomic concentration of O1s and Fe 2p at 100°C than at all other temperatures as shown in Figure 7-7 (a) and (b). This is an indication that less oxides of iron are formed at 100°C than at other temperatures, but gave increased carbon-based compounds as shown in Figure 7-7 (b).

In addition, a sudden increase in atomic concentration of B 1s occurred at 135°C compared to all other temperatures. This is an indication that easier release of adsorbed boron from the substrate due to increase in temperature occurred as observed in the literature [311].
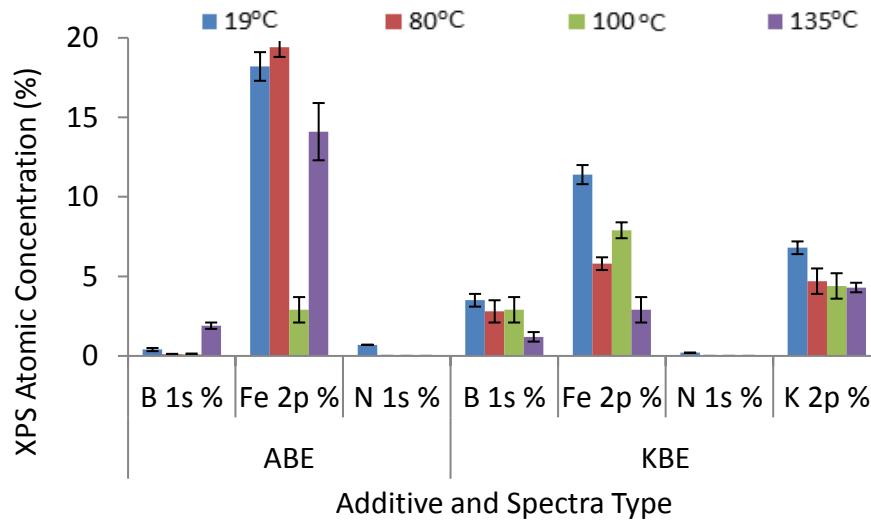
(a)
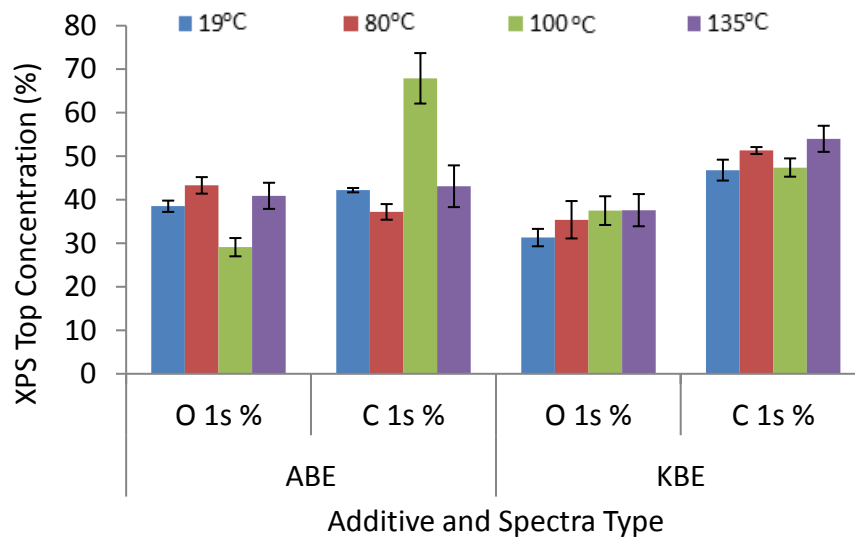
(b)

Figure 7-7 XPS top layer atomic concentrations on ABE- and KBE-containing tribofilms at different temperatures, 3 hr test duration and 1.0 wt. % additive concentrations of; (a) B 1s, Fe 2p, N 1s and K 2p, (b) O 1s and C 1s. Error bar is measured as standard deviation over three analysis points

This could have been responsible for the better antiwear performance of ABE tribofilms at 135°C than 100°C during the 3 hr and 6 hr tests as shown in section 5. A major observation on KBE-based tribofilm is the higher atomic concentration of Fe 2p peaks at 19°C and 100°C than at 80°C and 135°C. The higher atomic concentration of Fe 2p on KBE-based tribofilms favours the antiwear performance of KBE at 19°C more than 135°C. In addition, XPS peaks of N 1s was present only at 19°C tribotests temperature on both ABE and KBE-containing tribofilms, but gave noisy signals on tribofilms at all other tribo-test temperatures. On the tribofilms containing ABE additive, significant change in the atomic concentration of C 1s peaks as shown in Figure 7-7 (b) did not take place except at 100°C tribotests temperature. However, there are no significant changes on the atomic concentration of C 1s on KBE-containing tribofilms at all tribotests temperatures.

This is an indication that increased carbon based compounds on ABE-containing tribofilms formed at 100°C test temperature must have played a positive role in its antiwear performance. This was not the situation with KBE-based tribofilms, as it appears that fewer carbon based compounds within the KBE tribofilms are formed at 100°C. This could be responsible for its poor antiwear performance as shown in Chapter 5. This is an indication that the response of the chemistry of tribofilms from certain boron-containing additives in the base oil at 100°C tribotests temperature could form boundary films that could either enhance or be detrimental to their antiwear performance. A previous study had attributed the poor antiwear performance of tribofilms from some borate additives at 100°C to unreacted borates [167].

However, results from this study had indicated that certain borate additives could form carbon-based compounds on borate tribofilms in order to resist wear at 100°C tribotest temperature. This behaviour did not exclude the possible effects of other borate and iron-based compounds that could be affected. The insignificant changes in the atomic concentration of C 1s peaks at all tribotests temperatures is an indication that carbon-based compounds on KBE tribofilms are more stable than ABE. In order to understand the activity of oxygen-containing compounds on borate tribofilms, long scan XPS spectra of different element are necessary. A comparison of long scan XPS results of B 1s peaks on the borate tribofilms at 100°C and 135°C for the 3 hrs test

149

durations are shown in Figure 7-8 (a) to (d) and Table 7-5 for O 1s, C 1s and Fe 2p. This is necessary, since major changes in the formation of B_2O_3 from H_3BO_3 dehydration are known to take place between 80°C and 135°C [35, 163, 224].
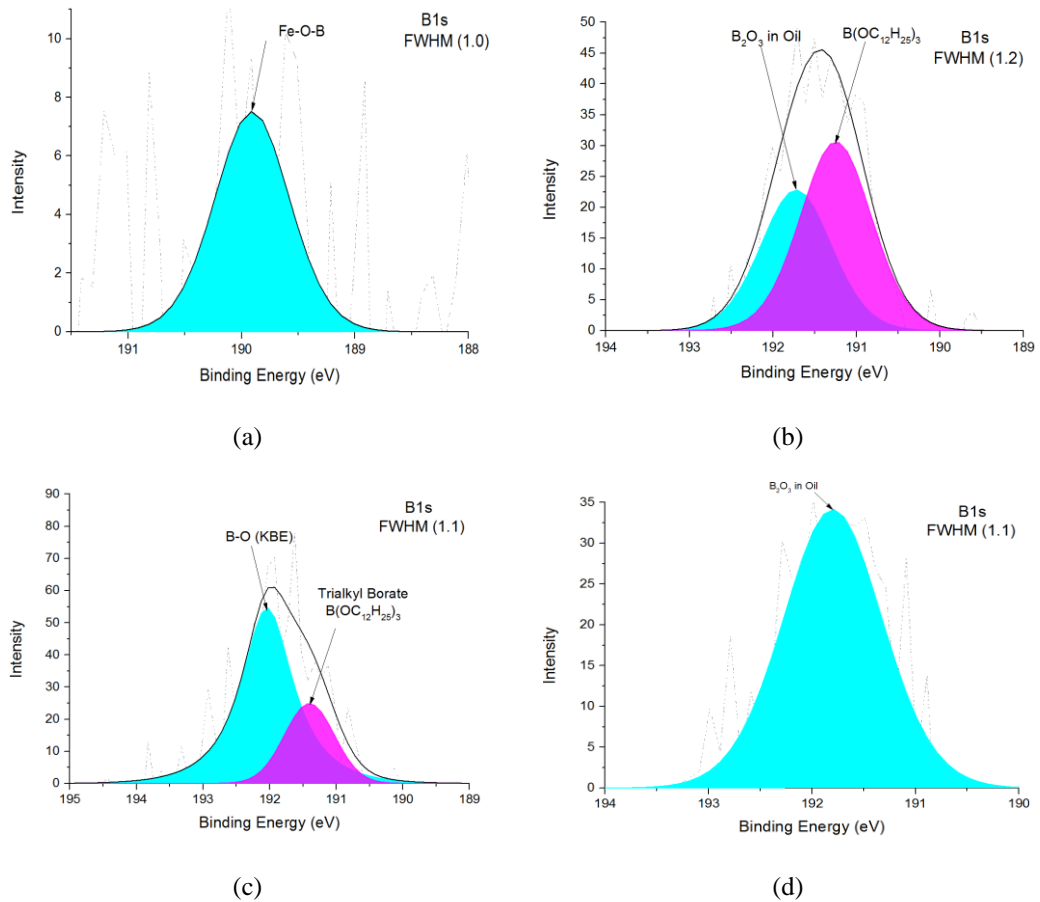
Figure 7-8 Representative XPS spectra of B 1s peaks at 3 spots on the tribofilms from the 3 hr tribological test at 1.0 wt. % additive concentration for; (a) ABE at 100°C, (b) ABE at 135°C, (c) KBE at 100°C and (d) KBE at 135°C

The key changes in Figure 7-8 (a) and (b) on ABE tribofilms between 100°C and 135°C shows additional formation of trialkyl borate at 191.2 eV [158] at 135°C along with boron oxide in oil at 191.8 eV that is also found on tribofilms formed at 100°C. The reverse was the case on KBE tribofilms formed between these temperatures as the presence of boron oxide from the oil could be attributed to adverse antiwear performance. The summary of XPS peaks of O 1s, C 1s and Fe 2p on tribofilms containing ABE and KBE at 100°C and 135°C are shown in Table 7-3 (a) to (c).

Table 7-3 XPS peaks on tribofilms by additives at 1.0 wt. % concentration in oil at 100 and 135ºC for 3 hrs tests durations for;(a) O 1s, (b) C 1s, (c) – Fe2p and

Additive Type	Binding Energies (eV)			Compounds or Bond Types	
	100ºC	135ºC		100ºC	135ºC
ABE	533	533.6		B-O	B-O
	531.8	531.7		C-O-B	C-O-B
	530.9	530.4		Oxides	Fe_2O_3
	529.5	532.8		FeO	C-OH
KBE	533.4	533.4		B-O	B-O
	532.1	532.4		C-OH	C-OH
	531.2	531.4		C-O-B	C-O-B
	529.8	530.4		FeO	O_2 in KO_2
(a)					
ABE	288.3	286.9		C=O	C-O
	286.6	285.9		C-O	C-O
	284.9	284.7		C-C/C-H	C-C/C-H
KBE	288.2	288.3		C=O	C=O
	286.0	286.1		C-O	C-O
	284.7	284.8		C-C/C-H	C-C/C-H
(b)					
ABE	710.6	712.8		Fe oxides	FeOOH
		710.9		-	Fe_2O_3
		709.5		-	FeO
KBE	711.8	709.9		FeOOH	Oxides
	709.7	-		Oxides	-
(c)					

Figure 7-8 (c) gave a summary of XPS peaks of Fe 2p on ABE tribofilms from 135°C tribotests temperatures which gave FeOOH at 712.9 eV [198], Fe_2O_3 at 710.9 eV [196, 197] and Fe O at 709.5 eV [196, 197]; but gave only iron oxides that were present at 100°C. Table 7-3 (c) gave a summary of XPS peaks of Fe 2p on ABE tribofilms from 135°C tribotests temperatures gave FeOOH at 712.9 eV [198], Fe_2O_3 at 710.9 eV [196, 197] and FeO at 709.5 eV [196, 197], but gave only iron oxides that were present at 100°C. Hence, the presence of B_2O_3 in the oil and FeOOH could have played a role in the better antiwear performance of ABE at 135°C than 100°C. In addition, there was the presence of FeOOH and other oxides at 100°C on KBE-containing tribofilms; but FeOOH was absent at 135°C. These results along with tribological results in Chapter 5 indicated that FeOOH presence on ABE-based tribofilm at 135°C enhances its antiwear performance.

On the contrary, the presence of FeOOH on KBE-containing tribofilms at 100°C could be linked to the adverse antiwear results compared to FeOOH absence on KBE tribofilm at 135°C. This is an indication that the presence or absence of FeOOH on borate tribofilms could positively or negatively affect their antiwear performance. The contradictory chemistry of ABE-based tribofilms compared to KBE between 100°C and 135°C could have been related to the composition of their wear-resistant borate glass; KBE additives contains oxides of iron and potassium; unlike ABE with only iron oxides as shown in Table 7-3 (c) and (d).

A summary of XPS results for C 1s on ABE and KBE-containing tribofilms at 100°C and 135°C tribotests temperatures are shown in Table 7-3 (b). XPS peaks of C 1s for ABE and KBE tribofilms between 100°C and 135°C are similar. The peaks of K 2p at 292.8 eV corresponding to O 1s at 530.4 eV as shown in Table 7-3 (a) on KBE-containing tribofilms can be attributed to KO_2 [199, 200] at 100°C and 135°C tribological tests. This could have been due to a number of factors such as; high temperature, dehydration of boric acid, differences in wear-resistance glass, changing composition of metallic oxides, and boric oxide structural units in the wear-resistant glass. The noisy XPS peaks of B1s are characteristic of boron not producing intense signal due to low atomic concentration of boron to iron. In addition, similar studies on some boron-containing tribofilm had displayed comparative noisy B1s peaks as obtained in literature of similar studies [125, 190].

7.4 XPS results of tribofilms species from durability tests (3r3)

7.4.1 Introduction

In this sub-section, XPS analysis of tribofilms from oils containing ABE and KBE additive at 1.0 wt. % concentration in the base oil for 3 hr test duration, which was temporarily stopped. With the oil replaced by PAO, the test was continued for another 3 hrs to give 3r3 tests. The schematic representation of the process is shown in Figure 7-9. In this analysis, the chemistry of preformed tribofilms after tribological tests with PAO at 100 and 135ºC are analysed using XPS.
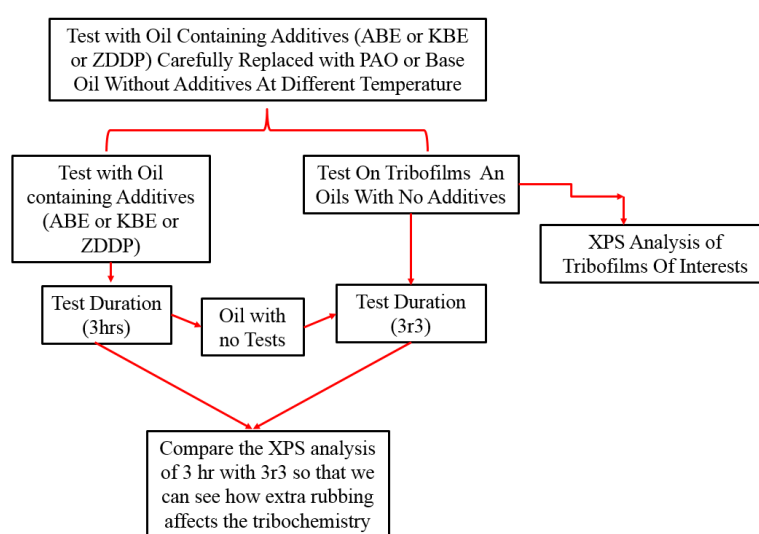
Figure 7-9 Schematic diagram of tribofilms from 3r3 or durability tests

7.4.2 XPS results of tribofilms species due to sliding process (3r3)

The long scan XPS results for B 1s peaks on the borate-containing tribofilms at 100ºC and 135ºC for 3r3 tests are shown in Figure 7-10 (a) to (d). This is to elucidate on how certain compounds on the borate tribofilms affects its durability at 100ºC and 135ºC tribotest temperature. These temperatures are chosen based on boric acid instability within these temperature range as discussed in Chapter 2. A notable feature of B1s spectra on pre-formed ABE tribofilm at 100ºC as shown in Figure 7-10 (a) is the binding energy of B 1s at 191.6 eV corresponding to O 1s at 531.7 eV that is assigned to boron oxide in oil. A comparison to B 1s obtained on tribofilms from 135ºC tribotests at 192.2 eV gave B_2O_3 in borate ester [158, 190].

153

The peaks of B1s on KBE-based tribofilms from the 3r3 tests at 100°C is different to those at 135°C; only trialkyl borate was formed at 191.2 eV [158] and 100°C tribotests compared to three boron compounds formed at 135°C. These are B_2O_3 at 194.1 eV dominated by BO_3 structural units [168, 312], 191.8 eV (boron oxide in oil) and 188.6 eV (Iron borides) [313, 314]. The XPS peaks of C 1s on ABE tribofilms from tribological tests at 100°C and 135°C as shown in Table 7-4 (a) indicates the presence of carbonates at 289-290 eV [158, 296, 298]. On the other hand, carbides at 283.0 eV [158, 315, 316] were formed on KBE tribofilms at 100 and 135°C.

(a)

(b)

(c)

(d)
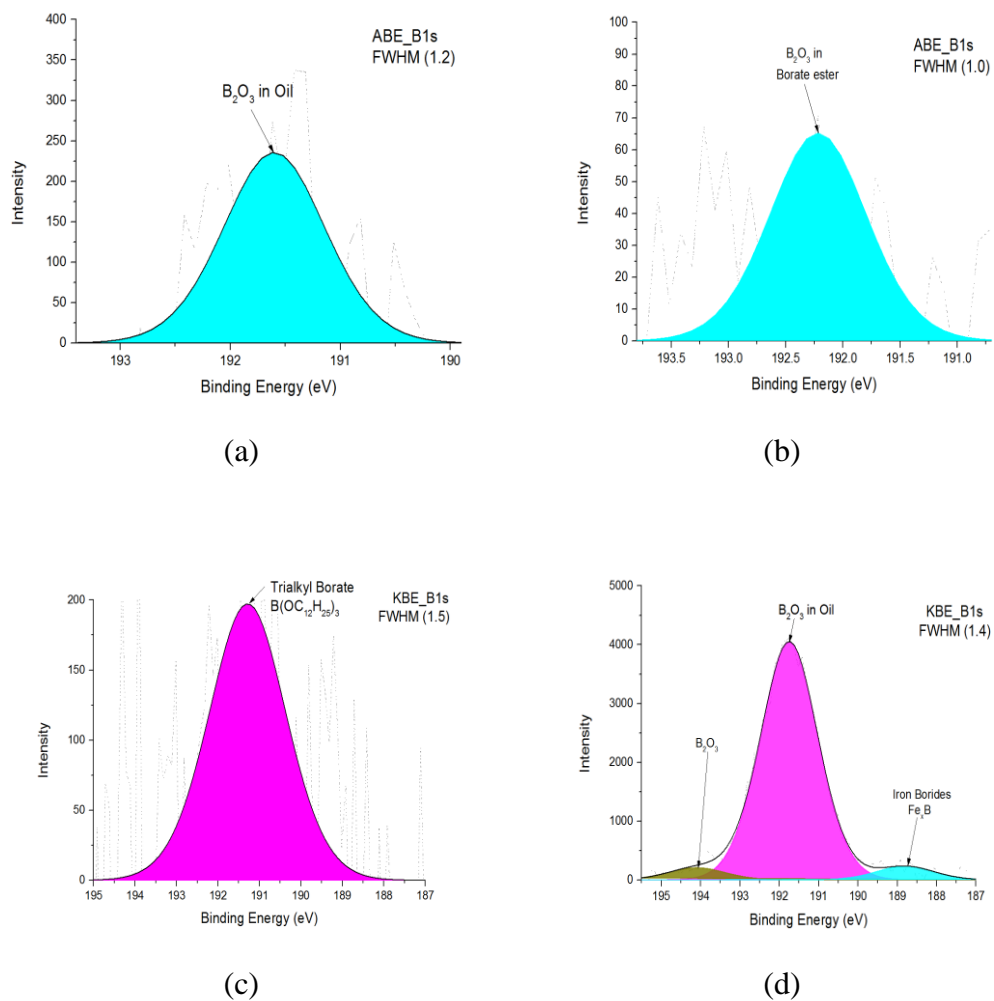
Figure 7-10 Representative XPS spectra of B1s peaks on tribofilms formed by KBE additives at 1.0 wt. % concentrations from 3r3 tests at (a) 100°C and (b) 135°C, and (c) 100°C and (d) 135°C

The presence of carbides on preformed KBE tribofilms could be attributed to enhanced durability at 135ºC tribotests temperature; but carbides was not formed at 100ºC. In addition, preformed ABE tribofilms had carbonates that could be attributed to its poor durability performance. The summary of XPS peaks of Fe 2p and K 2p on tribofilms of ABE and KBE at 100ºC and 135ºC are shown in Table 7-5 (a) and (b) respectively. In addition, Figure 7-11 compares the top layer atomic quantification of B 1s and K 2p peaks on KBE-containing tribolayer of preformed tribofilms at 100ºC and 135ºC tribotests temperatures.
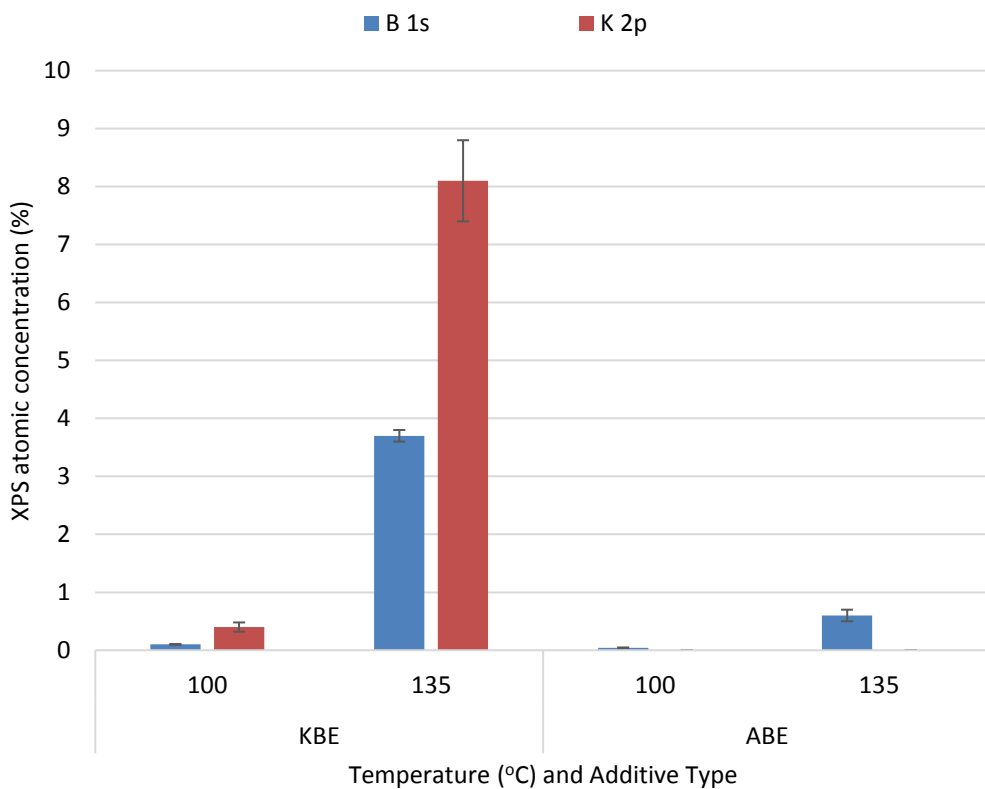
Figure 7-11 Average top layer XPS atomic concentrations on ABE and KBE tribofilms from 3r3 tests for B 1s and K 2p. Error is measured as the standard deviation over three analysis points

The results indicated that XPS peak intensity of B 1s and K 2p on preformed KBE tribofilm at 135ºC appeared to be very high compared to 100ºC tribotests temperature. This is an indication that temperature increase caused boron and potassium to be

released from pre-formed KBE tribofilms to form certain oxides of boron and potassium which provided comparable durability to preformed ZDDP tribolayer.

However, preformed ABE exhibited similar increase in B 1s, but did not provide comparable durability performance to KBE and ZDDP. The atomic concentration of K 2p on pre-formed KBE-based tribofilm at 100°C as shown in Figure 7-11 gave 0.4 atm. % compared to 3 hrs (4.4 atm. %) as shown in Figure 7-7 (a) and 9.4% for 6 hrs continuous test durations as shown in Table 7-2 (a).

However, XPS peak intensity of B 1s and K 2p on preformed KBE tribofilm at 135°C appeared to be very high compared to 100°C tribotests. This is an indication that K 2p atomic concentration was affected by both temperature and sliding process which can be attributed to the only stable oxides of potassium (KO_2) [199, 200].

The XPS long scan results of ABE and KBE-containing boundary films from the 3r3 tribotests as shown in Table 7-5 (a) both have the binding energy of Fe 2p at 707.3 eV and 100°C that can be attributed to metallic iron [158, 317]. XPS quantifications indicates the presence of metallic iron KBE and ABE tribofilms formed during the 3r3 tests at 100°C. This indicated that KBE tribofilms had higher metallic iron (8.9 ± 0.6 atm. %) than ABE (3.7 ± 0.3 atm. %), where they both gave poor durability compared to ZDDP.

However, this was not the case at 135°C test temperature where no metallic iron was formed. Table 7-4 (a) and (b) shows the XPS peaks of O 1s and C 1s and Table 7-5 (a) and (b) for Fe 2p and K 2p peaks respectively. The peaks of Fe 2p at 711.6 eV corresponding to O 1s at 531.3 eV can be assigned to FeOOH.

In addition, O 1s at 532.1 eV and 529.9 eV are attributed to C-OH [193] and oxides [158]. The presence of FeOOH and boron oxide in oil were not able to enhance durability performance of pre-formed ABE tribofilms at 100°C and 135°C based on the antiwear performance results in Chapter 5.

The results indicated that increasing the bulk oil temperature during the tribological test have metallic iron more protected at 135°C than at 100°C to provide enhanced durability. However, durability of tribofilms formed by KBE-containing oils was more enhanced than ABE.

Table 7-4 XPS peaks on borate tribofilms formed at 1.0 wt % additive concentration and sliding process of 3r3 tests at 100 and 135°C; (a) O 1s, (b) C 1s

Additive Type	Binding Energies (eV)			Compounds or Bond Types	
	100°C	135°C		100°C	135°C
ABE	533.3	533.3		B-O	B-O
	532.0	531.6		C-OH	C-O-B
	531.2	529.7		C-O-B	Oxides
	529.8	532.8		FeO	C-OH
KBE	533.3	533.9		B-O	C=O
	532.3	532.5		C-OH	C-OH
	531.5	531.4		C-O-B	C-O-B
	530.8	530.0		O_2 in KO_2	Oxides
	529.7	-		FeO	-

(a)

Additive Type	Binding Energies (eV)			Compounds or Bond Types	
ABE	289.2	290.4		Carbonate	Carbonate
	288.3	288.9		C=O	C=O
	287.1	287.8		Ads. ABE	Ads. ABE
	286.1	286.5		C-O	C-O
	284.8	285.1		C-C/C-H	C-C/C-H
KBE	288.9	289.0		C=O	C=O
	287.6	288.8		Ads. KBE	C=O
	286.1	286.4		C-O	C-O
	284.6	285.0		C-C/C-H	C-C/C-H
	282.8	283.0		Carbides	Carbides

(b)

The higher durability of preformed KBE-containing tribofilms could have been aided by the formation of iron borides as shown in Figure 7-10. Based on the antiwear mechanism for inorganic nanoparticle borate ester shown in Figure 2-22, trapped KBE nanoparticle in the preformed tribofilms has boron in boron oxide bind directly to metallic iron due to shear- and extreme-pressure effects. Tribochemical reaction between boron oxide and substrate produced a wear resistant film consisting of iron boride (FeB) to provide tenacious film for wear protection at $135^{\circ}C$ tribotest temperature.

Table 7-5 XPS peaks on borate tribofilms formed by 1.0 wt. % additive concentration and sliding process of 3r3 tests at 100 and $135^{\circ}C$ (a) Fe2p and (b) K 2p

Additive Type	Binding Energies (eV)			Compounds or Bond Types		
		$100^{\circ}C$	$135^{\circ}C$		$100^{\circ}C$	$135^{\circ}C$
ABE		713.5	712.9		Sat. Fe	FeOOH
		711.6	710.0		FeOOH	Oxides
		709.9	-		Oxides	-
		707.1	-		Metallic Iron	-
KBE		712.5	714.0		FeOOH	Sat. Fe
		710.1	710.5		Oxides	Fe Oxides
		707.2	-		Metallic Iron	-
(a)						
KBE		292.7	292.9		KO_2	KO_2
(b)						

7.5 Depth profile analysis of tribofilms at 3 hr tests and $100^{\circ}C$

In order to further understand the large differences in the antiwear performance of the two borate additives at $100^{\circ}C$, XPS depth profile results of major elements on ABE and KBE-based tribofilms are shown in Figure 7-12 (a) and (b) respectively. Figure 7-12 (a) and (b) indicated that, XPS atomic concentration of B 1s peaks was

observed to have increased from zero at the surface to a maximum of about 1.03 nm on both tribofilms containing ABE and KBE.
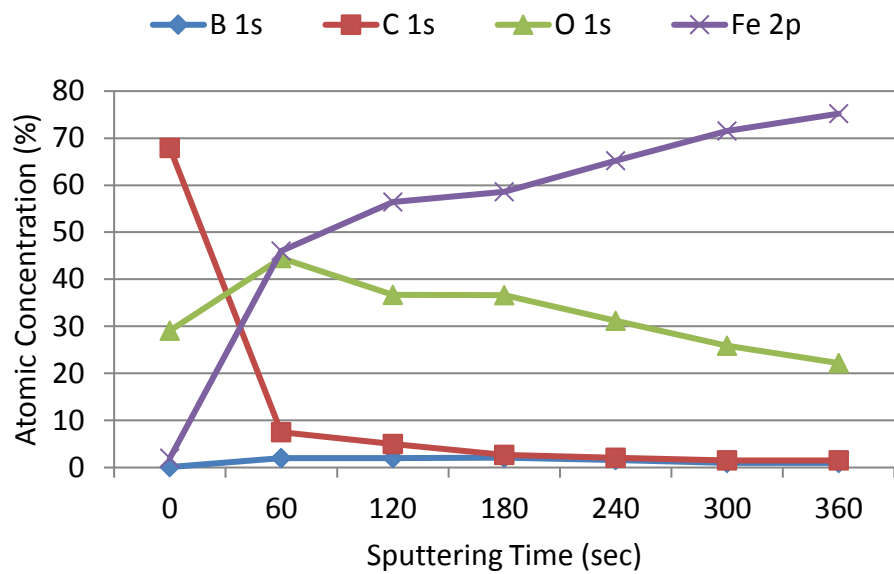
(a)
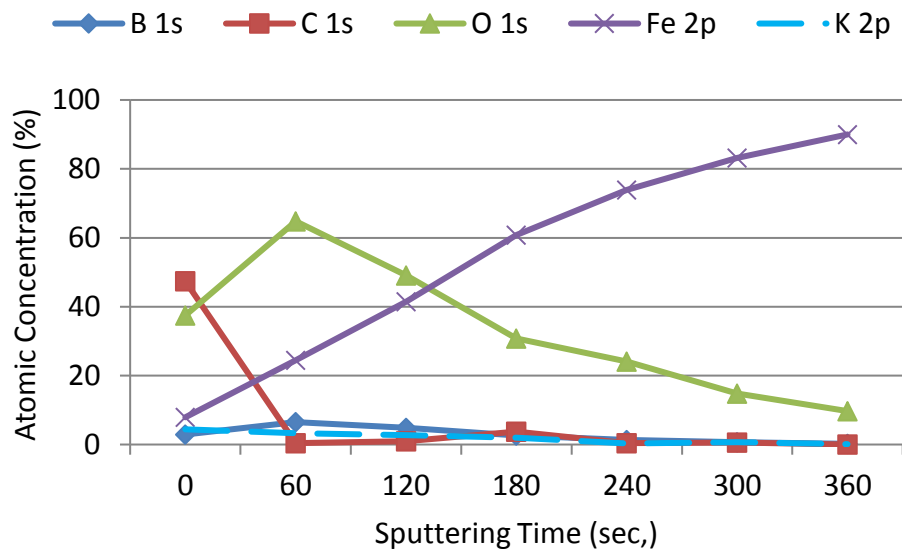
(b)

Figure 7-12 Average XPS depth profile of borate tribofilms formed at 100°C and 3 hrs tests from;(a) ABE and (b) KBE-containing oils at 1.0 wt. % concentration. The error bars are excluded for clarity

However, KBE-containing tribofilms gave a higher atomic concentration of B 1s than on ABE. In addition, the atomic concentration of B 1s at 1.03 nm on KBE tribofilms was higher than on ABE. This can be attributed to the higher concentration of boron in KBE additive than ABE as described in Chapter 3. At the maximum sputtering depth of 6.18 nm, the rate of decrease in B 1s on KBE tribofilms was higher than ABE. The higher increase in depth of B1s on ABE based tribofilms at 100°C is indicative of its adsorption mechanism [119, 198], unlike BTE tribofilms that relies more on adhesion and electrophoresis mechanism for wear resistant [201]. This is an indication that on ferrous substrate more permeating films of boron oxide were formed on ABE tribofilms than KBE that could have played a role in its better antiwear performance than KBE-based tribofilms at this temperature.

At the surface of the tribofilm and up to 1.03 nm depth, the XPS peaks of O 1s on KBE-based tribofilms gave higher atomic concentration than ABE-containing tribofilm, as shown in Figure 7-12 (a) and (b). However, between 4.12 nm and 6.18 nm depths, tribofilms containing ABE additive gave higher B 1s atomic concentration than KBE-containing tribofilm.

The lower atomic concentration of O 1s peaks at depths above 3.1 nm within KBE tribofilms compared to ABE indicated that changes in certain metallic oxides took place. The influence of atomic concentration of K 2p on KBE-containing tribofilm is limited to 4.12 nm as shown in Figure 7-12 (b). This suggests that any likely fusion of oxides of potassium and boron to form inorganic borate glass is limited to 3.0 nm depth range.

A key component of borate wear-resistant glass on ferrous substrate is Fe 2p peaks which is indicative of iron interaction with oxygen and carbon as shown in Figure 7-12 (a) and (b). The result indicates that atomic concentration of Fe 2p peaks on ABE-containing tribofilm is higher than KBE only at 1.03 and 2.06 nm, but lower at all other concentrations.

7.6 Raman analysis of tribofilms species at varying temperatures

The room temperature Raman spectroscopy indicating different frequency range at different temperature, sliding time and process on tribofilms containing ABE and KBE tests are shown in Figure 7-13 (a) to (f). In this study, bands involving different

vibrations of the BO$_3$ and BO$_4$ species were characterized using band assignments described in the literature from similar works.

Trigonal BO$_3$ species in B$_2$O$_3$ was identified by bands around 700 and 1321 cm^{-1}, while the tetragonal species was identified by Raman shifts around 630, 879, 1050 and 1380 cm^{-1} [181, 318-320]. The area ratios of these bands were utilised based on changes in the glass structures of ABE and KBE–containing tribofilm as shown in Figure 7-13 (a) to (f). Raman intensities of tribofilms formed at different temperatures, sliding process had bands of varying iron oxides. These ranged from magnetite (Fe$_3$O$_4$) at 309, 534, 614 and 663 cm^{-1} [299, 321] and haematite (α-Fe$_2$O$_3$) at 226, 294, 410 and 1320 cm^{-1} [299, 304, 321, 322].

However, the focus of this section is the transformation that takes place in B$_2$O$_3$ structural units. The tribofilms containing ABE compared to KBE from different tribotests ran at different temperatures were observed to have more iron oxides and oxyhydroxide. Their presence might have played a significant role in the antiwear performance of ABE-containing tribofilm at different temperatures during the 3 hr and 6 hr tests. However, at the end of 3r3 tests, the level of haematite and goethite on pre-formed ABE tribofilms dropped significantly which could have affected its durability performance as shown in section 5.3.

Acquired Raman spectra of different frequencies are used to identify bands involving BO$_3$ and BO$_4$ species vibrations. The fractions of BO$_4$ units (N$_4$ fraction) can be determined from the ratio of total area of different bands involving BO$_4$ species to the total area of bands associated with borate species Equation 7-1 as obtained from the literature [181, 211, 323, 324], enables the identification of borate structural unit transformation using N$_4$ speciation technique. In order to characterize the N$_4$ species formed on ABE and KBE tribofilms at a range of temperatures for different sliding time and process, a deconvolution of the Raman peaks is shown in Figure 7-13. A summary of the resulting N$_4$ on ABE and KBE tribofilms at different temperature and wear process are shown in Figure 7-14.

$$N_4 = \frac{Area\ of\ \sum BO_4^-}{Area\ of\ \sum BO_3^- \ + \ Area\ of\ \sum BO_4^-}$$

Equation 7-1
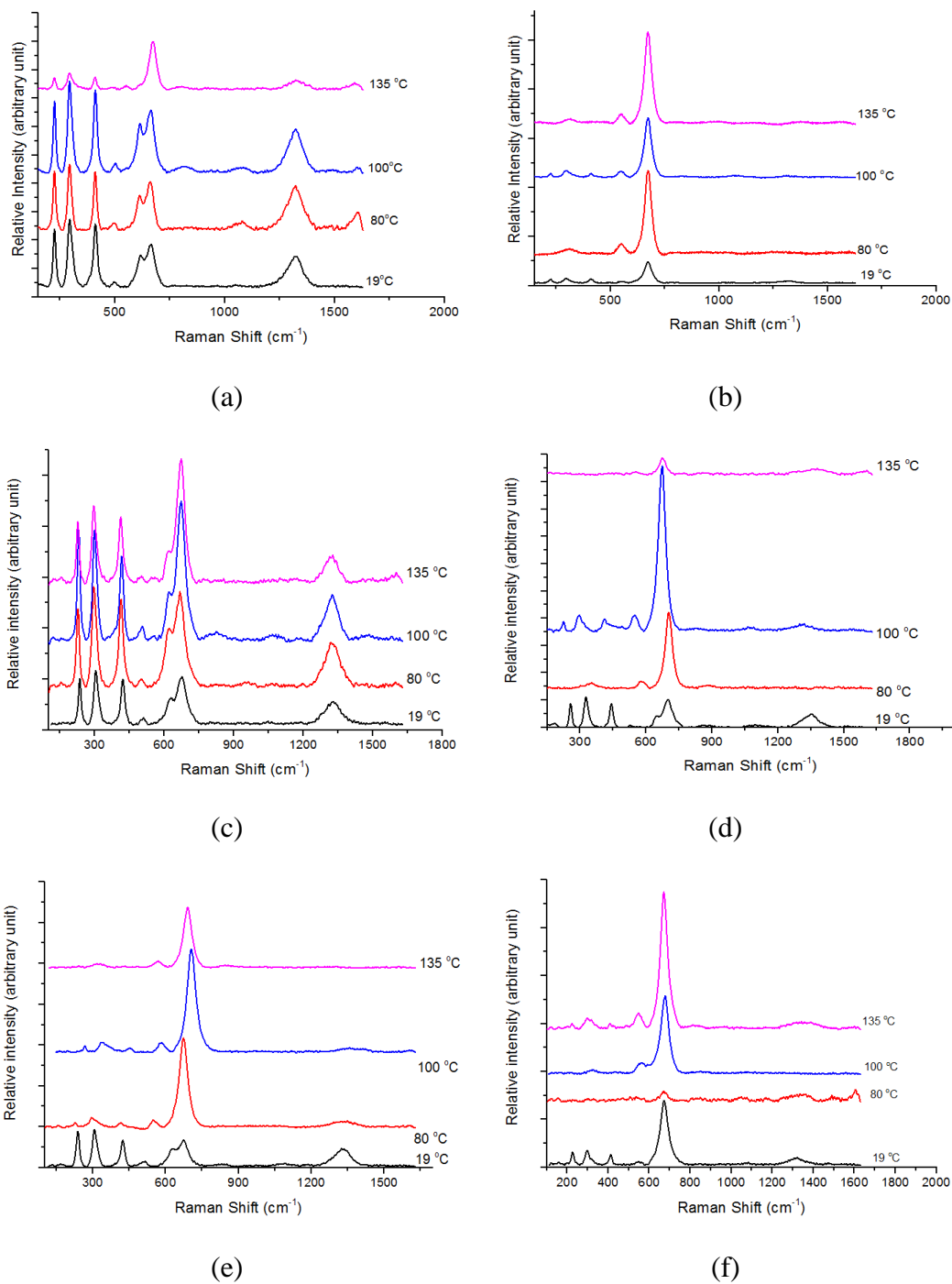
Figure 7-13 Changes in Raman intensity of borate tribofilms formed at different sliding process, temperatures and 1.0 wt. % additive concentrations;(a) ABE-(3hr), (b) KBE-(3h), (c) ABE-(6hr), (d) KBE-(6hr), (e)ABE-(3r3) and (f) KBE-(3r3). The spectra are plotted on the same scale and have been shifted vertically for clarity

The proportion of BO_4 tetrahedral in boric oxide structural units in ABE-containing tribofilm for 3 and 6 hr tests did not fall below 0.16 at the end of different sliding times. However, this was found to reduce significantly when the sliding process changed to 3r3, irrespective of the test temperature. On the other hand, changes in conversion of BO_3 structural units to BO_4 on tribofilms from temperature range of 19°C to 100°C on KBE-based tribofilms did not go beyond 0.18 for all sliding processes.
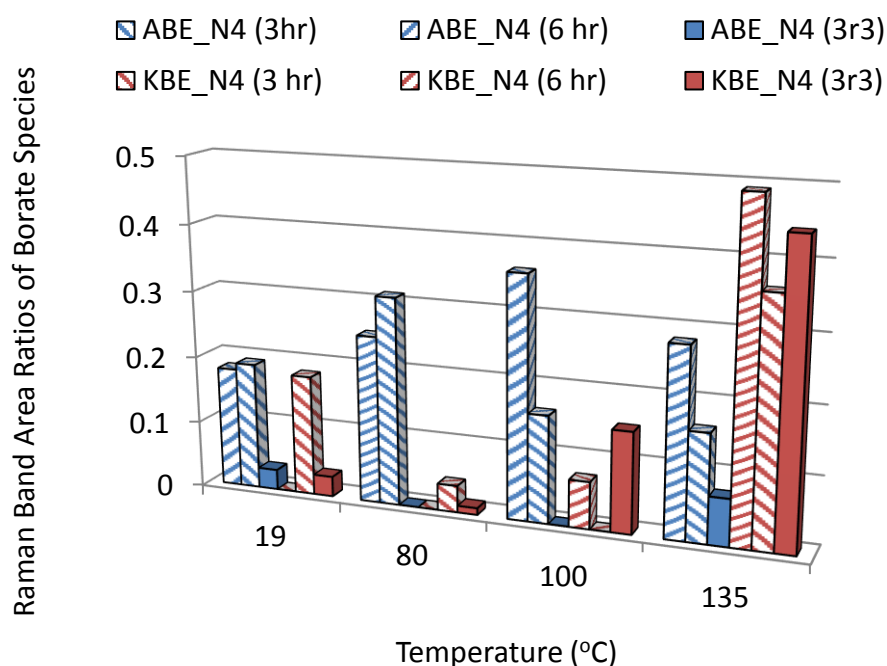
Figure 7-14 Raman speciation of BO_4 in B_2O_3 on tribofilms formed by borate additives at 1.0 wt. % concentration for a range of temperatures and wear processes

At 135°C bulk oil temperature, N_4 value on KBE-containing tribofilms increased significantly to a range between 0.36 and 0.49 for all sliding conditions. This is an indication that at the highest temperature, structural transformation of BO_3 units to BO_4 was more significant on tribofilms containing KBE additives at 135°C than on ABE. The antiwear performance and durability of KBE-based tribofilm at 135°C as shown in Chapter 5 could have been positively influenced partly due to this transformation and partly due to changes in alkali oxide (potassium oxide) and boron oxide concentrations, as shown in Figure 7-11.

The antiwear performance of ABE-containing tribofilms as shown in Chapter 5 appeared to be positively affected by structural transformation at 3 hr and 6 hr tests at all temperatures, but preformed ABE gave poor durability due to low N_4 values at 100ºC and 135ºC tribological test temperature.

This could be attributed to the nature and composition of the wear-resistant borate glass on ABE-containing tribofilms, which had been shown to be composed of a more stable iron oxide-boric oxide glass, unlike iron oxide-boron oxide-alkali oxide glass system on KBE tribofilms. Hence, the result of this study suggests that boron oxide anomaly affects antiwear performance and durability of tribofilms from alkali-based nanoparticle dispersion borate ester as lubricant additives more than that with organoborate at high temperature.

7.7   Chemistry of tribofilms from dissolved-water contamination

The tribochemistry of ABE and KBE tribofilms are presented in this section to provide a better understanding of how the antiwear performances of borate boundary films are influenced by different levels of water contamination since their friction reducing and antiwear mechanisms are known to rely on moisture in the surrounding air.

7.7.1   XPS results of tribofilm species from humidity test

The atomic concentrations of B 1s, C 1s, O 1s, Fe 2p and N 1s on the surfaces of the borate tribofilms at different humidity condition and K 2p peaks for KBE are shown in Figure 7-15. Changes in environmental conditions from dry air to moisture-rich environment greatly affects XPS atomic concentrations of C 1s, Fe 2p and O 1s on tribofilms containing KBE and ABE. In addition, changes in XPS atomic concentration of K 2p in KBE also occurred.

These changes are indications that reacted layers formed by ABE and KBE borate additives are different due to changes in humidity conditions. The major highlights of long scan XPS spectra of ABE and KBE tribofilms at 5% and 95% RH were compared to conditions of dissolved water contamination at 65% RH as shown in Figure 7-16 for Fe 2p peaks. In addition, the summary of XPS peaks of O 1s and B 1s are shown in Table 7-6 (a) and (b), and Table 7-7 (a), (b) and (c) for C 1s, N 1s and K 2p respectively. The peaks of Fe 2p at 5% RH on ABE tribofilms consisted of different

phases of iron oxy-hydroxides, oxide of iron and unusually high concentration of metallic iron. This was identified at a binding energy of 706.8 eV [158, 197, 317] as shown in Figure 7-16 (a). However, when dissolved water contamination was increased to a relative humidity of 95%, there was no indication of metallic iron oxidation by boron on ABE tribofilms as shown in Figure 7-16 (e).
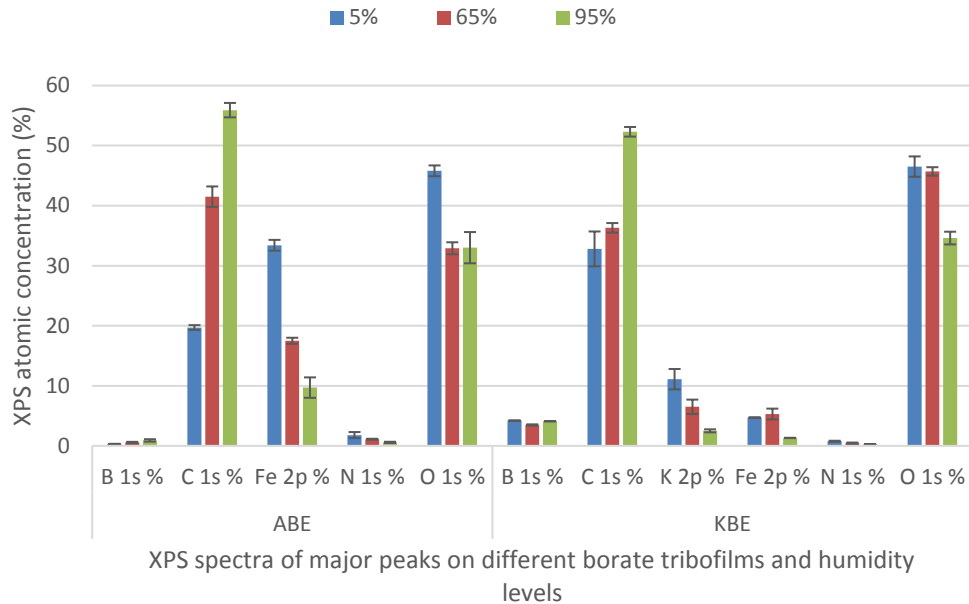
Figure 7-15 Average XPS atomic concentration of element peaks on tribofilms by oils with 1.0 wt. % borate additive concentrations and 19°C tribotest temperature exposed to different humidity conditions for; B 1s, C 1s, N 1s, O 1s, Fe 2p and K 2p. Error is measured as standard deviation of three analysis points

On the other hand, the peaks of Fe 2p on KBE-containing tribofilms formed at 5% and 95% RH as shown in Figure 7-16 (b) and (f) respectively indicates the presence of metallic iron on built-up KBE tribofilms along with oxides and oxy-hydroxides of iron. The presence of iron borides had been suggested to form 'non-active antiwear agent' from non-active atom such as boron permeating into the metal surface to form protective friction and wear reducing layer [314, 325]. Hence, the formation of iron borides on KBE tribofilms formed at 95% RH could have contributed to its increasing antiwear performance compared to ABE and ZDDP tribofilms as shown in Figure 7-16 and Table 7-7. At 65% RH, no metallic iron was detected on KBE and

ABE-containing tribofilms. This is an indication that boron binds directly with the oxygen in iron oxide and not with the metallic iron [158, 161].
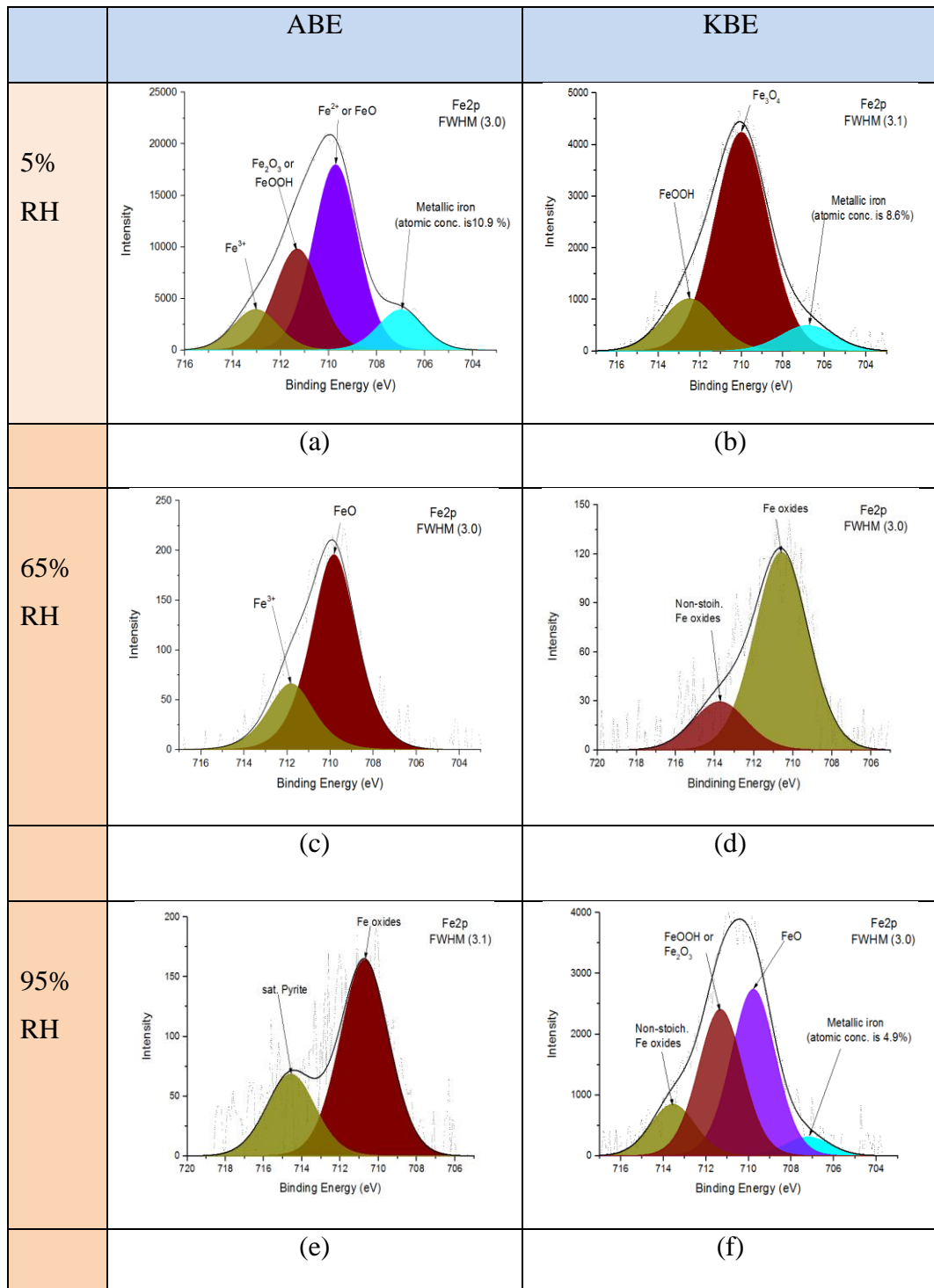
Figure 7-16 Long scan results for XPS peaks of Fe 2p at different relative humidity, 19°C test and 1.0 wt. % additive concentration for; (a) ABE-5%, (b) KBE-5%, (c) ABE-65%, (d) KBE-65%, (e) ABE-95%, and (f) KBE- 95%

Table 7-6 XPS binding energy of compounds or bonds on tribofilms formed by oils containing 1.0 wt. % additive concentration at 19°C for; (a) O 1s and (b) B 1s

Additive Type	Binding Energies (eV)			Compounds or Bond Types		
	5% RH	65% RH	95% RH	5% RH	65% RH	95% RH
ABE	-	-	529.6	-	-	FeO
	530.8	529.5	530.8	Oxides	Fe oxides	Oxides
	531.7	530.9	531.8	C-O-B	Oxides	C-O-B
	532.5	531.9	532.8	C-OH	FeOOH	C-OH
	533.7	533.2	533.8	B-O	B-O	B-O
KBE	529.7	-	529.7	FeO or KO_2	-	FeO or KO_2
	531.3	530.6	531.1	C-O-B	FeO or KO_2	C-O-B
	532.1	531.6	532	FeOOH	C-O-B	FeOOH
	532.8	532.9	532.8	C-OH	C-OH	C-OH
	533.9	-	533.9	B-O	-	B-O
(a)						
ABE	191.4	191.6	191.6	$B(OC_{12}H_{25})_3$	B_2O_3 in oil	B_2O_3 in oil
	I91.7		191.3	B_2O_3 in oil		$B(OC_{12}H_{25})_3$
KBE	192.2	191.9	192.3	B_2O_3	B_2O_3	B_2O_3
	-	-	191.5	-	-	B_2O_3 in oil
	-	-	188.7	-	-	Fe_xB
			193.3			$B(HO)_3$
(b)						

A summary of B 1s peaks as shown in Figure 7-16 (b) indicates that, as humidity increases from 5% to 95%, changes in B 1s took place from organic borate or trialkyl borate [131, 158] to boron oxide or oxygen in boron oxide and iron oxide [288, 326]

167

on ABE-based tribofilms. However, changes in B 1s peaks on KBE-based tribofilms with increasing level of dissolved-water contamination was mainly from oxygen in boron oxide and iron oxide, B_2O_3 and iron borides at 188.7 eV [193, 327].

Table 7-7 XPS binding energy of compounds or bonds on tribofilms from 1.0 wt. % amount of additive in oil at 19°C for; (a) C 1s, (b) N 1s and (c) K 2p

Additive Type	Binding Energies (eV)			Compounds or Bond Types		
	5% RH	65% RH	95% RH	5% RH	65% RH	95% RH
ABE	282.9	-	284.7	Carbides	-	C-C/C-H
	284.7	284.7	285.9	C-C/C-H	C-C/C-H	C-C
	286.0	285.4	286.9	C-O	C-C	C-O
	287.4	286.3	287.8	Ads. ABE	C-O	Ads. ABE
	288.6	288.1	288.8	C=O	C=O	C=O
KBE	84.9	-	283.4	C-C/C-H	-	Carbides
	286.5	284.9	285.1	C-O	C-C/C-H	C-C
	288.1	286.2	286.4	C=O	C-O	C-O
	289.1	288.3	288.1	Carbonates	C=O	C=O
(a)						
ABE	401.1	400.7	400.1	Graphitic N_2	Organic N_2	Organic N_2
	399.5	-		N-O/N-C-O	-	-
	397.2	-		Iron nitride	-	-
KBE	400.1	-	-	Organic N_2	-	-
(b)						
KBE	292.9	292.9	292.9	KO_2	KO_2	KO_2
(c)						

The major highlights of C 1s and N 1s are shown in Table 7-7 (a) where XPS peaks of C 1s on tribofilms formed by ABE and KBE containing oils at different humidity

levels formed different compounds and bonds. These are; adsorbed ABE at 5% and 95% RH at 287.4-287.8 eV [158], carbonates at 288-289 eV [158, 296, 298] at all humidity conditions for both borate additive types. The XPS peaks of N 1s on tribofilms formed by ABE containing oil at 5% RH gave N-containing compounds or bonds that were completely different to organic nitrogen (400.1 - 400.7 eV) [195] formed at 65% and 95% RH. These nitrogen compounds must have contributed to the poor antiwear performance of ABE tribofilms at 5% RH compared to KBE and ZDDP tribofilms under this test conditions. The XPS peaks of K 2p on KBE tribofilms existed at 292.9 eV on all the tribofilms formed at 5%, 65% and 95% RH that indicated the presence of oxides of potassium, such as (KO_2) [200].

7.7.2 Raman results of tribofilm species from humidity tests

Figure 7-17 (a) and (b) shows how humidity affected tribofilms chemistry from oils containing ABE and KBE using Raman vibration spectroscopy. This is to provide a better understanding of the changes that took place on tribofilms of worn plates over a range of dissolved water contamination during tribological tests. The key features of Figure 7-17 (a) and (b) are: decreasing intensities of haematite bands at 226, 294 and 410 cm^{-1}, and magnetite bands at 309, 534, 614 and 663 cm^{-1} [299, 321] with increasing relative humidity.

Raman sensitive boron compounds identified are; bands around 495 and 879 cm^{-1} was identified as boric acid [138, 160], boroxol groups in B_2O_3 peaks at 809 cm^{-1} [171, 210, 300, 301] and boroxol linked to at least one BO_4 tetrahedra located around 769-785 cm^{-1} [208, 213, 302]. The presence of carbonates was identified at 1060 $\pm$ 10 cm^{-1} bands [191, 213]. Raman peaks near 1300 $\pm$ 10 cm^{-1} could be in-phase wagging and deformation of - CH_3 - and - CH_3 - groups [206] or BO_3 linked to BO_4 units [178, 208, 213, 302] or α-Fe_2O_3 [304, 328, 329] that were relatively unaffected by changes in humidity.

The behaviour of distinct borate groups, iron oxides and iron oxy-hydroxides could have great influence on the tribological performance of tribofilms from borate additives. Changes in Raman shifts of oxides and hydroxides of iron were more significant on ABE than KBE-containing tribofilms. Hence, humidity effect on tribofilms containing ABE appeared to affect oxides and oxy-hydroxides of iron more than KBE-based tribofilms except at 65% RH. This is an indication that under certain

moisture level in air, the chemistry of boron-based tribolayer appear to change with respect to the prevailing moisture conditions of the surrounding air.
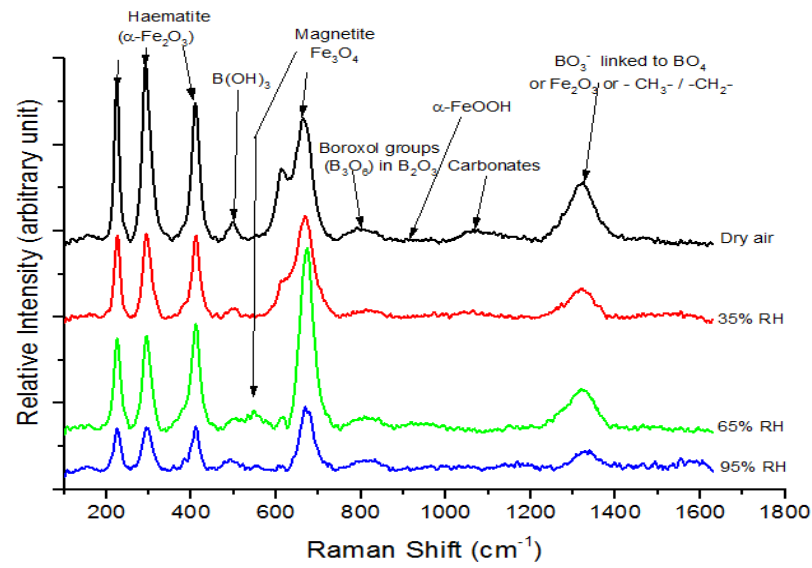
(a)
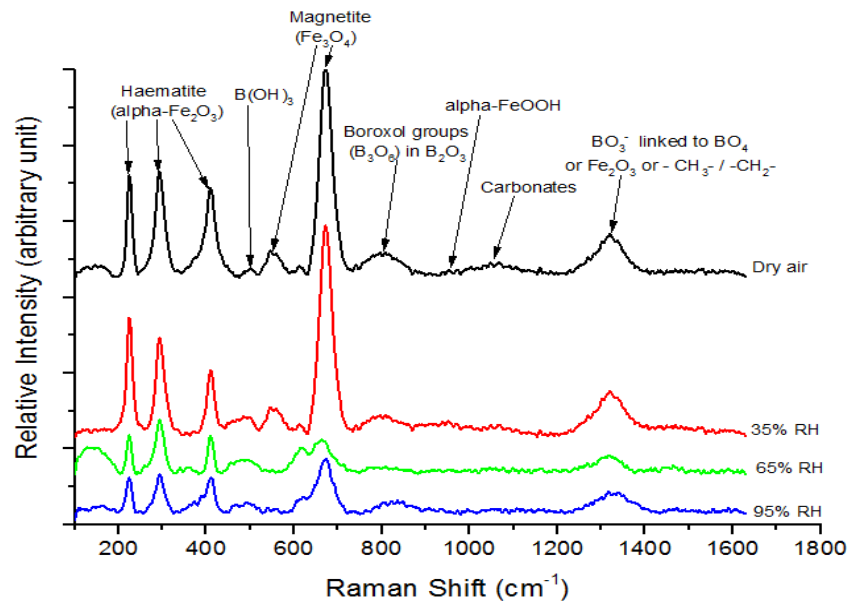
(b)

Figure 7-17 Room temperature Raman spectra of tribofilms formed by oils with 1.0 wt. % additive concentrations and 19°C for; (a) ABE, and (b) KBE. The spectra are plotted on the same scale and have been shifted vertically for clarity

These changes in the chemistry of borate tribofilms under different humidity conditions had been shown to promote friction reduction [24]. However, results from this study in conjunction with results from Chapter 5 indicates that changes in the chemistry of borate tribofilms under different humidity conditions do not only affect friction reduction, but also its wear resistant performance.

7.8   Chemistry of tribofilms due to free-water contamination

Figure 7-18 (a) and (b) shows how the Raman shifts on tribofilms from oils containing ABE and KBE changes with free-water contamination respectively. The key features of Figure 7-18 are: decreasing intensities of haematite bands at 226, 294 and 410 cm^{-1}, and magnetite bands at 309, 534, 614 and 663 cm^{-1} [299, 321] with increasing water concentration in the oil. Raman sensitive boron compounds identified are; bands around 495 and 879 cm^{-1} was identified as boric acid [138, 160], boroxol groups in B_2O_3 peaks at 809 cm^{-1} [171, 210, 300, 301] and boroxol linked to at least one BO_4 tetrahedra located around 769-785 cm^{-1} [208, 213, 302].

The presence of carbonates was identified at 1060 ± 10 cm^{-1} bands [191, 213]. In addition, Raman peaks near 1300 ± 10 cm^{-1} could either be anyone of the followings: in-phase wagging and deformation of - CH_3 - and - CH_3 - groups [206], BO_3 linked to BO_4 units [178, 208, 213, 302] or Fe_2O_3 [303, 304]. Raman results on water contaminated ABE-based tribofilms was able to provide comparable antiwear performance to KBE up to 1.0 wt. % free water. This can be attributed to the higher level of haematite on ABE than KBE tribofilms. However, haematite had been shown to be hard and less protective of the contacting asperities in the literature [275, 330]. At free-water contamination above 1.0 wt. %, the absence of carbonate could have contributed to poor antiwear performance.

On the other hand, the influence of free-water on tribofilms containing KBE gave β-FeOOH at 311 cm^{-1} [322, 331] at different water concentration except at 1.0 wt. % where haematite was detected. These were able to provide wear protection up to 1.5 wt. %. Hence, an indication that boroxol group linked to BO_4 structural units enhanced antiwear performance of the borate tribofilms contaminated with added water in the range of 1- 0.5 wt. % before high wear rates sets in when compared to ZDDP.
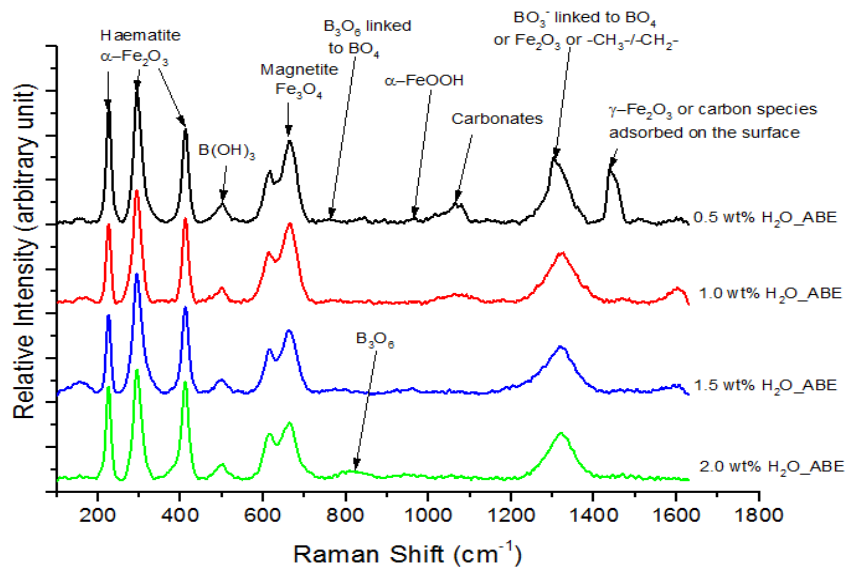
(a)
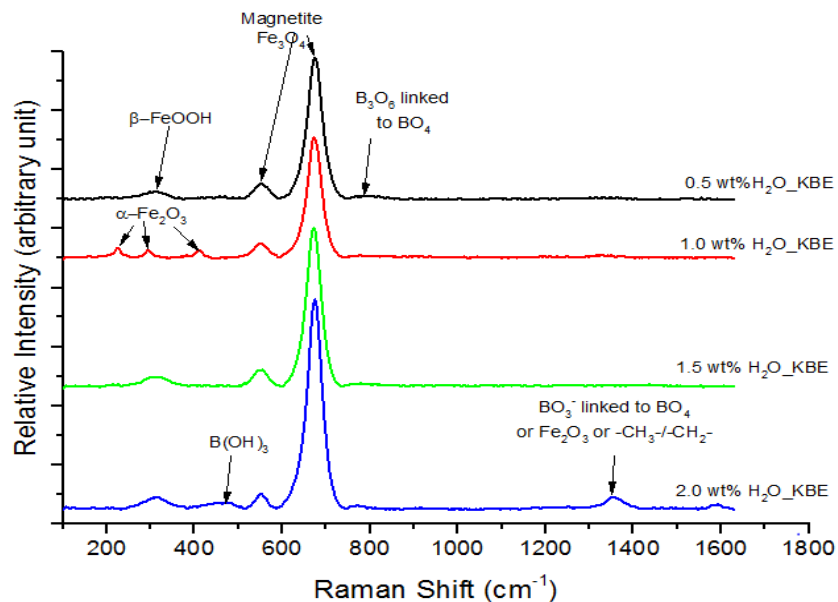
(b)

Figure 7-18 Raman spectra of tribofilms from free-water in oil tests at different water concentration formed by oils with 1.0 wt. % additive concentrations, 80°C tribotest temperature and 6 hrs test durations for; (a) ABE, and (b) KBE. The spectra are plotted on the same scale and have been shifted vertically for clarity.

The effects of humidity on borate tribofilms indicates the presence of boric acid and substantial amount of random three-dimensional network of nearly flat BO_3 triangles

in boron oxide converted into boroxol. On the other hand, free-water affects boron anions by the formation boric acid, replacement of one or two BO_3 triangles of the six-member rings by BO_4 tetrahedral on KBE tribofilms. A similar behaviour was observed on ABE tribofilms except at 2.0 wt. % water concentration where the boroxol structural units was also formed along with BO_3 linked to BO_4 units at other concentrations.

7.9 Summary

This chapter explored the chemistry of tribofilms formed by the borate additives with regards to varying conditions such as; concentration, temperature, humidity and free water contamination with the following key observations:

- The poor antiwear performance of non-synthetic boron compounds at high concentrations was not directly due to boric acid as was previously known, but was shown by this study to be due to high concentration of boron on the tribofilms which leads to the formation of small fractions of hard, abrasive boron nitride and carbides

- Tribofilms formation by oils containing synthetic boron-based additives were observed in this study to be affected not only by temperature and wear process, but also by the type of metallic oxide that fused with boron oxide to form wear-resistant borate glass on borate tribofilms

- The result from this study indicated that in the presence or absence of iron oxy-hydroxides, the antiwear performance of some boron-containing lubricant additives could be significantly affected

- Tribofilms containing borate additives are known to exhibit poor antiwear performance at 100^oC due to unreacted borate additives, but the results from this study had shown that the quantity of alkali-based compounds within KBE-based tribofilms have significant effect.

- A high degree of transformation of BO_3 structural units into BO_4 groups in boron oxide on KBE tribofilms provided was more tenacious than ABE at 135^oC

- The result of this study suggests that boric oxide anomaly is more likely to affect the antiwear performance and durability of tribofilms containing alkali borate ester than organoborate ester additives in lubricating oils for IC engines

- In the absence of moisture, a high concentration of metallic iron on the wear scar of both borate tribofilms gave high wear rates due to insufficient boron oxide to passivate the contacting asperities and presence of carbides acting as third body abrasives

- In environments saturated with moisture, some metal borate nanoparticle dispersion can undergo tribo-oxidative reaction of boron oxide and metallic iron to form non-active wear-resistant iron borides on KBE tribofilms

- Evidence from this study indicated that dissolved water contamination on borate tribofilms enhanced antiwear performance by trigonal borate anions structural transformation to boroxol groups

- On the other hand, free-water contamination was able to permit the boroxol groups to link the BO_4 tetrahedral structural units for antiwear protection up to 1.5 % water concentration.

Chapter 8

Discussion

8.1   Overview of discussion

The discussion chapter of this PhD research work will consider different themes of the result chapters. Following the analysis of results, detailed key findings will be compared to available literatures in order to examine areas of agreement and disagreement. The key areas to be examined are: (1) comparison of borate additives to ZDDP in terms of resistance to hydrolysis, (2) tribochemistry of borate-containing reacted layers compared to ZDDP at different test conditions, and (3) how borate friction reducing and antiwear mechanisms are affected by different extrinsic test conditions.

8.2   Effect of additive concentration on borate antiwear films

In order to form suitable borate salts and borate esters for additives in lubricating oils, various schemes are employed to produce synthetic borate additives from non-synthetic borates. The synthetic borates are expected to overcome borate susceptibility to hydrolysis as addressed in the literature review of Chapter 2. Assessment of thermo-oxidative and hydrolytic stabilities of borate additives with respect to ZDDP will provide valuable information for discussion on the behaviour of borate tribofilms at different test conditions.

8.2.1   Hydrolytic and thermo-oxidative stability additives

The results of hydrolytic and thermo-oxidative stabilities of antiwear additives in Chapter 4 indicates that BTE additives has the lowest resistance to hydrolysis and thermo-oxidative stability based on Figure 4-1. This is an indication that under thermal and tribo-oxidative conditions, the effect of hydrolysis will easily break down molecules in lubricating oils containing BTE more than ABE and KBE. This can be attributed to sp2 hybridization of B atom that has an empty 2p orbitals. The presence of a nucleophiles with a lone pair of electron like water [290, 332] could have attacked

boron atom in BTE additives more than ABE and KBE. The hydrolysis mechanism of borate ester is shown in Figure 8-1.

Hydrolysis by-products of borate ester is known to yield boric acid and alcohol [10, 119]. The poor hydrolytic stability of BTE is likely to yield more boric acid and alcohol than in oils containing ABE and KBE additives. However, the main friction-reducing compounds on reacted layers formed by borate additives is boric acid [27, 220]. In addition, the lower thermal and oxidative decomposition temperatures of BTE suggests that more volatile products are formed than oils containing ABE, KBE, ZDDP and PAO. These volatile products could be alcohol (ROH), moisture and some boric acid. However, boric acid is known to be volatile with steam [35, 164, 333] and start to decompose between 70-80°C [162, 163].
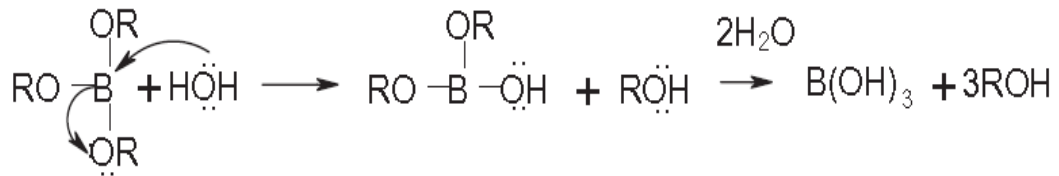
Figure 8-1 The hydrolysis mechanism of borate ester [10]

Hence, sudden weight loss upon thermal and oxidative decomposition of oils containing BTE additives ahead of other borate additives is an indication that hydrolysis will affect its thermal and tribo-oxidative behaviour more than other borate additives.

8.2.2 Additive concentration effects on friction coefficient reduction

The friction coefficient performance of ABE and BTE-containing tribofilms were respectively found to be consistent with results from similar studies as observed in the literature [158, 228, 334]. Similarly, friction coefficient performance of KBE was found to be consistent with results from the literature [201]. However, at higher concentration of potassium borate in lubricating oils, a significant reduction in friction coefficient is obtained. This is in good agreement with results from the literature [157, 335]. On the other hand, the friction response of ZDDP tribofilm at low concentration as shown in Figure 5-1 (a) agrees with results from the literature [89]

and at 1.2 wt. % concentration [21]. The difference in friction coefficient of ZDDP tribofilms obtained in this study could be related to test durations and quantities of phosphorus in ZDDP. Increasing additive concentration of ZDDP did not result into decreased friction coefficient, unlike the borates; despite its smoother morphology as shown in Figure 6-4.

The friction reducing mechanism of borate containing oil is attributed to boric acid (H_3BO_3) due to its low shear strength that is similar to MoS_2 [27, 159, 222]. In addition, boric acid is known to be lubricious on surfaces in tribological contacts due to reactions with moisture in air of the surrounding environment [154, 221, 223] as shown in Figure 2-20. This was attributed to the weak van der Waals forces between lamellar sheets of boric acid [220-223].

The friction coefficient performance by ABE and KBE tribofilms was better than BTE at all additive concentration. This observation supported the suggestion that hydrolysis of borate ester yields boric acid. However, boric acid is known to be insoluble and abrasives in oils [11, 118, 119, 121]. This could adversely affect tribological performance as suggested in the literature.

The established friction reducing and self-replenishing mechanism of tribofilms formed by borate additives assumed that sheet-like crystals of boric acid are stable at all temperatures. Evidence from Figure 7-3 and Figure 7-6 indicated that Raman intensity on borate tribofilms containing ABE additive at different concentration have higher boric acid than KBE and BTE. However, an increase in Raman intensity of boric acid did not result into significant friction coefficient reduction by ABE tribofilms compared to KBE. However, Raman intensity of boric acid on KBE tribofilms was consistent with its friction reduction performance as shown in Chapter 7. On the other hand, Raman intensity of boric acid on BTE tribofilms appeared to be intermediate between ABE and KBE at different concentrations. These results suggests the presence of boric acid is necessary in the control of friction coefficient on borate tribofilms. However, its formation can be affected by hydrolysis, amount of boron present and other extrinsic factors such as temperature and presence of third body abrasives. One major adverse effect of hydrolysis on BTE tribofilms is the need for low concentration of boron and boric acid for comparable friction coefficient performance with ABE and KBE tribofilms.

177

At the test temperature for this experiment, a change of state could occur to influence the amount of boric acid present. However, results from the literature had indicated that boric acid under prolonged heating is stable up to about 70-80°C [162, 163]. This suggests that under thermal and tribo-oxidative conditions at 100°C temperature, boric acid from oils containing boron additives could decompose or vaporize with steam. Its decomposition to form boron oxide was shown in the literature to be stage-wise. Firstly, it decompose to form metaboric acid around 100°C before finally dehydrating at 130°C to form boron oxide [162, 163].

Another friction reduction mechanism of boric acid was attributed to the passivation of high energy edge sites on boric acid by physisorbed water molecules that allows lamellar sheets of boric acid to easily shear and friction reduction [24]. However, at bulk oil test temperatures of about 100°C, evaporation of steam from the oil can take place. This could result into less physisorbed water molecules to passivate the edge site of boric acid, yet friction coefficient was not too poor. This could have been due to boron oxide affinity for moisture which it does not release easily [269], unlike boric acid that is known to be volatile with steam as suggested in the literature [35, 162, 164].

The peaks of B 1s atomic concentration on tribofilms from BTE in Chapter 7 shows rapid increase of about 14 and 19 times higher at 1.0 and 2.5 wt. % respectively than 0.5 wt. % additive concentrations. This is an indication that more boron compounds are formed on BTE tribofilms with increase in additive concentration. However, coefficient of friction provided by BTE tribofilm was higher than ABE and KBE. The high boric acid formed on BTE tribofilms at high concentration are expected to give lower friction coefficient reduction than ABE and KBE, if the mechanism of weak van der Waal's of boric acid is considered. However, friction results shown in Figure 5-1 (a) and Figure 5-2 indicated otherwise. In addition, if the passivation of high energy edge- site of boric acid mechanism is assumed, it is possible to assume that insufficient physisorbed water molecules to passivate the high energy edge-site of boric acid at the test temperature of 100°C.

The Raman intensity of boric acid on borate tribofilm at different concentrations as shown in Figure 7-6 (a) indicates two distinct behaviour. One is for the organic borate ester additives (ABE and BTE), and the other is for inorganic nanoparticle borate ester

(KBE). On the tribofilms formed between 0.5 and 2.5 wt. % concentration on ABE and BTE tribofilms, high boric acid gave friction coefficient reduction of 9% and 6 %, as shown in Figure 5-1 (a). On the other hand, tribofilms formed by KBE with lower Raman intensity of boric acid gave friction coefficient reduction of about 24 % between 0.5 and 2.5 wt. % additive concentration.

The difference in friction reduction behaviour of BTE at different concentration in comparison to ABE and KBE could be related to hydrolytic stability and test temperature. In addition, increased XPS atomic concentration of B 1s peaks on BTE tribofilms at higher additive concentration as shown in Chapter 7 and lower boric acid from Raman result analysis suggests that other boron compounds are formed. However, the presence of these boron compounds acts as third body abrasives on BTE tribofilms and consequently did not enhance friction reduction.

8.2.3 Effect of additive concentration on antiwear performance

Results of antiwear behaviour of borate-containing tribofilms are more different on the plates than pins as additive concentration increases as shown in Chapter 5. This could be related to dissimilar physical and chemical characteristics of tribofilms from these borate antiwear additives.

At low additive concentration (i.e. 0.5 wt. %), similar antiwear behaviour in comparison to ZDDP was provided by the borates on the pins. However, the tribofilms formed by ABE-containing oils gave better antiwear performance on the plates than other additives at this low concentration. The better antiwear behaviour results by ABE-containing tribofilms as shown in Figure 5-1 was similar to ZDDP antiwear behaviour at different concentration as observed in the literature [336]. At 1.0 wt. % additive concentration, the antiwear performance of ABE-containing tribofilm was comparable to ZDDP and better than KBE and BTE.

On the plates, the antiwear performance of tribofilms from BTE on the plates was poor compared to plates lubricated by only PAO. However, wear rates on tribofilms formed by oils containing BTE significantly increased with increasing additive concentration. This is unlike antiwear performance of ABE-based tribofilms, which decreases with increasing additive concentration. However wear protection by KBE-based tribofilms was more favoured at the highest concentration than at 0.5 and

1.0 wt. %. The poor antiwear performance of BTE confirmed the results from similar studies [161]. In addition, results of the antiwear performance of ZDDP at 1.0 wt. % and PAO is in good agreement with the literature [21, 239].

FIB-SEM analysis results indicated that tribofilms formed by borate containing oils have thickness in the range of 60 to 230 nm that are similar to results from the literature [80, 117, 153]. In addition, the thickness of ZDDP tribofilms is in good agreement with estimates between 80 and 100 nm in the literature [91, 189]. However, the study of Pereira et al. disagreed [188], as it estimated ZDDP film thickness as 180 ± 60 nm using FIB-SEM, where the high standard deviations from the result was attributed to tribofilms heterogeneity. This is another indication that thicker tribofilm does not necessarily result into better antiwear performance.

The tribofilm from BTE-containing oils at 1.0 wt. % gave the highest thickness compared to other additives as shown in Chapter 6. However, this did not provide lower wear rates. AFM and nanoindentation results indicated that BTE morphology and nanomechanical properties vary significantly with increased concentration in the oil compared to other additives. The presence of B_2O_3 on ABE tribofilms at all concentrations from XPS and Raman analysis supported results from similar studies on the tribochemistry of ABE tribofilms [152]. The morphology, hardness and boron content on ABE tribofilms did not vary significantly with increasing additive concentration. This is unlike tribofilms containing BTE at different concentration, based on physical and chemical examination which indicates large differences.

The antiwear performance at different additive concentration shown in Chapter 5, indicated that wear-rates are higher on worn plates than the pins. This is consistent with results of similar studies from the literature [82, 201, 337]. In addition, increased concentration of KBE additive at 0.5 and 1.0 wt. % gave high surface roughness and thicker tribofilms compared to ABE, but did not provide better antiwear performance on the plates. However, the antiwear behaviour of tribolayer formed by metal borate as lubricant additives in the literature could be affected by concentration [201, 338]. The chemistry of reacted layer and nanomechanical properties have an important role to play in the antiwear behaviour of borate tribofilms. An increase in additive concentration between 1.0 wt. % and 2.5 wt. % resulted in significantly better antiwear performance of ABE and KBE tribofilms than BTE. A corresponding change also

occurred on BTE tribofilms not only with its surface morphology, but also the atomic concentration of B 1s. This is an indication that increased activity of reacted layers on BTE resulted in adverse antiwear performance. Surface characterisation by Raman was able to identify the boroxol group on tribofilms formed by BTE at 0.5 wt. %, but formed trigonal BO_3 units linked to BO_4 tetrahedra at 1.0 and 2.5 wt. % .

These changes can be linked to the XPS results in form of bridging oxygen and non-bridging oxygen which occurred on the borate tribofilms formed on the plates. In addition, reduced intensity of magnetite indicates the involvement of native iron oxide in the tribochemical reaction process as identified in previous work from the literature [158]. This could have resulted in increased film thickness and surface roughness to give poor antiwear performance.

The very high B 1s atomic concentration from the XPS analysis suggests that more boron oxide could be formed. However, the antiwear mechanism of borate ester is attributed to digestion or fusion of boron oxide with metallic oxides and carbonates [80, 158, 339]. On BTE tribofilms at 1.0 and 2.5 wt. %, XPS results identified its degradation through the presence of C-O bonds. This is an indication that BTE was mechanically degraded during the friction process as identified in the literature [340]. Raman results shows that B_2O_3 in form of trigonal BO_3 units is linked to BO_4 tetrahedral units only.

This is unlike boron oxide on BTE tribofilms at 0.5 wt. % concentration that formed not only boroxol groups (B_3O_6), but also BO_3 linkage to BO_4 units. This is an indication that at higher concentration of BTE above 0.5 wt. %, the boron oxide formed is not only high, but also structurally different to give poor antiwear performance. The result of Raman intensity of boric acid to boron oxide for all the borate antiwear additives indicates that as additive concentration increases above 0.5 wt. %, boron oxide formed on ABE tribofilms did not vary significantly, unlike BTE-based tribofilms which decreased considerably at higher concentrations to give poor antiwear performance.

On the other hand, KBE tribofilms gave the highest boric acid to boron oxide ratio at 1.0 wt. %, which also gave poor antiwear performance like BTE at 1.0 and 2.5 wt. %. However, at higher concentration of KBE, boric acid to boron oxide ratio reduced to give better antiwear performance.

This is an indication that antiwear performance of KBE is greatly dependent on the ratio of boric acid to boron oxide. Studies from the literature had indicated that antiwear performance of KBE tribofilms is dependent on the amount of potassium borate nanoparticle reaching the friction zone as suggested in the literature [157, 341]. However, a similar studies on the antiwear performance of potassium borates had identified that at low concentration, low wear rates is possible [338]. The tribofilm formed by BTE at 1.0 wt. % concentration had significant hardness difference compared to those at higher concentrations. This can be attributed to the presence of B-OH units that indicated the presence of boric acid [342-344]. On the other hand, KBE tribofilms had similar boric acid ratio to boron oxide compared to tribofilms formed by BTE at 0.5 wt. % additive concentration that gave better wear rates.

The tribofilms containing KBE and BTE are observed to have similar morphology, but different hardness. Higher hardness of BTE tribofilms compared to KBE additive at 2.5 wt. % concentration could be attributed to the presence of BN and carbide particles. However, the hardness of worn sample lubricated by KBE was mainly composed of boron oxide as shown in Chapter 6. This is comparable to the hardness of boric acid and /or glassy boron oxide as shown in the literature [40, 345].

The hardness of worn samples lubricated by oils containing BTE at 2.5 wt. % as obtained in Chapter 6 are comparable to those obtained in the literature for thin films of BN (10.5 GPa) [41]. However, this increase did not enhance antiwear performance of BTE tribofilms, but rather gave severe wear compared to other additives. This behaviour could be attributed to hard boron nitride and carbides acting as third body abrasives. The concept of third body in borate tribochemistry had earlier been attributed to boric acid crystals as shown in Figure 8-2.
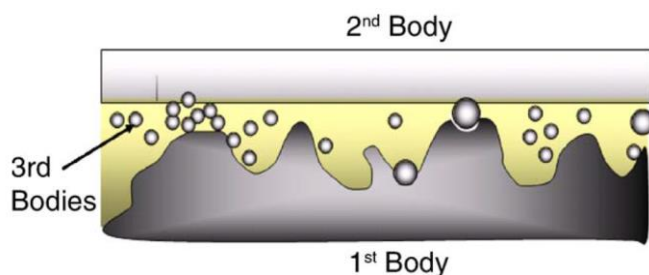
Figure 8-2 Boric acid particles acting as third body in a fluid lubricant **[222]**

However, results from this study suggests that hydrolysis effect due to thermal and tribo-oxidative degradation of BTE on a ferrous substrate did not only form boric acid, but also harder boron nitride (BN) and carbides acting as third body abrasive. This is based on results in Chapter 4, Chapter 6 and Chapter 7. Hence, results from this study indicated that the antiwear mechanisms of organoboron additives are affected more by hydrolysis than nanoparticle metal borate ester. This could be due to different modes of boron oxide formation, as shown in the literature [124, 125, 127, 201, 226].

On tribofilms formed by metal borate nanoparticle dispersion as antiwear additives, boron oxide formation did not rely entirely on boric acid decomposition, but by decomposition of the metal borate due to shear effect of the sliding tribo-contact under boundary lubrication condition [125, 226]. However, as concentration of borate ester in the base oil increases, hydrolysis sets in to prevent the effectiveness of the established antiwear mechanism for organoborate as lubricant additives shown in Figure 8-3.
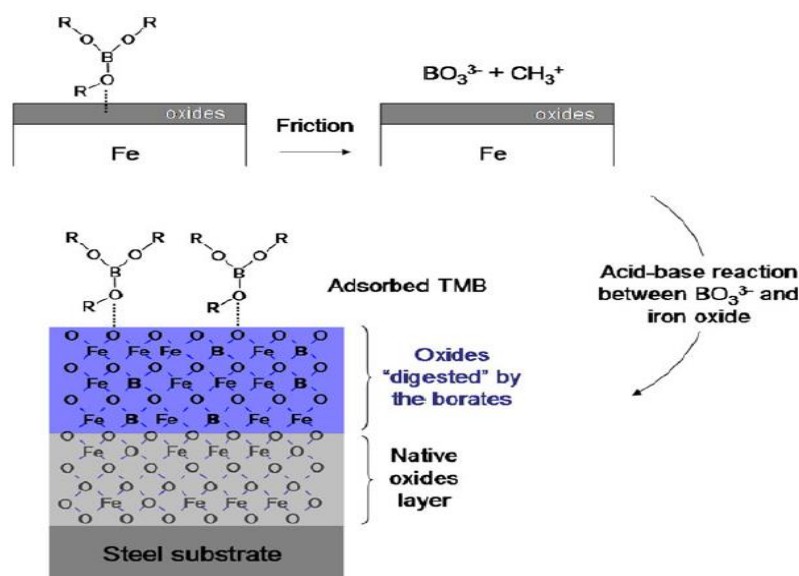
Figure 8-3 Existing borate tribofilms antiwear mechanism **[158]**

The poor tribological performance of borate ester that is susceptible to hydrolysis (BTE) with increasing additive concentration under thermal and tribo-oxidative

conditions is not directly due to boric acid formation as was previously understood, but due to a combination of the following factors;

- Amount of boric acid formed relative to boron oxide

- Type of borate ester (organoborate or inorganic borate ester)

- Dominant structural units of boron oxide

- Presence or absence of third body abrasives other than boric acid

At low additive concentration of borate ester, results from this study are in agreement with the established antiwear mechanism. Hence, tribochemistry study of antiwear films from boron-based lubricant additives indicates that boric acid are produced more on tribofilms formed by organic borates than inorganic nanoparticle borate ester. However, this did not result into better friction coefficient reduction on tribofilms formed by organic borate additives than inorganic nanoparticle borate ester. In addition, this study has been able to show that boric acid ratio to boron oxide formed on borate tribofilm could be a potentials indicator of their wear resistance.

8.3 Temperature effect on borate tribolayer

There had been very few studies on the effect of temperature on the tribological behaviour of tribofilms from borate-containing oils with good resistance to hydrolysis as shown in Chapter 2. A discussion on the effect of temperature on physical and chemical behaviour of reacted layers from oils containing synthetic borates will elucidate more on the influence of heat on borate tribochemistry.

8.3.1 Temperature effect on friction coefficient of tribofilms

Under the influence of frictional heating (at room temperature of $19^{o}C$), changes in coefficient of friction on the borate tribofilms at 3 and 6 hr test conditions as shown in Figure 8-4 are higher than ZDDP. The friction response of borate-containing tribofilms formed without heating the bulk oil is consistent with results from the literature [81, 82, 152, 277]. In addition, results of friction coefficient behaviour of ZDDP tribofilms under friction flash temperature is also consistent with similar studied in the literature [73, 81, 82]. Changes in friction coefficient due to changes in sliding process occurred on tribofilms formed by ZDDP and borate tribofilms. In

addition, considerable change did not occur on the nanomechanical properties and morphology of borate-based tribofilms after the sliding distance was doubled. The friction reduction performance for tribofilms formed by the borate additives was attributed to the formation of plate-like crystallites [220] of boric acid with its low shear strength [27]. A further analysis of Figure 5-3 (a) and Figure 7-13 resulted into Figure 8-4 (a) and (b) respectively. This indicates how temperature and sliding process affected changes in Raman intensity of boric acid and friction coefficient performance of the borate tribofilms.

The self-replenishing behaviour of friction reducing boric acid was effective only on KBE tribofilms at 100°C during both sliding processes, and at 80°C between 3r3 and 3 hr sliding process. This increase in boric acid on KBE tribofilms as shown in Figure 8-4 (a) did not result into a corresponding decrease in friction coefficient. On the other hand, ABE-containing tribofilms gave decreased boric acid level at all test temperature and sliding process as shown in Figure 8-4 (a). This did not result into significant changes in friction coefficient at 19°C, but gave an increase of 25 ± 3 % between 80 and 135°C when the sliding distance was doubled (from 3 hr to 6 hr).

However, changes in sliding process between 3r3 and 3 hr resulted in a 25% increase in friction coefficient at 19°C. At test temperatures between 80 and 135°C, a decrease in friction coefficient occurred, but was not too significant. This is an indication that certain morphology of boric acid formed during these processes could adversely affect friction coefficient at varying temperature and sliding process. Figure 8-4 suggests that durability of ABE-based tribofilms in terms of friction coefficient performance is better than KBE at 80 and 135°C. However, durability of KBE tribofilms was better at 100°C when the sliding duration was doubled. This result at 100°C tribotests temperature is in good agreement with the literature [81]. However, some friction coefficient results of ZDDP tribofilms from the literature indicates an increasing function of temperature at a test duration of 6 hrs [21, 346].

The friction coefficient results for ZDPP tribofilms at 100°C tribotests temperature is in good agreement with the literature [81]. However, friction coefficient results of ZDDP tribofilms from the literature indicated an increasing function of temperature at a test duration of 6 hrs [21, 346]. In addition, the increasing and decreasing friction

response behaviour of ZDDP obtained during the 3 hr test duration in this study supported results from similar studies in the literature [21, 73].
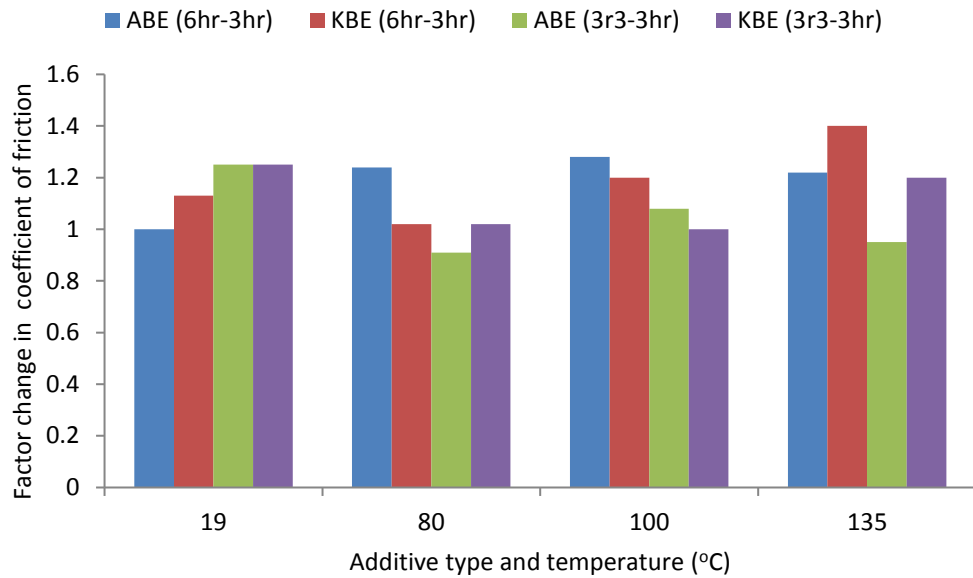
(a)
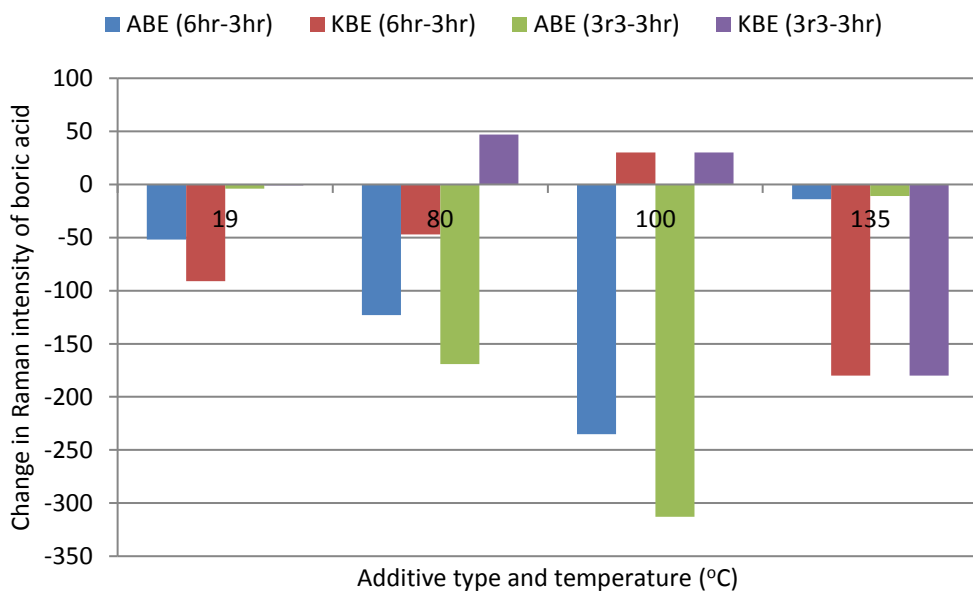
(b)

Figure 8-4 Effects of temperature, sliding time (6hr-3hr) and sliding process (3r3-3hr) on; (a) friction coefficient , and (b) Raman intensity of boric acid intensity formed by borate tribofilms at 1.0 wt. % additive concentration

Durability behaviour of built-up ZDDP tribofilms in terms of friction coefficient is in good agreement with results from the literature [111], but was not comparable to synthetic borates. This could be related to changes in the amount of phosphorus (P) on tribofilms containing ZDDP as suggested in the literature [89]. On the other hand, tribofilms from borate additives used in this study gave increasing friction coefficient with temperature that was in agreement with results of similar studies in the literature [12, 347]. However, this did not support results from similar works on borided steel surfaces which gave friction coefficient reduction [141]. The frictional response of borate tribofilms to sliding distance and temperature could be related to the effect of bulk oil temperature on the friction reducing boric acid.

It has been shown in the literature that orthoboric acid starts to decompose at about $80^{\circ}C$ to form metaboric acid [162, 163]. However, friction reduction of lubricious boric acid is attributed to reactions between boron oxide and moisture in the surrounding air as shown in Chapter 4, and subsequent dehydration back to boron oxide as from $80^{\circ}C$ [12].

Hence, friction reducing mechanism of boric acid formed on borate tribofilms is not significantly affected at low temperature; irrespective of the sliding distance, but could be considerably affected at temperatures between 80 and $135^{\circ}C$. On the other hand, durability of borate tribofilms in terms of friction coefficient reduction was not significantly affected at $19^{\circ}C$, but was greatly affected at higher temperatures. This is an indication that lubricity and tenacity (in terms of friction coefficient reduction) of boric acid on tribofilms from borate additives on a ferrous substrate is not only affected by temperature, but also by the sliding process.

8.3.2 Temperature effect on wear-resistance and durability

Tribological test results due to thermal and frictional heating indicates that increased antiwear performance of built-up ZDDP tribofilms with increasing temperature for 3 hr and 6 hr test durations was consistent with observation from the literature [21]. The antiwear performance of ZDDP tribofilms at temperatures between 25 and $150^{\circ}C$ from tribological tests similar to this study was shown to increase due to the formation of long chain polyphosphates that protects the contacting asperities [21].

On the other hand, built-up borate tribofilms was observed to provide decreasing antiwear performance up to 100°C that is consistent with results from similar studies [131, 273, 347]. However, better antiwear performance was provided by both borates at higher temperature above 100°C that is consistent with results from the literature [131, 169, 347]. At temperatures between 80°C and 135°C, changes in chemical and mechanical properties of the borate tribofilms greatly affected antiwear performance of KBE more than ABE and ZDDP. This could be related to different antiwear mechanism of metal borates [125, 127, 201] compared to ABE and ZDDP.

The antiwear and durability of borate and ZDDP tribofilms could be related to their nanomechanical properties. Previous studies from the literature had shown that ZDDP tribofilms formation depends on temperature, sliding distance and wear process [21, 47, 48, 89]. However, results from this study indicates that changes in nanomechanical properties of metal borate nanoparticle dispersion are more affected than tribofilms formed by oils containing organoboron and ZDDP additives.

However, durability performance of metal borates was comparable to ZDDP at the highest temperature due to increase in atomic concentration of boron and potassium on worn sample of KBE as shown in the XPS results. An increase in the amount of potassium dioxide (KO_2) on the wear-resistant alkali borate glass could have provided comparable durability to ZDDP. In addition, iron boride was formed due to chemical reaction products of boron oxide with metallic iron within the tribofilms. On the other hand, boron atomic concentration increase on ABE tribofilms did not affect its durability performance at the highest test temperature.

In addition, durability of both borate tribofilms was adversely affected at 100°C. This could not only be attributed to stage-wise decomposition of boric acid to boron oxide at 100°C, but also to boron not binding directly with oxygen in iron oxides [158, 161, 338]. However, this behaviour changed when bulk oil temperature was increased to 135°C. This was due to higher temperatures above the stage-wise decomposition barrier of boric acid and the ability of boron to bind directly with oxygen in the metal oxides.

Changes in the antiwear behaviour of the borates and ZDDP tribofilms due to sliding process and temperature are deduced from wear rates results in Chapter 5. This was deduced by subtracting the wear rates at 3 hr from 6 hr (changes in sliding time) and

3 hr from 3r3 (changes in sliding processes). Figure 8-5 shows a summary of these changes in order to make a good comparison. The results indicated that at 19ºC tribotests temperature, the borates are more affected by sliding distance than ZDDP. In addition, durability of borate tribofilms appeared to be better that ZDDP at 19ºC.

As tribotests temperature increases, the effect of sliding distance did not affect KBE tribofilms until 100ºC and ABE at 135ºC. However, changes in wear-resistant due to sliding distance of ZDDP tribofilms was only affected between 19 and 80ºC, but remained unchanged between 100 and 135ºC.

Response of Additive type to changes in temperature with sliding process
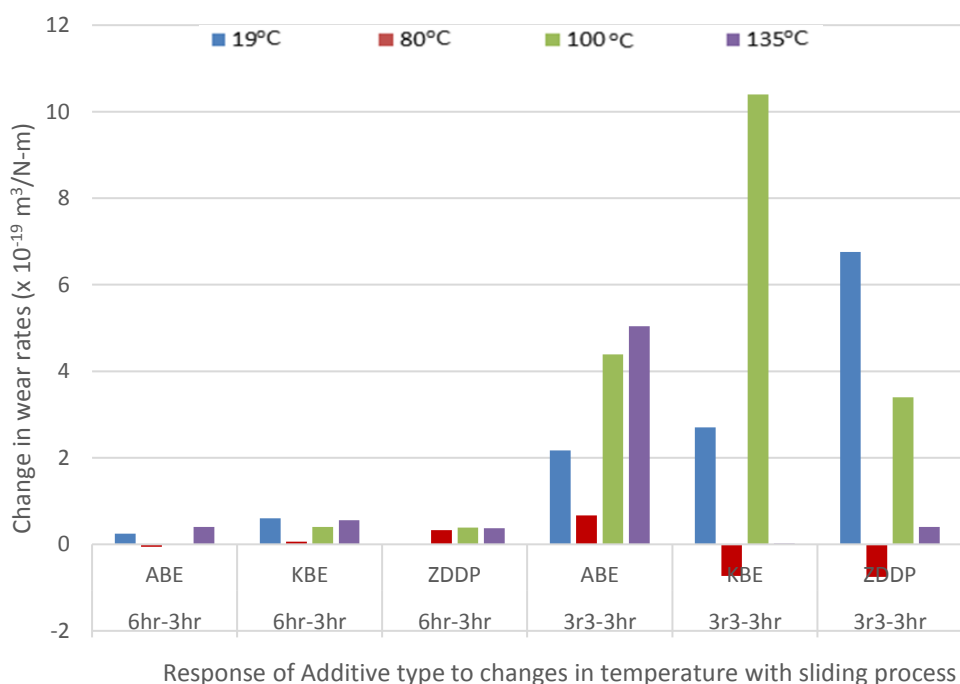
Figure 8-5 Changes in wear rates of tribofilms formed at additive concentration of 1.0 wt. % with temperature and sliding process

The behaviour of ZDDP tribofilms at temperatures below 100ºC was attributed to the formation of longer chain polyphosphate on the surface of its tribofilm, which increased in thickness at higher temperatures as shown in the literature [21]. Results from this study suggest that formed long chain polyphosphates on ZDDP tribofilms could sustain wear performance at twice the sliding distance. The increase in image height sensor (81 nm), surface roughness (9.3 nm) of ZDDP tribofilm between 100 and 130ºC supported the suggestion that long chain polyphosphate thickness

increased due to temperature as shown in Chapter 6. The response of tribofilms formed by the borate additive due to sliding distance and temperature is different to ZDDP. This could be related to differences not only in their tribofilms chemistry, but also of morphology and nanomechanical properties.

The tribofilms formed by ZDDP is known to be composed of short chain polyphosphate mixed with iron and zinc orthophosphate layers covered by a long thin pyrophosphate layer bonded to the substrate by interfacial sulphides [80]. The zinc orthophosphate glass formation was observed to be affected not only by temperature, but also by wear process [21, 47, 48, 63].

On the other hand, wear-resistant borate glass formed by borate tribofilms due to digestion of abrasive metallic oxide and carbonates by boron oxide [80, 339]. At tribotest temperatures between 80 and 135°C, changes in durability of preformed ABE tribofilms was less compared to KBE and ZDDP, except at 19°C. However, preformed KBE tribofilms durability was not only better than ZDDP at 19°C, but also comparable at 135°C.

This behaviour could be related to the high resistance to elastic and plastic deformation of preformed KBE tribofilms. The poor durability behaviour of ZDDP tribofilm has been related to the thickness and nanomechanical properties of zinc oxide reaction layer formed by the reaction of adsorbed dialkyl dithiophosphate on the native iron oxide/hydroxide [346, 348].

The only tribotests temperature that preformed ZDDP tribofilms gave better changes in durability than ABE and KBE is at 100°C which could be related to different physical, structural and chemical behaviour of their wear resistant glass. In the study of fully-formulated gear oils and lubricating oils containing a mixture of ZDDP and borate composition, the actual role of boron in the antiwear performance and durability was not fully understood of [81, 82]. The results from this study indicates that boron in the additive package could have enhanced the wear-resistant and durability of tribofilms formed due to only frictional flash temperature. In addition, ZDDP could also have provided enhance antiwear and durability at 100°C tribotest temperature.

8.3.3 Temperature effects on borate glass former

Raman spectroscopy results of BO_3 transformation to BO_4 structural units from this study indicates that structural changes occurred at all temperatures during the 3hr tests, but fewer at 3r3 tests on ABE tribofilms. These changes did not affect the antiwear performance of ABE tribofilms; except for its durability at $100^{\circ}C$ and $135^{\circ}C$. On the other hand, significant changes occurred on KBE tribofilms at $19^{\circ}C$ and $135^{\circ}C$. However, the highest transformation of BO_3 to BO_4 structural units occurred at $135^{\circ}C$, irrespective of the sliding distance. The transformation remained high on pre-formed KBE tribofilm which gave better durability (3r3 tests). This is in good agreement with results of similar studies where transformation from trigonal units in the borate ester additives to tetrahedral structural units on thermal and tribofilms containing boron was observed in the literature study described in Chapter 2 [168].

The established borate antiwear mechanism based on HSAB principle [158] had assumed that only BO_3^{-3} structural units on the borate tribofilms was involved in enhanced antiwear performance. However, results from this study has shown that if the metallic oxide is an alkali oxide, transformation of some BO_3^{-3} to BO_4^{-} structural units can take place due to tribological test temperature. This can affect the antiwear and durability of the alkali metal-containing borate tribofilms when the concentration of the alkali oxide and boron oxide that forms the wear-resistant glass exceeds a certain limit. In fresh borate ester additives, trigonal structure was shown to dominate, and transformation to other structural units [168]. However, borate-containing thermal and tribofilms are known to be composed of trigonal species and tetrahedral structural units some of which are also described in Chapter 2.

Figure 8-6 shows a comparison of wear rates and hardness behaviour of borate tribofilms to ZDDP due to changes in temperature and sliding distance. These analysis were deduced from Figure 5-3 (b) and Figure 6-12 for wear rates and hardness respectively. The results indicated that nanomechanical and wear rates response of borate tribofilms at the various temperatures for the borate tribofilms are different to ZDDP. Figure 8-6 indicates that at 80 and $100^{\circ}C$, considerable fractional changes in wear rates are identical to changes in hardness of tribofilms formed by KBE additive. For ABE-based tribofilms, this occurred at only $100^{\circ}C$, and for ZDDP at $19^{\circ}C$. However, considerable fractional change in wear rates and hardness of all tribofilms

occurred at 135°C. The fractional changes in hardness of tribofilms formed by oils containing KBE additives were observed to decrease with increasing temperature as shown in Figure 8-6. This was observed to adversely affect its antiwear performance. The behaviour of KBE-based tribofilms can also be related to its low N_4 that is indicative of its boron oxide in the wear resistant glass consisting of more BO_3 groups with some isolated BO_4 groups like F_3BO_6 [349-355]. The fusion of boron oxide dominated by BO_3 structural units with iron oxide is known to be less rigid compared to that with more BO_4 structural units [174, 175, 179].
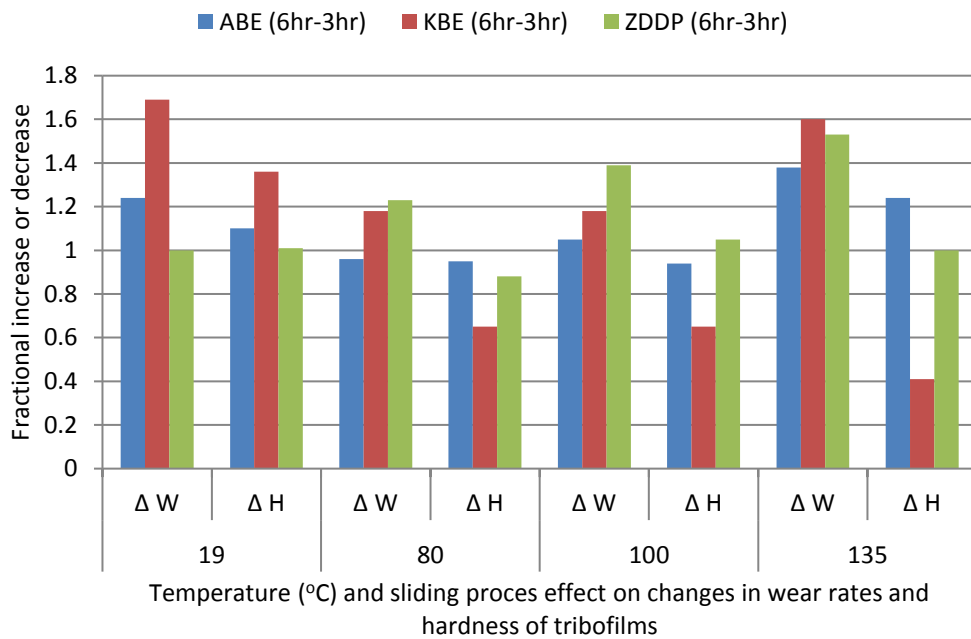
Figure 8-6 Fractional effect of temperature, sliding distance (6he-3hr) and sliding process (3r3-3hr) on wear rates and hardness of tribofilms formed at 1.0 wt. % additive concentration

Increase in tribotests temperature to 135°C resulted into high rate of wear was provided by tribofilms from all the antiwear additives when the sliding distance was doubled, despite high N_4 on the borate tribofilms. The wear-resistant glass structure of KBE is significantly different to ABE in terms of antiwear performance and durability due to thermal effects. The physical attributes of higher rigidity resulted into increased hardness and elastic modulus of KBE tribofilms formed at 135°C than at 100°C which provided better antiwear performance and durability than ABE.

Hence, antiwear performance and durability of metal borate dispersions in ZDDP containing oils [81, 82] could have partly been influenced by structural changes in boron anions. However, iron oxide is known to form stable glasses with different types of glass former, such as SiO_2, P_2O_5, B_2O_3 and TeO_2 [356]. Structural changes in boron oxide on ABE tribofilms at all temperatures during 3 hr and 6 hr tests formed wear resistant glass with iron that was not significantly affected by changes in nanomechanical properties. This resulted in comparable wear rate performance compared to ZDDP at $100^{o}C$ as supported by results of similar test at $100^{o}C$ in the literature [81, 82, 131]. However, lack of BO_3 conversion to BO_4 units on pre-formed ABE tribofilm can be attributed to its poor durability performance at $100^{o}C$ and $135^{o}C$.

8.3.4 Effect of boron penetration depths on tribofilms thickness

The XPS depth profile analysis of tribofilms formed by ABE and KBE additives at 1.0 wt. % concentration provided an understanding of different antiwear behaviour at $100^{o}C$. This is necessary since boron is known to have small atomic radius of about (85-88 pm) [202, 203] compared to most metals. In addition, boron atom is known to have electron-deficient p-orbitals which makes it possible to act as an electron carrier for; d-or f orbitals, and free electrons of the sliding metallic surfaces [198, 357, 358].

Figure 8-7 indicates that B 1s atomic concentration on ABE tribofilms was lower at the surface than KBE up to about 4.12 nm depth. However, ABE tribofilms had higher B 1s atomic penetration deep into the substrate up to 4.12-6.18 nm than KBE as shown in Figure 5-3. Results from similar studies on depth profile of B 1s on borate tribofilms had boron concentration within the boundary film decreasing from about 7.5 nm [169], 6.0 nm [201] and 9.0-18 nm [193].

The depth profile results on KBE tribofilms is similar to that obtained from the literature [201]. This can be attributed to potassium borate used in this study to be in hydrated form [128, 157]. The behaviour of borate additives on ferrous surfaces has been attributed to the small boron atomic radius which can capture free electron from the sliding metallic surfaces to become negatively charged. The resulting metallic surface will at the same time be positively charged to form a strong attraction between the borate ester and sliding metallic surfaces. Hence a strong adsorption of borate ester on sliding metallic surface could have favoured the formation of dense adsorbed film

on ABE tribofilms than KBE to provide better antiwear performance [198]. Result from this study, indicated that friction reducing and wear-resistant boron compounds are formed on the ferrous substrate due to interactions with surface oxides and hydroxides. These could act as reservoirs for replenishing the top-layer of the tribofilm.
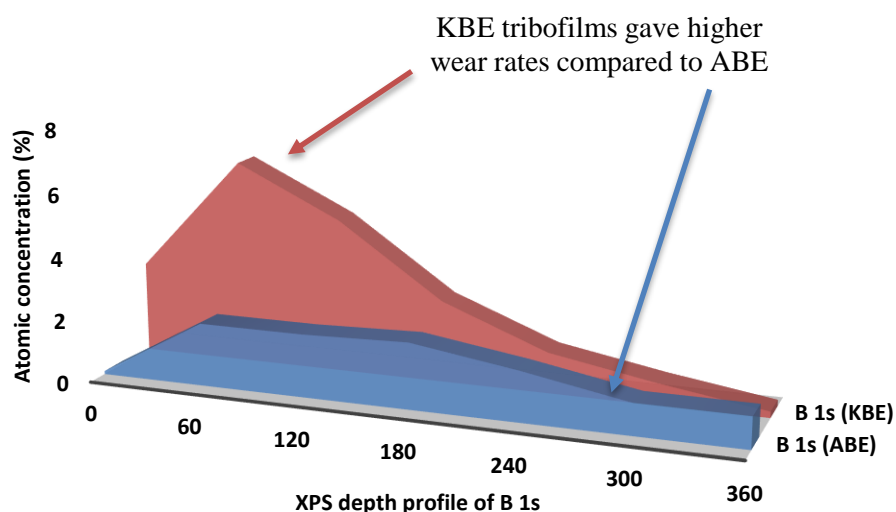
Figure 8-7 Variation in atomic concentration of B 1s with depth on borate tribofilms formed at 1.0 wt. % additive concentration, sliding distance of 3 hr and 100°C tribotest temperature

In addition, the behaviour of B 1s depths into metallic substrate are different. Synthetic organoborate acts as permeating film [11, 198], unlike synthetic metal borate nanoparticles which acts like protective wear resistant films [11, 125]. This result underscores the basis for self-replenishing behaviour of borate tribofilms additives as an interchange of dehydration of specific amount of boric acid and formation of its anhydride (boron oxide). In view of the effect of different chemical states of boron penetration depth within the tribofilms and metallic substrates, that wear-resistant borate glass should be considered to have its tribofilms deeply rooted in the various oxides of the micro-structure of the ferrous matrix.

8.3.5 Composition of elements in wear-resistant glass

The atomic concentration of metallic oxides that fused with the boron oxide (B_2O_3) on the top layer of ABE and KBE tribofilms formed at 3 hr, 6 hr and 3r3 tribotests under the influence of both frictional and thermal heating at 100°C and are shown in Figure 8-8. The result indicated that significant changes in the atomic concentrations O 1s and Fe 2p on ABE tribofilms did not take place, but B 1s atomic concentration increased when the sliding distance was doubled. This increase did not have considerable effect on nanomechanical properties and antiwear performance.
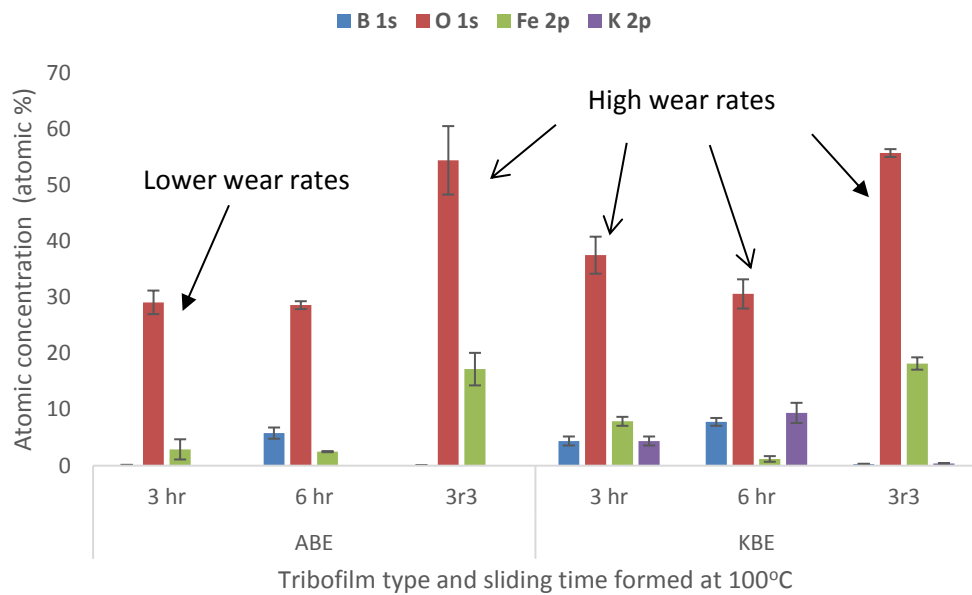
Figure 8-8 Changes in XPS atomic concentration of wear-resistant glass forming elements on borate tribofilms formed by additive containing oils at 1.0 wt. % concentration and 100°C tribotest temperature with sliding distance. Error is measured as standard deviation over three analysis points

However, ABE tribofilms at 100°C from 3hr test gave film thickness of about 66.4 ± 25.7 nm from FIB-SEM results in Chapter 6, which suggests that film thickness at 6 hr could be higher. The AFM morphology of ABE tribofilms suggests marginal difference, except in its nanomechanical response. When the test temperature was increased to 135°C, thermally induced increase in B 1s atomic concentration occurred at the surface to enhance antiwear performance, but did not improve durability.

This is an indication that changes in the composition of boron oxide on ABE-based tribofilms can adversely affect its durability, but not necessarily its antiwear performance between 100°C and 135°C. On the other hand, considerable changes occurred on all the oxides that could form wear-resistant glass on KBE-based tribofilms. The tribofilms containing KBE gave poor antiwear performance and durability at 100°C. However, when the temperature was increased to 135°C, the atomic concentration of all oxide forming elements increased compared to the corresponding 3 hr test at the same temperature as shown in Figure 8-9.
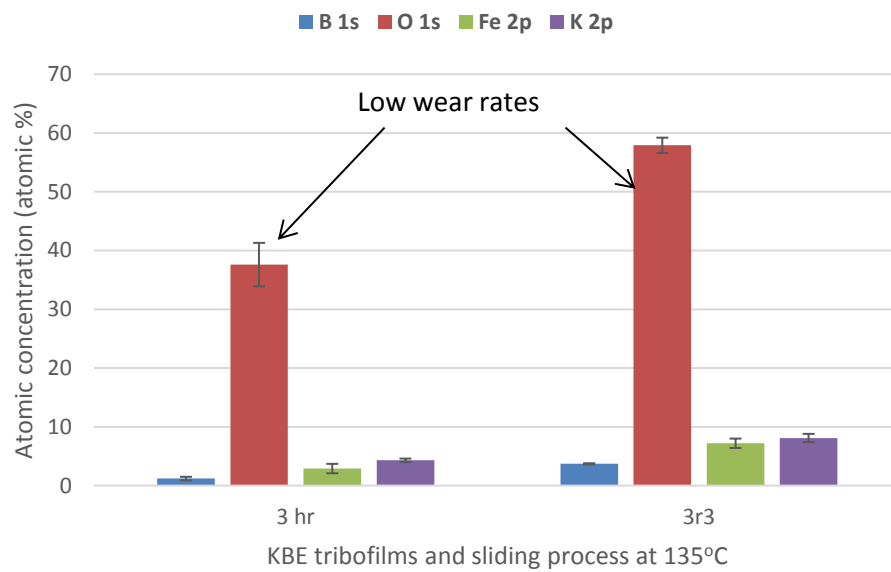
Figure 8-9 Effect of changes in XPS atomic concentration of wear-resistant glass forming elements on KBE-based tribofilms formed at 1.0 wt. % concentration and 135°C tribotest temperature with sliding time (3 hr) and sliding process (3r3). Error is measured as standard deviation over three analysis points

The result indicated that high temperature enhance durability of preformed KBE tribofilm when compared to ZDDP. A similar test in gear and lubricating oil compositions containing both metal borate nanoparticle and ZDDP resulted in a highly tenacious tribofilm [81, 82]. The result from this study indicated that at 100°C under which the test was carried out, hydrated potassium borate nanoparticle could not have contributed to enhanced durability of oils containing both potassium borate and ZDDP at 100°C.

196

8.4 Effect of water contamination on borate tribofilms

This section will discuss the effect of dry air and water contamination on friction coefficient performance and antiwear behaviour of borate tribofilms. Discussions will focus on tribochemistry results in comparison to literature studies on similar subjects in order to elucidate how friction and antiwear mechanisms of borate tribofilms are affected by free and dissolved water contamination.

8.4.1 Influence of moisture on friction on borate tribofilm

The effects of different levels of dissolve water contamination between dry-air and extremely wet conditions indicated that borate additives absorbed more dissolved water than ZDDP. This is could result into borate tribofilms behaving differently to ZDDP when subjected to different levels of water contamination.

At environmental humidity levels between dry air (5 % RH) and moisture-rich surrounding (95% RH), the coefficient of friction reduction by the borates was about (19-33%). The percentage reduction in friction coefficient reduction by the borate additives used in this study are comparable to results of similar works in the literature [24, 187]. However, higher friction coefficient reduction with increased humidity was obtained on borided surfaces [145, 184, 185]. On the other hand, friction reduction by ZDDP tribofilms was in the range of 30% that was comparable to that obtained from similar study in the literature [83].

Lubricious boric acid had been shown to provide low friction coefficient of about 0.02-0.04 [359]. On the other hand, the friction coefficient variation with increasing humidity of oxides of iron thin layers was between 0.4-0.7 [275]. XPS analysis of the top layer of the borate tribofilms detected boric acid on KBE samples only at 95% RH tests, but Raman analysis was able to shows the existence of boric acid at different intensity on all the borate tribofilms. This is an advantage of using Raman spectroscopy technique on borate tribofilms over XPS.

A summary of Raman intensity of boric acid and boron oxide on borate-containing tribofilms are shown in Figure 8-10. These are boron compounds known to be responsible for friction reduction and antiwear performance respectively under the influence of dissolved water contamination.

197

The compound responsible for friction reduction on borate tribofilms has been attributed to boric acid [220, 222] due to hydrogen bonds connecting the planar boron-oxygen groups to each other, e.g. van der Waals'. In dry air, high level of boric did not provide lower friction compared to ZDDP, despite the presence of boric acid as shown in Chapter 5.

In dry air, the friction reduction behaviour of ABE is different to KBE. This could be related to different amount of boric acid and haematite (α-Fe$_2$O$_3$) formed. Since haematite is known to be hard and less protective [274]. As humidity level increases up to 35 %, significant changes in boric acid level occurred on both borate tribofilms. However, a further increase in moisture level up to 95% RH resulted into considerable changes in boric acid level on the borate tribofilms. However, these changes occurred more on KBE tribofilms than ABE.
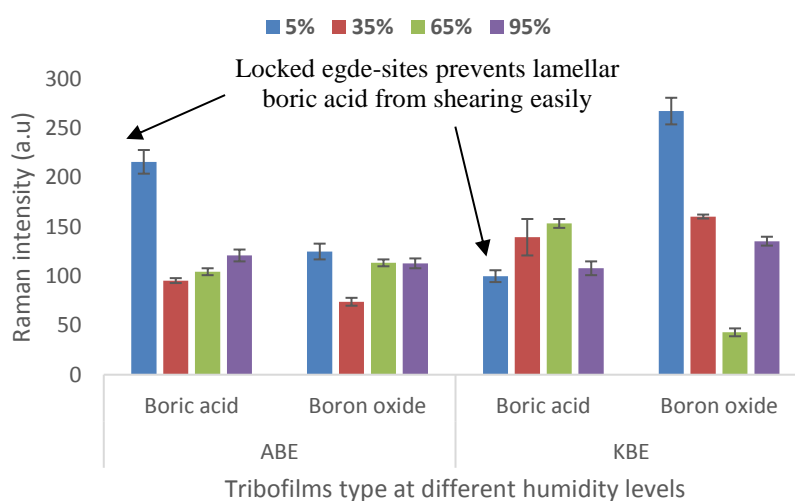
Figure 8-10 Humidity effect on Raman intensity of boric acid and boron oxide formed on tribofilms from oils at 1.0 wt. % additive concentration, 3 hr sliding distance and 19°C tribotest temperature. The error bar is standard deviation over three analysis points

Hence, results from this study supported the suggestion in the literature that water adsorption is required to unlock the edge site of boric acid for easy shear to yield low friction [187]. In dry air, there was no enough macroscopic physisorbed water vapour molecule to unlock the high edge-site of the basal plane for lamella boric acid to easily

shear and give ultra-low friction [24, 187]. Hence, result from this study is in good agreement with literature studies from similar studies that water vapour level on borate tribofilms could significantly influence the lubricity of boric acid.

8.4.2 Effect of moisture on wear reduction of borate tribofilms

The antiwear performance of borate tribofilms used in this study increases with rising humidity level. However, tribological results on borided ceramics [145] and boron carbide surfaces [184, 185] gave similar decreasing wear rates with increasing humidity. In addition, decreasing antiwear behaviour of ZDDP with increasing humidity is consistent with results from literature [83]. This is an indication that antiwear behaviour of borate tribofilms is different to ZDDP.

The reaction layer of ZDDP tribofilms in this study was thick enough under extremely dry conditions to give better antiwear performance compared to ABE and KBE. As humidity increases, the thickness of ZDDP reaction layer as shown by the AFM results reduced to give higher wear rates.

This results was similar to the morphology characterisation of ZDDP tribofilms in dry air and thermal heating [83]. However, this effect on ZDDP tribofilms has been attributed to depolymerisation of longer chain polyphosphates to shorter chain length polyphosphates, decreasing reaction layer thickness and formation of sulphates on the counter body in the literature studies in Chapter 2 [83].

XPS and Raman spectroscopy results revealed the presence of B_2O_3, H_3BO_3, Fe_3O_4, Fe_2O_3 and FeOOH (Iron oxy-hydroxide). The Raman spectroscopy showed the structural units of B_2O_3 as composed of both boroxol group (B_3O_6) and trigonal groups (BO_3) linked to BO_4 tetrahedral units as shown in Figure 7-17 (a) and (b). The boroxol groups consists of hexagonal ring of 3 boron atoms and three oxygen atoms with 3 corner oxygen atoms outside the ring. However, the formation of boron oxide is linked to boric acid dehydration as shown in Figure 8-11.

In addition, borate antiwear mechanism was also linked to the fusion of metallic oxide with boron oxide [80]. In dry air, XPS results revealed the presence of high concentration of metallic iron on tribofilms formed by both borate additives to give poor antiwear performance. The presence of carbides and carbonates and high

concentration of metallic iron were found on ABE and KBE boundary films respectively.

Since there was no evidence of boron binding directly to metallic iron, no borides was formed in dry air. Hence, the only possible reason for the high concentration of metallic iron is for the wear-resistant glass to be too thin as to protect the contacting asperities of the metallic substrate. This could be possible during the running-in stage as suggested in the literature [184, 185].

On the other hand, KBE tribolayer from dissolved water contamination tests at 95% RH showed evidence that oxidation of metallic iron occurred. At 95 % RH, tribofilms formed by KBE had iron borides to give reduced wear rates. This was in agreement with results from similar studies in the literature [125, 338], but disagrees with the view that boron is incapable of oxidative attack on metallic iron [117, 158]. Raman results indicates changes in intensities of boron oxide which is composed of boron oxide structural units such as; boroxol group (B_3O_6) and trigonal groups (BO_3) linked to BO_4 tetrahedral that could affect wear rates.

The structural transformation from trigonal units in B_2O_3 to boroxol and trigonal BO_3 linked to BO_4 structural units are summarized in Figure 8-11.
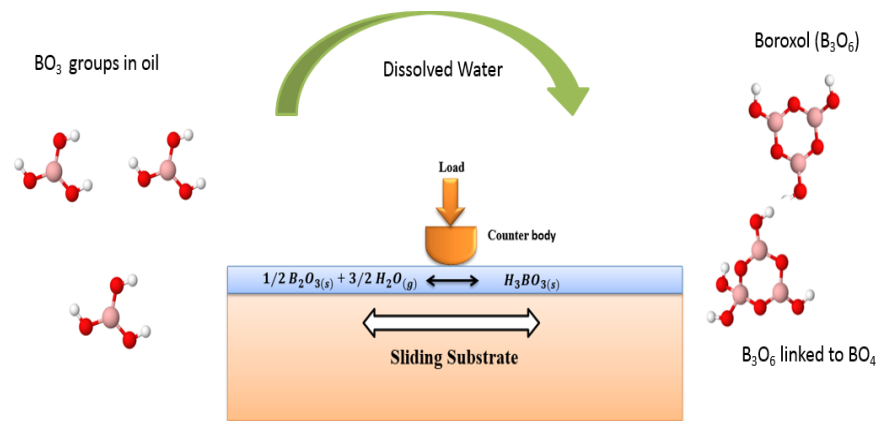
Figure 8-11 Effect of dissolved water contamination on borate anions

This result indicated that boron has the ability to coordinate with three and four oxygen atoms and subsequent linkage to the boroxol group which allowed it to resist dissolved water contamination effect more than ZDDP. In addition, the structural transformation in boron oxide could have occurred due to changes in the viscosity or

density of the oils [35]. Hence, BO_3 is not the only structural units in boron oxide that gives better antiwear performance, but also its linkage to BO_4 structural groups.

The antiwear mechanism of borate tribofilms rely on boroxol digestion of abrasive iron oxides based on HSAB principle [22, 158]. Evidence from the ratios of changes in Raman intensity of haematite to magnetite shows that adsorbed water affects the metallic oxides present on the wear-resistant glass, as shown in Figure 8-12. Changes in the behaviour of metallic oxides on ABE and KBE tribofilms with respect to humidity are different except at 95 % RH; where ratios of their iron oxides are similar.
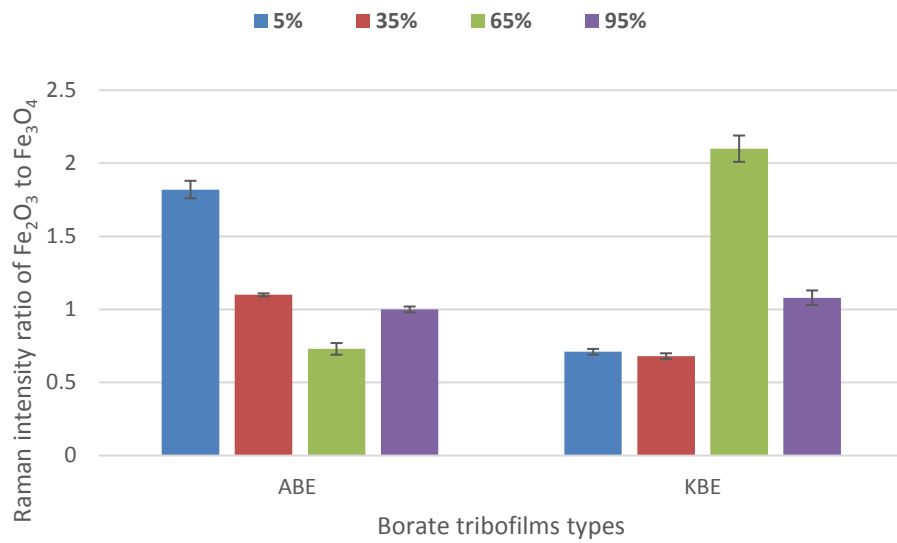
Figure 8-12 Humidity effect on Raman intensity of haematite ratio to magnetite on borate tribofilms formed at 1.0 wt. % additive concentration, 3 hr sliding distance and 19°C tribotest temperature. Error bars are standard deviations over three analysis points.

Tribofilms containing ABE exhibits decreasing iron oxide ratios up to 65 % RH before an increase at 95 % RH. This is unlike KBE tribofilms that exhibited nearly constant haematite to magnetite ratios up to 35 % RH, which rose at 65 % RH. The low and high Raman intensity ratios of haematite to magnetite at 65 % RH on ABE and KBE tribofilms respectively did not affect the antiwear performances of their tribofilms, but could have influenced the friction coefficient performance of ABE.

In dry air, the presence of boric acid, boron oxide and metallic oxide on the borate tribofilms could not provide better wear reduction than ZDDP. This could be related to the presence of third body abrasives on metallic iron. The major third body abrasive is boric acid with its locked edge-site due to the absence of moisture.

At increased moisture level, Raman results indicated the presence of boric acid and other borate poly-anions in boron oxide up to 95 % RH. The Lewis acidity of boron towards OH^- prevents boric acid from dissociation in aqueous solution, but rather will yield tetra hydroxyl borate ion and H^+ [360, 361] as shown in Equation 8- 1.

$$B(OH)_3 + H_2O \quad \leftrightarrow \quad B(OH)_4^- \ + \ H^+ \qquad \qquad \text{Equation 8- 1}$$

$$K_a = 7.3 \text{ x } 10^{-10} \text{ mol/l}; \ pK = 9.14$$

The oxidizing effect of moisture on borate tribofilms had boric acid dissociation in water that yields H^+. This could have resulted into oxidation and reduction reactions between haematite and magnetite [362] as shown in Equation 8- 2 and Equation 8- 3. Hence the various changes in the Raman intensity ratio of haematite and magnetite as shown in Figure 8-12 indicates that the boron oxide and boric acid formed are capable of interacting with the iron oxides and iron oxy-hydroxides.

$$3Fe_2O_3 \ + \ 2H^+ \ + \ 2e^- \quad \leftrightarrow \quad 2Fe_3O_4 \ + \ H_2O \qquad \qquad \text{Equation 8- 2}$$

$$Fe_3O_4 \ + \ 2\,H_2O \qquad \leftrightarrow \qquad 3FeOOH \ + \ 4H^+ \ + \ 2e^- \qquad \qquad \text{Equation 8- 3}$$

8.4.3 Effect of free water on friction behaviour of tribofilm

The tribological effect of added water up to about 1.5 wt. % free water in the boron-containing oil in comparison to ZDDP indicates that lower friction reduction was provided by ABE tribofilms compared to ZDDP and KBE. This performance could be linked to friction reducing boric acid with its unlocked edge sites as shown in Figure 8-13. However, the amount of boric acid appears to be immaterial as KBE tribofilms at 1.5 wt. % added water gave the lowest boric acid intensity.

The presence of haematite is known to form hard and less protective films on steel surface to give high friction [274, 275]. However, the possible surface oxides identified to produce friction coefficient reduction on ferrous surfaces in tribological contact are β-FeOOH [216] and magnetite (Fe_3O_4) [274, 275, 363]. The variation in Raman intensity ratio of haematite to magnetite is shown in Figure 8-14 due to free

water contamination. This indicates that boric acid controlled friction reduction on ABE tribofilm. However, very high intensity of magnetite on KBE tribofilms compared to boric acid indicates that Fe_3O_4 controlled its frictional behaviour.
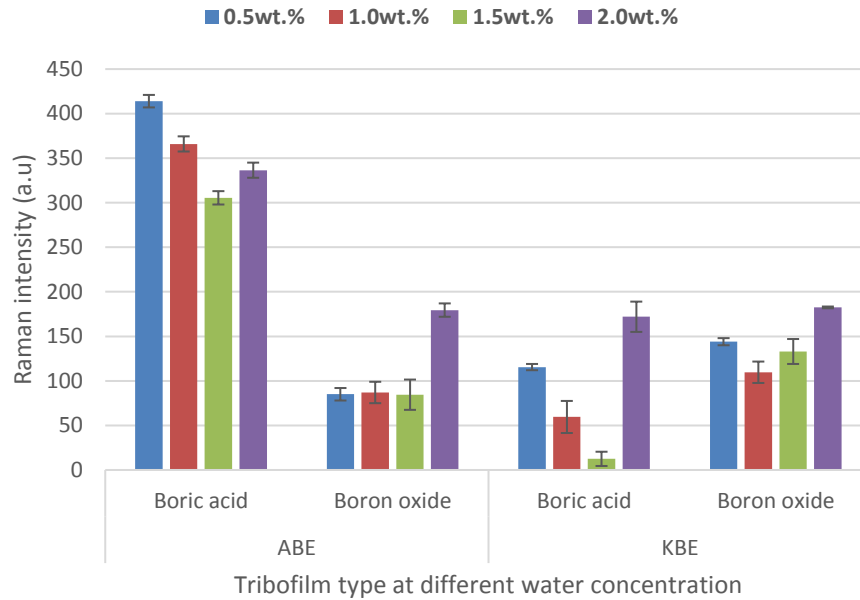
Figure 8-13 Raman intensity of boric acid and boron oxide on borate tribofilms formed at 1.0 wt. % additive concentration, tribotest temperature of 80°C, sliding distance of 6 hr and contaminated by added water in oils at different concentrations. The error bars are standard deviation over three analysis points

The difference in friction coefficient behaviour of borate additives with increasing free water could be attributed to coordination of nitrogen atoms to boron in their molecular structures. This could be attributed to the synthetic ABE having nitrogen coordination with borate ester which possess a lone electron pair to form a complex with the empty 2p orbital of the more electrophilic boron atom to prevent any possible attack by water [119, 121, 122, 364]. On the other hand, water tolerance of KBE was based on the small amount of water soluble Oxo-anions which disrupt the crystal structure of hydrolysis by-products as suggested in the literature [128, 231].

However, results of thermo-oxidative stability tests in Chapter 4, indicated that accelerated hydrolysis on both borate-containing oils was better than non-synthetic borate (BTE). The effect of tribo-oxidative conditions due to added water

contamination by ABE and KBE tribofilms formed passivating films that will inhibit corrosion as observed in the literature [13, 365, 366] and promote friction coefficient reduction. Literature studies had suggested that water molecules passivate high-energy edge sites that allowed macroscopically-lamellar compounds to easily shear and give low friction coefficient [24].
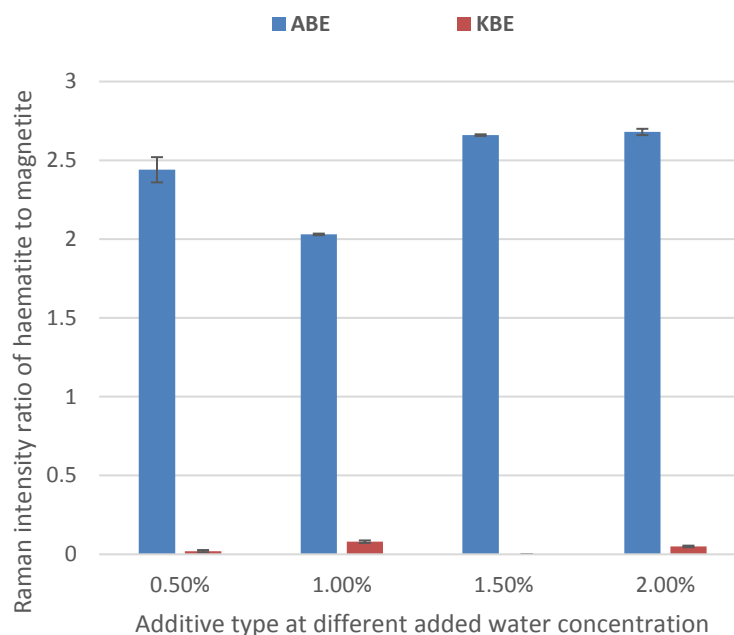
Figure 8-14 Effect of added water on Raman intensity ratio of haematite to magnetite for borate tribofilms formed at 1.0 wt. % additive concentration, 6 hr sliding distance and 80°C tribotest temperature. Error bars are standard deviations of three analytical points

In another observation from the literature, low-shear strength of boric acid and its self-replenishing mechanism which once aligned in the sliding direction can reduce friction. The results of this study indicated that the combinations of the two friction reducing mechanisms are necessary and sufficient to provide better friction coefficient performance than ZDDP.

8.4.4 Influence of free-water on wear-resistant tribofilms

Changes in antiwear performance of the borate tribofilms with increasing water contamination are different to ZDDP. The antiwear performance of ZDDP tribofilms

in this study got worse as the level of free water contamination increases. This was consistent with results from observation in the literatures [83]. However, this behaviour was attributed to de-polymerization of its wear resistant glass from long chain phosphates to shorter chain length phosphates [83]. The tribofilms formed by borate additives under free-water contaminated conditions gave increased antiwear performance when the level of free-water contamination is above 1.5 wt. % concentration.

However, the chemistry of reacted layers by the two borate additives are different. On tribofilms formed by ABE, the Raman intensity of carbonates as shown in Chapter 7 indicated its disappearance at water concentration above 1.0 wt. %. This could be linked to poor antiwear behaviour as shown in Figure 5-4 (b). However, boron oxide had been noted in the literature to form wear-resistant borate glass by carbonate and iron oxide digestion [80, 339]. Figure 8-14 obtained in this study indicated an increase in Raman intensity of haematite at 1.0 wt. % added water which resulted into hard and less protective haematite that not only affected friction reduction, but also poor antiwear performance as observed in the literature [48].

Under free water contamination, KBE-based tribofilms had boron oxide that was mainly composed of BO_3 linked to BO_4 tetrahedra units along with metallic oxides with no boroxol groups, at all water in oil concentrations. This was also the case with ABE tribofilms, except at 2.0 wt. % added water, where the boroxol group was also formed. Tribo-oxidative induced free water in oils containing KBE was mainly composed of magnetite and β-FeOOH. This could be attributed to the better antiwear performance than ABE at 1.5 wt. %. The above results is an indication that either moisture from the surrounding air or free-water inherent in the oil will be necessary to trigger tribochemical reactions as proposed by the established borate antiwear mechanism [158, 298]. In addition, borate antiwear mechanism due to HSAB principle overlooked the ability of boron oxide to fuse with carbonates and alkali oxides to form wear resistant glass. Hence, the glass forming potentials of tribofilms formed by ABE additive in the oil at added water concentration level above 1.5 wt. % becomes ineffective, irrespective of its structural units and chemical composition

8.5 Antiwear mechanisms of borate tribofilms

The established antiwear mechanisms for borate tribofilms are in three separate categories. One is exclusively for tribofilms formed by organoboron compounds based on HSAB principle [158] and the other is for metal borates nanoparticle dispersions based on the wear resistant of iron boride formed from chemical reaction between boron trioxide and substrate iron [125]. However, the third category relies on the ability of boron atoms to permeate easily through the surface and subsurface to form a high-strength adsorption film from the tribochemical reaction process [198, 298, 367]. In addition, the effect of boric acid was excluded despite its immediate formation upon exposure of boron oxide to moisture of the surrounding environment as shown by results in section 4.24 and section 4.25. Results from this study has been able to show that these three mechanisms are linked by boron oxide formation and easy permeation of boron into the substrate. Hence, the antiwear mechanisms of tribofilms containing boron could not be complete if boric acid, oxides and oxyhydroxides of iron are excluded.

8.5.1 Effect of borate concentration on antiwear mechanism

The effect of hydrolysis and thermo- and tribo-oxidation on the antiwear functions of tribofilm of synthetic and non-synthetic borate additives are summarized in Figure 8-15.
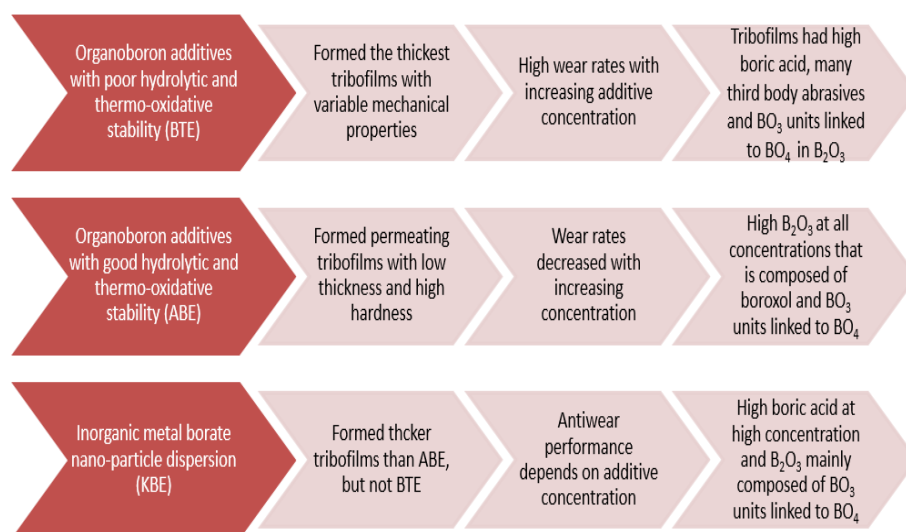
Figure 8-15 Effect of concentration on tribochemistry organic and inorganic borate

This result indicated that high wear rates by borate tribofilms is not directly due to boric acid, but of its stage-wise decomposition to form boron oxide at elevated temperature and/or formation of third body abrasives. Another key observation is that thicker borate tribofilms with high hardness do not necessarily produce lower wear rates. In addition, boron oxide formed by tribofilms with the best wear rates at all concentration not only have BO_3 units linked to BO_4 in B_2O_3, but also have boroxol groups. However, antiwear behaviour of reacted layer formed by metal borate nanoparticle dispersion used in this study indicates their susceptibility to high plastic flow, but unable to be sacrificed in place of the underlying substrate like ZDDP. Hence, enough concentration of additives is needed for enhanced antiwear performance.

8.5.2   Effect of temperature on borate antiwear mechanism

The tribochemistry of boron-containing additives at different concentration at 100°C indicated poor antiwear behaviour of KBE and BTE at 1.0 wt. %. In order to understand how the antiwear performance and durability of borate tribofilm responds to different level of thermal heating, a summary of the tribochemistry results are shown in Figure 8-16. The effect of temperature on tribofilms from both organic and inorganic borate esters as lubricant additives can be resolved into two broad categories; stage-wise decomposition of boric acid and boron oxide anomaly.

Boric acid formed by tribofilms from boron-based lubricant additives had earlier been shown to be dependent on the amount of boron present on the top layer of the tribofilm. In borate tribochemistry, the established borate antiwear mechanisms had assumed that boric acid decomposes to form boron oxide directly [27, 154, 159, 221]. However, results from this study had indicated that, between 80 and 135°C tribotest temperature incomplete decomposition of boric acid occurred that resulted into significant changes in the wear resistant performance and durability of both borate tribofilms.

In addition, the established antiwear mechanism of tribofilms formed by organoboron additives [158], consideration was given to only trigonal BO_3 groups in B_2O_3 to influence antiwear performance. Results from this study has shown that when metal

cation fuse with boron oxide due to high temperature, some of the BO_3 groups are converted to a more rigid BO_4 tetrahedra structural units. This was in good agreement with results of similar studies on borate tribofilms using XANES [167, 168]. This significantly affected the antiwear performance and durability of KBE-containing borate more than tribofilms formed by organoboron-based oils. In the borosilicate glass industries, this phenomenon was termed 'boric oxide anomaly' [35, 172, 284].
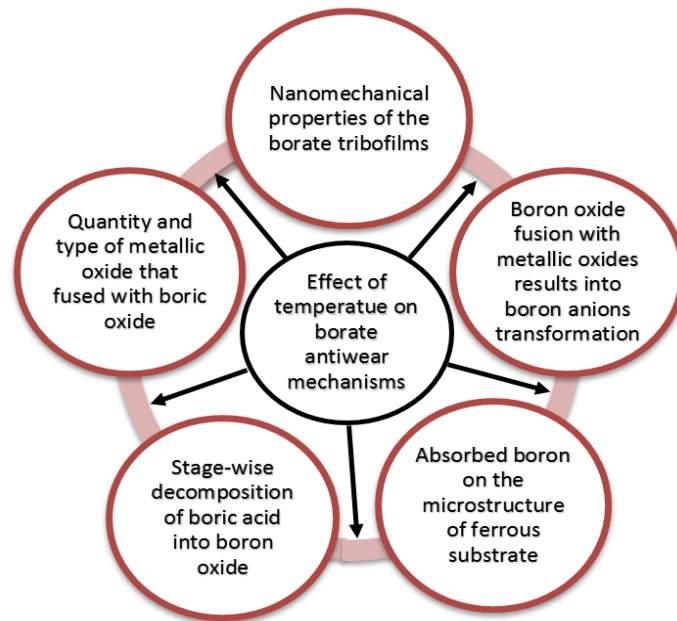
Figure 8-16 Effects of temperature on borate antiwear mechanism

Evidence from this study confirmed the anomalous behaviour of boron oxide in the wear-resistant borate tribofilms. This significantly affected the antiwear performance and durability of alkali-containing borate additives. Hence, the chemistry of reacted layer from alkali-containing borate ester as lubricant additives are likely to be affected by boron oxide anomaly at high temperatures than the organoboron additives.

8.5.3 Water contamination effect on borate antiwear mechanism

Enhanced antiwear performance by the borate tribofilms occurred with increased level of water contamination. In dry air, tribochemistry results from this study suggest that digestion process of abrasive iron oxides by boron oxide was not effective in order to provide a protective tribolayer of the metallic substrate. This occurred despite the presence of boroxol groups, BO_3 linked to BO_4 tetrahedra units and initial dissolved

water inherent in the oil. Wear rates reduction occurred due to increasing level of absorbed water and added water up to 1-1.5 wt. % on both borate-containing tribofilms. A summary of the interaction of boric acid, boron oxide and its structural units, iron oxides and iron oxyhydroxide on borate tribofilms is shown in Figure 8-17.
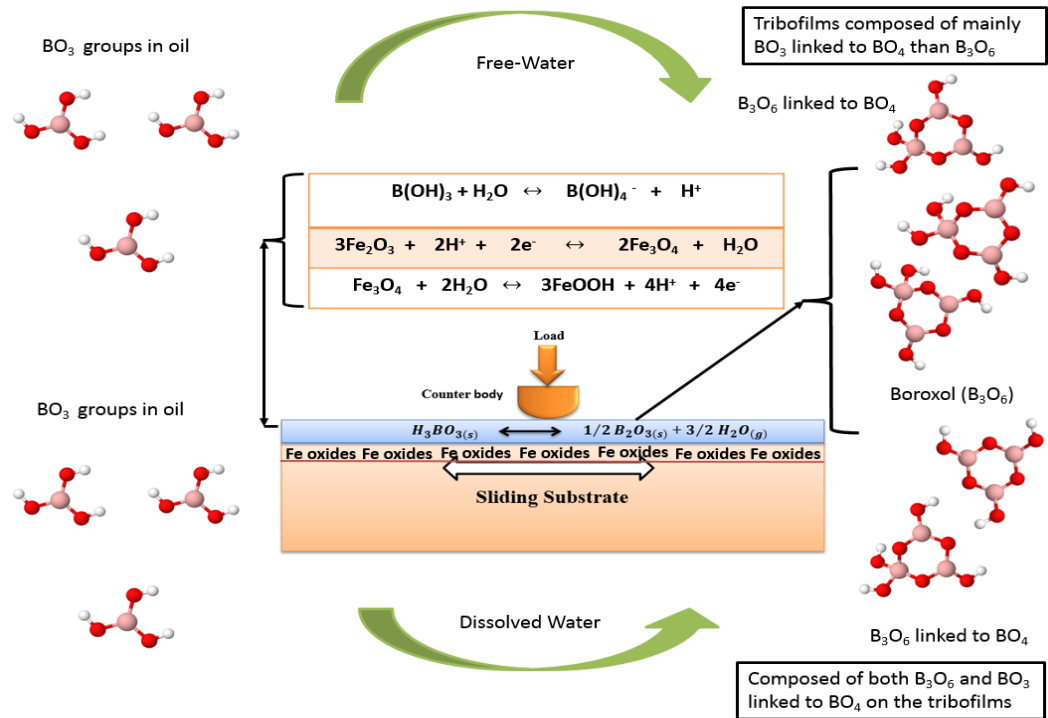
Figure 8-17 Sketch of heat and water contamination effects on borate antiwear mechanism

Previous literature studies on borate antiwear mechanism had relied on HSAB principle [22] due to preferential reactions between the boroxol groups (a borderline base) and Fe^{2+} (a borderline acid) [158]. However, this study has shown that Lewis acid behaviour of boric acid in aqueous solution forms H^+ (a hard acid) as shown in Equation 8- 1 and free electrons on the metallic sliding surface [198, 357, 358]. This could trigger tribochemical reaction between the metallic oxides to form iron oxy-hydroxides as shown in Equation 8- 3. The functions of boric acid on borate tribofilms formed at different test conditions were noted in the literature to provide friction coefficient reduction as shown in Figure 2-20. However, results from this study, indicates that boric acid also aid the digestion of abrasive iron oxide by boron oxide, as shown in Figure 8-17. In addition to boric acid enhancement of boron oxide

digestion of abrasive iron, less abrasive oxyhydroxides of iron could be formed to affect antiwear and durability performance of borate tribofilms.

Chapter 9

Conclusions and Future Work

9.1 Conclusions

In this chapter, various conclusions from the work in this thesis are presented. This study has provided insight the effects of hydrolysis, heat and water contamination on S- and P- free oils containing different types of boron additives in comparison to ZDDP. Physical analysis of borate and ZDDP tribofilms at different test conditions gave fresh understanding to friction reducing and antiwear mechanisms of tribofilms formed by borate additives in lubricating oils. In addition, chemical characterization of the borate tribofilms elucidate on how these extrinsic conditions affects their friction reducing and antiwear mechanisms. Hence, key findings are summarized and some suggestions have been made for future work.

9.2 Key findings

- It has been shown in this study that some borate additives in oils with good resistance to hydrolysis for use in internal combustion engines did not only have good thermo-oxidative resistance to copper corrosion, but also high thermal and oxidative decomposition temperatures. Hence, using copper corrosion tests only to determine hydrolytic stability of borate oils is necessary, but not sufficient enough to fully assess the effects of hydrolysis of borate additives

- The synthetic borate additives used in lubricating oils for this study were found to absorb more moisture from the surrounding air than ZDDP-containing oils. This study showed that moisture absorption by the borate additives was due to boron oxide in the additives more than boric acid

- The antiwear performance of synthetic borate additives (ABE and KBE) with high hydrolytic and thermo-oxidative stability increased with increasing concentration of additives in the oil compared to ZDDP. However, this study

211

showed that increased concentration of non-synthetic borate (BTE) in the oil resulted into catastrophic wear rates

- It has been shown in this study that tribofilms formed by BTE-containing oils are thick and hard, but did not provide enhanced antiwear performance, unlike ABE which was not as thick, but gave better antiwear performance. This study had shown that different chemistry of reacted layers formed by ABE and BTE could be responsible. In addition to the major achievements of this study, the hardness of tribofilms formed by organic borates additives (ABE and BTE) were shown be significantly higher than inorganic borate ester (KBE) at all additive concentrations

- Another major achievement by this study on the chemistry of non-synthetic borate tribofilms (BTE) revealed that its poor antiwear performance is not directly due to high boric acid formed, but also due to the presence of high atomic concentration of boron, stage-wise decomposition of boric acid and particles acting as third body abrasives. The third body abrasive particles were found to be carbides and boron nitride

- In the study of temperature effect on friction coefficient of borate tribofilms from boron containing oil, it has been shown that self-replenishing mechanism of boric acid was significantly affected by temperature increase and sliding process

- The result of this study has shown that low hardness of tribofilms formed by alkali-based borate additives and ZDDP can occur due to increased temperature. However, enhanced antiwear performance was provided by ZDDP tribofilms with increasing temperature, unlike borate tribofilms

- Surface analysis results by this study confirmed that transformation of boron oxide structural units, and changes in alkali oxide and boric oxide content on tribofilms occurred on tribofilms formed by KBE-containing oils between 135ºC and 100ºC. This was observed to adversely affect its durability more at 100ºC than 135ºC. Hence, this study has shown that boron oxide anomaly effect in borosilicate glass manufacture could significantly affect the antiwear

performance and durability of tribofilms formed by alkali-based borate additives

- The tribochemistry study of borate boundary films at different temperature in comparison to ZDDP by this study has shown that tribofilms from oils containing borates are more durable at 19°C, but less tenacious at 100°C. This was related to the significantly reduced level of boron and highly oxidized metallic iron

- A major findings by this study reveals that tribofilms formed by synthetic borate-containing oils under the influence of frictional flash temperature gave better tribological performance compared to ZDDP in moisture-rich environment, but poor antiwear performance in dry air

- In dry air, surface characterization of the borate tribofilms formed has been shown in this study to have considerable boric acid which could not easily shear along the sliding direction, but sheared easily in moisture-rich environments to provide better friction reduction

- This was attributed to the locked edge-site of lamellar boric acid which prevented its easy shear along the basal planes. In addition, carbides, carbonates and borides were found along with boric acid that acted as third body abrasives. These eventually gave poor antiwear performance compared to ZDDP

- In water-rich environments, this study shows that tribochemical surface polishing took place with increasing moisture level on both borate and ZDDP tribofilms. In addition, the borate tribofilms did not only have boron oxide with its different structural units and iron oxides, but also iron oxy-hydroxide, borides and carbonates

- A major findings of this research was that boron-based additives can act as an affective antiwear additives in internal combustion engines used in high humidity environments than ZDDP

- The established borate antiwear mechanism on tribofilms formed by oils containing boron relies on the fusion of boron oxide with iron oxides to form wear-resistant glass based on HSAB principle. A major findings from the

213

study of borate tribofilms at different extrinsic tribological conditions has shown that; moisture in the surrounding air, boric acid, iron oxy-hydroxides, carbonates and borides facilitated the digestion of abrasive iron oxides.

9.3 Future work

Following the results of research generated within this thesis, there is great potential to extend the current study for future consideration. These are discussed below;

- The tribochemistry of borate tribofilms formed in fully formulated oils by the combine effects of borate friction modifiers and borate antiwear additives in comparison to the traditional friction modifier and ZDDP
- The synergy of borate tribofilms with moisture contamination was studied mainly due to frictional flash temperature, future work on the combine effect of increased bulk oil temperature and dissolved water contamination will be necessary
- In this research, only alkali metal borate additives were assumed to represent the behaviour of all metal borate nanoparticle dispersions as lubricant additive. Hence, future tribological studies on the behaviour of alkaline earth metal borates as lubricant additives in IC engines would be necessary
- The study of borate tribofilms formed in this research considered only hardened steel as the surface for generating the tribofilms. However, borate tribofilms formed on some component parts of the IC engines in tribological contact from non-ferrous materials such as; diamond-like carbon (DLC) coated surfaces, zirconia and alumina among several others, could behave differently from that obtained in this study.
- This research had considered the tribological performance of borate tribofilms in pure sliding under boundary lubrication condition, additional future work needs to consider its behaviour under slide-roll conditions in comparison to ZDDP
- Future work on the influence of the combination of increased bulk oil temperature and humidity on borate tribochemistry in both model and fully formulated oils are necessary

- The use of other surface characterization techniques such as X-ray Absorption Near-edge Spectroscopy (XANES) could provide further insight into how the structural units of boron oxide and Mössbauer spectroscopy for iron oxides interacts in the boron oxide-iron oxide wear resistant glass on the tribofilms behave.

References

[1]   David W. Smith, D. o. B. A. E., Texas A & M Universit. (January, 2014, 10/06/2017). Available: http://animalagclimatechange.org/wp-content/uploads/Contribution_of_Greenhouse_Gases.pdf

[2]   Harde, H. (2017) Scrutinizing the carbon cycle and CO_2 residence time in the atmosphere, *Global and Planetary Change,* **152**, 19-26.

[3]   Holmberg, K., Andersson, P., and Erdemir, A. (2012) Global energy consumption due to friction in passenger cars, *Tribology International,* **47**, 221-234.

[4]   Shi, Y. (2016) Reducing greenhouse gas emissions from international shipping: Is it time to consider market-based measures?, *Marine Policy,* **64**, 123-134.

[5]   Sperling, D. and Gordon, D. (2008) Two billion cars: transforming a culture, *TR news,*

[6]   Van der Hoeven, M. (2011) CO2 emissions from fuel combustion–highlights, *IEA Statistics,*

[7]   Selby, T., Bosch, R., and Fee, D. (2005) Phosphorus additive chemistry and its effects on the phosphorus volatility of engine oils, *Journal of ASTM International,* **2**, 1-16.

[8]   Farrauto, R. J. and Heck, R. M. (1999) Catalytic converters: state of the art and perspectives, *Catalysis Today,* **51**, 351-360.

[9]   Heck, R. M. and Farrauto, R. J. (2001) Automobile exhaust catalysts, *Applied Catalysis A: General,* **221**, 443-457.

[10]   Spikes, H. (2008) Low-and zero-sulphated ash, phosphorus and sulphur anti-wear additives for engine oils, *Lubrication Science,* **20**, 103-136.

[11]   Choudhary, R. and Pande, P. (2002) Lubrication potential of boron compounds: an overview, *Lubrication Science,* **14**, 211-222.

[12]   Baş, H. and Karabacak, Y. E. (2014) Investigation of the effects of boron additives on the performance of engine oil, *Tribology Transactions,* **57**, 740-748.

[13]   Shah, F. U., Glavatskih, S., and Antzutkin, O. N. (2013) Boron in tribology: from borates to ionic liquids, *Tribology letters,* **51**, 281-301.

[14] Twigg, M. V., Collins, N. R., Morris, D., O'Connell, T. J., Ball, I. K., Arrowsmith, S.*, et al.*, "The effect of phosphorus and boron lubricant oil additives on catalyst and engine durability," SAE Technical Paper 0148-7191, 2004.

[15] Ceramics, A. (2012, 04/05/2017). *Borates looks to high-priced Future*. Available:

http://content.yudu.com/Library/A1vi5r/AsianCeramicsFeb12/resources/62.htm

[16] Kistler, R. B. and Helvaci, C. (1994) Boron and borates, *Industrial minerals and rocks,* **6**, 171-186.

[17] Schott, A. (2007) SCHOTT Technical Glasses (Physical and Technical Properties), *Firmenschrift, Oct,*

[18] Mufti, R. A. and Priest, M. (2009) Effect of engine operating conditions and lubricant rheology on the distribution of losses in an internal combustion engine, *Journal of Tribology,* **131**, 041101.

[19] Neville, A., Morina, A., Haque, T., and Voong, M. (2007) Compatibility between tribological surfaces and lubricant additives—how friction and wear reduction can be controlled by surface/lube synergies, *Tribology International,* **40**, 1680-1695.

[20] Tung, S. C. and McMillan, M. L. (2004) Automotive tribology overview of current advances and challenges for the future, *Tribology International,* **37**, 517-536.

[21] Morina, A., Neville, A., Priest, M., and Green, J. (2006) ZDDP and MoDTC interactions in boundary lubrication—the effect of temperature and ZDDP/MoDTC ratio, *Tribology international,* **39**, 1545-1557.

[22] Pearson, R. G. (1968) Hard and soft acids and bases, HSAB, part 1: Fundamental principles, *Journal of Chemical Education,* **45**, 581.

[23] Erdemir, A., Fenske, G., Erck, R., Nichols, F., and Busch, D., "Tribological properties of boric acid and boric-acid-forming surfaces: Part 2, Formation and self-lubrication mechanisms of boric acid films on boron-and boric-oxide-containing surfaces," Argonne National Lab., IL (USA)1990.

[24] Barthel, A. J., Luo, J., and Kim, S. H. (2015) Origin of ultra-low friction of boric acid: Role of vapor adsorption, *Tribology Letters,* **58**, 1-12.

[25]   Priest, P. M. (2005). *Introduction to Tribology and Real Surfaces. Work Unit 1.*

[26]   Hamrock, B. J., Jacobson, B. O., and Schmid, S. R., *Fundamentals of machine elements*: WCB/McGraw-Hill Singapore, 1999.

[27]   Erck, E. A. a. R. A. (1991) Relationship of hertzian contact pressure to friction behavior of self-lubricating boric acid films, *Surface and Coatings Technology,,* 435—438.

[28]   Singer, I., Bolster, R., Wegand, J., Fayeulle, S., and Stupp, B. (1990) Hertzian stress contribution to low friction behavior of thin MoS< inf> 2</inf> coatings, *Applied Physics Letters,* **57**, 995-997.

[29]   Stachowiak, G. and Batchelor, A. W., *Engineering tribology*: Butterworth-Heinemann, 2013.

[30]   Hamrock, B. J., Jacobson, B. O., Schmid, S. R., Jacobson, B., and Jacobson, B., *Fundamentals of machine elements*: WCB/McGraw-Hill Singapore, 1999.

[31]   Horosdysky., R. M. G. A. G., "Lubricant Composition Containing Borated Oxazolin Rriction Reducer," US 4,374,032

1983.

[32]   Shah, F. U., *Designed boron chemistry for tribological systems*: Luleå tekniska universitet, 2011.

[33]   Weintraub, E. (1909) Preparation and properties of pure boron, *Trans. Amer. Electrochem. Soc,* **16**, 165-184.

[34]   Erd, C. (1980) Supplement to Mellor's Comprehensive Treatise on Inorganic and Theoretical Chemistry, Vol. 5, *Boron, Part A, Boron-oxygen Compounds, Longman, London,* 7.

[35]   Smith, R. A. (1985) Boric oxide, boric acid, and borates, *Ullmann's encyclopedia of industrial chemistry,*

[36]   Han, W. Q. (2010) Anisotropic Hexagonal Boron Nitride Nanomaterials: Synthesis and Applications, *Nanotechnologies for the Life Sciences,*

[37]   Garcia-Bustos, E., Figueroa-Guadarrama, M., Rodríguez-Castro, G., Gómez-Vargas, O., Gallardo-Hernández, E., and Campos-Silva, I. (2013) The wear resistance of boride layers measured by the four-ball test, *Surface and Coatings Technology,* **215**, 241-246.

[38] Uslu, I., Comert, H., Ipek, M., Celebi, F., Ozdemir, O., and Bindal, C. (2007) A comparison of borides formed on AISI 1040 and AISI P20 steels, *Materials & design,* **28**, 1819-1826.

[39] Qin, J., He, D., Wang, J., Fang, L., Lei, L., Li, Y*., et al.* (2008) Is rhenium diboride a superhard material?, *Advanced Materials,* **20**, 4780-4783.

[40] Ma, X., Unertl, W., and Erdemir, A. (1999) The boron oxide–boric acid system: Nanoscale mechanical and wear properties, *Journal of materials research,* **14**, 3455-3466.

[41] Gocman, K., Kałdoński, T., Mróz, W., Burdyńska, S., and Prokopiuk, A. (2011) Structural and mechanical properties of boron nitride thin films deposited on steel substrates by pulsed laser deposition, *Journal of KONES,* **18**, 149-156.

[42] Mukhanov, V., Kurakevich, O., and Solozhenko, V. (2008) On the hardness of boron (III) oxide, *Journal of Superhard Materials,* **30**, 71-72.

[43] Twigg, M. V., Collins, N. R., Morris, D., O'CONNELL, T. J., Ball, I. K., Arrowsmith, S*., et al.* (2004) The effect of phosphorus and boron lubricant oil additives on catalyst and engine durability, *SAE transactions,* **113**, 948-959.

[44] Bovington, C. and Castle, R. (2002) Lubricant chemistry including the impact of legislation, *Tribology Series,* **40**, 141-146.

[45] Suarez, A. N., Grahn, M., Pasaribu, R., and Larsson, R. (2010) The influence of base oil polarity on the tribological performance of zinc dialkyl dithiophospate additives, *Tribology International,* **43**, 2268-2278.

[46] Bennett, P. A. (1959) A surface effect associated with the use of oils containing zinc dialkyl dithiophosphate, *ASLE Transactions,* **2**, 78-90.

[47] Yin, Z., Kasrai, M., Fuller, M., Bancroft, G. M., Fyfe, K., and Tan, K. H. (1997) Application of soft X-ray absorption spectroscopy in chemical characterization of antiwear films generated by ZDDP Part I: the effects of physical parameters, *Wear,* **202**, 172-191.

[48] Martin, J. M. (1999) Antiwear mechanisms of zinc dithiophosphate: a chemical hardness approach, *Tribology letters,* **6**, 1-8.

[49] Spikes, H. (2004) The history and mechanisms of ZDDP, *Tribology Letters,* **17**, 469-489.

[50]   Luther, H., E, B., and Staeck, D. (1969) Investigation of decomposition of dialkyl dithiophosphates in hydrocarbons, *Erdol und kohle erdgas petrochemie,* **22**, 530-&.

[51]   Christmann, L. J., "Salts of organic di-thiophosphates," ed: Google Patents, 1933.

[52]   Kennerly, G. and Patterson, W. (1956) Kinetic studies of petroleum antioxidants, *Industrial & Engineering Chemistry,* **48**, 1917-1924.

[53]   Burn, A. (1966) The mechanism of the antioxidant action of zinc dialkyl dithiophosphates, *Tetrahedron,* **22**, 2153-2161.

[54]   Howard, J., Ohkatsu, Y., Chenier, J., and Ingold, K. (1973) Metal complexes as antioxidants. I. The reaction of zinc Dialkyldithiophosphates and related compounds with peroxy radicals, *Canadian Journal of Chemistry,* **51**, 1543-1553.

[55]   Al-Malaika, S., Coker, M., and Scott, G. (1988) Mechanism of antioxidant action: Nature of transformation products of dithiophosphates—Part 1. Their role as antioxidants in polyolefins, *Polymer degradation and stability,* **22**, 147-159.

[56]   Willermet, P., Mahoney, L., and Haas, C. (1979) The effects of antioxidant reactions on the wear behavior of a zinc dialkyldithiophosphate, *ASLE Transactions,* **22**, 301-306.

[57]   Willermet, P., Mahoney, L., and Bishop, C. (1980) Lubricant Degradation and Wear III. Antioxidant Reactions and Wear Behavior of a Zinc Dialkyldithiophosphate in a Fully Formulated Lubricant, *Asle transactions,* **23**, 225-231.

[58]   Masuko, M., Ohkido, T., Suzuki, A., and Ueno, T. (2003) Fundamental study of changes in friction and wear characteristics due to ZnDTP deterioration in simulating engine oil degradation during use, *Tribology Series,* **43**, 359-366.

[59]   Watkins, R. (1982) The antiwear mechanism of zddp's. Part II, *Tribology International,* **15**, 13-15.

[60]   Spedding, H. and Watkins, R. (1982) The antiwear mechanism of zddp's. Part I, *Tribology International,* **15**, 9-12.

[61] Tan, Y. (2011) Experimental methods designed for measuring corrosion in highly resistive and inhomogeneous media, *Corrosion science,* **53**, 1145-1155.

[62] Huq, M., Chen, X., Aswath, P., and Elsenbaumer, R. (2005) Thermal degradation behavior of zinc dialkyldithiophosphate in presence of catalyst and detergents in neutral oil, *Tribology Letters,* **19**, 127-134.

[63] Fuller, M. L. S., Kasrai, M., Bancroft, G. M., Fyfe, K., and Tan, K. H. (1998) Solution decomposition of zinc dialkyl dithiophosphate and its effect on antiwear and thermal film formation studied by X-ray absorption spectroscopy, *Tribology international,* **31**, 627-644.

[64] Nicholls, M. A., Do, T., Norton, P. R., Kasrai, M., and Bancroft, G. M. (2005) Review of the lubrication of metallic surfaces by zinc dialkyl-dithiophosphates, *Tribology International,* **38**, 15-39.

[65] Jayne, D. T., Shanklin, J. R., and Stachew, C. F., "Controlling the corrosion of copper alloys in engine oil formulations: antiwear, friction modifier, dispersant synergy," SAE Technical Paper2002.

[66] García-Antón, J., Monzó, J., Guiñón, J., Gómez, D., and Costa, J. (1990) Study of corrosion on copper strips by petroleum naphtha in the ASTM D-130 test by means of electronic microscopy (SEM) and energy dispersive X-ray (EDX), *Fresenius' Journal of Analytical Chemistry,* **337**, 382-388.

[67] Jones, R. and Coy, R. (1981) The chemistry of the thermal degradation of zinc dialkyldithiophosphate additives, *Asle Transactions,* **24**, 91-97.

[68] Coy, R. and Jones, R. (1981) The thermal degradation and EP performance of zinc dialkyldithiophosphate additives in white oil, *ASLE transactions,* **24**, 77-90.

[69] Yamaguchi, E. and Ryason, P. (1993) Inelastic electron tunneling spectra of lubricant oil additives on native aluminum oxide surfaces, *Tribology transactions,* **36**, 367-374.

[70] Dacre, B. and Bovington, C. H. (1982) The Adsorption and Desorption of Zinc Di-Isopropyldithiophosphate on Steel, *ASLE Transactions,* **25**, 546-554.

[71] Sheasby, J., Caughlin, T., and Habeeb, J. (1991) Observation of the antiwear activity of zinc dialkyldithiophosphate additives, *Wear,* **150**, 247-257.

[72]   So, H., Lin, Y., Huang, G. G., and Chang, T. S. (1993) Antiwear mechanism of zinc dialkyl dithiophosphates added to a paraffinic oil in the boundary lubrication condition, *Wear,* **166**, 17-26.

[73]   Lin, Y. and So, H. (2004) Limitations on use of ZDDP as an antiwear additive in boundary lubrication, *Tribology International,* **37**, 25-33.

[74]   Jahanmir, S. (1987) Wear reduction and surface layer formation by a ZDDP additive, *Journal of tribology,* **109**, 577-586.

[75]   Oura, K., Lifshits, V., Saranin, A., Zotov, A., and Katayama, M., "Surface Science: An Introduction. 2003," ed: Berlin: Springer.

[76]   Desjonqueres, M.-C. and Spanjaard, D., *Concepts in surface physics*: Springer Science & Business Media, 2012.

[77]   Lùeth, H., *Surfaces and interfaces of solids*: Springer-Verlag, 1993.

[78]   Gosvami, N., Bares, J., Mangolini, F., Konicek, A., Yablon, D., and Carpick, R. (2015) Mechanisms of antiwear tribofilm growth revealed in situ by single-asperity sliding contacts, *Science,* **348**, 102-106.

[79]   Ray, N. (1974) Composition—property relationships in inorganic oxide glasses, *Journal of Non-Crystalline Solids,* **15**, 423-434.

[80]   Kapadia, R., Glyde, R., and Wu, Y. (2007) In situ observation of phosphorous and non-phosphorous antiwear films using a mini traction machine with spacer layer image mapping, *Tribology international,* **40**, 1667-1679.

[81]   Kim, S., Sit, C., Komvopoulos, K., Yamaguchi, E., and Ryason, P. (2000) Boundary lubrication of steel surfaces with borate, phosphorus, and sulfur containing lubricants at relatively low and elevated temperatures, *Tribology transactions,* **43**, 569-578.

[82]   Komvopoulos, K., Chiaro, V., Pakter, B., Yamaguchi, E., and Ryason, P. (2002) Antiwear tribofilm formation on steel surfaces lubricated with gear oil containing borate, phosphorus, and sulfur additives, *Tribology transactions,* **45**, 568-575.

[83]   Cen, H., Morina, A., Neville, A., Pasaribu, R., and Nedelcu, I. (2012) Effect of water on ZDDP anti-wear performance and related tribochemistry in lubricated steel/steel pure sliding contacts, *Tribology International,* **56**, 47-57.

[84] Duncanson, M. (2005) Detecting and controlling water in oil, *Practicing Oil Analysis Magazine,* 22-24.

[85] Cann, P., Spikes, H., and Cameron, A. (1983) Thick film formation by zinc dialkyldithiophosphates, *ASLE Transactions,* **26**, 48-52.

[86] Kennedy, S. and Moore, L., "Additive effects on lubricant fuel economy," SAE Technical Paper1987.

[87] Holinski, R. (1979) The influence of boundary layers on friction, *Wear,* **56**, 147-154.

[88] Kubo, K., Kibukawa, M., and Shimakawa, Y., Effect on friction of lubricants containing zinc dithiophosphate and organomolybdenum compound, in *I Mech E Conference Publictions, Institution of Mechanical Engineers*, 1985, 121-131.

[89] Gao, H., McQueen, J., Black, E., Gangopadhyay, A., and Jensen, R. (2004) Reduced phosphorus concentration effects on tribological performance of passenger car engine oils, *Tribology transactions,* **47**, 200-207.

[90] Cann, P. and Cameron, A. (1984) Studies of thick boundary lubrication— influence of zddp and oxidized hexadecane, *Tribology international,* **17**, 205-208.

[91] Fujita, H. and Spikes, H. (2004) The formation of zinc dithiophosphate antiwear films, *Proceedings of the Institution of Mechanical Engineers, Part J: Journal of Engineering Tribology,* **218**, 265-278.

[92] Fujita, H., Glovnea, R., and Spikes, H. (2005) Study of zinc dialkydithiophosphate antiwear film formation and removal processes, part I: experimental, *Tribology transactions,* **48**, 558-566.

[93] Yin, Z., Kasrai, M., Bancroft, G., Fyfe, K., Colaianni, M., and Tan, K. (1997) Application of soft X-ray absorption spectroscopy in chemical characterization of antiwear films generated by ZDDP Part II: the effect of detergents and dispersants, *Wear,* **202**, 192-201.

[94] Ray, N. H. (1979) The structure and properties of inorganic polymeric phosphates, *British Polymer Journal,* **11**, 163-177.

[95] Brow, R. K., Tallant, D. R., Myers, S. T., and Phifer, C. C. (1995) The short-range structure of zinc polyphosphate glass, *Journal of Non-Crystalline Solids,* **191**, 45-55.

[96]   Brow, R. K. (2000) Review: the structure of simple phosphate glasses, *Journal of Non-Crystalline Solids,* **263**, 1-28.

[97]   Eapen, K., Patton, S., and Zabinski, J. (2002) Aktary, M., MT McDermott and GA MacAlpine, Morphology and nanomechanical properties of ZDDP antiwear films as a function of tribological contact time 12 (2002) 155 Arvind Singh, R., GSVL Narasimham and SK Biswas, Estimation of surface temperature of a pin wearing on a disk 12 (2002) 203 Ashurst, WR, see Maboudian, R. 12 (2002) 95, *Tribology Letters,* **12**,

[98]   Morina, A., Green, J., Neville, A., and Priest, M. (2003) Surface and tribological characteristics of tribofilms formed in the boundary lubrication regime with application to internal combustion engines, *Tribology Letters,* **15**, 443-452.

[99]   Ye, J., Kano, M., and Yasuda, Y. (2002) Evaluation of local mechanical properties in depth in MoDTC/ZDDP and ZDDP tribochemical reacted films using nanoindentation, *Tribology Letters,* **13**, 41-47.

[100]   Nicholls, M. A., Do, T., Norton, P. R., Bancroft, G. M., Kasrai, M., Capehart, T. W*., et al.* (2003) Chemical and mechanical properties of ZDDP antiwear films on steel and thermal spray coatings studied by XANES spectroscopy and nanoindentation techniques, *Tribology Letters,* **15**, 241-248.

[101]   Martin, J. M., Grossiord, C., Le Mogne, T., Bec, S., and Tonck, A. (2001) The two-layer structure of Zndtp tribofilms: Part I: AES, XPS and XANES analyses, *Tribology International,* **34**, 523-530.

[102]   Chryssikos, G. D., Duffy, J., Hutchinson, J., Ingram, M., Kamitsos, E., and Pappin, A. (1994) Lithium borate glasses: a quantitative study of strength and fragility, *Journal of non-crystalline solids,* **172**, 378-383.

[103]   Bancroft, G., Kasrai, M., Fuller, M., Yin, Z., Fyfe, K., and Tan, K. H. (1997) Mechanisms of tribochemical film formation: stabilityof tribo-and thermally-generated ZDDP films, *Tribology Letters,* **3**, 47-51.

[104]   Hsu, S. M. and Gates, R. (2005) Boundary lubricating films: formation and lubrication mechanism, *Tribology International,* **38**, 305-312.

[105]   Williams, J. (2004) The behaviour of sliding contacts between non-conformal rough surfaces protected by'smart'films, *Tribology Letters,* **17**, 765-778.

[106]   Pearson, R. G., *Chemical hardness*: Wiley-VCH, 1997.

[107]   Warren, O., Graham, J., Norton, P., Houston, J., and Michalske, T. (1998) Nanomechanical properties of films derived from zinc dialkyldithiophosphate, *Tribology Letters,* **4**, 189-198.

[108]   Graham, J., McCague, C., and Norton, P. (1999) Topography and nanomechanical properties of tribochemical films derived from zinc dialkyl and diaryl dithiophosphates, *Tribology letters,* **6**, 149-157.

[109]   Haque, T., "Tribochemistry of lubricant additives on non-ferrous coatings for reduced friction, improved durability and wear in internal combustion engines," University of Leeds, 2007.

[110]   Bec, S., Tonck, A., Georges, J.-M., Coy, R., Bell, J., and Roper, G., Relationship between mechanical properties and structures of zinc dithiophosphate anti–wear films, in *Proceedings of the Royal Society of London A: Mathematical, Physical and Engineering Sciences*, 1999, 4181-4203.

[111]   Morina, A., Neville, A., Green, J., and Priest, M. (2005) Additive/additive interactions in boundary lubrication—a study of film formation and tenacity, *Tribology and Interface Engineering Series,* **48**, 757-767.

[112]   Asseff, P. A., Kasai, T., and Towle, A., PD 23 (3) Interrelation Between Fuels, Lubricants and Automotive Engine Anti-Pollution Devices, in *9th World Petroleum Congress*, 1975.

[113]   Guibet, J.-C. and Faure-Birchem, E., *Fuels and engines: technology, energy, environment* vol. 2: Éditions Technip, 1999.

[114]   Kaleli, H. (2001) The impact of crankcase oil containing phosphorus on catalytic converters and engine exhaust emissions, *Industrial Lubrication and Tribology,* **53**, 237-255.

[115]   Rokosz, M., Chen, A., Lowe-Ma, C., Kucherov, A., Benson, D., Paputa Peck, M.*, et al.* (2001) Characterization of phosphorus-poisoned automotive exhaust catalysts, *Applied Catalysis B: Environmental,* **33**, 205-215.

[116]   Cook, J. F., "Antiwear lubricants containing boron esters," ed: Google Patents, 1961.

[117]   Kreuz, K., Fein, R., and Dundy, M. (1967) EP films from borate lubricants, *ASLE Transactions,* **10**, 67-76.

[118]   Steinberg, H., *Organoboron chemistry*: Interscience Publishers, 1964.

[119] Zheng, Z., Shen, G., Wan, Y., Cao, L., Xu, X., Yue, Q., *et al.* (1998) Synthesis, hydrolytic stability and tribological properties of novel borate esters containing nitrogen as lubricant additives, *Wear,* **222**, 135-144.

[120] Braid, M. and Horodysky, A. G., "Hindered phenyl esters of cyclic borates and lubricants containing same," ed: Google Patents, 1986.

[121] Yao, J. and Dong, J. (1995) Improvement of hydrolytic stability of borate esters used as lubricant additives, *Lubrication engineering,* **51**,

[122] Thomas J. C.Karrol, S. G. D., "Synergistic Organoborate Compositions And Lubricating Compositions Containing Same," US Patent US 2004/0138073 A1, Jul. 15, 2004, 2004.

[123] Adams, J. H., "Lubricant containing potassium borate," ed: Google Patents, 1976.

[124] Hu, Z. and Dong, J. (1998) Study on antiwear and reducing friction additive of nanometer titanium borate, *Wear,* **216**, 87-91.

[125] Hu, Z., Dong, J., Chen, G., and He, J. (2000) Preparation and tribological properties of nanoparticle lanthanum borate, *Wear,* **243**, 43-47.

[126] Hu, Z., Shi, Y., Wang, L., Peng, Y., Chen, G., and Dong, J. (2001) Study on antiwear and reducing friction additive of nanometer aluminum borate, *Lubrication engineering,* **57**, 23-27.

[127] Hu, Z. S., Lai, R., Lou, F., Wang, L., Chen, Z., Chen, G., *et al.* (2002) Preparation and tribological properties of nanometer magnesium borate as lubricating oil additive, *Wear,* **252**, 370-374.

[128] Harrison, J. J., Nelson, K. D., and Buitrago, J. A., "Dispersed hydrated potassium borate compositions having improved properties in lubricating oil compositions," ed: Google Patents, 2004.

[129] Canter, N. (2008) Friction-reducing characteristics T, *Tribology & Lubrication Technology,* **1**, 1.

[130] Wang, Y., Li, J., and Ren, T. (2009) Tribological study of a novel borate ester containing dialkylthiophosphate group as multifunctional additive, *Industrial Lubrication and Tribology,* **61**, 33-39.

[131] Li, W., Wu, Y., Wang, X., and Liu, W. (2012) Tribological study of boron-containing soybean lecithin as environmentally friendly lubricant additive in synthetic base fluids, *Tribology Letters,* **47**, 381-388.

[132] Li, Z., Zhang, Y., Ren, T., and Zhao, Y. (2014) Tribological studies of highly hydrolytically stable N-containing long chain alkyl phenylborate esters in mineral oil, *Proceedings of the Institution of Mechanical Engineers, Part J: Journal of Engineering Tribology,* 1350650114530878.

[133] Jianwei, Y., Fenfang, L., and Yihui, H. (2010) Tribological performance of two potential environmentally friendly ashless vegetable oil additives, *China Petroleum Processing & Petrochemical Technology,* **12**, 43-48.

[134] Zhu, F., Fan, W., Wang, A., and Zhu, Y. (2009) Tribological study of novel S–N style 1, 3, 4-thiadiazole-2-thione derivatives in rapeseed oil, *Wear,* **266**, 233-238.

[135] Dicky, D. and Dyah, S. P. (2012) Bio-Lubricants Development: The Potential Use of Boron-Containing Additives,

[136] Boyde, S. (2000) Hydrolytic stability of synthetic ester lubricants, *Journal of Synthetic Lubrication,* **16**, 297-312.

[137] Beran, E. (2010) Effect of chemical structure on the hydrolytic stability of lubricating base oils, *Tribology International,* **43**, 2372-2377.

[138] Erdemir, A., Bindal, C., Zuiker, C., and Savrun, E. (1996) Tribology of naturally occurring boric acid films on boron carbide, *Surface and Coatings Technology,* **86**, 507-510.

[139] Erdemir, A., Halter, M., and Fenske, G. (1997) Preparation of ultralow-friction surface films on vanadium diboride, *Wear,* **205**, 236-239.

[140] Tian, S., Jiang, L., Guo, Q., and Wu, G. (2014) Effect of surface roughness on tribological properties of TiB 2/Al composites, *Materials & Design,* **53**, 129-136.

[141] Taktak, S. (2006) Tribological behaviour of borided bearing steels at elevated temperatures, *Surface and Coatings Technology,* **201**, 2230-2239.

[142] Martini, C., Palombarini, G., Poli, G., and Prandstraller, D. (2004) Sliding and abrasive wear behaviour of boride coatings, *Wear,* **256**, 608-613.

[143] Cimenoglu, H., Atar, E., and Motallebzadeh, A. (2014) High temperature tribological behaviour of borided surfaces based on the phase structure of the boride layer, *Wear,* **309**, 152-158.

[144] E. Garcia-Bustos a, M. A. F.-G. a., G.A. Rodríguez-Castro b, O.A. Gómez-Vargas b, and E.A. Gallardo-Hernández a, I. C.-S. b. ((2013)) The wear

resistance of boride layers measured by the four-ball test, *Surface & Coatings Technology,* 241–246.

[145] Umeda, K., Enomoto, Y., Mitsui, A., and Mannami, K. (1993) Friction and wear of boride ceramics in air and water, *Wear,* **169**, 63-68.

[146] Chakraborty, S., Debnath, D., Mallick, A. R., and Das, P. K. (2014) Mechanical, Tribological, and Thermal Properties of Hot-pressed ZrB2-B4C Composite, *International Journal of Applied Ceramic Technology,*

[147] Kimura, Y., Wakabayashi, T., Okada, K., Wada, T., and Nishikawa, H. (1999) Boron nitride as a lubricant additive, *Wear,* **232**, 199-206.

[148] Han, W. Q. (2009) Anisotropic Hexagonal Boron Nitride Nanomaterials: Synthesis and Applications, *Nanotechnologies for the Life Sciences,*

[149] Mahathanabodee, S., Palathai, T., Raadnui, S., Tongsri, R., and Sombatsompop, N. (2013) Effects of hexagonal boron nitride and sintering temperature on mechanical and tribological properties of SS316L/h-BN composites, *Materials & Design,* **46**, 588-597.

[150] Habig, K.-H. (1995) Fundamentals of the tribological behaviour of diamond, diamond-like carbon and cubic boron nitride coatings, *Surface and Coatings Technology,* **76**, 540-547.

[151] Erdemir, A. and Donnet, C. (2006) Tribology of diamond-like carbon films: recent progress and future prospects, *Journal of Physics D: Applied Physics,* **39**, R311.

[152] Hao, L., Li, J., Xu, X., and Ren, T. (2010) Preparation, characterization, and tribological evaluation of triethanolamine monooleate-modified lanthanum borate nanoparticles, *Proceedings of the Institution of Mechanical Engineers, Part J: Journal of Engineering Tribology,* **224**, 1163-1171.

[153] Zhao, C., Jiao, Y., Chen, Y. K., and Ren, G. (2014) The Tribological Properties of Zinc Borate Ultrafine Powder as a Lubricant Additive in Sunflower Oil, *Tribology Transactions,* **57**, 425-434.

[154] HU Zhi-biao, L. H.-j., Fu Qian-gang, Xue Hui, Sun Guo-ling (June 2007 2007) Fabrication and tribological properties of B2O3 as friction reducing coatings for carbon-carbon composites, *New Carbon Materials,* **22,**,

[155] Ray, N. H. (1975) Inorganic oxide glasses as ionic polymers, *British Polymer Journal,* **7**, 307-317.

[156] Yan, J., Zeng, X., van der Heide, E., and Ren, T. (2014) The tribological performance and tribochemical analysis of novel borate esters as lubricant additives in rapeseed oil, *Tribology International,* **71**, 149-157.

[157] Canter, N. (2009) Boron nanotechnology-based lubricant additive, *Tribology & Lubrication Technology,* **65**, 12-13.

[158] Philippon, D., De Barros-Bouchet, M.-I., Lerasle, O., Le Mogne, T., and Martin, J.-M. (2011) Experimental simulation of tribochemical reactions between borates esters and steel surface, *Tribology Letters,* **41**, 73-82.

[159] A. Erdemir av*, C. B. a., C. Zuiker a, E. Savrun b ((1996)) Tribology of naturally occurring boric acid films on boron carbide, *Surface and Coatings Technology,,* 507-510.

[160] Jallad, K. N., Ben-Amotz, D., and Erdemir, A. (2002) Raman chemical Imaging of tribological surfaces, *Tribology transactions,* **45**, 239-245.

[161] Shirahama, S. and Hirata, M. (1989) The effects of engine oil additives on valve train wear, *Lubrication Science,* **1**, 365-384.

[162] Pankajavalli, R., Anthonysamy, S., Ananthasivan, K., and Rao, P. V. (2007) Vapour pressure and standard enthalpy of sublimation of H 3 BO 3, *Journal of nuclear materials,* **362**, 128-131.

[163] Balcı, S., Sezgi, N. A., and Eren, E. (2012) Boron oxide production kinetics using boric acid as raw material, *Industrial & Engineering Chemistry Research,* **51**, 11091-11096.

[164] Balasubramanian, R., Lakshmi Narasimhan, T., Viswanathan, R., and Nalini, S. (2008) Investigation of the vaporization of boric acid by transpiration thermogravimetry and Knudsen effusion mass spectrometry, *The Journal of Physical Chemistry B,* **112**, 13873-13884.

[165] Liu, W., Xue, Q., Zhang, X., Wang, H., and Huang, C. (1992) The performance and antiwear mechanism of tridodecyl borate as an oil additive, *Lubrication engineering,* **48**, 475-479.

[166] BAILAR, J., *Comprehensive Inorganic Chemistry*: Pergamon Press, 1973.

[167] Varlot, K., Kasrai, M., Bancroft, G., Yamaguchi, E., Ryason, P., and Igarashi, J. (2001) X-ray absorption study of antiwear films generated from ZDDP and borate micelles, *Wear,* **249**, 1029-1035.

[168]   Zhang, Z., Yamaguchi, E., Kasrai, M., and Bancroft, G. (2004) Interaction of ZDDP with borated dispersant using XANES and XPS, *Tribology transactions,* **47**, 527-536.

[169]   Yamaguchi, E. S., Roby, S. H., and Yeh, S. (2005) Time-dependent film formation from ZnDTPs and nonphosphorus antiwear agents, *Tribology transactions,* **48**, 57-68.

[170]   Johnsson, E. (2015) Investigation of tribological mechanisms of a boron additive in lubricants and fuel enhancer,

[171]   Krogh-Moe, J. (1969) The structure of vitreous and liquid boron oxide, *Journal of Non-Crystalline Solids,* **1**, 269-284.

[172]   Doweidar, H. (1990) Consideration of the boron oxide anomaly, *Journal of materials science,* **25**, 253-258.

[173]   Mozzi, R. L. and Warren, B. (1970) The structure of vitreous boron oxide, *Journal of Applied Crystallography,* **3**, 251-257.

[174]   Saddeek, Y. B. (2004) Structural analysis of alkali borate glasses, *Physica B: Condensed Matter,* **344**, 163-175.

[175]   Kodama, M. and Kodama, S., Velocity of sound and elastic properties of alkali borate glasses, in *Proc. Second Int. Conf. on Borate Glasses, Crystals, and Melts*, 1997, 181-8.

[176]   Hansson, A. (1961) On Crystal Structure Of Hydrated Sodium Perborate, *ACTA Chemica Scandinavica,* **15**, 934-&.

[177]   Menzel, H. and Schulz, H. (1940) A contribution to the knowledge of the acids of boron and of the alkaliborates. X. Kernite (Rasorite) Na^ sub 2^ B^ sub 4^ O^ sub 7^ 4H2O), *Z. anorg. Chem,* **245**, 157-220.

[178]   Padmaja, G. and Kistaiah, P. (2009) Infrared and Raman spectroscopic studies on alkali borate glasses: evidence of mixed alkali effect, *The Journal of Physical Chemistry A,* **113**, 2397-2404.

[179]   Kodama, M., Hirashima, T., and Matsushita, T. (1993) Anomalous behaviour of ultrasonic velocity in caesium borate glasses, *Physics and chemistry of glasses,* **34**, 129-139.

[180]   Akagi, R., Ohtori, N., and Umesaki, N. (2001) Raman spectra of $K_2O–B_2O_3$ glasses and melts, *Journal of non-crystalline solids,* **293**, 471-476.

[181] Cochain, B., Neuville, D., Henderson, G., McCammon, C., Pinet, O., and Richet, P. (2012) Effects of the Iron Content and Redox State on the Structure of Sodium Borosilicate Glasses: A Raman, Mössbauer and Boron K-Edge XANES Spectroscopy Study, *Journal of the American Ceramic Society,* **95**, 962-971.

[182] Fleet, M. and Muthupari, S. (1999) Coordination of boron in alkali borosilicate glasses using XANES, *Journal of non-crystalline solids,* **255**, 233-241.

[183] Kauzmann, W. (1948) The Nature of the Glassy State and the Behavior of Liquids at Low Temperatures, *Chemical Reviews,* **43**, 219-256.

[184] Larsson, P., Axen, N., and Hogmark, S. (1999) Tribofilm formation on boron carbide in sliding wear, *Wear,* **236**, 73-80.

[185] Cuong, P. D., Ahn, H.-S., Yoon, E.-S., and Shin, K.-H. (2006) Effects of relative humidity on tribological properties of boron carbide coating against steel, *Surface and Coatings Technology,* **201**, 4230-4235.

[186] Barthel, A. and Kim, S. (2013) Surface chemistry dependence of water adsorption on solid substrates in humid ambient and humidity effects on wear of copper and glass surfaces, *Tribology-Materials, Surfaces & Interfaces,* **7**, 63-68.

[187] Alazizi, A., Barthel, A. J., Surdyka, N. D., Luo, J., and Kim, S. H. (2015) Vapors in the ambient—A complication in tribological studies or an engineering solution of tribological problems?, *Friction,* **3**, 85-114.

[188] Pereira, G., Munoz-Paniagua, D., Lachenwitzer, A., Kasrai, M., Norton, P. R., Capehart, T. W.*, et al.* (2007) A variable temperature mechanical analysis of ZDDP-derived antiwear films formed on 52100 steel, *Wear,* **262**, 461-470.

[189] Kim, B., Mourhatch, R., and Aswath, P. B. (2010) Properties of tribofilms formed with ashless dithiophosphate and zinc dialkyl dithiophosphate under extreme pressure conditions, *Wear,* **268**, 579-591.

[190] Sun, Y., Hu, L., and Xue, Q. (2009) Tribological properties and action mechanism of N, N-dialkyl dithiocarbamate-derived S-hydroxyethyl borate esters as additives in rapeseed oil, *Wear,* **266**, 917-924.

[191] Kamitsos, E., Karakassides, M., and Patsis, A. (1989) Spectroscopic study of carbonate retention in high-basicity borate glasses, *Journal of non-crystalline solids,* **111**, 252-262.

[192] Joyner, D. J., Johnson, O., and Hercules, D. M. (1980) A study of the iron borides. 1. Electron spectroscopy, *Journal of the American Chemical Society,* **102**, 1910-1917.

[193] Qiao, Y., Liu, W., Qi, S., Xue, Q., Xu, B., and Ma, S. (1998) The tribochemical mechanism of the borate modified by N-containing compound as oil additive, *Wear,* **215**, 165-169.

[194] Baldwin, B. A. (1977) Relative antiwear efficiency of boron and sulfur surface species, *Wear,* **45**, 345-353.

[195] Ren, T.-h., Liu, W.-m., Xue, Q.-j., and Wang, H. (1993) The effect of molecular structure of n-containing heterocyclic compounds on their wear properties, *Lubrication Science,* **5**, 205-212.

[196] Brion, D. (1980) Etude par spectroscopie de photoelectrons de la degradation superficielle de FeS 2, CuFeS 2, ZnS et PbS a l'air et dans l'eau, *Applications of Surface Science,* **5**, 133-152.

[197] Descostes, M., Mercier, F., Thromat, N., Beaucaire, C., and Gautier-Soyer, M. (2000) Use of XPS in the determination of chemical environment and oxidation state of iron and sulfur samples: constitution of a data basis in binding energies for Fe and S reference compounds and applications to the evidence of surface species of an oxidized pyrite in a carbonate medium, *Applied Surface Science,* **165**, 288-302.

[198] Yang, G., Zhang, Z., Li, G., Zhang, J., Yu, L., and Zhang, P. (2011) Synthesis and tribological properties of S-and P-free borate esters with different chain lengths, *Journal of Tribology,* **133**, 021801.

[199] Vannerberg, N.-G. (1962) Progress in Inorganic Chemistry, Vol. 4, *lnterscience, New York,* **5**, 133.

[200] Lindner, U. and Papp, H. (1988) XPS and ISS characterization of potassium or copper containing Fe/Mn oxide catalysts for Fischer-Tropsch synthesis, *Applied surface science,* **32**, 75-92.

[201] Morizur, M. and Teysset, O. (1992) Antiwear actions of additives in solid dispersion, *Lubrication Science,* **4**, 277-299.

[202] Slater, J. C. (1964) Atomic radii in crystals, *The Journal of Chemical Physics,* **41**, 3199-3204.

[203] Lee, J.-H., Yi, J.-S., Yang, K.-J., Park, J.-H., and Oh, R.-D. (2003) Electrical and optical properties of boron doped CdS thin films prepared by chemical bath deposition, *Thin Solid Films,* **431**, 344-348.

[204] Hassan, A., Torell, L., Börjesson, L., and Doweidar, H. (1992) Structural changes of B_2O_3 through the liquid-glass transition range: A Raman-scattering study, *Physical Review B,* **45**, 12797.

[205] Song, L., Ci, L., Lu, H., Sorokin, P. B., Jin, C., Ni, J*., et al.* (2010) Large scale growth and characterization of atomic hexagonal boron nitride layers, *Nano letters,* **10**, 3209-3215.

[206] Demas, N. G., Timofeeva, E. V., Routbort, J. L., and Fenske, G. R. (2012) Tribological effects of BN and MoS2 nanoparticles added to polyalphaolefin oil in piston skirt/cylinder liner tests, *Tribology Letters,* **47**, 91-102.

[207] Bindal, C. and Erdemir, A. (1996) Ultralow friction behavior of borided steel surfaces after flash annealing, *Applied physics letters,* **68**, 923-925.

[208] Meera, B. and Ramakrishna, J. (1993) Raman spectral studies of borate glasses, *Journal of non-crystalline solids,* **159**, 1-21.

[209] Walrafen, G. E., Samanta, S., and Krishnan, P. (1980) Raman investigation of vitreous and molten boric oxide, *The Journal of Chemical Physics,* **72**, 113-120.

[210] Hannon, A. C., Grimley, D. I., Hulme, R. A., Wright, A. C., and Sinclair, R. N. (1994) Boroxol groups in vitreous boron oxide: new evidence from neutron diffraction and inelastic neutron scattering studies, *Journal of non-crystalline solids,* **177**, 299-316.

[211] Pascuta, P., Lungu, R., and Ardelean, I. (2010) FTIR and Raman spectroscopic investigation of some strontium–borate glasses doped with iron ions, *Journal of Materials Science: Materials in Electronics,* **21**, 548-553.

[212] Kamitsos, E., Karakassides, M., and Chryssikos, G. D. (1987) Vibrational spectra of magnesium-sodium-borate glasses. 2. Raman and mid-infrared investigation of the network structure, *Journal of Physical Chemistry,* **91**, 1073-1079.

[213] Kamitsos, E. and Chryssikos, G. D. (1991) Borate glass structure by Raman and infrared spectroscopies, *Journal of molecular structure,* **247**, 1-16.

[214] Fukumi, K., Ogawa, K., and Hayakawa, J. (1992) Intensities of Raman bands in borate glasses, *Journal of non-crystalline solids,* **151**, 217-221.

[215] Yu, X., Jiang, Z., Wei, D., Zhou, C., Huang, Q., and Yang, D. (2013) Tribological properties of magnetite precipitate from oxide scale in hot-rolled microalloyed steel, *Wear,* **302**, 1286-1294.

[216] Sone, Y., Suzumura, J., Ban, T., Aoki, F., and Ishida, M. (2008) Possibility of in situ spectroscopic analysis for iron rust on the running band of rail, *Wear,* **265**, 1396-1401.

[217] De Faria, D., Venâncio Silva, S., and De Oliveira, M. (1997) Raman microspectroscopy of some iron oxides and oxyhydroxides, *Journal of Raman spectroscopy,* **28**, 873-878.

[218] Li, H., Zhang, Q., Yap, C. C. R., Tay, B. K., Edwin, T. H. T., Olivier, A.*, et al.* (2012) From bulk to monolayer MoS2: evolution of Raman scattering, *Advanced Functional Materials,* **22**, 1385-1390.

[219] Simeone, D., Mallet, C., Dubuisson, P., Baldinozzi, G., Gervais, C., and Maquet, J. (2000) Study of boron carbide evolution under neutron irradiation by Raman spectroscopy, *Journal of nuclear materials,* **277**, 1-10.

[220] Erdemir, A., Fenske, G., and Erck, R. (1990) A study of the formation and self-lubrication mechanisms of boric acid films on boric oxide coatings, *Surface and coatings technology,* **43**, 588-596.

[221] A. Erdemir, G. R. F. a. R. A. E. ((1990)) A Study of The Formation and Self-lubrication Mechanisms of Boric Acid Films on Boric Oxide Coatings, *Surfaces and Coatings Technology,* 588—596.

[222] Lovell, M., Higgs, C., Deshmukh, P., and Mobley, A. (2006) Increasing formability in sheet metal stamping operations using environmentally friendly lubricants, *Journal of materials processing technology,* **177**, 87-90.

[223] M. A. Kabir, C. F. H. I., Michael R. Lovell (2008) A Pin-on-Disk Experimental Study on a Green Particulate-Fluid Lubricant, *Journal of Tribology,* **130**, 1-5.

[224] Kocakuşak, S., Akcay, K., Ayok, T., Koöroğlu, H., Koral, M., Savaşçi, Ö.*, et al.* (1996) Production of anhydrous, crystalline boron oxide in fluidized bed reactor, *Chemical Engineering and Processing: Process Intensification,* **35**, 311-317.

[225] Qiu, S., Zhou, Z., Dong, J., and Chen, G. (2001) Preparation of Ni nanoparticles and evaluation of their tribological performance as potential additives in oils, *Journal of Tribology,* **123**, 441-443.

[226] Hu*, J. X. D. a. Z. S. (1998) A study of the anti-wear and friction-reducing properties of the lubricant additive, nanometer zinc borate, *Tribology International,* **Vol. 31, No. 5,**, 219–223.

[227] Chemical, T.-i. E. *Chemicals Datasheet SpectrSyn 6*. Available: http://www.tri-iso.com/html2pdf/html2ps.php?url=exxonmobil-chemical-company%2Fspectrasyn-6.html%3Fnothumbs%3D1

[228] Karol, T. J. and Donnelly, S. G., "Synergistic organoborate compositions and lubricating compositions containing same," ed: Google Patents, 2009.

[229] Mang, T. and Dresel, W. (2001) Tribology of gears, lubricants and lubrications, *Chapter,* **10**, 210-211.

[230] Company, R. T. V. H. (10/06/2017). *VANLUBE ® 289 Lubricant Additive*. Available: https://www.rtvanderbilt.com/TDS%20Vlbe289.pdf

[231] Harrison, J. J. and Nelson, K. D., "Lubricant composition comprising alkali metal borate dispersed in a polyalkylene succinic anhydride and a metal salt of a polyisobutenyl sulfonate," ed: Google Patents, 2003.

[232] Archoil Oils, F. a. L. (28/05/2017). *AR9100 Nanoborate Friction Modifier* Available: https://www.carid.com/images/archoil/products/pdf/ar9100-data-sheet.pdf

[233] Brotherton, R. J., Weber, C. J., Guibert, C. R., and Little, J. L., "Boron Compounds," in *Ullmann's Encyclopedia of Industrial Chemistry*, ed: Wiley-VCH Verlag GmbH & Co. KGaA, 2000.

[234] Lappert, M. (1956) Organic compounds of boron, *Chemical Reviews,* **56**, 959-1064.

[235] Brotherton, R. J., Weber, C. J., Guibert, C. R., and Little, J. L. (1985) Boron compounds, *Ullmann's Encyclopedia of Industrial Chemistry,*

[236] SIGMA-ALDRICH. *Trimethyl Borate Technical Data Sheet*. Available: http://www.sigmaaldrich.com/catalog/product/sial/92330?lang=en&region=GB

[237] Qu, J., Luo, H., Chi, M., Ma, C., Blau, P. J., Dai, S.*, et al.* (2014) Comparison of an oil-miscible ionic liquid and ZDDP as a lubricant anti-wear additive, *Tribology International,* **71**, 88-97.

[238] Inc., A. *Archoil AR9100 Friction Modifier*. Available: http://www.archoil.com/wp-content/uploads/2013/12/9100Sheet.pdf

[239] Morina, A., Neville, A., Priest, M., and Green, J. (2006) ZDDP and MoDTC interactions and their effect on tribological performance–tribofilm characteristics and its evolution, *Tribology Letters,* **24**, 243-256.

[240] Priest, M. and Taylor, C. (2000) Automobile engine tribology—approaching the surface, *Wear,* **241**, 193-203.

[241] Tribology-abc. *Hertzian contact pressure calculator-initial point contact*. Available: http://www.tribology-abc.com/calculators/e2_1.htm

[242] Hamrock, B. J. and Dowson, D. (1977) Isothermal elastohydrodynamic lubrication of point contacts: Part III—Fully flooded results, *Journal of Tribology,* **99**, 264-275.

[243] Bauer, C. and Day, M. (2007) Water contamination in hydraulic and lube systems, *Practicing Oil Analysis Magazine,* **9**,

[244] Tunac, C. and Zimmerman, J., "Market Investigation for Oil Analysis Instruments," DTIC Document1999.

[245] KITTIWAKEPARKER. *Oil Test and Analysis Solutions*. Available: http://www.onsitecatalog.com/catalogs/1685/4362/pdf-file/Katalog_2012.pdf

[246] Mourhatch, R. and Aswath, P. B. (2011) Tribological behavior and nature of tribofilms generated from fluorinated ZDDP in comparison to ZDDP under extreme pressure conditions—Part II: Morphology and nanoscale properties of tribofilms, *Tribology International,* **44**, 201-210.

[247] Li, Y.-R., Pereira, G., Lachenwitzer, A., Kasrai, M., and Norton, P. R. (2008) Studies on ZDDP thermal film formation by XANES spectroscopy, atomic force microscopy, FIB/SEM and 31P NMR, *Tribology Letters,* **29**, 11-22.

[248] Kaemmer, S. B. (2011) Introduction to bruker's scanasyst and peakforce tapping afm technology, *Bruker application note. Bruker Nano Inc., Santa Barbara, CA,*

[249] Narain, K., "An Introduction to Nanomechanical Testing," W. Micro Materials Ltd., Ed., ed. UK: krish@micromaterials.co.uk.

[250] Beake, B., Goodes, S., Jones, S., Gray, A., Harris, A., Pickford, N.*, et al.* (2006) NanoTest On-line Help File Version 1.0 and NanoTest Manual Version 3.0, *Micro Materials Ltd,*

[251] Oliver, W. C. and Pharr, G. M. (2004) Measurement of hardness and elastic modulus by instrumented indentation: Advances in understanding and refinements to methodology, *Journal of materials research,* **19**, 3-20.

[252] Oliver, W. C. and Pharr, G. M. (1992) An improved technique for determining hardness and elastic modulus using load and displacement sensing indentation experiments, *Journal of materials research,* **7**, 1564-1583.

[253] He, J. and Veprek, S. (2003) Finite element modeling of indentation into superhard coatings, *Surface and Coatings Technology,* **163**, 374-379.

[254] Tsui, T. and Pharr, G. (1999) Substrate effects on nanoindentation mechanical property measurement of soft films on hard substrates, *Journal of Materials Research,* **14**, 292-301.

[255] Pharr, G. and Oliver, W. (1992) Measurement of thin film mechanical properties using nanoindentation, *Mrs Bulletin,* **17**, 28-33.

[256] Pollock, H., Maugis, D., and Barquins, M. (1986) Microindentation techniques in material science and engineering, *ASTM STP,* **889**, 47-71.

[257] Doerner, M., Gardner, D., and Nix, W. (1986) Plastic properties of thin films on substrates as measured by submicron indentation hardness and substrate curvature techniques, *Journal of Materials Research,* **1**, 845-851.

[258] Fairley, N. C., "Version 2.1. 25," ed.

[259] Seah, M. (1990) Quantification of AES and XPS, *Practical surface analysis,* **1**, 201-255.

[260] Briggs, D. and Seah, M. P. (1983) Practical surface analysis by Auger and X-ray photoelectron spectroscopy, *D. Briggs, & M. P. Seah,(Editors), John Wiley & Sons, Chichester 1983, xiv+ 533,*

[261] Seah, M. P. and Briggs, D., *Practical Surface Analysis: Auger and X-ray Photoelectron Spectroscopy*: John Wiley & Sons, 1990.

[262] Coates, J. (1998) Vibrational Spectroscopy: Instrumentation for Infrared and Raman Spectroscopy∗, *Applied spectroscopy reviews,* **33**, 267-425.

[263] Gouadec, G. and Colomban, P. (2007) Raman Spectroscopy of nanomaterials: How spectra relate to disorder, particle size and mechanical properties, *Progress in Crystal Growth and Characterization of Materials,* **53**, 1-56.

[264] Konijnendijk, W. L. and Stevels, J. M. (1975) The structure of borate glasses studied by Raman scattering, *Journal of Non-Crystalline Solids,* **18**, 307-331.

[265] Krogh-Moe, J. (1962) The crystal structure of lithium diborate, Li2O. 2B2O3, *Acta Crystallographica,* **15**, 190-193.

[266] Krogh-Moe, J. (1962) Structural interpretation of melting point depression in the sodium borate system, *Phys. Chem. Glasses,* **3**, 101-110.

[267] FOCUSLAB. *Copper Strip Corrosion ASTM D130*. Available: http://my.umbc.edu/system/shared/attachments/33558a3a66c8c1e778cbd3df 308dcc1d/593d5d28/group-documents/000/001/952/4dea382d82666332fb564f2e711cbc71/coppercorros ion.pdf?1334852745

[268] Lehrle, R. S., Duncan, R., Liu, Y., Parsons, I. W., Rollinson, M., Lamb, G.*, et al.* (2002) Mass spectrometric methods for assessing the thermal stability of liquid polymers and oils: study of some liquid polyisobutylenes used in the production of crankcase oil additives, *Journal of analytical and applied pyrolysis,* **64**, 207-227.

[269] Chang, C. E. and Wilcox, W. R. (1971) Vitreous boron oxide: Drying and moisture absorption, *Materials Research Bulletin,* **6**, 1297-1304.

[270] Slobod, R. and Krogh, M. (1950) Nitrous oxide as a constituent of the atmosphere, *Journal of the American Chemical Society,* **72**, 1175-1177.

[271] Erdemir, A., Erck, R. A., and Robles, J. (1991) Relationship of hertzian contact pressure to friction behavior of self-lubricating boric acid films, *Surface and Coatings Technology,* **49**, 435-438.

[272] Shen, G., Zheng, Z., Wan, Y., Xu, X., Cao, L., Yue, Q.*, et al.* (2000) Synergistic lubricating effects of borate ester with heterocyclic compound, *Wear,* **246**, 55-58.

[273] Varlot, K., Martin, J., Grossiord, C., Vargiolu, R., Vacher, B., and Inoue, K. (1999) A dual-analysis approach in tribochemistry: application to ZDDP/calcium borate additive interactions, *Tribology Letters,* **6**, 181-189.

[274] Godfrey, D. (1999) Iron oxides and rust (hydrated iron oxides) in tribology, *Lubrication Engineering-Illinois-,* **55**, 33-38.

[275] Zhu, Y., Olofsson, U., and Chen, H. (2013) Friction between wheel and rail: a pin-on-disc study of environmental conditions and iron oxides, *Tribology letters,* **52**, 327-339.

[276] Walker, J., Kamps, T., and Wood, R. (2013) The influence of start–stop transient velocity on the friction and wear behaviour of a hyper-eutectic Al–Si automotive alloy, *Wear,* **306**, 209-218.

[277] Zhi Zheng a, G. S. a.,), Yong Wan a, Lili Cao a, Xiangdong Xu a, Qixian Yue b,Tianjian Sun, B. (1998) Synthesis, hydrolytic stability and tribological properties of novel borate esters containing nitrogen as lubricant additives, *Wear,* 135–144.

[278] Erdemir, A. (2001) Solid lubricants and self-lubricating films, *Modern tribology handbook,* **2**, 787.

[279] Bec, S., Tonck, A., Georges, J., Yamaguchi, E., and Ryason, P. (2003) Surface Force Apparatus Studies of Adsorbed Borate Films, *Tribology transactions,* **46**, 522-533.

[280] Komvopoulos, K., Do, V., Yamaguchi, E., and Ryason, P. (2004) Nanomechanical and nanotribological properties of an antiwear tribofilm produced from phosphorus-containing additives on boundary-lubricated steel surfaces, *Journal of tribology,* **126**, 775-780.

[281] Aktary, M., McDermott, M. T., and McAlpine, G. A. (2002) Morphology and nanomechanical properties of ZDDP antiwear films as a function of tribological contact time, *Tribology letters,* **12**, 155-162.

[282] Glaeser, W., *Materials for tribology* vol. 20: Elsevier, 1992.

[283] Philip, J. (1997) NMR and NQR Studies of Borates and Borides, *Borate Glasses, Crystals and Melts,* 1.

[284] Raman, T., Rao, G., and Chakravorty, D. (1978) Mössbauer effect studies of alkali borate glasses, *Journal of Non-Crystalline Solids,* **29**, 85-107.

[285] Zhong, J. and Bray, P. J. (1989) Change in boron coordination in alkali borate glasses, and mixed alkali effects, as elucidated by NMR, *Journal of non-crystalline solids,* **111**, 67-76.

[286] Silver, A. and Bray, P. (1958) Nuclear Magnetic Resonance Absorption in Glass. I. Nuclear Quadrupole Effects in Boron Oxide, Soda-Boric Oxide, and Borosilicate Glasses, *The Journal of Chemical Physics,* **29**, 984-990.

[287] Lu, Y., Shen, Y., Li, K., and Chen, H. (2006) Effects of nitrogen content on nanostructure evolution, mechanical behaviors and thermal stability in Ti–B–N thin films, *Surface and Coatings Technology,* **201**, 1228-1235.

[288] Gong, Q., Yu, L., and Ye, C. (2002) The tribological behaviour and mechanism of action of sulphur-containing borate esters in rape seed oil, *Journal of Synthetic Lubrication,* **19**, 19-30.

[289] Strohmeier, B. R. (1989) Surface characterization of aluminum foil annealed in the presence of ammonium fluoborate, *Applied surface science,* **40**, 249-263.

[290] Zhongyi, H., Liping, X., Liang, Q., Sheng, H., Aixi, C., Jianwei, Q.*, et al.* (2014) Tribological properties and hydrolysis stability study of benzothiazole borate derivative, *Lubrication Science,* **26**, 81-94.

[291] Wagner, C., Riggs, W., Davis, L., Moulder, J., and Muilenberg, G. (1975) Handbook of X-ray Photoelectron Spectroscopy; Perkin–Elmer Corporation, Physical Electronics Division: Eden Prairie, MN, 1979, *There is no corresponding record for this reference,*

[292] Fatima, N., Holmgren, A., Marklund, P., Minami, I., and Larsson, R. (2015) Degradation mechanism of automatic transmission fluid by water as a contaminant, *Proceedings of the Institution of Mechanical Engineers, Part J: Journal of Engineering Tribology,* **229**, 74-85.

[293] Martin, J. M., Matta, C., Bouchet, M.-I. D. B., Forest, C., Le Mogne, T., Dubois, T.*, et al.* (2013) Mechanism of friction reduction of unsaturated fatty acids as additives in diesel fuels, *Friction,* **1**, 252-258.

[294] Xu, N., Zhang, M., Li, W., Zhao, G., Wang, X., and Liu, W. (2013) Study on the selectivity of calcium carbonate nanoparticles under the boundary lubrication condition, *Wear,* **307**, 35-43.

[295] Nedelcu, I., Piras, E., Rossi, A., and Pasaribu, H. (2012) XPS analysis on the influence of water on the evolution of zinc dialkyldithiophosphate–derived reaction layer in lubricated rolling contacts, *Surface and Interface Analysis,* **44**, 1219-1224.

[296] Mistry, K., Neville, A., Morina, A., and Webster, M. (2008) Lubricant/surface interactions under extreme pressure conditions: corrosion inhibitor interacting extreme pressure/anti-wear additives on steel surface, *Proceedings of the Institution of Mechanical Engineers, Part J: Journal of Engineering Tribology,* **222**, 315-323.

[297] Wang, J., Wu, W., and Feng, D. (1992) Introduction to electron spectroscopy (XPS/XAES/UPS), *National Defense Industry Press, Beijing,* 249-260.

[298] Hua, F. J., Bo-Shui, C., Lin, D., Jiu, W., and Wei-Jiu, H. (2004) The synthesis and tribological behaviour of boron-nitrogen-modified fatty acid water-based lubricant additives, *Journal of Synthetic Lubrication,* **21**, 129-137.

[299] De Faria, D. and Lopes, F. (2007) Heated goethite and natural hematite: Can Raman spectroscopy be used to differentiate them?, *Vibrational Spectroscopy,* **45**, 117-121.

[300] Bronswijk, J. and Strijks, E. (1977) The Raman spectrum of vitreous and crystalline B2O3, *Journal of Non-Crystalline Solids,* **24**, 145-147.

[301] Ferlat, G., Seitsonen, A. P., Lazzeri, M., and Mauri, F. (2012) Hidden polymorphs drive vitrification in B2O3, *Nature materials,* **11**, 925-929.

[302] Kamitsos, E., Karakassides, M., and Chryssikos, G. D. (1987) A vibrational study of lithium borate glasses with high Li2O content, *Physics and chemistry of glasses,* **28**, 203-209.

[303] Ohtsuka, T., Kubo, K., and Sato, N. (1986) Raman spectroscopy of thin corrosion films on iron at 100 to 150 C in air, *Corrosion,* **42**, 476-481.

[304] Oh, S. J., Cook, D., and Townsend, H. (1998) Characterization of iron oxides commonly formed as corrosion products on steel, *Hyperfine interactions,* **112**, 59-66.

[305] Gohar, I., Megahed, A., Doweidar, H., Oraby, A., and Atta, A. (1991) An account on modifier and networkformer ions concentration in lead borate glasses containing iron and their effects on some physical properties, *Solid state communications,* **77**, 911-915.

[306] Domnich, V., Gogotsi, Y., Trenary, M., and Tanaka, T. (2002) Nanoindentation and Raman spectroscopy studies of boron carbide single crystals, *Applied Physics Letters,* **81**, 3783-3785.

[307] Kuhlmann, U. and Werheit, H. (1994) Raman effect of boron carbide (B4. 3C to B10. 37C), *Journal of alloys and compounds,* **205**, 87-91.

[308] Erdemir, A., Bindal, C., and Fenske, G. (1996) Formation of ultralow friction surface films on boron carbide, *Applied physics letters,* **68**, 1637-1639.

[309] Thevenot, F. (1990) Boron carbide—a comprehensive review, *Journal of the European Ceramic society,* **6**, 205-225.

[310] Hill, J. Raman Spectroscopy of Boron Nitride,

[311] Dreiling, I., Raisch, C., Glaser, J., Stiens, D., and Chassé, T. (2012) Temperature dependent tribooxidation of Ti–B–N coatings studied by Raman spectroscopy, *Wear,* **288**, 62-71.

[312] Bois, L., L'Haridon, P., Laurent, Y., Gouin, X., Grange, P., Létard, J.-F.*, et al.* (1996) Characterization of a boro-silicon oxynitride prepared by thermal nitridation of a polyborosiloxane, *Journal of alloys and compounds,* **232**, 244-253.

[313] Jianwei, Y., Fenfang, L., and Yihui, H. (2010) Tribological performance of two potential environmentally friendly ash less vegetable oil additives, *China Petrol. Process. Petrochem. Technol,* **12**, 43-48.

[314] Hu, Z., Yie, Y., Wang, L., Chen, G., and Dong, J. (2000) Synthesis and tribological properties of ferrous octoxyborate as antiwear and friction-reducing additive of lubricating oil, *Tribology Letters,* **8**, 45-50.

[315] Vannerberg, N. (1962) Progress in Inorganic Chemistry, Vol. 4, *lnterscience, New York,* **5**, 133.

[316] Furlan, A., Jansson, U., Lu, J., Hultman, L., and Magnuson, M. (2015) Structure and bonding in amorphous iron carbide thin films, *Journal of Physics: Condensed Matter,* **27**, 045002.

[317] Piras, F. M., Rossi, A., and Spencer, N. D. (2003) Combined in situ (ATR FT-IR) and ex situ (XPS) study of the ZnDTP-iron surface interaction, *Tribology Letters,* **15**, 181-191.

[318] Frost, R. L., Scholz, R., López, A., Xi, Y., and Belotti, F. M. (2014) Infrared and Raman Spectroscopic Characterization of the Borate Mineral Vonsenite, *Spectroscopy Letters,* **47**, 512-517.

[319] Manara, D., Grandjean, A., and Neuville, D. (2009) Advances in understanding the structure of borosilicate glasses: A Raman spectroscopy study, *American Mineralogist,* **94**, 777-784.

[320] Bunker, B., Tallant, D., Kirkpatrick, R., and Turner, G. (1990) Multinuclear nuclear magnetic resonance and Raman investigation of sodium borosilicate glass structures, *Physics and chemistry of glasses,* **31**, 30-41.

[321] Hanesch, M. (2009) Raman spectroscopy of iron oxides and (oxy) hydroxides at low laser power and possible applications in environmental magnetic studies, *Geophysical Journal International,* **177**, 941-948.

[322] Ohtsuka, T. (1996) Raman spectra of passive films of iron in neutral borate solution, *Materials Transactions, JIM,* **37**, 67-69.

[323] Barrow, N. (2006) Superstructural Units In Borate Glasses,

[324] Martin, S. W. and Angell, C. (1984) Glass formation and transition temperatures in sodium and lithium borate and aluminoborate melts up to 72 mol.% alkali, *Journal of non-crystalline solids,* **66**, 429-442.

[325] Fenfang, L., Boshui, C., and Junxiu, D. (2001) Preparation and tribological performance of lanthanum alkoxyborate, *Lubrication Science,* **13**, 193-198.

[326] Guoliang, W. J. W. (2001) Dong Junxiu (Logistical Engineering University, Chongqing); Study on the Lubricating Behaviors of N-Containing Borate Ester Additives [J], *Lubrication Engineering,* **1**,

[327] Fang, J., Xia, Y., Lin, Y., and Liu, W. (2009) Tribological behavior of plasma nitrided 1Cr18Ni9Ti austenitic stainless steel under the effect of lubricant additives, *Journal of Tribology,* **131**, 031603.

[328] Dünnwald, J. and Otto, A. (1989) An investigation of phase transitions in rust layers using Raman spectroscopy, *Corrosion Science,* **29**, 1167-1176.

[329] Yamashita, M., Miyuki, H., Matsuda, Y., Nagano, H., and Misawa, T. (1994) The long term growth of the protective rust layer formed on weathering steel by atmospheric corrosion during a quarter of a century, *Corrosion Science,* **36**, 283-299.

[330] Godfrey, D. (1987) Recognition and solution of some common wear problems related to lubricants and hydraulic fluids, *Lubricant Engineering,* **43**, 111-114.

[331] Boucherit, N., Delichere, P., Joiret, S., and Hugot le Goff, A., Passivity of iron and iron alloys studied by voltammetry and Raman spectroscopy, in *Materials Science Forum*, 1989, 51-62.

[332] Wang, Q., Zheng, G., Ai, J. J., and Wei, X. J., Study on the hydrolytic stability of borate ester, in *Applied Mechanics and Materials*, 2011, 499-503.

[333] Stackelberg, M. v., Quatram, F., and Dressel, J. (1937) Volatility of boric acid in steam. The system B 2 O 3-water, *Z. Elektrochem,* **43**, 14-28.

[334] He, Z., Lu, J., Zeng, X., Shao, H., Ren, T., and Liu, W. (2004) Study of the tribological behaviors of S, P-containing triazine derivatives as additives in rapeseed oil, *Wear,* **257**, 389-394.

[335] Canter, N. (2008) Friction-reducing characteristics of nano-boric acid, *Tribology & Lubrication Technology,* **64**, 10.

[336] Rastogi, R., Maurya, J., and Jaiswal, V. (2012) Low sulfur, phosphorus and metal free antiwear additives: Synergistic action of Salicylaldehyde N (4)-phenylthiosemicarbazones and its different derivatives with Vanlube 289 additive, *Wear,*

[337] Booth, J. E., "The feasibility of using electrostatic charge condition monitoring for lubricant additive screening," University of Southampton, 2008.

[338] LIU, W., ZHANG, B., HUANG, C., ZHANG, X., XUE, Q., and WANG, H. (1991) The antiwear properties of potassium borate as an oil additive, *Lubrication engineering,* **47**, 344-347.

[339] Ray, N. H., *Inorganic polymers*: Academic Press London, 1978.

[340] Wang, S., Wang, Y., Bian, C., Zhong, Y., and Jing, X. (2015) The thermal stability and pyrolysis mechanism of boron-containing phenolic resins: The effect of phenyl borates on the char formation, *Applied Surface Science,*

[341] Adams, J. H., "Synergistic Combinations Of Hydrated Potassium Borate,Antiwear Agents,And Organic Sulphide Antioxidants(US Patent)," 4,089,790, 1978.

[342] Broadhead, P. and Newman, G. (1971) The vibrational spectra of orthoboric acid and its thermal decomposition products, *Journal of Molecular Structure,* **10**, 157-172.

[343]   Durig, J., Green, W., and Marston, A. (1968) The low-frequency vibrations of molecular crystals. IV. Boric Acid, *Journal of Molecular Structure,* **2**, 19-37.

[344]   Kim, Y., Lim, J.-T., and Park, S. (1999) The structures and the hydrolysis rates of the dehydrates prepared from orthoboric acid (H 3 BO 3), *Journal of Physics and Chemistry of Solids,* **60**, 969-973.

[345]   V. A. Mukhanov, O. O. K., and V. L. Solozhenko (2008) On the Hardness of Boron (III) Oxide,

[346]   Heuberger, R., Rossi, A., and Spencer, N. D. (2007) XPS study of the influence of temperature on ZnDTP tribofilm composition, *Tribology Letters,* **25**, 185-196.

[347]   Weimin Liu, L. Y. a. Q. X. An investigation of the film formed in the borate oil immersion test, *Thm Sohd Fdms,,* 83-85.

[348]   Zhang, Z., Yamaguchi, E., Kasrai, M., Bancroft, G., Liu, X., and Fleet, M. (2005) Tribofilms generated from ZDDP and DDP on steel surfaces: Part 2, chemistry, *Tribology Letters,* **19**, 221-229.

[349]   Kawano, T., Morito, H., Yamada, T., Onuma, T., Chichibu, S. F., and Yamane, H. (2009) Synthesis, crystal structure and characterization of iron pyroborate (Fe 2 B 2 O 5) single crystals, *Journal of Solid State Chemistry,* **182**, 2004-2009.

[350]   Diehl, R. and Brandt, G. (1975) Refinement of the crystal structure of Fe3BO6, *Acta Crystallographica Section B: Structural Crystallography and Crystal Chemistry,* **31**, 1662-1665.

[351]   Diehl, R. and Friedrich, F. (1976) Growth of bulk single crystals of the weak ferromagnet Fe 3 BO 6 by a vapor phase reaction, *Journal of Crystal Growth,* **36**, 263-266.

[352]   Diehl, R., Räuber, A., and Friedrich, F. (1975) Vapour growth of bulk FeBO 3 single crystals, *Journal of Crystal Growth,* **29**, 225-233.

[353]   Leonov, I., Yaresko, A., Antonov, V., Attfield, J., and Anisimov, V. (2005) Charge order in Fe 2 OBO 3: An LSDA+ U study, *Physical Review B,* **72**, 014407.

[354]   Knyrim, J. S. and Huppertz, H. (2008) Synthesis and crystal structure of the high-pressure iron borate α-FeB 2 O 4, *Journal of Solid State Chemistry,* **181**, 2092-2098.

[355] Block, S., Burley, G., Perloff, A., and Mason Jr, R. D. (1959) Refinement of the crystal structure of triclinic magnesium pyroborate, *J. Res. Nat. Bur. Stand,* **62**, 95-100.

[356] Murawski, L. (1982) Electrical conductivity in iron-containing oxide glasses, *Journal of Materials Science,* **17**, 2155-2163.

[357] Nevshupa, R. A. (2004) Triboemission: an attempt of developing a generalized classification, *Tribology Science and Application, Herman MA (Ed.), CUN PAN, Warsaw,* 11-25.

[358] Kajdas, C. K. (2005) Importance of the triboemission process for tribochemical reaction, *Tribology International,* **38**, 337-353.

[359] Kano, M. (2006) Super low friction of DLC applied to engine cam follower lubricated with ester-containing oil, *Tribology International,* **39**, 1682-1685.

[360] Jolly, W. L., *Modern inorganic chemistry*: McGraw-Hill College, 1984.

[361] Housecroft, C. and Sharpe, A., "Inorganic Chemistry, d-block chemistry: coordination complexes," ed: Pearson Prentice Hall, England, 2005.

[362] Zhu, Y., Kelsall, G., and Spikes, H. (1994) The influence of electrochemical potentials on the friction and wear of iron and iron oxides in aqueous systems, *Tribology transactions,* **37**, 811-819.

[363] Goto, H. and Buckley, D. (1985) The influence of water vapour in air on the friction behaviour of pure metals during fretting, *Tribology international,* **18**, 237-245.

[364] Liping, X., Zhongyi, H., Liang, Q., Lin, M., Aixi, C., Sheng, H.*, et al.* (2014) Synthesis, Tribological and Hydrolysis Stability Study of Novel Benzotriazole Borate Derivative, *PloS one,* **9**, e83501.

[365] Adams, J. (1977) Borate--New Generation EP(Extreme Pressure) Gear Lubricant, *Lubric. Eng.,* **33**, 241-246.

[366] Junbin, Y. (1997) Antiwear function and mechanism of borate containing nitrogen, *Tribology international,* **30**, 387-389.

[367] Yang, G., Zhang, J., Zhang, S., Yu, L., Zhang, P., and Zhu, B. (2013) Preparation of Triazine Derivatives and Evaluation of Their Tribological Properties as Lubricant Additives in Poly-alpha Olefin, *Tribology International,*

Appendix A

A.1. Coefficient of Friction

First law of friction as it applies dry sliding contacts for metals, polymers and rubbers are shown in Equation A.1.- 1, Equation A.1.- 2 and Equation A.1.- 3.

$$F \propto W \quad \text{or} \quad F = \mu \cdot W \quad \text{(Metals)}$$

Equation A.1.- 1

$$F \propto W^{3/4} \quad \text{Or} \quad F = \mu \cdot W^{3/4} \quad \text{(Polymers)}$$

Equation A.1.- 2

$$F \propto W^{2/3} \quad \text{Or} \quad F = \mu \cdot W^{2/3} \quad \text{(Rubbers)}$$

Equation A.1.- 3

Where, μ is the constant of proportionality known as friction coefficient or coefficient of friction (COF). However, friction coefficient can be expressed in terms of the mechanical properties of the contacting sliding material is shown in Equation A.1.- 4

$$\mu = S/P_C$$

Equation A.1.- 4

Where S is the shear strength of the lubricant film interface in N/mm^2 of the sliding interface and P_C is the contact pressure in N/mm^2.

A.2. Wear modes and equations

Table A.2.- 1 Summary of wear modes [29]

Wear Type	Mechanical			Tribo- Chemical		Thermal	
Wear Mode	Abrasive	Adhesive	Flow	Fatigue	Corrosive	Diffusive	Melt

The general wear law is shown in Equation A.2.- 1. However, the relationship of Archard's wear law to adhesive and abrasive wear are respectively shown in Equation A.2.- 2 and Equation A.2.- 3.

$$v_i \quad \propto \quad A_r \, . \, L \quad \text{(Wear law)}$$

Equation A.2.- 1

(Adhesive wear)

Equation A.2.- 2

$$v_i = K \, . \, A_r = K \, . \, L . \, W / H = k_1 \, . \, L . \, W / 3H$$

(Abrasive wear)

Equation A.2.- 3

$$v_i = K \, . \, A_r = K \, . \, L . \, W / H = 2k_1 \, . \, k_2 \, L . \, W / 3H.$$

Where k_1 = adhesive wear constant in m³/N-m,

$k_2 = \dfrac{2tan\theta}{\pi}$ = abrasive wear constant in m³/N-m,

K = Archard's coefficient used as an index to determine severity of wear,

A_r = real contact area in m²,

W = applied load in Newton (N),

L = sliding distances in m,

H = hardness of the softer material in N/m²,

v_i = wear volume in m³

θ = slope of the hard conical asperity in degrees

A.3. Lubrication regimes

Lubricant film parameter (Λ) determination is determined from Equation A.3.- 1.

$$\Lambda = \frac{h_{min}}{\sqrt{R_{q1}^2 + R_{q2}^2}}$$

Equation A.3.- 1

Where, R_{q1} and R_{q2} are the root mean squares of the surface roughness of each of the contacting surfaces and h_{min} is the minimum lubricant film thickness which can be determined using the Hamrock and Dowson empirical equation for isothermal elliptical contact relations shown in Equation A.3.- 2. However, the dimensionless

parameters in the Equation A.3.- 2 can be obtained from Equation A.3.- 3, Equation A.3.- 4, Equation A.3.- 5, and Equation A.3.- 6

$$\frac{h_{min}}{R^*} = 3.63 U_{\Sigma}^{0.68} G_{\Sigma}^{0.49} W_{\Sigma}^{-0.073} (1 - e^{-0.68k}) \qquad \text{Equation A.3.- 2}$$

Dimensionless speed parameter, $\quad U_{\Sigma} = \frac{\eta_o U}{E^* R} \qquad \text{Equation A.3.- 3}$

Dimensionless material parameter, $G_{\Sigma} = \frac{E^*}{P_o} \qquad \text{Equation A.3.- 4}$

Dimensionless load parameter, $W_{\Sigma} = \frac{W}{E^* R^2} \qquad \text{Equation A.3.- 5}$

Entraining surface velocity, U in (m/s), $= \left(\frac{U_1 + U_2}{2}\right) \qquad \text{Equation A.3.- 6}$

Where;

η_o = lubricant viscosity at ambient pressure (N/m^2)

P_o = asymptotic isoviscous pressure (N.s/m^2)

W = contact load (N)

For point contact, $k_i \cong \mathbf{1.03}$ and for line contact, $k = \infty$

$\boldsymbol{v_q}$ = Poisson's ratio

$\mathbf{R_Q}$= radius of curvature of the contacting surfaces (m)

$\mathbf{E_q}$ = elastic modulus of the contacting surfaces (N/m^2)

In addition, the reduced elastic modulus (E*) and reduced radius of curvature (R*) are respectively obtained as shown in Equation A.3.- 7 and Equation A.3.- 8 if the ellipticity parameter, k is taken as 1.03 [242] for line contact.

Reduced Young Modulus, E^* (N/m^2) $= \left(\frac{1 - v_{q1}^2}{E_{q1}} + \frac{1 - v_{q2}^2}{E_{q2}} \right)^{-1}$ Equation A.3.- 7

Reduced radius of curvature, R^* (m) $= \left(\frac{1}{R_{Q1}} + \frac{1}{R_{Q2}} \right)^{-1}$ Equation A.3.- 8